

UNIVERSITY OF BELGRADE
FACULTY OF CIVIL ENGINEERING

Nina M. Gluhović

**BEHAVIOUR OF SHEAR CONNECTIONS REALISED BY
CONNECTORS FASTENED WITH CARTRIDGE FIRED PINS**

Doctoral Dissertation

Belgrade, 2019

УНИВЕРЗИТЕТ У БЕОГРАДУ
ГРАЂЕВИНСКИ ФАКУЛТЕТ

Нина М. Глуховић

**ПОНАШАЊЕ СМИЧУЋИХ СПОЈЕВА ИЗВЕДЕНИХ
МОЈДАНИЦИМА СА ЕКСЕРИМА СА ЕКСПЛОЗИВНИМ
УПУЦАВАЊЕМ**

докторска дисертација

Београд, 2019

Supervisor:

Prof. Zlatko Marković
University of Belgrade, Faculty of Civil Engineering

Members of the jury:

Prof. Zlatko Marković
University of Belgrade, Faculty of Civil Engineering

Asst. Prof. Milan Spremić
University of Belgrade, Faculty of Civil Engineering

Asst. Prof. Marko Pavlović
Delft University of Technology, Faculty of Civil Engineering
and Geosciences, Department of Engineering Structures, The
Netherlands

Defense date: _____

Ментор: Др Златко Марковић, редовни професор
Универзитет у Београду, Грађевински факултет

Чланови комисије: Др Златко Марковић, редовни професор
Универзитет у Београду, Грађевински факултет

Др Милан Спремић, доцент
Универзитет у Београду, Грађевински факултет

Др Марко Павловић, доцент
Delft University of Technology, Faculty of Civil Engineering
and Geosciences, Department of Engineering Structures, The
Netherlands

Датум одбране: _____

Acknowledgments

This work is supported by the Serbian Ministry of Education, Science and Technological Development through project TR-36048 and is entirely funded by Hilti Company, Liechtenstein.

Special thanks are addressed to supervisor Prof. Zlatko Marković for professional guidance and support. I would like to express great appreciation to my colleagues Asst. Prof. Milan Spremić and Asst. Prof. Marko Pavlović for enormous help in experimental and numerical investigation.

I would like to extend my appreciation to Mr. Herman Beck, Mr. Georgi Dimitrov and Mr. Daniel Bătrâneanu from Hilti Company for recognizing the importance of this research, for excellent collaboration and constructive discussions. Further, special thanks are addressed to Mr. Srđan Stojakov and Mrs. Ivana Bošković Pešić, from Hilti office in Belgrade for unselfish help during preparation of specimens for experimental investigation and professional guidance.

Also, I would like to extend my gratitude to my colleagues and technical staff of the Laboratory of Materials and the Laboratory of Structures, Faculty of Civil Engineering, University of Belgrade, Mladen Jović, Marina Aškračić, Savo Stavnjak and Radomir Petrović for their help in experimental works.

Special thanks are addressed to my dear colleagues Assoc. Prof. Jelena Dobrić and Asst. Prof. Nenad Fric for their unselfish help and support. Thanks are addressed to my colleagues Aljoša Filipović and Isidora Jakovljević.

Dedicated to my family.

BEHAVIOUR OF SHEAR CONNECTIONS REALISED BY CONNECTORS FASTENED WITH CARTRIDGE FIRED PINS

Abstract

New demands towards fast construction resulted in development of different types of prefabricated concrete slabs and shear connectors. Composite action between steel beam and concrete slabs can be achieved with group positioning of shear connectors in envisaged openings of prefabricated concrete slabs. The aim of presented investigation is to promote application of mechanically fastened shear connectors in prefabricated concrete slabs. X-HVB 110 shear connectors fastened to the steel base material with X-ENP-21 HVB cartridge fired pins are used in experimental and numerical analysis presented in this thesis. Presented investigation should improve understanding of X-HVB shear connectors behaviour which is currently based on their application in solid or composite concrete slabs. Also, this investigation should result in extension of currently small basis of experimental results, which are mostly part of the technical reports and are considered as proprietary. Feasibility study presented in this work highlighted the importance of further investigation of X-HVB shear connectors in group arrangement, at distances smaller than minimal recommended, in order to satisfy current recommendations for minimal partial shear connection degree in composite floor structures with profiled steel sheeting. Detail examination of X-HVB 110 shear connectors positioned in envisaged openings of prefabricated composite slabs is performed. The experiment aims at understanding the effects of the spacing between shear connectors, orientation of shear connectors relative to the shear force direction and installation power level used for installation of cartridge fired pins, when they are used for prefabricated composite construction. In order to generate all structural performance data, this investigation included experimental investigation of cartridge fired pins performed through shear and tension tests. Extensive finite element analysis is conducted in this research in order to develop and calibrate FE models of push-out test specimens of X-HVB 110 shear connectors, and shear and tension tests of cartridge fired pins, based on the results of presented experimental research. The novelty in the FE modelling approach developed in this study is phenomenological simulation of installation procedure of cartridge fired pins resulting in preloading of the pins and interaction with

the base material. Numerical FE models are developed through extensive calibration of main parameters which are introduced in FE simulation of firing the pins in tension tests and further sensitivity study. Parametric study of push-out FE models is performed for X-HVB 110 shear connectors through variation of concrete and steel base material properties. Main failure mechanisms which are obtained through experimental investigation of X-HVB 110 shear connectors in prefabricated concrete slabs are related to deformation capacity and pull-out of cartridge fired pins from the steel base material. Developed FE models of push-out test series matched the failure mechanisms obtained through experimental investigation. Pull-out of cartridge fired pins in FE models is defined by equivalent compressive contact stresses and friction at the interface between the base material and pins modelled as separate parts. This resembles the physical mechanism of the load transfer of cartridge fired pins and is a recommended modelling procedure as it gives good agreement with experimental results. Presented FE modelling approach of installation procedure of cartridge fired pins highlights the clamping of the fastener in steel base material as the most dominant anchorage mechanism. Prediction models for pull-out resistance of cartridge fired pins loaded in tension and shear resistance of X-HVB shear connectors are proposed based on the presented results of experimental and numerical investigation.

Keywords: Prefabricated steel-concrete composite construction, Mechanically fastened shear connectors, Cartridge fired pins, Push-out tests, Shear resistance, Pull-out resistance, Anchorage mechanisms, FE analysis.

Field of science: Civil and Structural Engineering

Subdivision: Steel Structures

UDC number: 624.012./14.(043.3)

ПОНАШАЊЕ СМИЧУЋИХ СПОЈЕВА ИЗВЕДЕНИХ МОЖДАНИЦИМА СА ЕКСЕРИМА СА ЕКСПЛОЗИВНИМ УПУЦАВАЊЕМ

Резиме

Савремени трендови у грађевинарству се најчешће огледају у повећаним захтевима за убрзаном градњом, што је утицало на развој нових врста префабрикованих бетонских плоча и средстава за спрезање. Спрезање префабрикованих бетонских плоча и челичних гредних носача најчешће се постиже постављањем можданика у отворе у бетонској плочи, који су за то предвиђени у процесу префабрикације. Предмет научног истраживања је понашање смичућих спојева остварених помоћу Х-НВВ можданика у префабрикованим бетонским плочама. Х-НВВ 110 можданици повезани су са челичним профилима уз помоћ два Х-ЕНР-21 НВВ механичка спојна средства (ексера) експлозивним упуцавањем. Приказано испитивање треба да допринесе бољем разумевању понашања Х-НВВ можданика у смичућим спојевима, које је тренутно засновано на испитивањима у пуним и спрегнутим бетонским плочама на профилисаним лимовима. Такође, испитивање треба да допринесе проширењу тренутно мале базе експерименталних испитивања, која су највећим делом садржана у техничким извештајима који нису лако доступни истраживачима. Упоредна анализа носивости заварених можданика са главом и Х-НВВ можданика у спрегнутим плочама са профилисаним лимом, презентована у овом раду, нагласила је потребу за додатним испитивањима ове врсте можданика када су они груписани на растојањима која су мања од минимално препоручених, како би се задовољиле тренутне препоруке у погледу минималног процента парцијалног смичућег споја. Детаљно експериментално испитивање Х-НВВ 110 можданика постављених у отворе префабрикованих бетонских плоча споредно је у овом раду. Испитивање је обухватило утицај положаја и међусобног растојања можданика у односу на правац смичуће силе као и различите јачине уградње ексера. У циљу јасног сагледавања понашања ове врсте можданика, експериментално испитивање ексера је спроведено кроз тестове смицања и затезања. Нумерички модели базирани на методи коначних елемената развијени су за потребе симулирања смичућих спојева са Х-НВВ 110 можданицима као и ексера са експлозивним упуцавањем који су оптерећени на смицање и затезање и

калибрисани су према резултатима експерименталног испитивања. Симулација уградње ексера са експлозивним упуцавањем која је дефинисана кроз нумеричке моделе резултовала је преднапрезањем ексера и дефинисањем посебних услова интеракције између ексера и основног материјала. Нумерички модели су развијени кроз опсежну калибрацију основних параметара који су кориштени за дефинисање процеса уградње и накнадно су анализирани кроз студију осетљивости спроведну на моделима са X-HVB 110 можданицима. Параметарска анализа спроведена је на моделима смичућих спојева X-HVB 110 можданика кроз промену механичких својстава бетона и основног челичног материјала. Основни модели лома који су се појавили кроз експериментално испитивање повезани су са деформацијом ексера и њиховим извлачењем из основног челичног материјала. Развијени нумерички модели смичућих спојева са X-HVB 110 можданицима потврдили су овакве видове лома. Носивост на извлачење ексера из основног челичног материјала дефинисана је кроз еквивалентни напон притиска и коефицијент трења који је развијен на контактної површини између ексера и основног челичног материјала. Овакав начин нумеричког моделирања процеса уградње ексера показао је добро слагање са резултатима експерименталног испитивања и наглашава укљештење ексера у основни челични материјал као најдоминантнији механизам анкеровања. Предиктивни изрази за носивост ексера на извлачење и носивост X-HVB можданика у смичућим спојевима дефинисани су у овом раду на основу презентованог експерименталног и нумеричког испитивања.

Кључне речи: Префабриковане спрегнуте конструкције, Можданица са механичким спојним средствима, Ексери са експлозивним упуцавањем, Тест на смицање, Носивост на смицање, Носивост на извлачење, Механизми анкеровања, Метод коначних елемената.

Научна област: Грађевинарство

Ужа научна област: Металне конструкције

УДК број: 624.012./14.(043.3)

Table of Contents

Acknowledgments	i
Abstract.....	ii
Резиме	iv
List of figures	x
List of tables	xvii
Notation	xx
Chapter 1. Introduction.....	1
1.1. Background.....	1
1.2. The advantage of shear connectors fastened with cartridge fired pins	1
1.3. Goal of the research	3
1.4. Objectives of the research.....	4
1.5. Methodology of the research	4
1.6. Outline of the thesis	5
Chapter 2. Literature review	7
2.1. Introduction.....	7
2.2. Shear connectors in prefabricated concrete slabs	7
2.3. Mechanically fastened shear connectors.....	8
2.3.1. X-HVB shear connectors in solid concrete slabs.....	8
2.3.2. X-HVB shear connectors in composite concrete slabs.....	15
2.3.3. Design recommendations and installation requirements	18
2.3.4. Other types of mechanically fastened shear connectors	21
2.4. Cartridge fired pins	24
2.4.1. Development and classification.....	24
2.4.2. Range of application and installation quality	25
2.4.3. Anchorage mechanisms of cartridge fired pins	29

2.4.4. Pull-out resistance of cartridge fired pins in tests.....	30
2.4.5. Different types of load and failure mechanisms	34
2.4.6. Design resistance of cartridge fired pins	36
2.5. Summary	42
Chapter 3. X-HVB shear connectors vs. headed studs shear resistance.....	43
3.1. Various application of X-HVB shear connectors	43
3.2. Reduction factor of X-HVB shear connectors in composite floor structures	45
3.3. Parametric analysis of X-HVB shear connectors in composite floor structures	47
3.4. Summary	49
Chapter 4. Experimental work.....	50
4.1. Experimental program of push-out tests	50
4.2. Specimens preparation	53
4.3. Material properties	55
4.3.1. Steel profile and X-HVB shear connector	56
4.3.2. Concrete	60
4.4. Push-out test set-up.....	64
4.5. Experimental results of push-out tests	66
4.5.1. Cyclic loading	67
4.5.2. Failure loading	68
4.5.3. Analysis of experimental results.....	71
4.5.4. Characteristic failure mechanisms	76
4.6. Measurement of material hardness after push-out tests.....	79
4.7. Shear and tension tests of cartridge fired pins	82
4.8. Summary	90
Chapter 5. Numerical analysis.....	93
5.1. Introduction.....	93

5.2. FE modelling of push-out experiments.....	93
5.2.1. Geometry and boundary conditions.....	93
5.2.2. Loading phases	96
5.2.3. Finite element mesh.....	99
5.2.4. Material models	101
5.3. FE models of shear and tension tests of cartridge fired pins	110
5.4. Comparison of FE analysis results with experimental investigation.....	113
5.4.1. Push-out FE models.....	113
5.4.2. FE models of shear and tension tests of cartridge fired pins	119
5.5. Summary.....	121
Chapter 6. Calibration of numerical models and parametric analysis of X-HVB shear connector	123
6.1. Calibration of pull-out FE models for cartridge fired pins	123
6.2. Sensitivity study of push-out FE models for various installation procedure parameters of cartridge fired pins.....	129
6.3. Parametric analysis of X-HVB shear connector push-out FE models.....	132
6.4. Summary.....	135
Chapter 7. Pull-out resistance of cartridge fired pins loaded in tension.....	137
7.1. Behaviour of cartridge fired pins through tension loading.....	137
7.2. Prediction model for pull-out resistance of cartridge fired pins	144
7.3. Summary.....	147
Chapter 8. Behaviour of X-HVB shear connectors in prefabricated concrete slabs	149
8.1. Summary.....	166
Chapter 9. Conclusions and future work	168
REFERENCES	171
Annex A – Concrete material properties	175

Annex B – Installation requirements	179
Annex C – Base plate material properties of cartridge fired pins shear and tension tests	184
Annex D – Development of FE models	188
Annex E – Influence of different parameters on FE analysis results of push-out tests	195
Curriculum vitae	
Биографија аутора	
Изјава о ауторству	
Изјава о истоветности штампане и електронске верзије докторског рада	
Изјава о коришћењу	

List of figures

Figure 2.1. X-HVB shear connectors and X-ENP-21 HVB cartridge fired pins.....	8
Figure 2.2. Shear resistance of HVB 105 shear connector in solid concrete slabs.....	11
Figure 2.3. HVB shear connectors – geometry and shear resistance.....	12
Figure 2.4. Influence of connectors orientation on shear resistance in solid concrete slabs	12
Figure 2.5. Results of push-out experiments on HVB shear connectors in solid concrete slabs	13
Figure 2.6. Influence of connector height and concrete strength on shear resistance in composite concrete slabs, adapted from [1]	15
Figure 2.7. Influence of profiled sheeting geometry on shear resistance, adapted from [1]	16
Figure 2.8. Influence of connector distance and number of connectors per profile sheeting rib on shear resistance, adapted from [1].....	17
Figure 2.9. Composite beams examination with HVB 100 shear connector [9], [10], [16]	18
Figure 2.10. Recommendations for X-HVB shear connectors positioning [5], [7].....	19
Figure 2.11. Push-out tests with Rib Connectors (Ribcon) [20]	22
Figure 2.12. Push-out tests with Strip Connectors (Stripcon) [20].....	22
Figure 2.13. Composite beam examination with Rib and Strip Connectors [20].....	23
Figure 2.14. Mechanically fastened shear connectors	24
Figure 2.15. Powder actuated fasteners [33]	26
Figure 2.16. Installation requirements of cartridge fired pins [7], [32].....	27
Figure 2.17. Application range limits for various types of cartridge fired pins	28
Figure 2.18. Failure of fasteners due to exceeding of upper application limits [32]	28
Figure 2.19. Anchorage mechanisms of X-ENP 21 HVB cartridge fired pins [32].....	29
Figure 2.20. Influence of the knurling of the fastener on the pull-out resistance [12] ..	31
Figure 2.21. Influence of base material thickness and depth of penetration on the pull-out resistance [12].....	32
Figure 2.22. Depth penetration influence on the pull-out resistance, adapted from [32]	32

Figure 2.23. Influence of base material strength and thickness on pull-out resistance [12]	33
Figure 2.24. Pull-out resistances of various types of powder actuated fasteners [37]... 33	33
Figure 2.25. Failure mechanisms of cartridge fired pins loaded in shear and tension [32]	34
Figure 2.26. Characteristic resistance of X-ENP-19 L15 cartridge fired pin [35]	36
Figure 3.1. Different types of shear connectors – possibilities for renovation of existing composite structures	44
Figure 3.2. Shear resistance reduction factor of X-HVB shear connectors for decking ribs transverse to the beam axis – $n_r=2$	45
Figure 3.3. Reduction of composite beam bending resistance for 3.0 m distance of composite beams (composite floor span)	48
Figure 4.1. Geometrical properties of shear connector and cartridge fired pin.....	50
Figure 4.2. Position of shear connectors in envisaged openings	51
Figure 4.3. Push-out test specimens layout	52
Figure 4.4. Prefabrication of concrete slabs in “ASA IBELIK” concrete plant.....	53
Figure 4.5. Push-out specimens assembling	54
Figure 4.6. Installation of X-ENP-21 HVB cartridge fired pins.....	54
Figure 4.7. Specimens after assembling	55
Figure 4.8. Tensile test coupons	56
Figure 4.9. Tensile tests procedure and test coupons after fracture.....	57
Figure 4.10. Nominal stress-strain curves	58
Figure 4.11. Standard tests to determine the material properties of concrete.....	61
Figure 4.12. Push-out specimen during examination	64
Figure 4.13. Layout of measurements for push-out specimens	65
Figure 4.14. Loading regime for push-out tests.....	65
Figure 4.15. Designation of main parameters for push-out tests analysis.....	66
Figure 4.16. Force-slip curves for cyclic loading	67
Figure 4.17. Experimental results for failure loading - HSF test series	68
Figure 4.18. Experimental results for failure loading - HSB test series.....	68
Figure 4.19. Experimental results for failure loading - HSFg test series	70

Figure 4.20. Experimental results for failure loading - HSFg-2 test series	70
Figure 4.21. Average results of push-out tests series	72
Figure 4.22. Stiffness of X-HVB shear connectors	75
Figure 4.23. Experimentally obtained slip corresponding to the serviceability limit state	75
Figure 4.24. Specimens of phase 1 after testing procedure - cut through concrete slab	76
Figure 4.25. Infill concrete zone and steel beam after testing of phase 1.....	77
Figure 4.26. Specimens after testing procedure - reduced distance between shear connectors - phase 2 and 3.....	78
Figure 4.27. Material hardness test for push-out test steel beam.....	79
Figure 4.28. Impresses obtained for measuring position 4.....	80
Figure 4.29. Shear and tension test specimens	82
Figure 4.30. Specimens after installation of cartridge fired pins.....	84
Figure 4.31. Examination of shear test specimens - ST	84
Figure 4.32. Examination of tension test specimens - TT	85
Figure 4.33. Force-relative deformation curves of shear test specimens - ST	86
Figure 4.34. Results of shear test specimens (ST) examination.....	87
Figure 4.35. Tension test (TT) specimens results.....	88
Figure 4.36. Force-deformation curves for tension test specimens (TT)	89
Figure 4.37. Pull-out resistance of cartridge fired pins	89
Figure 5.1. Geometry of FE models for push-out specimens	94
Figure 5.2. Double vertical symmetry boundary conditions of FE models.....	94
Figure 5.3. Support boundary conditions of FE models.....	95
Figure 5.4. Geometry of shear connector and cartridge fired pin of FE models	95
Figure 5.5. Various approaches for FE models of connector and cartridge fired pin....	96
Figure 5.6. Predefined temperature fields of cartridge fried pins.....	97
Figure 5.7. Von Mises stresses and deformed shape (scale x5) after the preloading step in FE analysis - HSF test series	98
Figure 5.8. Smoothed amplitudes of FE analysis steps - HSF test series.....	99
Figure 5.9. FE model mesh for shear connector and pin.....	100
Figure 5.10. FE model mesh for concrete slab and steel profile	100

Figure 5.11. Orthotropic material properties of cartridge fired pins - preloading step in FE analysis.....	102
Figure 5.12. Connector material properties - FE analysis	103
Figure 5.13. Quad-linear material model of steel profile - FE analysis	103
Figure 5.14. Stress-strain relation for concrete compression behaviour - HSF and HSB push-out FE models	108
Figure 5.15. Compression damage - HSF and HSB push-out FE models.....	108
Figure 5.16. Concrete behaviour in tension - HSF and HSB push-out FE models	109
Figure 5.17. Geometry of FE models for shear and tension tests of cartridge fired pins	110
Figure 5.18. Quad-linear material model of steel base material - FE models of ST specimen	111
Figure 5.19. Analysed material models of steel base material - FE models of TT specimen	112
Figure 5.20. Experimental and FE analysis force-slip curves - HSF test series.....	113
Figure 5.21. Experimental and FE analysis force-slip curves - HSB test series	113
Figure 5.22. Experimental and FE analysis force-slip curves - HSFg test series.....	114
Figure 5.23. Experimental and FE analysis force-slip curves – HSFg-2 test series....	114
Figure 5.24. Experimental and FE analysis results – concrete compressive damage .	116
Figure 5.25. Experimental and FE analysis results – concrete compressive damage - cut through prefabricated concrete slabs	117
Figure 5.26. Tensile strains in prefabricated concrete slabs – FE analysis	117
Figure 5.27. Deformation of shear connector – HSF FE model.....	118
Figure 5.28. Deformation of shear connector – HSB FE model	118
Figure 5.29. Experimental and FE analysis results - force-relative displacement curves for shear test specimens (ST).....	120
Figure 5.30. Failure of shear test specimen (ST) of cartridge fired pins - FE analysis	120
Figure 5.31. Deformation of shear test specimen (ST) - FE analysis.....	120
Figure 5.32. Experimental and FE analysis results - pull out resistance of tension test specimens (TT)	121

Figure 6.1. Parametric analysis results for pin installation procedure of tension tests – base material S275.....	125
Figure 6.2. Parametric analysis results for pin installation procedure of tension tests– base material S355.....	126
Figure 6.3. Comparison of parametric analysis results for pin installation procedure of tension tests – true stress-strain material model	127
Figure 6.4. Comparison of parametric analysis results of tension tests – analysis of two material models influence.....	129
Figure 6.5. Sensitivity study results for various installation procedure of cartridge fired pins – HSF test series	130
Figure 6.6. Sensitivity study results for various installation procedure of cartridge fired pins – HSB test series	131
Figure 6.7. Influence of material model of steel base material on FE analysis results – HSF test series	131
Figure 6.8. Influence of material model of steel base material on FE analysis results – HSB test series.....	132
Figure 6.9. Influence of concrete class on shear resistance – HSF test series.....	133
Figure 6.10. Influence of concrete class on shear resistance – HSB test series	133
Figure 6.11. Influence of steel base material strength on FE analysis results – HSF test series	134
Figure 6.12. Influence of steel base material strength on FE analysis results – HSB test series	134
Figure 7.1. Comparison of experimental and FE analysis results with pull-out resistances for smooth shank powder actuated fasteners, adapted from [37].....	138
Figure 7.2. Comparison with characteristic resistance of ENP2-21 L15MXR fastener	138
Figure 7.3. Stress accumulated in steel base material after installation procedure and corresponding to pull-out of cartridge fired pin	139
Figure 7.4. Stress and preloading force in cartridge fired pin after installation procedure	140
Figure 7.5. FE analysis results for tension test specimens	140

Figure 7.6. Geometry of steel base plate hole	141
Figure 7.7. Stress obtained over cartridge fired pin hole height (path 1) and perimeter (path 2).....	142
Figure 7.8. Contact pressure on steel base material after installation procedure and corresponding to pull-out of cartridge fired pin	143
Figure 7.9. Analytical vs. experimental results of ENP2-21 L15MXR and X-ENP-21 HVB cartridge fired pin.....	146
Figure 7.10. Comparison of proposed prediction model with experimental results of various types of fasteners, $f_u=400$ MPa.....	146
Figure 7.11. Comparison of proposed prediction model with experimental results of various types of fasteners with smooth shank, $f_u=400$ MPa.....	147
Figure 8.1. Failure mechanisms of X-HVB shear connectors – experimental vs. FE analysis	149
Figure 8.2. Deformation of connector and cartridge fired pins – FE analysis.....	150
Figure 8.3. Cartridge fired pins forces – first row of shear connectors relative to the shear force direction.....	151
Figure 8.4. Axial and shear force in cartridge fired pins – minimal distance between shear connectors.....	152
Figure 8.5. Axial and shear force in cartridge fired pins – group arrangement of shear connectors.....	153
Figure 8.6. Average pins forces relative to shear resistance and slip capacity - minimal distance between shear connectors	154
Figure 8.7. Average pins forces relative to shear resistance and slip capacity - group arrangement of shear connectors	155
Figure 8.8. Concrete pressure corresponding to 90 % of shear resistance	156
Figure 8.9. Concrete pressure corresponding to 90 % of shear resistance – minimal distance of shear connectors	157
Figure 8.10. Concrete pressure corresponding to 90 % of shear resistance – reduced distance between shear connectors	158
Figure 8.11. Shear resistance for one shear connector – installation power level 3.5 and forward orientation of shear connectors	159

Figure 8.12. Steel base material stress – behind pin (left) and in front of pin (right) relative to the shear force direction 160

Figure 8.13. Stress in steel base material for forward orientation of shear connectors and installation power level 3.5..... 161

Figure 8.14. Comparison of shear resistance for FE analysis results and according to prediction model..... 164

List of tables

Table 2.1. Characteristic and design resistance of X-HVB shear connectors in solid slabs [5], [7].....	14
Table 3.1 Headed stud vs. X-HVB shear connector resistance, adapted from [45]	43
Table 4.1. Geometrical properties of push-out specimens.....	53
Table 4.2. Steel beam material properties.....	59
Table 4.3. Shear connector material properties	59
Table 4.4. Quantities of infill concrete admixtures	60
Table 4.5. Concrete material properties at the age of push-out tests - phase 1.....	63
Table 4.6. Concrete material properties at the age of push-out tests - phase 2.....	63
Table 4.7. Concrete material properties at the age of push-out tests - phase 3.....	63
Table 4.8. Results of standard push-out tests - HSF series	69
Table 4.9. Results of standard push-out tests - HSB series	69
Table 4.10. Results of standard push-out tests - HSFg series.....	71
Table 4.11. Results of standard push-out tests - HSFg-2 series.....	71
Table 4.12. Comparison of experimental results with recommendations given in ETA-15/0876 assessment [7] and EN 1994-1-1:2004 [11]	73
Table 4.13. Comparison of experimental results of four push-out test series.....	74
Table 4.14. Shear resistance per one cartridge fired pin.....	74
Table 4.15. Results of hardness measurement with Poldi hammer	81
Table 4.16. Tension test specimens properties	83
Table 4.17. Average values of base plate material properties	83
Table 4.18. Results of shear test specimens (ST) examination.....	87
Table 4.19. Pull-out resistance per cartridge fired pin of ST specimens	88
Table 4.20. Results of tension test specimens - TT	89
Table 5.1. Experimental and FE analysis results of push-out specimens	115
Table 6.1. Analysed parameters of pin installation procedure for tension tests with base material S275 – true stress-strain material model	123
Table 6.2. Analysed parameters of pin installation procedure for tension tests with base material S355 – true stress-strain material model	124

Table 6.3. Analysed parameters for base material S275 and S355 – quad-linear material model	128
Table 6.4. Various installation procedure of cartridge fired pins – sensitivity study of push-out FE models	130
Table 7.1. Comparison of experimental and FE analysis results with prediction model of pull-out resistance of X-ENP-21 HVB cartridge fired pin	145
Table 8.1. Shear resistance for forward orientation of shear connectors – comparison with prediction model for various base material strengths	163
Table 8.2. Shear resistance for forward orientation of shear connectors – comparison with prediction model for various concrete classes	164
Table 8.3. Characteristic shear resistance of X-HVB shear connectors - ETA-15/0876 assessment [7] and prediction model.....	165
Table 8.4. Shear resistance of X-HVB shear connector	166
Table A.2. Infill concrete material properties of phase 1 push-out tests	176
Table A. 3. Infill concrete material properties of phase 2 push-out tests.	176
Table A.4. Infill concrete material properties of phase 3 push-out tests	176
Table A.5. Prefabricated concrete slabs strength at 28 days.....	177
Table A.6. Infill concrete strength of phase 1 at 28 days	177
Table A.7. Infill concrete strength of phase 2 at 28 days	177
Table A.8. Infill concrete strength of phase 3 at 28 days	178
Table A.9. Modulus of elasticity of prefabricated concrete slabs at 28 days	178
Table C.1. Base plate material properties - ST specimens	186
Table C.2. Base plate material properties - TT2-2 specimens.....	186
Table C.3. Base plate material properties - TT3-2 and TT3-3.5 specimens.....	186
Table D.1. Calibration of parameters without preloading of pins in FE analysis – HSF test series	189
Table D.2. Calibration of different connector and washer geometry in FE analysis - HSF test series	190
Table D.3. FE models for different approaches of pins’ preloading - HSB test series	192
Table D.4. Calibration of parameters for preloading of upper part of the pin - HSF and HSB series	193

Table E.1. Influence of different parameters on push-out FE analysis results 195

Notation

Roman upper case letters:

A	cross-section area of round and flat tensile coupon; elongation after fracture defined in material specifications;
A_e	embedded surface of cartridge fired pin, determined according Eq. 7.5 and Eq. 7.6;
A_{net}	net cross-section area of the connected part [28];
A_{nv}	net area subjected to shear [42];
A_{80}	minimum percentage elongation after fracture [14];
C_1	material coefficient that defines the transition point in the strain hardening region [56];
C_2	material coefficient [56];
D	diameter of steel ball used for examination with Poldi hammer;
D_c	concrete compressive damage variable of concrete damage plasticity model [51];
D_t	concrete tensile damage variable of concrete damage plasticity model [51];
E	modulus of elasticity of steel;
E_{cm}	secant modulus of elasticity of concrete [50];
$E_{cm}(t)$	modulus of elasticity of concrete at an age of t days [50];
E_{sh}	strain hardening modulus [56];
$F_{b,Rd}$	design bearing resistance of cartridge fired pins loaded in shear [28];
$F_{b,Rk}$	characteristic bearing resistance of cartridge fired pins loaded in shear [22];
$F_{n,Rd}$	design net-section resistance of cartridge fired pins loaded in shear [28];
$F_{p,Rd}$	design pull-through resistance per fastener loaded in tension [28];

F_{bs}	base stress parameter (455 MPa) [42];
$F_{t,Ed}$	design tensile force per cartridge fired pin for the ultimate limit state [28];
$F_{o,Rd}$	design pull-out resistance per fastener loaded in tension [28];
F_{press}	pressure force developed during installation procedure between cartridge fired pin and steel base material;
F_u	tensile strength [42];
F_{uh}	tensile strength of hardened powder actuated fastener steel [42];
F_{u1}	tensile strength of member in contact with fastener head or washer [42];
$F_{v,Ed}$	design shear force per cartridge fired pin for the ultimate limit state [28];
$F_{v,Rd}$	design shear resistance of cartridge fired pins [28];
$F_{v,Rk}$	characteristic shear resistance of cartridge fired pin [28];
F_{y2}	yield stress of member not in contact with powder actuated fastener head or washer [42];
H_e	hardness of check test piece (examination with Poldi hammer);
H_x	hardness of tested material (examination with Poldi hammer);
$H_{x,1E}$	hardness of tested material for measuring position 1E (examination with Poldi hammer);
K	ratio of the second stress invariant on the tensile meridian to the compressive meridian [54];
L_R	characteristic bearing resistance of cartridge fired pins loaded in shear [22];
L_0	original gauge length of tensile test coupon [48];
N_{con}	number of shear connectors per one push-out test specimen;
N_{Rk}	characteristic tension resistance of powder actuated fastener for connection of profiled sheeting to the steel base material [35];

N_{spc}	number of specimens within test series;
P_{max}	upper force bound during cyclic loading of the push-out specimen;
P_{min}	lower force bound during cyclic loading of the push-out specimen;
P_{nb}	nominal bearing and tilting strength (resistance) per powder actuated fastener [42];
P_{nos}	nominal pull-out strength (resistance) in shear per powder actuated fastener [42];
P_{nov}	nominal pull-over strength of sheet per powder actuated fastener [42];
P_{ntp}	nominal tensile strength (resistance) of powder actuated fasteners [42];
P_{nv}	nominal net-section rupture strength [42];
P_{pull}	pull-out resistance of cartridge fired pin for tension loading according Eq. 7.1, 7.3 and 7.4;
P_{Rd}	design value of the shear resistance of a single connector;
$P_{\text{Rd,t,t}}$	design value of the shear resistance of a single connector used with profiled steel sheeting transverse to the beam and with transverse orientation of shear connectors [7];
$P_{\text{Rd,t,l}}$	design value of the shear resistance of a single connector used with profiled steel sheeting transverse to the beam and longitudinal orientation of shear connectors [7];
$P_{\text{Rd,l}}$	design value of the shear resistance of a single connector used with profiled steel sheeting parallel to the beam [7];
$P_{\text{Rd,red}}$	design value of the shear resistance of a single connector reduced for thicknesses of base material lower than 8.0 mm [7];
P_{Rk}	characteristic value of the shear resistance of a single connector;
$P_{\text{Rk,SLS}}$	force level corresponding to the serviceability limit state, approximately 70 % of ultimate shear force;

P_{ult}	shear resistance of push-out test specimen in experimental and FE analysis or shear resistance of cartridge fired pins loaded in shear, i.e. ultimate shear force;
$P_{pull,anl}$	pull-out resistance of cartridge fired pin for tension loading according to prediction model given with Eq. 7.1;
$P_{pull,exp}$	experimentally obtained pull-out resistance of cartridge fired pin for tension loading;
$P_{pull,fea}$	pull-out resistance of cartridge fired pin for tension loading according to FE analysis;
$P_{ult,anl}$	shear resistance of X-HVB shear connectors obtained through prediction model given in Eq. 8.1;
$P_{ult,exp}$	experimentally obtained shear resistance of X-HVB shear connectors;
$P_{ult,fea}$	shear resistance of X-HVB shear connectors obtained through FE analysis;
$P_{ult,pin}$	shear resistance per one cartridge fired pin for shear test specimens; pull-out resistance per one cartridge fired pin for tension test specimens;
$P_{\delta 3}$	shear force obtained for 3.0 mm of relative displacement for shear test specimens of cartridge fired pins;
$P_{\delta 3,pin}$	shear force per one cartridge fired pin obtained for 3.0 mm of relative displacement for shear test specimens;
R_e	conventional yield strength of a skin-passes product [14];
R_m	tensile strength [48];
R_n	nominal strength resistance of powder actuated fastener [42];
R_u	required strength (resistance) of powder actuated fastener for LRFD [42];
V_{Rk}	characteristic shear resistance of powder actuated fastener for connection of profiled sheeting to the steel base material [35];
V_x	coefficient of variation of a property X [47];

X_k characteristic value of a material property [47];

Roman lower case letters:

b_{sc} width of X-HVB shear connector, according to ETA-15/0876 assessment [7];

d nominal diameter of cartridge fired pin shank [28] or fastener diameter measured at the near side of embedment [42]; diameter of round tensile coupon;

d_{ac} average embedment diameter computed as average of installed fastener diameters measured at near side and far side of embedment material or d_s for PAF installed such that entire point is located behind far side of embedment material [42];

d_e diameter of the impress on the check test piece (examination with Poldi hammer);

d_h diameter of hole [42];

d_{max} maximum hole (pin) diameter, adopted as 4.5 mm;

d_{min} minimum hole (pin) diameter adopted as 3.5 mm;

d_s nominal shank diameter [42];

d_w diameter of the washer of cartridge fired pin [28];

d_w' actual diameter of fastener head or washer in contact with retained substrate [42];

d_x diameter of the impress on the tested material (examination with Poldi hammer);

e_{net} clear distance between end of material and edge of fastener hole [42];

e_1 distance from the centre of the fastener to the adjacent end of the connector;

h_c	thickness of concrete above the main flat surface of the top of the ribs of the sheeting [11];
h_e	embedded depth of cartridge fired pin;
h_{NVS}	fastener stand-off after installation, i.e. distance from the fastener head and cover material in the connection;
h_p	overall depth of the profiled steel sheeting excluding embossments;
h_{sc}	overall nominal height of a shear connector;
h_{wc}	coped flat web depth [42];
b_0	mean width of a concrete rib or minimum width of re-entrant profiled sheeting;
$f_{c,cube}$	concrete compressive cube strength;
$f_{c,cyl}$	concrete compressive cylinder strength;
$f_{ct,sp}$	concrete splitting tensile strength;
$f_{ctm}(t)$	axial tensile strength at an age of t days [50];
f_{ctm}	mean value of axial tensile strength of concrete [50];
f_{cm}	mean value of concrete cylinder compressive strength [50];
$f_{cm}(t)$	mean concrete compressive strength at an age of t days [50];
f_{ck}	characteristic compressive cylinder strength of concrete at 28 days [50];
f_{cuE}	compressive stress in the concrete at point “E” of sinusoidal descending part of stress-strain curve (lower point) [51];
f_{cuF}	compressive stress in the concrete at point “F” at final residual strength of concrete, i.e. final residual strength of concrete [51];
f_{cu1}, f_{cuD}	compressive stress in the concrete at point “D” of sinusoidal descending part of stress-strain curve (upper point), equal to ε_{cu1} [51];
$f_{C1\varepsilon u}$	stress corresponding to transition point in the strain hardening region [56];

f_u	ultimate strength of steel;
$f_{u,mean}$	mean value of tensile strength of four tensile test coupons;
$f_{u,relation}$	tensile strength determined based on the relation (examination with Poldi hammer);
$f_{u,tensile\ test}$	tensile strength determined according to the results of tensile test coupons;
f_y	yield strength of steel;
f_{02}	0.2 % proof stress of non-linear material;
k_n	characteristic fractile factor [47];
$k_{t,t}$	reduction factor for resistance of a single connector used with profiled steel sheeting transverse to the beam and transverse orientation of shear connectors [7];
$k_{t,l}$	reduction factor for resistance of a single connector used with profiled steel sheeting transverse to the beam and longitudinal orientation of shear connectors [7];
k_{init}	initial stiffness of a single shear connector;
k_1	reduction factor for resistance of a single connector used with profiled steel sheeting parallel to the beam [7];
k_{SLS}	stiffness of a single shear connector for loading level corresponding to the serviceability limit state;
k	hardness coefficient (examination with Poldi hammer); coefficient which depends of shear connector orientation relative to the shear force direction and should be adopted as 8.5 for forward orientation of shear connectors and 6.8 when shear connector orientation is not prescribed; factor depending on fastener stand-off after installation ($k = 2.23$ for range of appropriate installation) [22];
k_{u3}	elastic stiffness of lateral restraint for push-out test specimens;

n	number of fasteners on critical cross section [42]; number of cartridge fired pins [22];
n_b	number of fasteners along failure path being analysed [42];
n_r	number of shear connectors in one rib;
s	coefficient which depends on the type of cement used in concrete mixtures [50];
t	thickness of steel plate [28], or base steel thickness of section (Eq. 2.22); the thickness of coped web (Eq. 2.23) [42]; age of concrete in days [50]; thickness of shear connector;
t_I, t_1	thickness of the cover material in the connection [35], or thickness of member in contact with powder actuated fastener head or washer [42];
t_{II}, t_2	thickness of the base material [35], or thickness of member not in contact with powder actuated fastener head or washer [42];
$t_{II,act}$	actual base material thickness [7];

Greek upper case letters:

Φ	safety factor for factored resistance of powder actuated fastener for Load and Resistance Factor Design and Limit State Design [42];
Ω	safety factor for factored resistance of powder actuated fastener for Allowable Strength Design [42];

Greek lower case letters:

α	coefficient which value depends on the age of the concrete t [50]; reduction factor of sinusoidal descending part of the concrete compressive stress-strain curve [51];
α_a, α_d	ascending and descending parameters for concrete compressive stress-strain curve according to [57];

α_{iD}	tangent factor at point “D” (upper point) of sinusoidal descending part of concrete compressive stress-strain curve [51];
α_{iE}	tangent factor at point “E” (lower point) of sinusoidal descending part of concrete compressive stress-strain curve [51];
α_w, α_b	coefficient differentiating type of powder actuated fastener [42];
β_{cc}	coefficient which depends on the age of the concrete t (age of concrete in days [50]);
γ_v	partial factor for design shear resistance of a shear connector [11];
γ_M, γ_{M2}	partial safety factor for joints [28];
δ_{total}	total longitudinal slip of shear connection;
δ_{init}	initial longitudinal slip accumulated during cyclic loading;
δ_{ui}	relative displacement of sensor i corresponding to ultimate shear force obtained for shear test specimens of cartridge fired pins;
δ_{ult}	total displacement measured from four sensors corresponding to ultimate shear force obtained for shear test specimens of cartridge fired pins;
δ_{uk}	characteristic value of slip capacity obtained for 90% of ultimate shear force on descending branch of load-slip curve;
$\delta_{uk,FEA}$	characteristic value of slip capacity obtained from FE analysis;
$\delta_{uk,test}$	characteristic value of slip capacity obtained from experimental investigation;
ε	strain (in general, Eq. 5.2), flow potential eccentricity in concrete damage plasticity model [51];
ε_c	uniaxial concrete compressive strain [50];
ε_{cuD}	compressive strain in the concrete at point “D” of sinusoidal descending part of stress-strain curve (upper point), equal to ε_{cu1} [51];

ε_{cuE}	compressive strain in the concrete at point “E” of sinusoidal descending part of stress-strain curve (lower point) [51];
ε_{cuF}	compressive strain in the concrete at point “F” at final residual strength of concrete [51];
ε_{cul}	nominal ultimate strain, adopted as $3.50 \cdot 10^{-3}$ according to [50];
ε_{c1}	strain at peak stress, adopted as $2.05 \cdot 10^{-3}$ according to [50];
ε_{sh}	strain hardening strain [56];
ε_{true}	true strain (in general, Eq. 5.2);
ε_{tu}	cracking strain [54];
ε_y	yield strain [56];
ε_u	ultimate strain [56];
θ_s	shear stress ratio;
μ	relative coordinate between points D-E of sinusoidal descending part of concrete compressive stress-strain curve [51], global friction coefficient prescribed in FE models;
μ_e	friction coefficient of embedded part of pin which should be adopted as 0.25 for installation power level 2.0 and 0.3 for installation power level 3.5 for tension loading of cartridge fired pins;
σ	stress (in general, Eq. 5.1);
σ_{b0}	biaxial compressive strength in concrete damage plasticity model [54];
σ_c	concrete uniaxial compressive stress [50];
σ_{c0}	uniaxial compressive strength in concrete damage plasticity model [54];
σ_{true}	true stress (in general, Eq. 5.1);
ψ	dilation angle in concrete damage plasticity model [54];

Abbreviations:

ASD	Allowable Strength Design;
ASTM	American Society for Testing and Materials;
AISI	American Iron and Steel Institute;
DAMAGEC	concrete compressive damage variable [54];
EAD	European Assessment Document;
ETA	European Technical Assessment;
FE	finite element;
LRFD	Load and Resistance Factor Design;
LSD	Limit State Design;
PATMI	Powder Actuated Tool Manufacturers Institute;
PAF	powder actuated fastener;
SLS	serviceability limit state;

Chapter 1. Introduction

1.1. Background

Construction industry is constantly facing new demands towards fast construction and the smallest possible quantity of work at construction site. In the recent decades, development of different types of prefabricated concrete slabs has taken an important place in the field of composite constructions. Prefabrication of concrete slabs reduces construction time and represents a solution which is widely used for various types of composite steel-concrete buildings.

Composite action between steel beams and prefabricated concrete slabs is often achieved with shear connectors positioning in envisaged openings of slabs and therefore their discontinuity in comparison to the uniformly distributed shear connectors along the beam span. Development of new types of shear connectors represents alternative solution to the traditionally used welded headed studs and often reduces the construction time and overall construction cost. Application of various types of shear connectors results in significant differences in required equipment and amount of work at the construction site, preparation of base material for shear connectors installation and required temperature and weather conditions during installation procedure. Main properties, such as: shear resistance, stiffness and ductility, are the most important characteristics of shear connectors. Therefore, all these features will influence the determination of shear connector application for specific construction.

1.2. The advantage of shear connectors fastened with cartridge fired pins

Mechanically fastened shear connectors represent a new group of connectors for composite steel-concrete construction which are fastened to the steel base material with cartridge fired pins. They represent a unique system comprised of two elements, shear connector and mechanical fasteners. Therefore, their overall behaviour is, among other factors, also related to the behaviour and failure mechanisms of fasteners. X-HVB shear connectors are well-known representative of this group of shear connectors.

X-HVB shear connectors are fastened to the steel base material with two X-ENP-21 HVB cartridge fired pins. Installation of these fasteners (pins) is performed with special powder actuated fastening tool. They are often defined in literature as cartridge

fired pins or powder actuated fasteners. Development of these alternative shear connectors for composite steel-concrete construction, was conditioned with development of fasteners for their connection to the base material and first national approvals for their application in Europe, were granted in 1970s.

Shear connectors fastened with cartridge fired pins are alternative for the headed studs and bolted shear connectors for steel-concrete composite construction. Behaviour of X-HVB shear connectors in composite shear connections is expected to be different from the behaviour of headed studs as the most widely used shear connectors, which behaviour is described in various literature, research information and design codes. Experimental and numerical analysis of mechanically fastened shear connectors can lead towards wider application in composite construction and to extension of currently available recommendations for their application, which nowadays can be obtained only by manufacturer.

The main characteristic of X-HVB shear connectors is significantly lower installation time in comparison to the headed studs and bolted shear connectors. Installation of cartridge fired pins is performed with relatively simple hand-held installation tool which does not require electricity source at construction site. The installation procedure itself is a simple procedure, without welding or any other technological procedure. Also, the quality of installation procedure is not affected with special atmospheric or temperature conditions at the construction site, resulting in less work interruptions. Moreover, installation of this type of shear connector does not require additional preparation of base material or predrilling of holes in the base material. Base material coatings (zinc coatings or paintings) for corrosion protection do not affect the installation quality and should not be removed from the base material before connector installation. Also, the installation quality can be simply performed, through visual checking of the fastener stand-off over the surface of the fastened material. For fasteners that do not allow an accurate visual check, the use of stand-off template is recommended.

Shear resistance of connectors fastened with cartridge fired pins in solid concrete slabs is determined by resistance and failure mechanisms of cartridge fired pins which are used for connection with the base material. Overall resistance and deformation capacity is the result of local deformation of connector fastening leg around cartridge fired pins, bending of fasteners and local deformation of concrete in the contact zone of

the connector. Shear resistance of X-HVB shear connectors in solid concrete slabs is significantly lower in comparison to the welded headed studs and bolted shear connectors. Shear resistance of this type of shear connector in composite slabs with profiled sheeting is reduced only for very narrow profiled sheeting ribs. For specific types of profiled sheeting, shear resistance is not reduced in comparison to the solid slabs. Moreover, their installation in composite slabs with profiled steel sheeting is simple and fast, not requiring any additional work or predrilling of the holes. Therefore, continuous profiled sheeting can be used on the construction site, which reduces the profile cross-section and amount of work in comparison to the single span profiled sheeting.

Shear connectors fastened with cartridge fired pins may be used for construction of new buildings and for reconstruction or strengthening of floor structures in the old buildings. Moreover, the main prerequisite of the cost-efficient use of this type of shear connector is achieved considering fast and simply installation procedure. Therefore, they can be competitive to the traditionally used welded headed studs, particularly for composite floor structures with profiled sheeting. Current design recommendations for composite steel-concrete structures do not define prediction models for shear resistance of mechanically fastened shear connectors. In addition, main failure mechanisms of shear connectors fastened with cartridge fired pins are related to the failure of fasteners. Verification of the shear connector and fastener resistance thus has to be provided by tests. Further experimental and numerical analysis of this type of shear connector and cartridge fired pins should lead to the extension of currently small basis of experimental results and should improve understanding of their overall behaviour and their wider usage.

1.3. Goal of the research

The aim of the research presented in this thesis is the investigation of X-HVB shear connectors behaviour and encouragement of their application in prefabricated concrete slabs. This investigation should improve understanding of X-HVB shear connectors behaviour which is currently based on their application in solid or composite concrete slabs with continuous arrangement of shear connectors over the beam span. Characterization of behaviour and failure mechanisms and determination of prediction

models for shear resistance of this type of shear connectors in prefabricated concrete slabs with grouped shear connectors are the main goals of this research.

1.4. Objectives of the research

The analysis of the previous experimental investigations of X-HVB shear connectors and fasteners which are used for their connection to the steel base material, needs to be performed as a first step and is followed with small feasibility study of their application on wide range of floor structures with composite concrete slabs. Further, experimental investigation of X-HVB shear connectors is performed through standard push-out tests. The influence of group arrangement of shear connectors in prefabricated concrete slabs on shear resistance, stiffness and slip capacity is analysed based on the results of experimental investigation. Experimental investigation of cartridge fired pins through tension and shear tests is necessary for understanding of overall behaviour and failure mechanisms of the new type of shear connectors which are in the scope of this thesis. Experimental investigation is followed with development of numerical FE models which are calibrated with results of experimental investigation and further used for the parametric study. Numerical models of X-HVB shear connectors are used to recognize main parameters for shear connection behaviour, definition of main failure mechanisms and quantification of main parameters for shear resistance of this type of shear connector.

1.5. Methodology of the research

In the scope of this thesis, analytical, experimental and numerical methods are performed through:

- Investigation and analysis of the previous experimental investigations of shear connectors with cartridge fired pins and new innovative shear connectors which are also connected to the steel base material with cartridge fired pins. Also, investigation included previous examination of cartridge fired pins and design recommendations which can be find in different design codes.
- Experimental investigation of X-HVB shear connectors through standard push-out tests and experimental investigation of cartridge fired pins through tension and shear tests is performed. Moreover, standard tests to obtain properties of

materials used in the tests (steel base material, concrete and shear connectors) are performed.

- Numerical 3D finite element models of shear connectors push-out tests and tension and shear tests of cartridge fired pins with damage material models are built and calibrated based on the results of experimental investigation.
- Developed and calibrated numerical FE models of shear connectors and cartridge fired pins are used for parametric study.
- Prediction models for shear resistance of X-HVB shear connectors and pull-out resistance of cartridge fired pins are proposed based on the results of experimental and numerical investigation.

1.6. Outline of the thesis

The thesis is organized in following chapters:

Chapter 2 gives an overview of the most important characteristics of X-HVB shear connectors, their development, previous examination and recommendations for application in steel-concrete composite structures obtained by manufacturer. Also, the literature review chapter gives information about other types of mechanically fastened shear connectors, which can be used in composite construction. The second part of this chapter presents the most important characteristics of cartridge fired pins and their design recommendations which can be found in European and North American design codes.

Chapter 3 presents a small feasibility study which deals with application of X-HVB shear connectors in wide range of floor structures with composite concrete slabs. Comparison of composite beams design resistance with two types of shear connectors, headed studs and X-HVB shear connectors is presented.

Chapter 4 presents program and results of experimental investigation of standard push-out tests of X-HVB 110 shear connector in prefabricated concrete slabs and shear and tension tests of X-ENP-21 HVB cartridge fired pins. Also, results of experimental investigation of material properties of steel profile, shear connector and concrete slab are presented.

Chapter 5 deals with FE analysis of push-out models with X-HVB shear connectors and models for shear and tension tests of X-ENP-21 HVB cartridge fired pins. Results of experimental investigation are used for calibration of FE models. Material models used

in FE analysis are developed based on the results gained from the experimental investigation. Comparison of experimental results with results of FE analysis is presented in this chapter, considering obtained resistances, deformation and failure mechanisms.

Chapter 6 presents a calibration procedure of FE models of cartridge fired pins loaded in tension and sensitivity study of push-out FE models. Sensitivity study is performed through variation of the most important parameters which are used to simulate installation procedure of cartridge fired pins, such as: predefined field magnitude and expansion material properties of cartridge fired pins. Further, parametric study performed on push-out FE models is presented. Influence of concrete and steel base material properties on shear resistance of X-HVB 110 shear connector is presented.

Chapter 7 presents an analysis of cartridge fired pins pull-out resistance through obtained experimental and FE analysis results. Also, definition of prediction model of cartridge fired pins pull-out resistance is proposed herein.

Chapter 8 presents an analysis of X-HVB shear connectors behaviour in prefabricated concrete slabs based on FE models which are developed and calibrated for four push-out test series. The most important parameters for shear connector behaviour are recognized and presented. Prediction model for shear resistance of X-HVB shear connectors is proposed and presented.

Chapter 9 gives an overview of the most important conclusions which are drawn from experimental and FE analysis presented in this thesis. Also, propositions for future investigations in this field are given.

Chapter 2. Literature review

2.1. Introduction

Shear connectors fastened with cartridge fired pins represent a new type of shear connectors which are more or less competitive to the traditional welded headed studs or bolted shear connectors. Their overall behaviour is directly related to the behaviour and failure mechanisms of fasteners. The X-HVB shear connectors are well-known representative of this group of shear connectors and they are used for the experimental investigation in prefabricated concrete slabs, which is in the scope of this thesis. Currently available results of experimental investigation of X-HVB shear connectors include studies in solid and composite concrete slabs [1] and represent the basis and motivation for the investigation presented in this thesis. Therefore, this chapter gives an overview of the development process and the main outcomes from previous research of X-HVB shear connectors. Also, alternative types of shear connectors fastened with cartridge fired pins are briefly presented. Afterwards, review of the previous investigations of cartridge fired pins is given. Certain design rules for cartridge fired pins, which are given in different design codes, are also presented in this chapter.

2.2. Shear connectors in prefabricated concrete slabs

Prefabrication of concrete slabs is widely applicable in the composite construction of building and bridges. It is estimated that 50 % of already constructed steel framed buildings are built with prefabricated concrete slabs [2]. In the recent decades, several investigations of group arrangement of shear connectors for prefabricated composite construction have been performed. Experimental and numerical investigation of group arrangement of shear connectors in prefabricated concrete slabs has been performed in recent period at Faculty of Civil Engineering, University of Belgrade. Investigation of groups of welded headed studs positioned in envisaged openings of prefabricated concrete slabs was performed by Spremić [3]. Investigation included different arrangement of shear connectors in a group and different spacing between connectors. Extensive experimental investigation included six different specimens layout with longitudinal and transversal spacing of adjacent shear connectors which are smaller than minimal recommended. The findings of the study were that the reduction of the distance

between headed studs in force direction can be allowed. Experimental results confirmed that there is no need for the reduction of studs group shear resistance even in the cases when the distance between headed studs is smaller than minimal recommended. The second study, performed by Pavlović [4] throughout standard push-out tests and numerical analysis, in detail investigated behaviour of bolted shear connectors in prefabricated concrete slabs considering different methods of bolts installation, with two different bolts diameter. Connections with two nuts, one of which is embedded in the concrete, were proposed as the best solution. Investigation of X-HVB shear connectors in prefabricated concrete slabs which is presented in this thesis follows the progressing trends of contemporary structural engineering.

2.3. Mechanically fastened shear connectors

2.3.1. X-HVB shear connectors in solid concrete slabs

The X-HVB shear connector is L shaped cold-formed metal connector made from steel sheets with 2.0 or 2.5 mm thickness, comprising the fastening leg fixed to the steel base material with two X-ENP-21 HVB cartridge fired pins, as shown in Figure 2.1, and anchorage leg and head casted into the concrete slab. Therefore, this type of shear connector is often determined in literature as nailed shear connector or mechanically fastened shear connector.

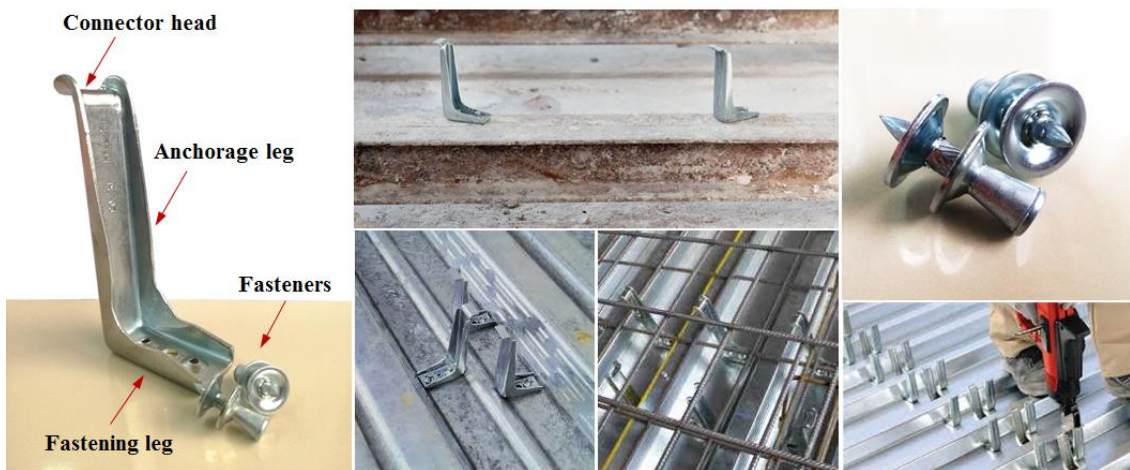


Figure 2.1. X-HVB shear connectors and X-ENP-21 HVB cartridge fired pins

Wide range of X-HVB shear connectors with various heights are currently applicable for composite steel-concrete construction. Nowadays, those are X-HVB 40, 50, 80, 95, 110, 125, 140 shear connectors. The X-HVB shear connectors can be used for

composite steel-concrete constructions with normal-weight concrete classes C20/25 - C50/60 and with light-weight concrete classes LC20/22 - LC50/55 and raw density greater than 1750 kg/m^3 [5], [6], [7]. These connectors may be used for connection to the structural steel base material S235, S275 and S355 in qualities JR, JO, J2, K2 according to EN 10025-2 [8] and minimal base material thickness for composite steel-concrete beams of 8.0 mm [5],[6], [7].

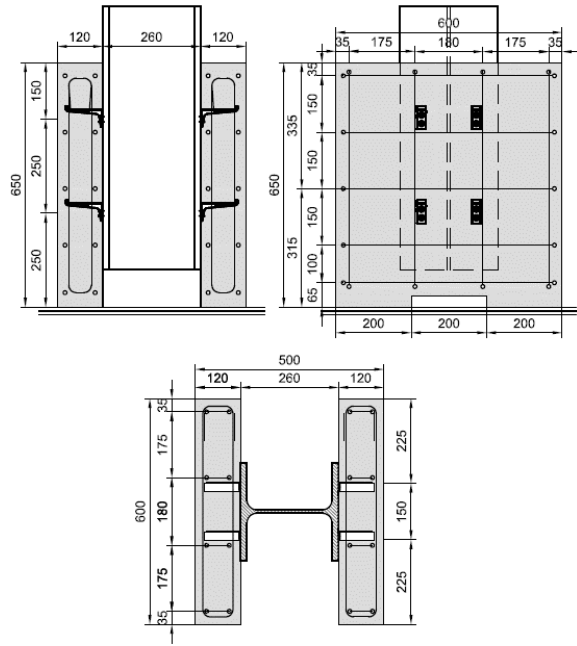
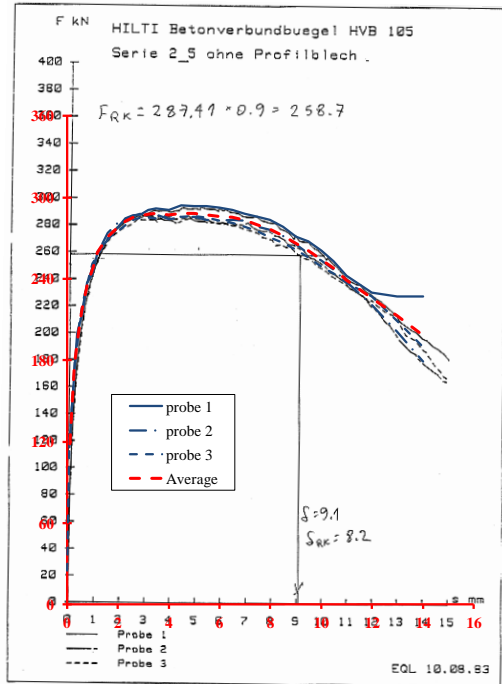
This type of shear connector is beneficial for renovation of old buildings, where applicability of welded studs is doubtful due to unknown weldability of old steel. Welding of headed studs on old unalloyed carbon steel might be brittle and not effective. In comparison to this behaviour of headed studs, X-HVB shear connectors with cartridge fired pins can be used for connection to the unalloyed carbon steel with minimum yield strength of 170 N/mm^2 [7]. Beside the main usage of this type of shear connectors, for composite steel-concrete floor beams, they are often used for lateral bracing of steel beams and end anchorage of profiled steel sheeting in composite floor construction [5]–[7]. Firstly, these shear connectors had a general designation HVB shear connectors. Current designation of this type of shear connector, according to X-HVB system solutions [5], European assessment document EAD 200033-00-0602 [6] and ETA-15/0876 assessment [7] is X-HVB shear connector. This, X-HVB designation has been used for the last twenty years. Accordingly, HVB designation is used in this chapter for presentation of main outcomes of previous experimental investigation, and X-HVB designation for current design recommendations.

Development and the wider usage of this type of shear connector was directly related to the development of cartridge fired pins. Usage of this type of fasteners is widely introduced in civil engineering and other ranges of industry for more than seventy years. Development of mechanically fastened shear connectors was in the program of the Hilti Company since 1977. Since then, several research programs were performed in order to obtain data for system evaluation and were followed with gathering of international technical assessments and approvals. The main experimental programs of push-out tests and beam tests were conducted during the 1980s, and two additional experimental programs were performed during the 1990s. However, there is still small amount of easily accessible information about mechanically fastened shear connectors in scientific journals and another professional literature. The results of experimental investigations are

mostly presented in technical reports of manufacturers which are considered proprietary. Also, non-proprietary technical reports are not easily available. Very few research results of mechanically fastened shear connectors and cartridge fired pins are available in scientific journals and conference proceedings. An overview of several published experimental investigations and overview of results published in technical reports which are obtained by kindness of Hilti Company is given below.

The first push-out test series of HVB shear connectors were conducted in 1983 by Hilti Company in order to obtain data for technical assessment approvals. Examination included 48 push-out test specimens with HVB 80 and HVB 105 shear connectors which were firstly developed. Push-out specimens comprised specimens with solid and composite concrete slabs with various types of profiled sheeting. Parameters which were analysed during examination are type of profiled sheeting, spacing of connectors, connectors position relative to the shear force direction, concrete strength and loading cycles. In addition to these experimental investigations, a numerous push-out tests of HVB 80 and HVB 105 shear connectors were performed in France (1984), Italy (1985) and United States (1986), analysing shear resistance and slip capacity and comparing the obtained results with mostly used headed stud shear connectors [9], [10].

The results of the first push-out tests series indicated that higher HVB shear connectors should be developed. Therefore, the second phase of push-out test series was carried out during 1987 - 1988 with HVB 100, HVB 110, HVB 125 and HVB 140 shear connectors by Hilti Company in Schaan, Liechtenstein. Also, additional push-out specimens were examined by ICOM (Institut de statique et structures – Construction métallique) in Lausanne, Switzerland during 1993 - 1995 in order to obtain data for technical assessments and approvals [9], [10]. Highlights and outcomes of these experimental investigations will be given here, comparing the most important tests series and analysed parameters. Firstly, the results of push-out tests with solid slabs will be given, followed with presentation of the main results drawn from examination of push-out tests with profiled sheeting. Finally, the results of composite beam tests with HVB shear connectors will be presented. Overview of the previous research is followed with the most important current design recommendations given in X-HVB system solutions [5] and ETA-15/0876 assessment [7].



a) HVB 105 results, adapted from [1]

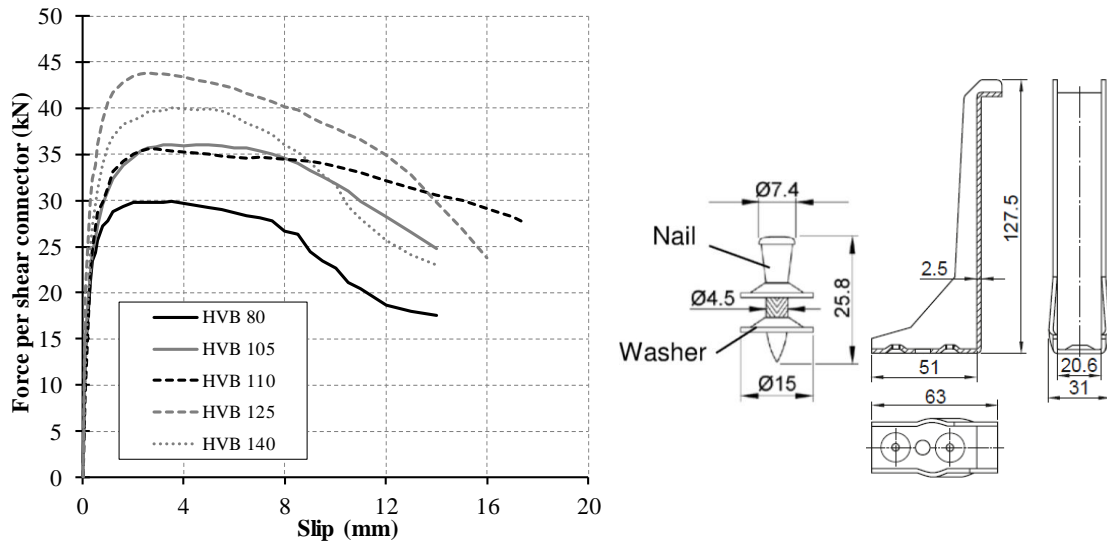
b) standard push-out test

Figure 2.2. Shear resistance of HVB 105 shear connector in solid concrete slabs

Results of initial push-out tests presented by Hilti Company are given in form of force-slip curves of individual specimens for different experimental series, as shown in Figure 2.2a [1]. Test set-up given in Figure 2.2b was in compliance with former recommendations for push-out tests given in EN 1994-1-1:2004 [11]. The results of individual test series are used to plot average force-slip curves, as given in Figure 2.2a in order to compare main parameters of various test series.

Comparison of derived average force-slip curves from the results of individual push-out test series given in Technical report XMA-17A/95 [1] for various types of HVB shear connectors in solid slabs, is presented in Figure 2.3a. Geometry of current X-HVB 125 shear connector is presented in Figure 2.3b. The number in the connectors designation defines the height of the connector in millimetres. Variation of shear connectors heights resulted in various shear resistances. Moreover, relatively similar behaviour regarding initial stiffness and characteristic value of slip capacity was achieved, clearly indicating necessity for development of shear connectors with various heights in order to take into account various concrete slabs heights. Additionally, ductile behaviour of all examined shear connectors was observed. According to EN 1994-1-1:2004 [11], shear connectors are ductile when obtain sufficient deformation capacity to justify the assumption of ideal

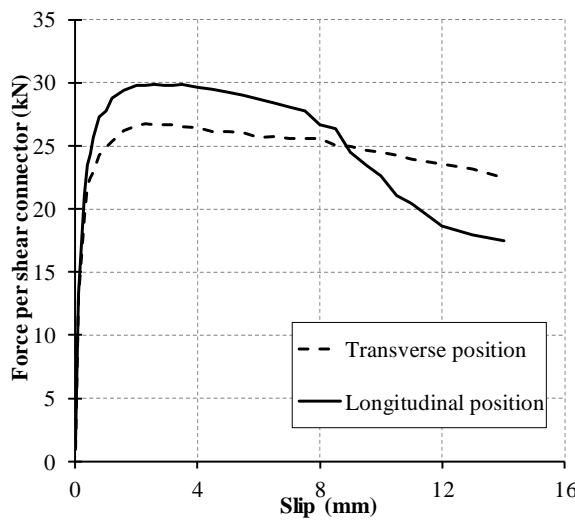
plastic behaviour of shear connection. If characteristic value of slip capacity is at least 6.0 mm, shear connector may be taken as ductile [11].



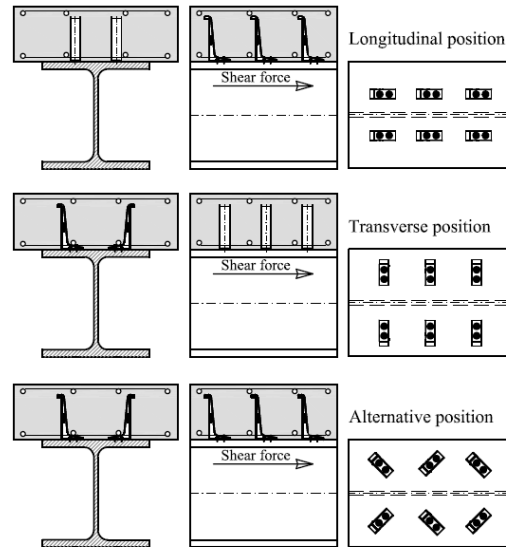
a) shear resistance in solid concrete slabs, adapted from [1]

b) X-HVB 125 shear connector [7]

Figure 2.3. HVB shear connectors – geometry and shear resistance



a) average force-slip curves for HVB 80, adapted from [1]

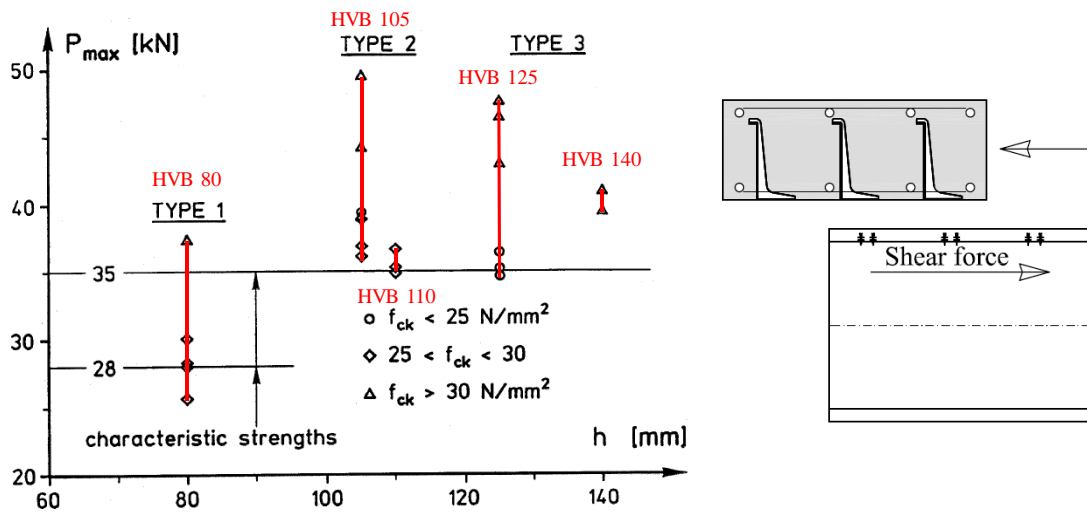


b) position of shear connectors

Figure 2.4. Influence of connectors orientation on shear resistance in solid concrete slabs

Initial experimental investigations of HVB shear connectors included three orientations of shear connectors relative to the shear force direction which can be used depending on the dimension of the steel beam flange, required number of shear

connectors and available space for their positioning, as shown in Figure 2.4b. Influence of the shear connectors position relative to the direction of shear force, longitudinal or transverse, is presented in Figure 2.4a, for HVB 80 shear connector in solid concrete slabs. Transverse position of shear connectors resulted in approximately 10 % lower shear resistance considering average force-slip curves given in Figure 2.4a.



a) shear resistance in solid slab, adapted from [10] b) failure mechanism
Figure 2.5. Results of push-out experiments on HVB shear connectors in solid concrete slabs

Figure 2.5a summarizes the results of push-out tests with solid slabs for various heights of shear connectors which are distinguished in three groups. Normal weight concrete with nominal 28 day concrete cube strength from 16 N/mm² to 60 N/mm² was used in these push-out tests and steel beams with steel grade from S235 to S355. Obtained failure mechanism in all push-out tests with solid slabs was failure of fasteners which are used for connection to the steel base material, as presented in Figure 2.5b. Connector failure or failure of the concrete was not observed. At loading levels which correspond to the serviceability limit state, lower slip was observed in comparison to the welded headed studs [9], [10]. Longitudinal position of shear connectors relative to the shear force direction was used for all series which results are given in Figure 2.5a. For three analysed connector groups, relatively large standard deviation of obtained results disabled the possibility to distinguish the influence of individual parameters on shear resistance [10]. Therefore, it was adopted that characteristic shear resistance of connector type 1 (HVB 80) is 28.0 kN and of connector type 2 and 3 (HVB 105, HVB 110, HVB 125 and HVB

140) is 35.0 kN, as shown in Figure 2.5a. This recommendation was prescribed as characteristic resistance in the first Technical reports [9], [10]. Also, it was suggested to calculate design resistance by dividing the characteristic shear resistance with partial safety factor of $\gamma_v = 1.25$, according to the former draft version of Eurocode 4.

Table 2.1. Characteristic and design resistance of X-HVB shear connectors in solid slabs [5], [7]

Designation	Characteristic resistance	Design resistance
	P_{Rk} (kN)	P_{Rd} (kN)
X-HVB 40	29.0	23.0
X-HVB 50	29.0	23.0
X-HVB 80	32.5	26.0
X-HVB 95	35.0	28.0
X-HVB 110	35.0	28.0
X-HVB 125	37.5	30.0
X-HVB 140	37.5	30.0

Nowadays, X-HVB shear connectors are the main representative of mechanically fastened shear connectors which are granted with “*General Construction Supervisory Authority Approval*” delivered by German approval and assessment body DIBt (*Deutsches Institut für Bautechnik*) [12]. Design resistance of shear connectors and implementation requirements are defined through previous versions of Technical approvals for application in Germany [13] and currently valid ETA assessment, ETA-15/0876 [7] which covers implementation of X-HVB shear connectors in composite structures for all European countries. This document incorporated new requirements for implementation of shear connectors in profiled sheeting and revised values of characteristic and design resistance for wide range of shear connectors heights, which are given in Table 2.1. X-HVB shear connectors are produced from steel DC04, according to EN 10130:2006 [14], through procedure of cold-forming with zinc plating of minimum 3.0 μm . According to ETA-15/0876 assessment [7], installation of X-HVB shear connectors should be performed with DX 76 HVB or DX 76 PTR HVB powder-actuated fastening tool, which performances can be found in operating instructions document [15].

In previous edition of Technical approval [13] characteristic resistance of shear connectors in solid concrete slabs was defined in function of concrete class. For example, characteristic resistance of shear connector X-HVB 125 was defined as 33.0 kN for

concrete C20/25, 38.0 kN for concrete C25/30 and 40.0 kN for higher concrete classes. Current ETA assessment, ETA-15/0876 [7], defines characteristic shear resistance of this shear connector of 37.5 kN for all concrete classes in the range of application, C20/25 - C50/60. Moreover, according to this assessment, X-HVB shear connectors are determined as ductile connectors according to requirements given in EN 1994-1-1:2004 [11] and therefore, should be used for plastic analysis of design moment resistance of composite cross-sections. The partial safety factor for shear connection $\gamma_v = 1.25$ is used for calculation of design resistance, according to recommendations given in EN 1994-1-1:2004 [11].

2.3.2. X-HVB shear connectors in composite concrete slabs

Mechanically fastened shear connectors can be used also in composite concrete slabs with profiled steel sheeting. Experimental investigation of push-out test series during the 1980s and 1990s included wide range of different profiled steel sheeting. Also, influence of concrete strength, spacing between connectors and number of connectors per profiled sheeting rib were analysed parameters.

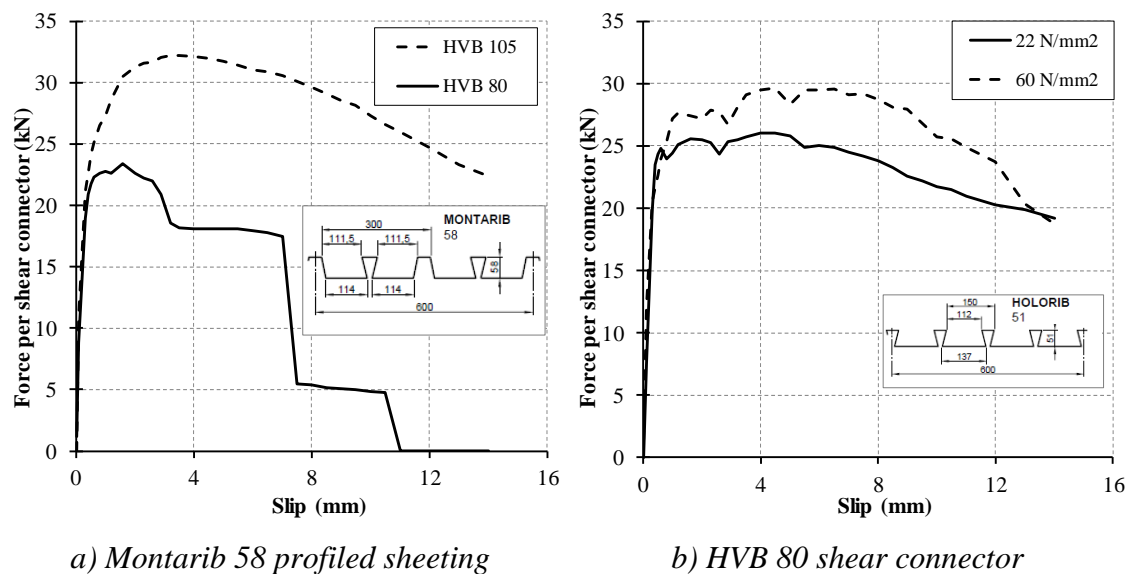


Figure 2.6. Influence of connector height and concrete strength on shear resistance in composite concrete slabs, adapted from [1]

Different behaviour and failure mechanisms were obtained for two shear connectors with heights of 80.0 mm and 105.0 mm in composite concrete slab with 58.0 mm height of profiled sheeting, as shown in Figure 2.6a. Lowering of shear resistance of approximately 10 % was obtained for both shear connectors in comparison to the same

resistance in solid concrete slabs. Also, brittle behaviour was noticed for HVB 80 shear connector in profiled sheeting with 58.0 mm height. However, significant increase in concrete strength did not influence the proportional increase in shear resistance of HVB 105 shear connector, as shown in Figure 2.6b.

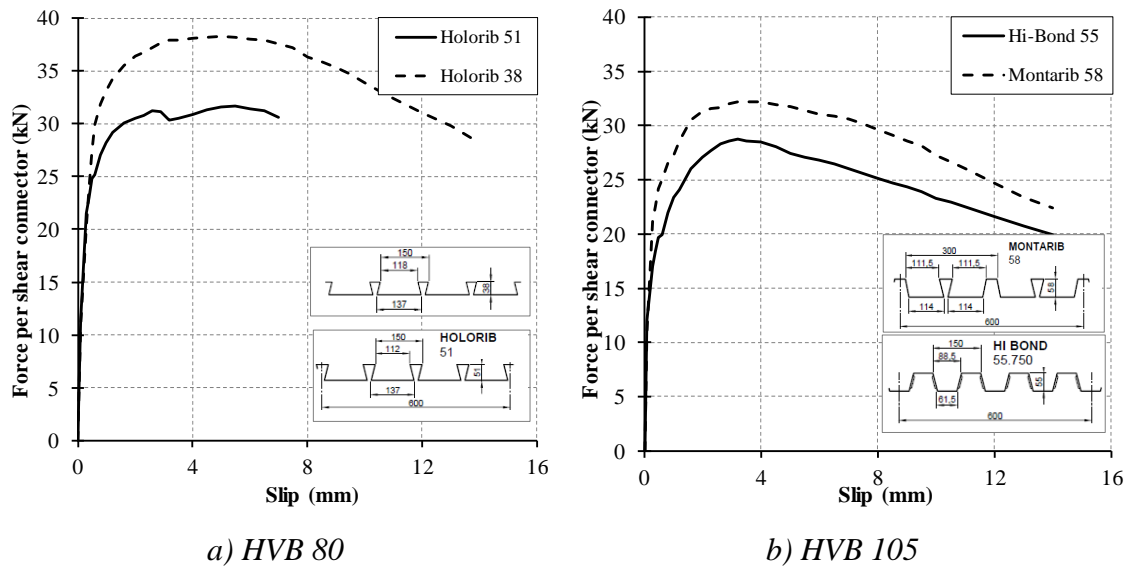


Figure 2.7. Influence of profiled sheeting geometry on shear resistance, adapted from [1]

The influence of profiled sheeting geometry on behaviour of HVB shear connectors was examined with various types of profiled sheeting. Main outcomes are given in Figure 2.7, comparing the influence of height and geometry of trapezoidal and re-entrant sheeting. Increase of height of re-entrant profiled sheeting for 13.0 mm resulted in approximately 20 % lower shear resistance and more brittle behaviour, as shown in Figure 2.7a. Profiled sheeting with approximately same height but with different geometry also had an influence on obtained shear resistance, without significant influence on slip capacity, as shown in Figure 2.7b. Two representatives of trapezoidal and re-entrant profiled sheeting were used for this comparison.

Further, impact of the connectors spacing on shear resistance and failure mechanisms was examined through push-out test series which were performed with HVB shear connectors. The main conclusions in form of adapted average force-slip curves from Technical reports [9], [10], [1] are given in Figure 2.8

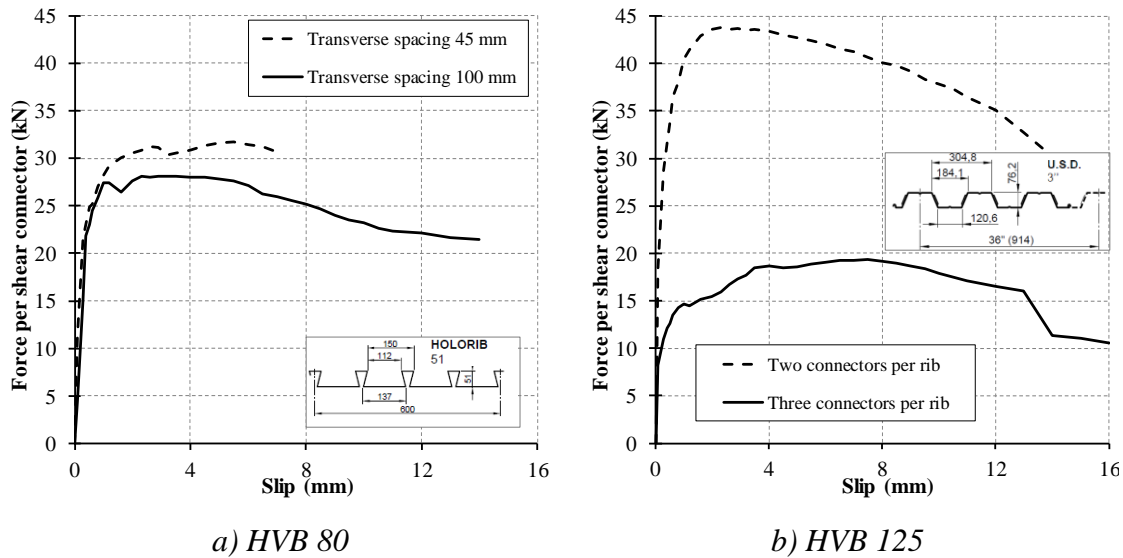


Figure 2.8. Influence of connector distance and number of connectors per profile sheeting rib on shear resistance, adapted from [1]

Lower transverse spacing of shear connectors within one rib of profiled sheeting resulted in relatively small increase of shear resistance but in significantly brittle behaviour, as shown in Figure 2.8a. Increase of shear connectors number per profiled sheeting rib resulted in significant reduction of shear resistance per shear connector, as given in Figure 2.8b. This was the main consequence of lowering of the transverse distances between connectors by increase of their number per profiled sheeting rib. Main failure mechanism which was obtained for push-out tests with profiled sheeting was failure of fasteners followed with significant deformation of connectors and profiled sheeting. Brittle behaviour of shear connection was obtained in push-out specimens where height of anchorage leg of HVB connector above the profiled sheeting was insufficient and usually manifested as failure of concrete in the zone above of the profiled sheeting. Depending on the connector height and geometry of profiled sheeting, other failure mechanisms can be obtained, such as: concrete pull-out around the connector or concrete failure around the connector fastening leg.

Very limited research on the analyses of behaviour of composite beams with HVB shear connectors is available when compared to the push-out tests. Technical reports from 1988 - 1989 [9], [10] presented the results of three composite beams examination. Composite beams with 6.0 m beam span, 2.0 m effective width and 120.0 mm composite slab height with profiled sheeting Hibond 55 were examined, as shown in Figure 2.9. HVB 100 shear connectors were positioned in ribs of profiled sheeting which were

transversally oriented relative to the supporting steel beam. Overall number of shear connectors per composite beam was varied in three examined beams, corresponding to 20 %, 40 % and 56 % of partial shear connection degree.

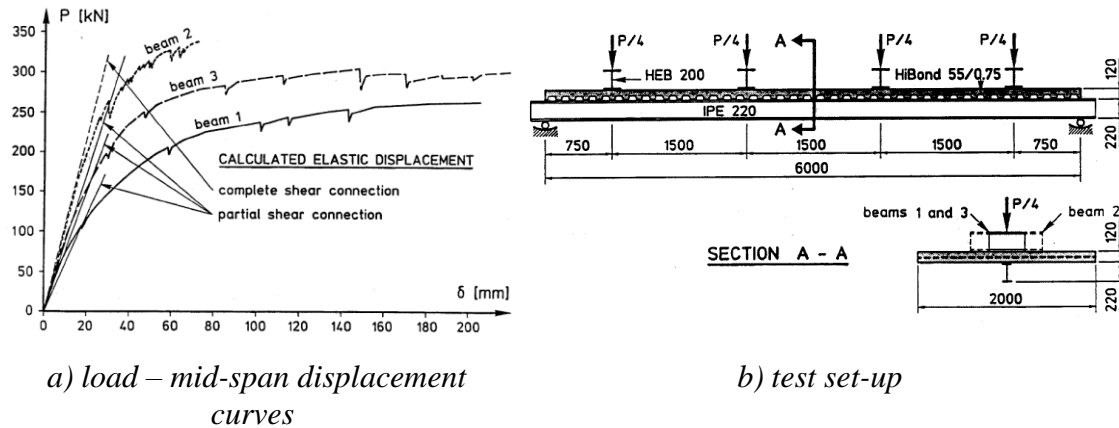


Figure 2.9. Composite beams examination with HVB 100 shear connector [9], [10], [16]

Composite beam tests with partial shear connection showed that behaviour remains ductile even with low degrees of partial shear connection [9], [10], [16]. The vertical displacement of composite beams 1 and 3 at maximum load was greater than 150.0 mm and slip at the ends of the beam was up to 14.0 mm [16]. At the end of testing procedure, concrete was completely crushed in the ribs of profiled sheeting for three analysed degree of partial shear connection. Moreover, composite action between steel beam and concrete above profiled sheeting ribs remained uninterrupted.

The results of experimental investigation of composite beams were compared by Crisinel [16] with design procedure for partial shear connection which was presented in draft version of Eurocode 4. Also, results of composite beam tests showed that for 15.0 m beams span in buildings, partial shear connection degree can be lowered to approximately 25 % without achievement of brittle behaviour. This partial shear connection degree is significantly lower than 40 % (50 % in draft version of Eurocode 4) which is defined for welded headed studs according to EN 1994-1-1:2004 [11].

2.3.3. Design recommendations and installation requirements

Observations from the previously explained experimental investigations of HVB shear connectors enabled the definition of initial requirements for minimum distances between connectors in order to avoid the reduction of shear resistance and brittle

behaviour. Some of the first detailing rules which must be respected considering connectors positioning in profiled sheeting rib and their height above profiled sheeting were defined in Technical reports [9], [10].

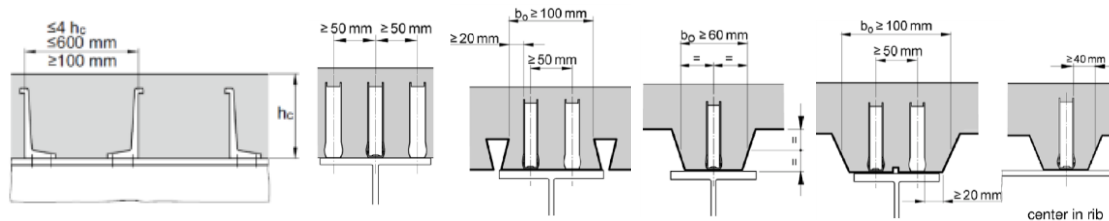
The most important current recommendations for connectors positioning in solid and composite concrete slabs are given in Figure 2.10. When unfavourable effects of corrosion are expected, minimum concrete slab thickness should be at least 20.0 mm higher than X-HVB shear connector height [5], [7]. Also, certain restrictions are defined for installation in composite concrete slabs, considering profiled sheeting geometry and height of X-HVB shear connector [5], [7]. Minimal base material thickness for connectors X-HVB 40 and X-HVB 50 is 6.0 mm and 8.0 mm for other shear connectors. If base material with smaller thicknesses than 8.0 mm is used, design resistance of shear connector should be reduced and calculated according to Eq. 2.1.

$$P_{Rd,red} = \frac{t_{II,act}}{8mm} \cdot P_{Rd} \geq 23.0 \text{ kN} \quad (2.1)$$

In previous expression:

$t_{II,act}$ is the actual base material thickness [mm];

P_{Rd} is the design value of shear resistance of single connector.



a) solid slabs

b) composite slabs with profiled sheeting

Figure 2.10. Recommendations for X-HVB shear connectors positioning [5], [7]

The similarity between load-slip behaviour and ductility of X-HVB shear connectors and welded headed studs permitted the use of the same formulation for design resistance reduction factor in composite slabs with profiled sheeting. Nowadays, reduction factors are precisely defined. For sheeting ribs parallel to the supporting beam, design resistance should be calculated using Eq. 2.2 [5], [7]. Reduction factor k_1 has the same definition as for welded headed studs defined in EN 1994-1-4:2004 [11].

$$P_{Rd,l} = k_1 \cdot P_{Rd} \quad (2.2)$$

with:

$$k_1 = 0.6 \cdot \frac{b_0}{h_p} \cdot \left(\frac{h_{sc}}{h_p} - 1 \right) \leq 1.0 \quad (2.3)$$

When profiled sheeting ribs are positioned transverse to the supporting beam, design resistance should be calculated according to Eq. 2.4. [5], [7]. Reduction factor $k_{t,l}$ for transverse profiled sheeting ribs and longitudinal position of shear connectors has approximately the same definition as for welded headed studs [11].

$$P_{Rd,t,l} = k_{t,l} \cdot P_{Rd} \quad (2.4)$$

with:

$$k_{t,l} = \frac{0.66}{\sqrt{n_r}} \cdot \frac{b_0}{h_p} \cdot \left(\frac{h_{sc}}{h_p} - 1 \right) \leq 1.0 \quad (2.5)$$

When profiled sheeting ribs and shear connectors are both positioned transverse to the supporting beam, which is the specificity of this type of shear connector, design resistance should be calculated according to Eq. 2.6 [5], [7]. The upper limit of reduction factors values of X-HVB shear connectors is 1.0, as given in Eq. 2.3, Eq. 2.5 and Eq. 2.7. The same upper limit for welded headed studs, in the widest range of application, is between 0.60 and 0.85, as given in EN 1994-1-1:2004 [11]. X-HVB shear connectors in composite beams with profiled sheeting can be considered as ductile according to requirements given in EN 1994-1-1:2004 [11].

$$P_{Rd,t,t} = 0.89 \cdot k_{t,t} \cdot P_{Rd} \quad (2.6)$$

with:

$$k_{t,t} = \frac{1.18}{\sqrt{n_r}} \cdot \frac{b_0}{h_p} \cdot \left(\frac{h_{sc}}{h_p} - 1 \right) \leq 1.0 \quad (2.7)$$

In previous expressions:

b_0 is the mean width of a concrete rib or minimum width of re-entrant profiled sheeting;

h_p is the overall depth of the profiled steel sheeting excluding embossments;

h_{sc} is the overall nominal height of a stud connector;

n_r is the number of shear connectors in one rib [-].

Also, it is important to highlight that current design recommendations for composite steel-concrete structures, EN 1994-1-4:2004 [11], ANSI/AISC 360-05 [17] and JSCE [18], do not define design resistance for mechanically fastened shear connectors. EN 1994-1-4:2004 [11] defines recommendations only for welded headed studs in solid and composite concrete slabs, while ANSI/AISC 360-05 [17] defines design resistance for headed studs and channel shear connectors. Moreover, JSCE [18] gives design resistance and installation requirements for headed studs, perforated-plate dowels and block connectors. Shear resistance of mechanically fastened shear connectors is related to the several failure mechanisms and most of them are associated to the failure of the cartridge fired pins or anchorage mechanisms. Their quantitative and qualitative definition has not yet been analytically explained. With the exception of shear connection in composite steel-concrete beams, mechanically fastened shear connectors such as X-HVB can be used in several other applications, such as: anchorage of profiled steel sheeting in composite floor construction or for concrete encased steel columns. Extensive experimental and numerical investigation of composite concrete slabs end anchorage with various types of profiled steel sheeting with headed studs and mechanically fastened shear connectors was performed through push-out tests and composite slab tests by Daniels et al. [19].

2.3.4. Other types of mechanically fastened shear connectors

In the recent period, new types of mechanically fastened shear connectors, Rib Connectors (Figure 2.11) and Strip Connectors (Figure 2.12) were developed by Fontana, Bärtschi and Beck and presented in their works [20], [21], [22]. For both types of shear connectors, shear connection between steel supporting beam and concrete was achieved with cartridge fired pins X-ENP-21 HVB. The Rib Connector is cold-formed steel angle with perforated edge which is in connection with surrounding concrete slab, performing a similar behaviour as for perforated sheer connectors [23]. This type of shear connector can be used in composite beams with solid concrete slabs and composite beams with profiled sheeting ribs parallel to the steel supporting beam. Obtained shear resistance of Rib connector is in the range from 500.3 kN to 616.5 kN. Failure of this connector was followed with shear failure and pull-out of fasteners which is similar to the failure of X-

2.13a. Specimens after failure are presented in Figure 2.13b. Obtained failure mechanisms for three examined specimens were shear failure and pull-out failure of fasteners. Detachment of concrete from profiled sheeting was obtained for all three analysed beams when the testing procedure was finished, as shown in Figure 2.13b.

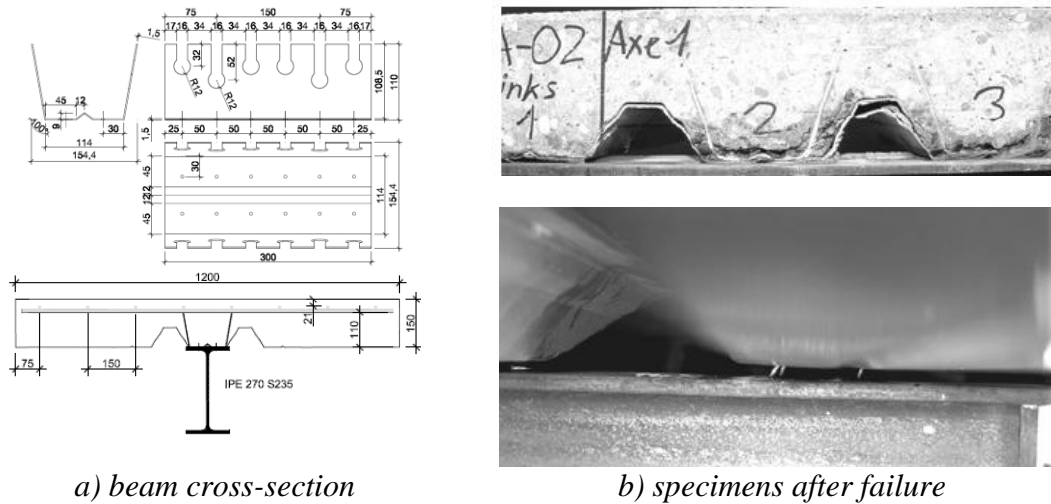


Figure 2.13. Composite beam examination with Rib and Strip Connectors [20]

In addition, another types of mechanically fastened shear connectors are available for application in composite construction. Shear connectors which are developed by Tecnaria Company are presented in Figure 2.14. These shear connectors, Diapason and CFT, are in the recent period also granted with European Technical assessments. Design resistance and installation requirements in solid slabs and composite slabs with profiled sheeting of CFT shear connectors are reported in ETA-18/0447 assessment [25]. Design resistance is defined in relation to the concrete class. In composite slabs with profiled sheeting, design resistance should be determined using reduction coefficients defined in EN 1994-1-1:2004 [11]. Moreover, for wide range of concrete classes and different orientations of shear connectors relative to the shear force direction in solid concrete slabs, CFT shear connectors with height lower than 70.0 mm could not be considered as ductile according to recommendations given in EN 1994-1-1:2004 [11]. Behaviour of CFT shear connectors in push-out tests is also presented by Tahir et al. [26]. Shear resistance per one shear connector in solid concrete slabs was between 42.0 kN and 55.8 kN and obtained failure mechanism was fracture and pull-out of fasteners [26]. Experimental data obtained from seven push-out test specimens, indicated that slip corresponding to the shear resistance was less than 3.1 mm and ductile behaviour of CFT

shear connectors was not achieved, according to requirements given in EN 1994-1-1:2004 [11].



a) CFT connector [25]



b) Diapason connector [27]

Figure 2.14. Mechanically fastened shear connectors

Implementation of Diapason shear connectors in composite construction is granted with ETA-18/0335 assessment [27]. In respect to the specific geometry, this type of shear connector can be used with or without reinforcement positioned through holes in the connector. Moreover, specific geometry reflects the design restrictions considering implementation in composite slabs with profiled sheeting, which are defined in ETA-18/0335 assessment [27]. Diapason shear connectors should be considered as ductile for application in solid and composite concrete slabs with profiled sheeting. Design resistance depends on the concrete class and for Diapason shear connectors is approximately 30 % higher in comparison to the CFT shear connector of the same height.

2.4. Cartridge fired pins

2.4.1. Development and classification

A wide range of mechanical fasteners which are attached to the steel base material with specific hand-held fastening tool are designated as powder actuated fasteners (PAF). However, the terminology is not standardized. In English, this type of fasteners is known as powder actuated fasteners or cartridge fired pins. In German, the word *Setzbolzen* is used as generic term for wide range of various types of mechanical fasteners. Also, *Stahlbau kalender* from 2011 [12] defines powder actuated fasteners as a group of nails, threaded studs and blunt tip threaded studs which have a common way of application. EN 1993-1-3:2009 [28] defines cartridge fired pins as mechanical fasteners which can be used for cold-formed members and sheeting. Therefore, term cartridge fired pin will be used

here to determine a specific type of powder actuated fasteners which has a wide range of application and also can be used for X-HVB shear connectors. For all other types of mechanical fasteners with same installation procedure, term powder actuated fastener will be used.

Development of the powder actuated fasteners dates back to the beginning of 20th century. First high velocity direct fastening tool was invented by Robert Temple in 1915 and was used by the navy in underwater applications, to make temporary repairs of ships [12], [29]. First high velocity direct fastening tool was used in construction industry in the United States in 1940s. Till 1958 high velocity direct fastening tool was replaced with low velocity piston-principle tool which was more secure for application. Nowadays, direct fastening tools are fully-automatic and semi-automatic tools for which driving force is provided by power load of the cartridge and meet strict safe requirements such as those given in ISO 11148-13:2007 [30] and EN 15895:2018 [31].

2.4.2. Range of application and installation quality

Wide range of powder actuated fasteners can be used in steel construction for fastening of profiled metal sheeting, cold-formed profiles and sandwich panels which is the main field of their application in constructions [12], [32], in addition to the mechanical fastening of shear connectors. There are several manufacturers of this type of fasteners, which are members of the Powder Actuated Tool Manufacturers Institute (PATMI). Moreover, design recommendations of these fasteners are based on the experimental investigations which are part of the proprietary technical reports. Relatively few results of experimental investigations are published in scientific journals, conference proceedings or other engineering literature. Typical powder actuated fasteners are shown in Figure 2.15. Fasteners from a) to d) are characteristic general-purpose powder actuated fasteners, fasteners e) and f) are specified for profiled sheeting and steel base materials, while fasteners g) and h) are designated as threaded studs. The overall length of the fasteners is from 15.0 mm to 120.0 mm with shank diameter from 2.5 mm to 5.0 mm. The most important characteristics of X-ENP 21 HVB cartridge fired pins which are used for X-HVB shear connectors will be presented here. Also, characteristics of similar fasteners will be presented and compared with X-ENP 21 HVB cartridge fired pin.

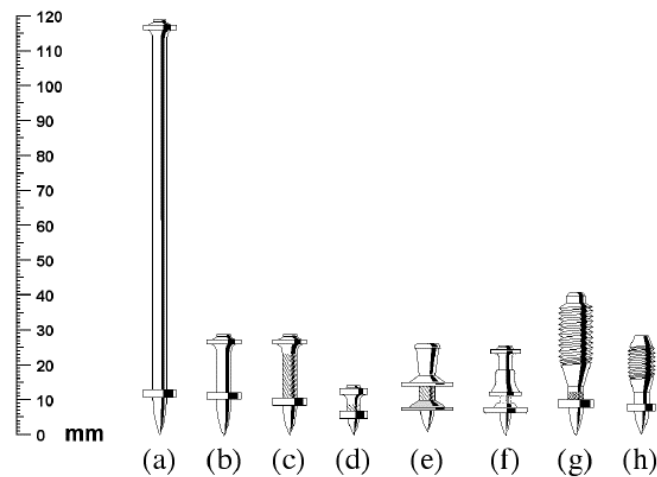


Figure 2.15. Powder actuated fasteners [33]

The first European Technical approvals were granted for powder actuated fasteners for fastening of profiled sheeting in 2004. As previously explained, implementation of X-HVB shear connectors in composite construction is granted by European Technical approvals ETA-15/0876 assessment [7] which also includes application limits for X-ENP 21 HVB cartridge fired pins. Other types of cartridge fired pins which can be used in steel construction for cold-formed profiles, profiled sheeting and sandwich panels are granted with technical approvals, such as ETA-08/0040 assessment [34] and ETA-04/0101 assessment [35].

X-ENP 21 HVB cartridge fired pins are used for fastening of X-HVB shear connectors to the steel supporting material with or without profiled sheeting. The fastener, the fastening tool and driving energy together represent the fastening system [12]. The high driving velocity, presented with maximum driving energy of approximately 600 J, enables installation of cartridge fired pins into steel supporting material. Installation of cartridge fired pins is highly dynamic procedure which has a significant influence on stress-state of fastened and base material. Goldspiegel et al. [36] proposed a numerical model for high-speed nailing procedure for connection of dissimilar materials with various mechanical properties. Nailing simulations have shown that final installation depth of cartridge fired pins is mainly governed by damage parameters of fastened materials [36].

X-ENP 21 HVB cartridge fired pins are made from zinc plated carbon steel. The strength and hardness of the cartridge fired pins have to be approximately 4 to 5 times higher than of steel base material, in order to accomplish the driving procedure. A

hardness of the cartridge fired pins is between 49 and 58 HRc, which amounts approximately 1850 N/mm² to 2200 N/mm² of ultimate strength [12]. A wire material which is used for manufacturing of cartridge fired pins is heat treatable carbon steel with 0.65 % of carbon and tensile strength of approximately 600 N/mm². The required hardness and ductility of cartridge fired pins are achieved through heat treatment, which should be applied carefully in order to avoid brittle behaviour of the fastener.

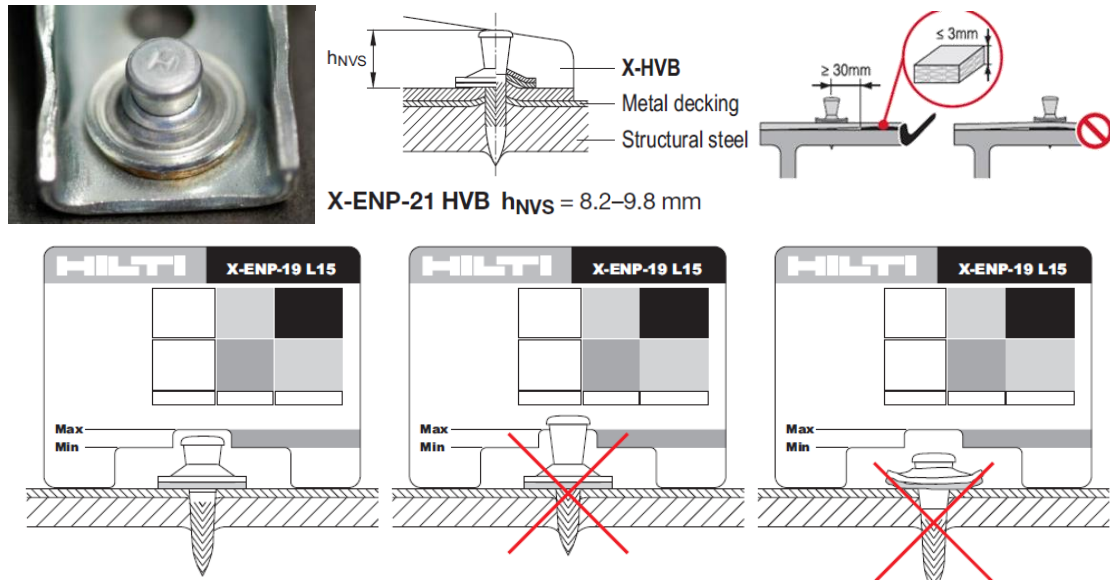
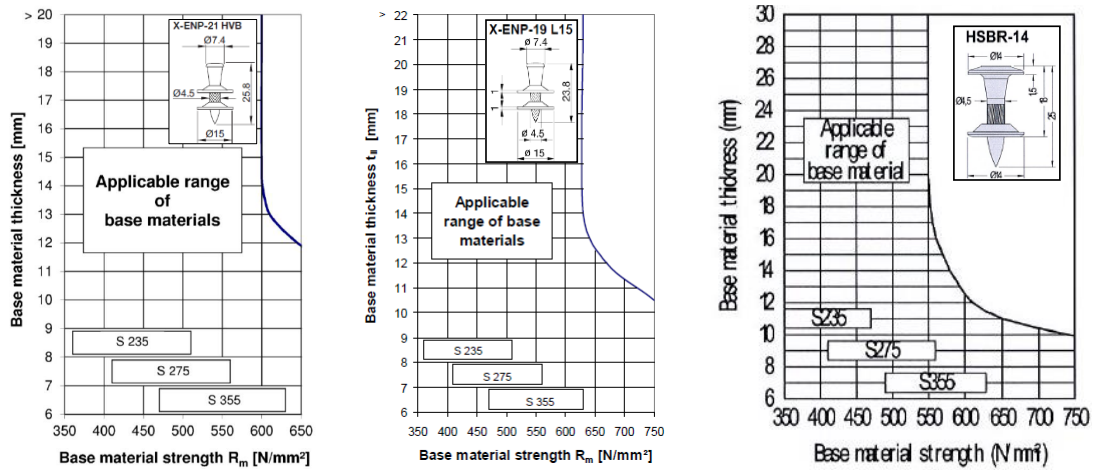


Figure 2.16. Installation requirements of cartridge fired pins [7], [32]

The quality of the installation procedure is determined by fastener stand-off after installation, h_{NVS} as shown in Figure 2.16, with clearly visible piston mark on the top of the pin washer. For appropriate installation, X-ENP 21 HVB cartridge fired pin stand-off amounts from 8.2 mm to 9.8 mm. If damage on the top of the washer or gap between top and bottom washer is visible, the fastener stand-off is outside of previously defined limits, and installation procedure should be adjusted.

Application range of X-ENP 21 HVB cartridge fired pins for shear connectors, depending of base material thickness and strength in accordance to the ETA-15/0876 assessment [7] is shown in Figure 2.17. This application range limits implicitly take into account the thickness of the cover material t_1 . Lower application limit is related to the minimum thickness of the base material, t_{II} and directly related to the obtained hold of the fastener in the base material. When the depth of penetration is greater than thickness of the base material, fastener penetrates right through the base material and fastener point is visible on the reverse side of the supporting material, as shown in Figure 2.16. When

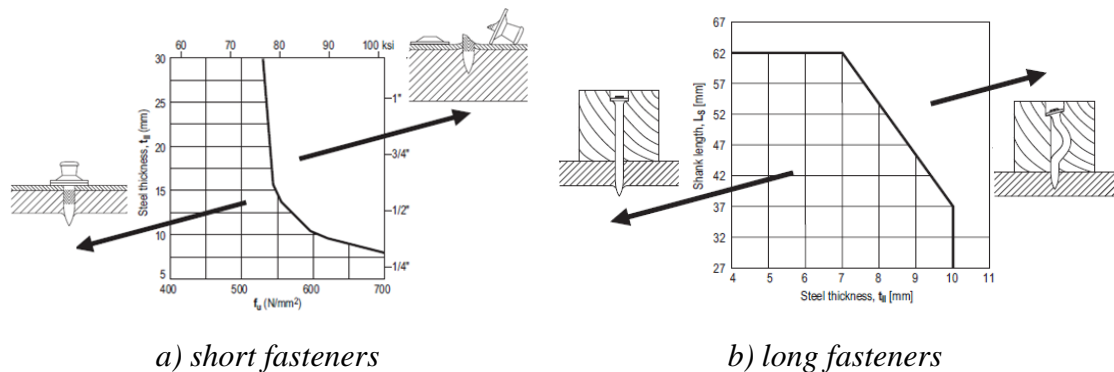
depth of penetration is lower than the base material thickness, term “solid steel” is used to describe this situation. Therefore, depth of penetration is equal to the depth of embedment. Above certain base material thickness t_{II} , such as 15.0 mm to 20.0 mm, further increase of thickness would not influence the increase in obtained hold. Application limits for various types of cartridge fired pins are given in Figure 2.17 and must be provided in the scope of the approval procedure.



a) X-ENP 21 HVB [7] b) X-ENP 19 L15 [35] c) HSBR-14 [34]

Figure 2.17. Application range limits for various types of cartridge fired pins

Upper application limit is related to the fastener driving ability and it exceeding can lead to the fastener shear breakage for short fasteners (siding and decking nails and threaded studs) and bending for long fasteners (nails used to fasten wood to steel) as the fastener is overstressed due to high driving resistance. Shear breakage of fasteners with failure surface of approximately at 45° angle to the shank length is shown in Figure 2.18a. Bending of long fasteners is shown in Figure 2.18b.



a) short fasteners

b) long fasteners

Figure 2.18. Failure of fasteners due to exceeding of upper application limits [32]

2.4.3. Anchorage mechanisms of cartridge fired pins

As previously explained, failure mechanisms of X-HVB shear connectors are mostly related to the shear failure and pull-out failure of cartridge fired pins. Pull-out failure is associated to failure of anchorage mechanisms that are developed during installation of cartridge fired pins. The term “anchorage” refers to the hold obtained by the fastener in the base material [12]. Anchorage mechanisms are in the scope of approval procedures and must be systematically verified. Metals with plastic deformation behaviour provide suitable anchorage mechanism for this type of fasteners and the most important base material is unalloyed structural steel according to EN 10025-2:2004 [8]. Anchorage mechanisms and principles which are pronounced considering cartridge fired pins are clamping, keying, welding and soldering, as shown in Figure 2.19.

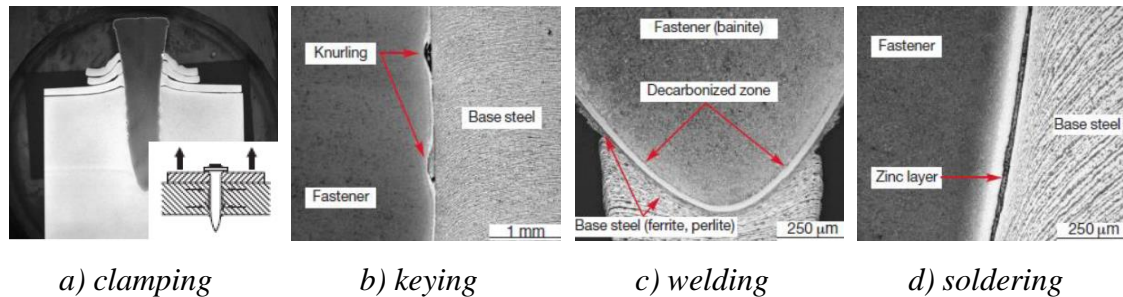


Figure 2.19. Anchorage mechanisms of X-ENP 21 HVB cartridge fired pins [32]

Clamping is the primary anchoring mechanism, shown in Figure 2.19a. This anchoring mechanism is a result of the radial dislocation of the base steel material resulting in plastic strains and residual stresses towards the body of the protruded pin. Installation procedure imposes the pressure in the base material to the fastener and friction at the contact surface.

Another anchorage mechanism is related to mechanical interlocking of the micro embossments on the side of the pin, also known as keying in case of cartridge fired pins, as shown in Figure 2.19b. This anchorage mechanism is directly related to the knurling of the fastener shank of X-ENP 21 HVB cartridge fired pin which obtains micro keying of fastener into the base material. Keying mechanism is the result of zinc and base material accumulation in knurled surface of the nails during very dynamic installation procedure.

Welding mechanism is observed mostly at the top point of a fastener where the temperature during installation can be expected to be the highest, as shown in Figure

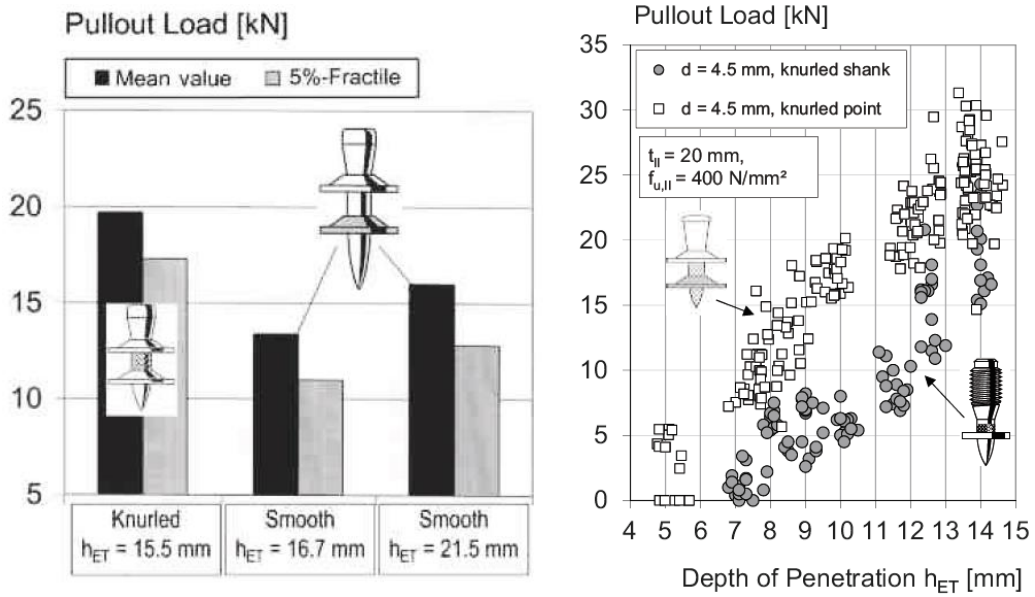
2.19c. During the installation procedure and due to development of very high temperatures at the point of the fastener, thin zinc layer is melting and obtains welding of the fastener point to the base material. Thin zinc layer of approximately 10.0 μm on the fastener represents corrosion protection during storage, transportation and installation. Therefore, welding can be obtained only for the fasteners installed in solid steel, or in the case when depth of penetration is equal to the embedded depth of fastener.

Anchoring mechanism which is shown in Figure 2.19d is soldering. This type of the anchorage is resulted by soldered zinc layer between fastener and base material further from the fastener point. Soldering is developed due to relatively high temperatures and friction in the contact zone of the base material and fastener.

Prediction models for determination of the pull-out resistance of cartridge fired pins are not present in available design regulations [12]. According to the currently available literature and design codes, anchorage capacity should be obtained by appropriate testing procedures. Moreover, contribution of each type of anchorage mechanism in overall anchorage is not constant and depends on the fastener type and base material. It is assumed that the clamping obtains the most important influence on fasteners pull-out resistance, which is explained through FE analysis presented in this thesis.

2.4.4. Pull-out resistance of cartridge fired pins in tests

Pull-out resistance of the fasteners is influenced by several various factors, such as depth of penetration, base material thickness, base material properties, fastener diameter and knurling of the fastener shank or tip. Effects of the knurling of the fasteners on the anchorage mechanisms and pull-out resistance are shown in Figure 2.20. Influence of the knurled shank and smooth shank of the fasteners which are installed in the same base material is shown in Figure 2.20a. The pull-out resistance of the smooth shank fastener is significantly lower than resistance of the fastener with knurled shank. Even the larger depth of penetration of the longer, smooth shank fastener can not compensate the absence of shank knurling and therefore much lower pull-out resistance. Moreover, knurling of the fastener shank is efficient only when sufficient embedment of the fastener in the base material is achieved. Comparison of the pull-out resistance of fasteners with and without knurled fastener tip is given in Figure 2.20b.

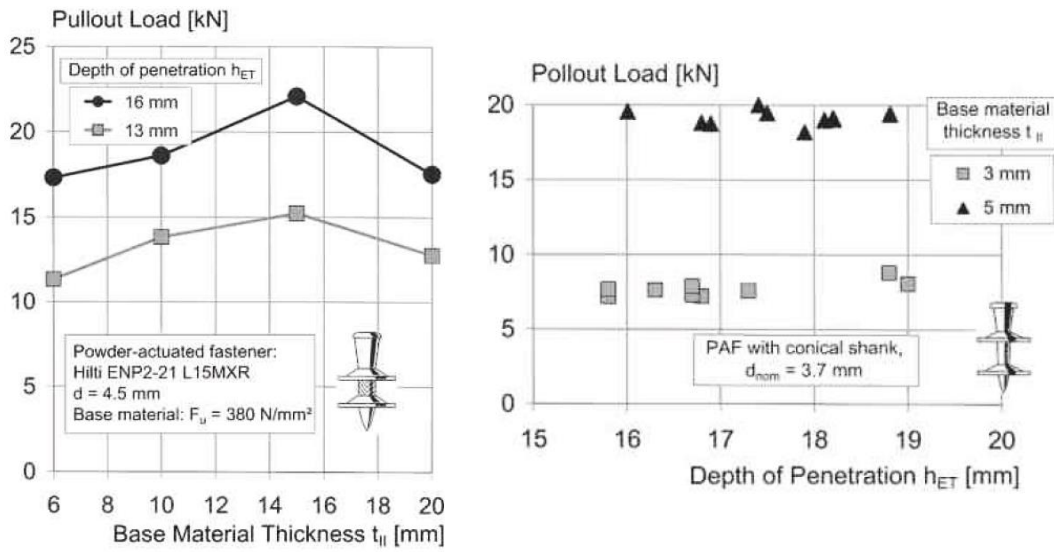


a) knurling of the fasteners shank

b) tip knurling

Figure 2.20. Influence of the knurling of the fastener on the pull-out resistance [12]

Results of cartridge fired pins pull-out tests evaluated for various base material thicknesses and depth of penetration are shown in Figure 2.21a. Each dot represents a characteristic pull-out resistance evaluated from series of 90 individual tests. Results presented in Figure 2.21 are obtained for test specimens when the depth of penetration is greater than thickness of the base material and fastener point is visible on the reverse side of the supporting material. As shown in Figure 2.21, characteristic pull-out resistance is increased with increase of the base material thickness when fastener penetrates through base material. The increase, however, is much lower than the increase in the area of contact between the fastener and the base material [12]. As shown in Figure 2.21a the optimum is achieved with similar value for depth of penetration and base material thickness. The influence of the base material thickness on the resistance is comparatively slight, considering that approximately same resistance is achieved with 6.0 mm and 20.0 mm base material thickness. Moreover, with base material thicknesses lower than 6.0 mm, their influence becomes considerable. Figure 2.21b represents the pull-out resistance of fasteners for which depth of penetration is several times larger than base material thickness. The effects of penetration depth on pull-out resistance can be experimentally investigated with varied driving energy in order to achieve various embedment depts. Pull-out resistance of X-ENP-19 L15 fastener with various depths of penetration with base material thickness of 20.0 mm is given in Figure 2.22.



a) base material $t_{II} \geq 6.0$ mm b) base material $t_{II} < 6.0$ mm
Figure 2.21. Influence of base material thickness and depth of penetration on the pull-out resistance [12]

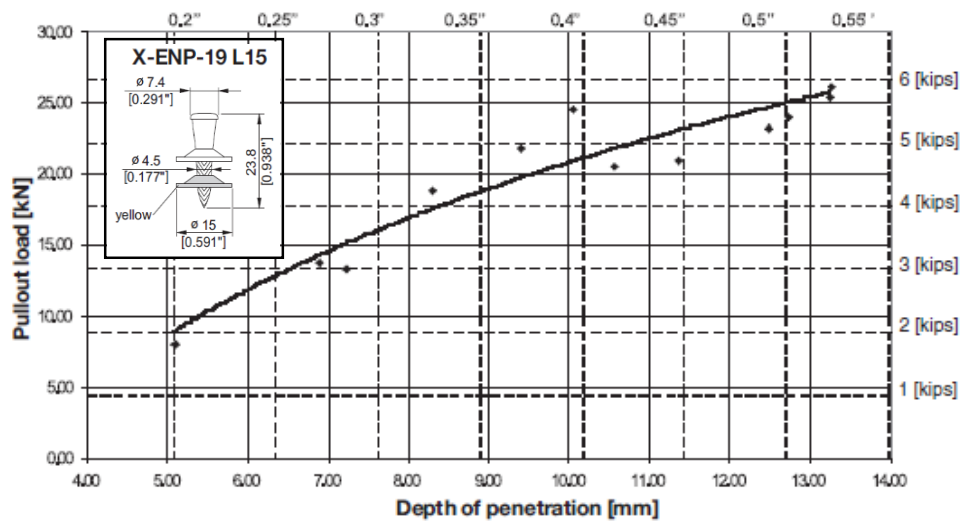
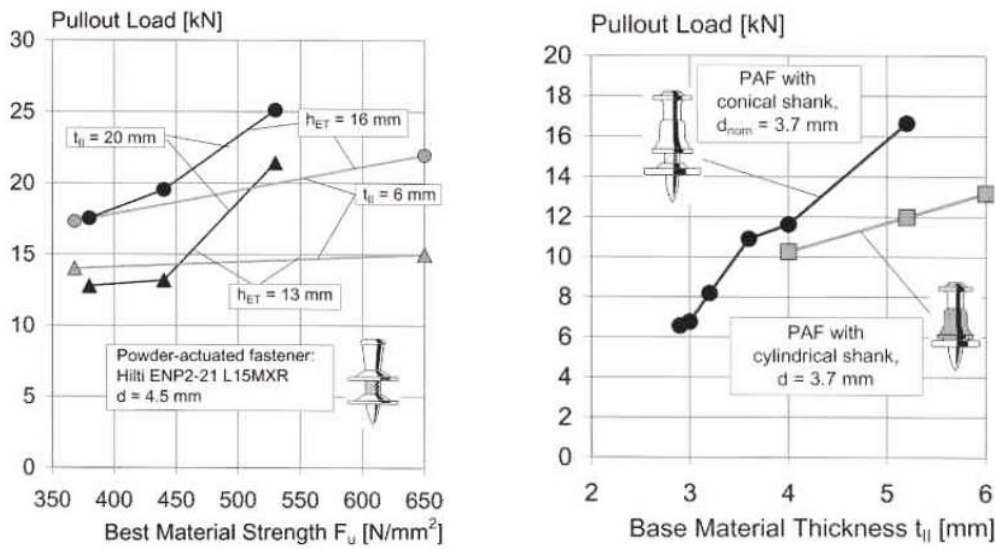


Figure 2.22. Depth penetration influence on the pull-out resistance, adapted from [32]

Influence of the base material strength on pull-out resistance of ENP2-21 L15MXR cartridge fired pin, for various base material thicknesses and depths of penetration is given in Figure 2.23a. Increase of pull-out resistance for higher tensile strength of base materials is more pronounced for higher base material thicknesses for full embedment of fastener in solid base material. The most notable increase is observed for base materials strength increase from 450 to 550 N/mm². Results of pull-out resistances for various types of

cartridge fired pins are given in Figure 2.23b, obtaining similar results as for group of X-ENP fasteners (ENP2-21 L15MXR, X-ENP-19 L15, X-ENP 21 HVB).



a) ENP2-21 L15MXR

b) PAF with cylindrical and conical shanks

Figure 2.23. Influence of base material strength and thickness on pull-out resistance [12]

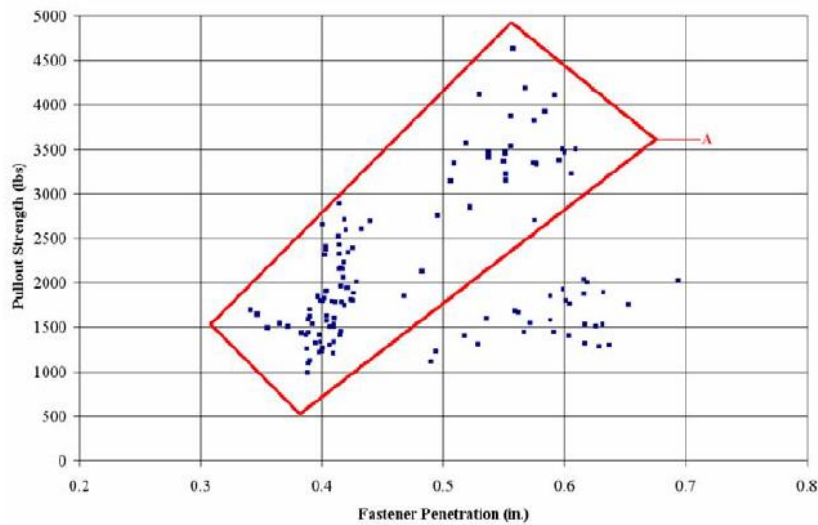


Figure 2.24. Pull-out resistances of various types of powder actuated fasteners [37]

Mujagic et al. [37] analysed results of pull-out resistances obtained from tension tests of various types of powder actuated fasteners with smooth shank, without knurling. Analysis included powder actuated fasteners from four manufacturers. Figure 2.24 presents the pull-out resistances of powder actuated fastener without knurled shank in function of embedded depth. The results included 127 individual tension tests.

Unfortunately, no information was provided regarding the information about precise geometry of fastener and base material strength for results presented in Figure 2.24. Results given in Figure 2.24 are dispersed in three distinct clouds with significant scattering of resistances for same embedded depth. Results outside the boundary denoted with A (see Figure 2.24) are also related to embedded depth of fastener, but are probably related to the excessive driving energy applied during installation procedure. Mujagic et al. [37] gave a low bound prediction for pull-out resistance of powder actuated fasteners for three base material thicknesses and highlighted that definition of unique code-based equation for pull-out resistance of various types of powder actuated fasteners would be an impossible task.

2.4.5. Different types of load and failure mechanisms

Various types of cartridge fired pins are used for connecting the profiled sheeting to the steel base material. According to the ETA-04/0101 assessment [35], X-ENP-19 L15 cartridge fired pin given in Figure 2.17b, can be used to attach profiled sheeting with thickness $t_I = 0.63 - 2.5$ mm (maximum 4.0 mm for 2 - 4 layers) to the steel base material with thickness $t_{II} = 6.0$ mm. Another type of the fastener which is also used for profiled sheeting attachment is HSBR 14 cartridge fired pin, which range of application is given in Figure 2.17c. This type of fastener can be used for attachment of thicker profiled sheeting, $t_I = 0.63 - 3.0$ mm (maximum 5.0 mm for 2-4 layers) to the steel base material with thickness $t_{II} = 6.0$ mm [34]. Cartridge fired pins connecting profiled sheeting are loaded in tension, shear or combined tension and shear loading.

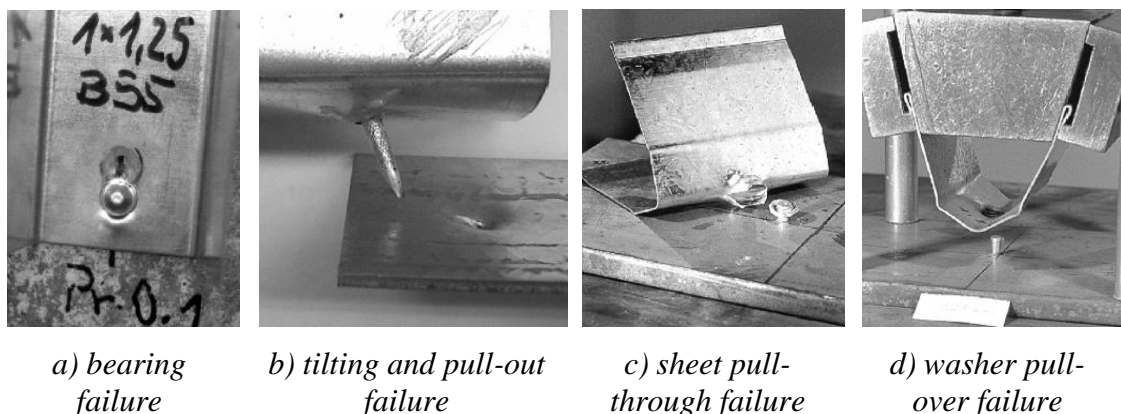


Figure 2.25. Failure mechanisms of cartridge fired pins loaded in shear and tension

[32]

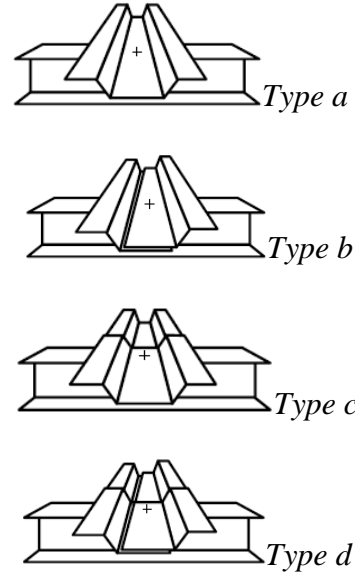
Shear loading of cartridge fired pins can result in several failure mechanisms, such as: shear of fastener, bearing failure, net section failure, end failure and tilting and pull-out [38]. Characteristic failure of the fastened material and failure of the base material is given in Figure 2.25a and Figure 2.25b, respectively. Failure of the fastened material is the most often failure mechanism for shear loading of cartridge fired pins. Bearing failure is characterized with overcome of clamping force of the washer and cutting of fastened metal sheeting with shank of cartridge fired pin, as shown in Figure 2.25a. For large thicknesses of fastened sheeting in comparison to the base material thickness, bearing failure of the base material can occur, which is followed with tilting and pull-out of the fastener, as given in Figure 2.25b. Shear failure of the X-ENP-19 L15 cartridge fired pin can be obtained with force of approximately 20.0 kN and 2.5 mm thickness of fastened metal sheeting.

Characteristic failure mechanisms of cartridge fired pins loaded in tension are: pull-out failure, fracture of fastener, pull-over and pull-through failure [38]. Sheeting pull-over failure is characterized with tearing and distortion of the fastened material around fastener head. When profiled metal sheeting is completely disconnected from the fastener, obtained failure mechanism is defined as pull-through, as shown in Figure 2.25c. Also, one of the possible failure mechanisms is washer pull-over the head of the fastener, as shown in Figure 2.25d, when the profiled metal sheeting is stronger or thicker than for the sheeting pull-over failure. Pull-out failure mechanism will occur for thicker profiled metal sheeting or increased number of layers, when anchorage mechanisms are overcome, as explained in previous chapter. Moreover, pull-out failure is governed with the shape and size of the fastener head and washer and for properly installed X-ENP-19 L15 cartridge fired pin this failure mechanism is not common failure mechanism [32]. Approximately 30.0 kN tension force is required for fracture of the fastener with 4.5 mm diameter, but this failure mechanism will hardly occur. As shown in previous chapter, pull-out resistance of the various types of cartridge fired pins is significantly lower than 30.0 kN. Therefore, other types of failure mechanisms due to tension loading is more frequent for cartridge fired pins.

Characteristic shear and tension resistances of X-ENP-19 L15 cartridge fired pin for various thicknesses of profiled sheeting are given in Figure 2.26, according to ETA-04/0101 assessment [35]. Design shear and tension resistance should be determined using

partial safety factor $\gamma_M = 1.25$, or other value which is determined within National Annex of EN 1993-1-8:2010 [39] or EN 1993-1-3:2009 [28].

Sheeting thickness	Characteristic resistance		Type of connection
	Shear	Tension	
t_1 (mm)	V_{Rk} (kN)	N_{Rk} (kN)	-
0.63	4.0	4.1	a, b, c, d
0.75	4.7	6.3	a, b, c, d
0.88	5.4	7.2	a, b, c, d
1.00	6.0	8.0	a, b, c, d
1.13	7.0	8.4	a, c
1.25	8.0	8.8	a, c
1.50	8.6	8.8	a
1.75	8.6	8.8	a
2.00	8.6	8.8	a
2.50	8.6	8.8	a



a) characteristic resistance for specific connection type b) type of connection

Figure 2.26. Characteristic resistance of X-ENP-19 L15 cartridge fired pin [35]

2.4.6. Design resistance of cartridge fired pins

Certain design resistances for cartridge fired pins are defined in EN 1993-1-3:2009 [28] and given in following equations. For fasteners loaded in shear, bearing resistance should be calculated according to Eq. 2.8 and resistance of net-section according to Eq. 2.9. Design recommendation for shear resistance of cartridge fired pins is not defined according to EN 1993-1-3:2009 [28] and should be determined by testing and using Eq. (2.10).

$$F_{b,Rd} = 3.2 \cdot f_u \cdot d \cdot t / \gamma_{M2} \quad (2.8)$$

$$F_{n,Rd} = A_{net} \cdot f_u / \gamma_{M2} \quad (2.9)$$

$$F_{v,Rd} = F_{v,Rk} / \gamma_{M2} \quad (2.10)$$

In previous expressions:

f_u is the ultimate strength of steel;

d is the nominal diameter of cartridge fired pin shank;

t is the thickness of steel plate;

γ_{M2} is the partial safety factor for joints;

A_{net} is the net cross-section area of the connected part;

$F_{v,Rk}$ is the characteristic shear resistance of cartridge fired pin.

For pins loaded in tension several failure mechanisms can be obtained. For cartridge fired pins loaded in tension through profiled sheeting, usual failure mechanism which can be obtained is pull-through failure mechanism. This failure is characterized with failure of material of profiled sheeting adjacent to the fastener head and according to EN 1993-1-3:2009 [28] should be calculated using Eq. 2.11 and Eq. 12 for static loads and for wind loads and combination of wind loads and static loads, respectively. Design resistances for pull-out failure mechanism and tension resistance of the fastener should be determined by testing, according to EN 1993-1-3:2009 [28]. When fasteners are loaded in combined, shear and tension loading, the resistance of the fastener should be determined according to Eq. 2.13.

$$F_{p,Rd} = d_w \cdot t \cdot f_u / \gamma_{M2} \quad (2.11)$$

$$F_{p,Rd} = 0.5 \cdot d_w \cdot t \cdot f_u / \gamma_{M2} \quad (2.12)$$

In previous expressions:

d_w is the diameter of the washer of cartridge fired pin.

$$\frac{F_{t,Ed}}{\min(F_{p,Rd}, F_{o,Rd})} + \frac{F_{v,Ed}}{\min(F_{b,Rd}, F_{n,Rd})} \leq 1.0 \quad (2.13)$$

In previous expressions:

$F_{t,Ed}$ is the design tensile force per cartridge fired pin for the ultimate limit state;

$F_{v,Ed}$ is the design shear force per cartridge fired pin for the ultimate limit state;

$F_{p,Rd}$ is the design pull-through resistance per fastener;

$F_{o,Rd}$ is the design pull-out resistance per fastener;

$F_{b,Rd}$ is the design bearing resistance per fastener;

$F_{n,Rd}$ is the design resistance of net-section.

Test methods for cartridge fired pins loaded in shear and tension are given in ECCS publications [38], [40] and AISI S905 standard [41]. When deformation capacity of the connection is needed, then the required conditions given in Eq. 2.14 and Eq. 2.15 should be fulfilled for fasteners loaded in shear and tension, respectively. When these conditions are not fulfilled, then the needed deformation capacity should be provided by other parts of the structure [28]. Moreover, the National Annex of EN 1993-1-3:2009 [28] may give further information on shear resistance of cartridge fired pins loaded in shear and pull-out resistance and tension resistance of cartridge fired pins loaded in tension.

$$F_{v,Rd} \geq 1.5 \sum F_{b,Rd} \quad \text{or} \quad \sum F_{v,Rd} \geq 1.5 \sum F_{n,Rd} \quad (2.14)$$

$$F_{o,Rd} \geq \sum F_{p,Rd} \quad \text{or} \quad F_{t,Rd} \geq \sum F_{o,Rd} \quad (2.15)$$

Design recommendations for various types of cartridge fired pins are incorporated in AISI S100-16 [42] since 2012. In this design code, the term powder actuated fasteners (PAF) was used, which is common term for North America. In general, the AISI S100-16 [42] incorporate three design methods: *Allowable Strength Design (ASD)*, *Load and Resistance Factor Design (LRFD)* and *Limit State Design (LSD)*. Both, ASD and LRFD are applicable in United States and Mexico, while LSD is applicable in Canada. ASD and LRFD are two distinct methods and they are not interchangeable. Moreover, LRFD and LSD are two identical design methods but obtained with different load factors γ_i based on the dead - live load probability. Three design methods are based on calculation of available strength (factored resistance) based on the nominal strength (resistance) R_n and appropriate safety factors Ω for ASD or resistance factors Φ for LRFD and LSD. Available strength (factored resistance) should be greater than required strength R_u . Detail definition of all three design methods is given in AISI S100-16 [42]. The design recommendations and provisions for installation given in this AISI S100-16 [42] for powder actuated fasteners will be given bellow.

Design recommendations given in AISI S100-16 [42] should be applied when thickness of the base material does not exceed 19.1 mm and thickness of the fastened material is less than 1.52 mm. Moreover, the washer diameter used in the following equations should not be greater than 15.2 mm and shank diameter should be between 2.69 mm and 5.23 mm. AISI S100-16 [42] also defines requirements for minimal edge and spacing distances as stipulated in ASTM E1190 [43].

For powder actuated fasteners loaded in tension design resistance is defined for tension fracture of fastener and pull-over strength. The nominal tensile strength (resistance) of powder actuated fasteners should be calculated according to Eq. 2.16. Powder actuated fasteners possess Rockwell hardness (HRC) values of 49 to 58 which can be properly related to tensile strength. Mujagic et al. [37] showed in their work that nominal tensile fracture strength (resistance) can be determined using the value of 1790 MPa for the HRC range in excess of 52.

$$P_{ntp} = (d/2)^2 \cdot \pi \cdot F_{uh} \quad (2.16)$$

with:

$$F_{uh} = F_{bs} \cdot e^{(HRC_p/40)} \quad (2.17)$$

$$\Omega = 2.65 \text{ (ASD)}; \Phi = 0.60 \text{ (LRFD)}; \Phi = 0.50 \text{ (LSD)}$$

In previous expressions:

d is the fastener diameter measured at the near side of embedment;

F_{uh} is the tensile strength of hardened powder actuated fastener steel;

F_{bs} is the base stress parameter (455 MPa);

HRC_p is the Rockwell C hardness of powder actuated fastener steel.

The nominal pull-over strength (resistance) of powder actuated fasteners should be determined using Eq. 2.18.

$$P_{nov} = \alpha_w \cdot t_1 \cdot d_w' \cdot F_{ul} \quad (2.18)$$

with:

$$\Omega = 3.00 \text{ (ASD)}; \Phi = 0.50 \text{ (LRFD)}; \Phi = 0.40 \text{ (LSD)}$$

In previous expression:

α_w is the coefficient differentiating type of powder actuated fastener;

t_1 is the thickness of member in contact with powder actuated fastener head or washer;

d_w' is the actual diameter of fastener head or washer in contact with retained substrate (≤ 15.2 mm);

F_{ul} is the tensile strength of member in contact with fastener head or washer.

AISI S100-16 [42] stipulate testing as only viable method for determining the pull-out strength of powder actuated fasteners. Currently available testing protocols are given in AISI S905 [41] and ASTM E1190 [43]. The available strength (factored resistance) should be determined using safety factor $\Omega = 4.0$ (ASD) and resistance factors $\Phi = 0.40$ (LRFD) and $\Phi = 0.30$ (LSD). Moreover, nominal tensile pull-out strengths of powder actuated fasteners for specific fastener diameters and embedment depths based on the experimental investigation are given in the work of Mujagic et al. [37].

Failure mechanisms for powder actuated fasteners which are loaded in shear are shear fracture, bearing and tilting, pull-out, net section checks, and nominal shear strength (resistance) limited by edge distance, according to AISI S100-16 [42]. The nominal shear strength (resistance) of powder actuated fasteners should be determined multiplying the nominal tension strength (resistance) by factor 0.6 and using safety factor $\Omega = 2.65$ (ASD) and resistance factors $\Phi = 0.60$ (LRFD) and $\Phi = 0.55$ (LSD).

Bearing and tilting strength of powder actuated fasteners should be calculated according to Eq. 2.19 which is proposed by Mujagic et al. [37] who performed investigation for two types of powder actuated fasteners and limitations regarding thicknesses of members which are not in contact with fastener head or washer t_2 and members which are in contact with fastener head or washer t_1 , $t_2 / t_1 \geq 2.0$ and $t_2 \geq 3.18$ mm. Since the investigation performed by Mujagic et al. [37] was performed for two types of fasteners the conservative value of equation factor $\alpha_b = 3.2$ was set according to recommendations given in EN 1993-1-3:2009 [28] (see Eq. 2.8) for all types of fasteners.

$$P_{nb} = \alpha_b \cdot d_s \cdot t_1 \cdot F_{ul} \quad (2.19)$$

with:

$$\Omega = 2.05 \text{ (ASD); } \Phi = 0.80 \text{ (LRFD); } \Phi = 0.65 \text{ (LSD)}$$

In previous expression:

α_b is the factor which value depends on type of powder actuated fastener;

d_s is the nominal shank diameter.

Pull-out of fasteners in shear is dominantly determined by fastener tilting. Failure and is obtained for wide range of t_2 / t_1 ratios. The bearing strength given in Eq. 2.19

considers the influence of tilting deformation on bearing strength for low ratios of t_2 / t_1 and therefore does not give a good prediction of connection resistance. Therefore, AISI S100-16 [42] stipulates the separate control of pull-out strength for whole range of thicknesses, $2.87 \text{ mm} \leq t_2 \leq 19.1 \text{ mm}$ and depth of penetration of at least of $0.6 t_2$ according to Eq. 2.20.

$$P_{\text{nos}} = d_{\text{ae}}^{1.8} \cdot t_2^{0.2} \cdot (F_{y2} \cdot E^2)^{\frac{1}{3}} / 30 \quad (2.20)$$

with:

$$\Omega = 2.55 \text{ (ASD)}; \Phi = 0.60 \text{ (LRFD)}; \Phi = 0.50 \text{ (LSD)}$$

In previous expression:

d_{ae} is the average embedment diameter computed as average of installed fastener diameters measured at near side and far side of embedment material or d_s for PAF installed such that entire point is located behind far side of embedment material;

t_2 is the thickness of member not in contact with powder actuated fastener head or washer;

F_{y2} is the yield stress of member not in contact with powder actuated fastener head or washer;

E is the modulus of elasticity of steel.

Based on the work of Beck and Engelhardt [44], AISI S100-16 [42] stipulates calculation of net section rupture strength based on the Eq. 2.21 with hole diameter which is 1.10 times the powder actuated fastener diameter. Net area subjected to shear should be calculated according to Eq. 2.22 when each fastener pulls through the material and Eq. 2.23 for beam end connections.

$$P_{\text{nv}} = 0.6 \cdot F_u \cdot A_{\text{nv}} \quad (2.21)$$

with:

$$A_{\text{nv}} = 2 \cdot n \cdot t \cdot e_{\text{net}} \quad (2.22)$$

$$A_{\text{nv}} = (h_{\text{wc}} - n_b \cdot d_h) \cdot t \quad (2.23)$$

$$\Omega = 3.00 \text{ (ASD)}; \Phi = 0.50 \text{ (LRFD)}; \Phi = 0.75 \text{ (LSD)}$$

In previous expressions:

- F_u is the tensile strength;
- A_{nv} is the net area subjected to shear;
- n is the number of fasteners on critical cross section;
- t is the base steel thickness of section (Eq. 2.22); the thickness of coped web (Eq. 2.23);
- e_{net} is the clear distance between end of material and edge of fastener hole;
- h_{wc} is the coped flat web depth;
- n_b is the number of fasteners along failure path being analysed;
- d_h is the diameter of hole.

Moreover, the same criteria given in Eq. 2.21 should be used for shear strength limited by edge distance based in the nominal shank diameter d_s . Also, AISI S100-16 [42] defines combined shear and tension resistance according to same design procedure given in EN 1993-1-3:2009 [28] and Eq. 2.13.

2.5. Summary

Overview of mechanically fastened shear connectors for composite action of steel and concrete with main focus on X-HVB shear connectors is presented. This type of shear connector is used in experimental and numerical investigation focusing on analytical definition of obtained failure mechanisms. Failure of cartridge fired pins, as mechanical fasteners for connection of X-HVB shear connectors, is the main failure mechanism of shear connectors. Therefore, overview of the previous experimental investigations and design recommendations of cartridge fired pins is also presented in this chapter.

Most of the results of experimental investigations of X-HVB shear connectors and cartridge fired pins both are contained in the technical reports which are considered as proprietary of the manufacturers and therefore not available to the researchers and engineers. This chapter presents summarized results of the most important conclusions drawn from previous experimental investigations of X-HVB shear connectors available in literature and presented in proprietary technical reports obtained by kindness of Hilti Company.

Chapter 3. X-HVB shear connectors vs. headed studs shear resistance

3.1. Various application of X-HVB shear connectors

In order to gain a better insight in the possible application of X-HVB shear connectors in composite structures, it is important to compare their shear resistance with resistance of extensively used welded headed studs. According to ETA-15/0876 assessment [7], characteristic shear resistance of X-HVB shear connectors in solid concrete slabs is from 29.0 kN to 37.5 kN, for 40.0 mm to 140.0 mm connector height, respectively (see Table 2.1). This is less than 50 % of shear resistance of 19.0 mm headed stud with height of 120.0 mm and concrete class C25/30 [45].

Table 3.1 Headed stud vs. X-HVB shear connector resistance, adapted from [45]

Shear connectors	Design resistance of one connector P_{Rd} (kN)		Reduction coefficients for shear connectors used with profiled steel sheeting transverse to the beam
	Solid concrete slab	Composite slab (profiled sheeting)	k_t (-)
<p>Headed studs $d=19$ mm [11]</p>	73.7	55.3	$k_t = \min\left(0.75; \frac{0.7}{\sqrt{n_r}} \cdot \frac{b_0}{h_p} \left(\frac{h_{sc}}{h_p} - 1\right)\right)$ $h_{sc}=120 \text{ mm}$ $n_r=1$
<p>X-HVB 125 [7]</p>	28.0	23.8	$k_t = \min\left(1.0; \frac{0.66}{\sqrt{n_r}} \cdot \frac{b_0}{h_p} \left(\frac{h_{sc}}{h_p} - 1\right)\right)$ $h_{sc}=125 \text{ mm}$ $n_r=2$
	28.0	28.0	

* concrete class C25/30, $f_{ck}=25$ MPa, $E_{cm}=31$ GPa; headed studs with height 120 mm, 19 mm diameter and steel material with $f_y=350$ MPa and $f_u=450$ MPa; profiled sheeting with thickness $t \leq 1$ mm and dimensions according to drawings.

Comparison of design resistances of headed stud shear connector with 19.0 mm diameter and X-HVB 125 shear connector in solid and composite concrete slab is presented in Table 3.1. Approximately three X-HVB 125 shear connectors should be used to replace one headed stud with 19.0 mm diameter in solid concrete slab, considering obtained shear resistance. For specific re-entrant profiled sheeting geometry given in Table 3.1, two X-HVB 125 shear connectors can replace one 19.0 mm diameter headed stud. Headed stud shear connector with 19.0 mm diameter is frequently used shear connector for composite floor structures which can accomplish full shear connection for wide range of composite floor layouts (different beam spans and distances) and geometries of profiled sheeting.

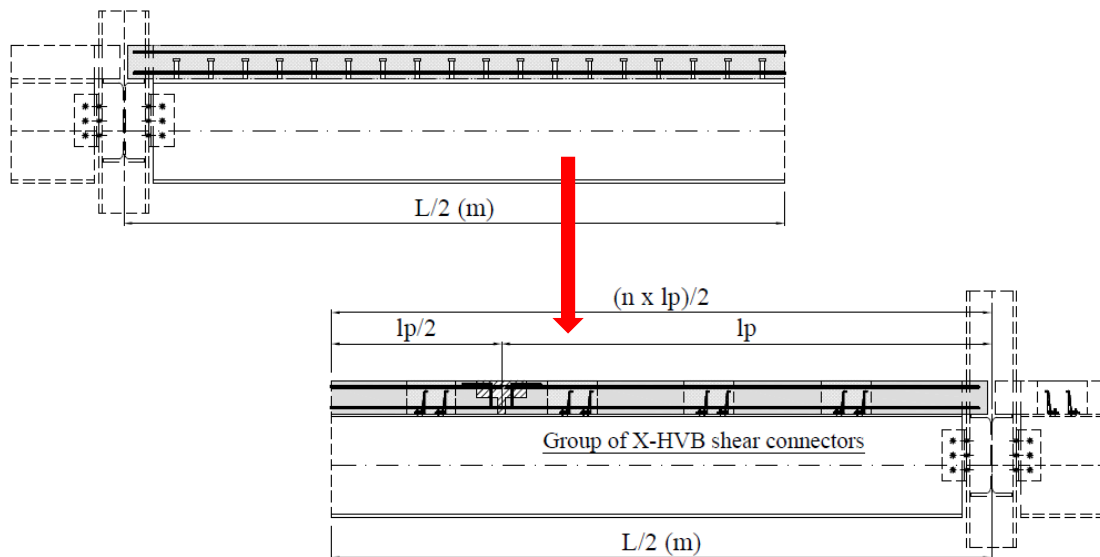


Figure 3.1. Different types of shear connectors – possibilities for renovation of existing composite structures

Comparative analysis of shear resistance of headed studs and X-HVB shear connectors can be of particular importance in case of renovation of existing composite structures, when solid concrete slabs with headed studs should be replaced with prefabricated concrete slabs with envisaged openings and X-HVB shear connectors, as given in Figure 3.1. Installation of X-HVB shear connectors should meet current requirements given in ETA-15/0876 assessment [7] considering recommendations for minimal distances between shear connectors. Analysis of group arrangement of X-HVB shear connectors in envisaged openings of prefabricated concrete slabs at distances smaller than minimal recommended is presented in this thesis through experimental and

numerical analysis. Also, group arrangement of shear connectors is of particular importance for composite floor structures when positioning of shear connectors are restricted with dimensions of profiled sheeting ribs.

3.2. Reduction factor of X-HVB shear connectors in composite floor structures

Analysis of shear resistance reduction factors of X-HVB shear connectors in composite concrete slabs with transverse position of ribs relative to the beam axis and two shear connectors per one rib is shown in Figure 3.2. X-HVB shear connectors with lower height than 80.0 mm are not applicable in composite construction with profiled steel sheeting, according to ETA-15/0876 assessment [7]. The analysis presented in Figure 3.2 included five different types of profiled sheeting with various decking rib width / height ratios.

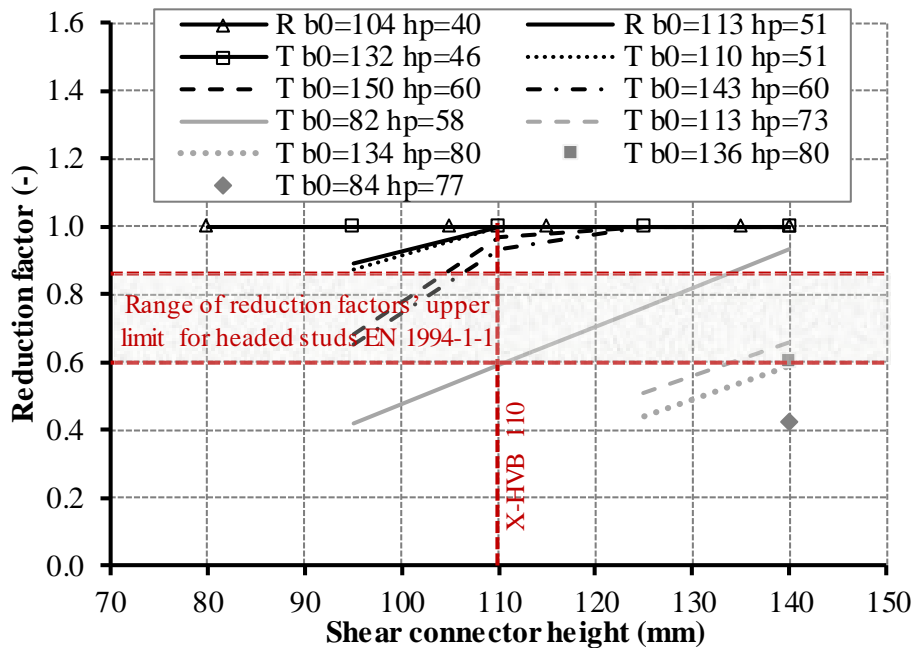


Figure 3.2. Shear resistance reduction factor of X-HVB shear connectors for decking ribs transverse to the beam axis – $n_r=2$

Manufacturer recommendations [7] both for allowed decking rib width and decking rib / connector height ratios are considered. Analysis included trapezoidal and re-entrant profiled sheeting, designated with T and R in Figure 3.2, respectively. Also, Figure 3.2 gives designation of mean width of concrete rib for trapezoidal (T) profiled sheeting or minimum width of re-entrant (R) profiled sheeting b_0 and overall depth of profiled sheeting h_p instead of profiled sheeting designation obtained by manufacturer. These

designations have been presented in Figure 3.2 in order to gain better insight in influence of two main geometrical properties of analysed profiled sheeting (b_0 and h_p) on the value of shear resistance reduction factor.

Upper limit for shear resistance reduction factor of X-HVB shear connectors is 1.0, according to ETA-15/0876 assessment [7] in comparison to the 0.60 - 0.85 which is used for welded headed studs with diameters up to 20.0 mm (see Figure 3.2), according to EN 1994-1-1:2004 [11]. Installation of X-HVB shear connectors in wide trapezoidal and re-entrant profiled sheeting (T and R designation respectively, see Figure 3.2) with height h_p up to 46.0 mm and width of concrete rib b_0 in range from 104.0 to 132.0 mm would not induce reduction of X-HVB shear connector resistance for whole range of connectors heights, as shown in Figure 3.2. For height of profiled steel sheeting $h_p = 51.0$ mm and width of concrete rib $b_0 = 110.0 - 113.0$ mm of both analysed profiled sheeting geometries (trapezoidal T and re-entrant R, see Figure 3.2) obtained reduction of shear resistance is up to 13 %, but only for X-HVB shear connectors lower than 110.0 mm. Application of higher X-HVB shear connectors with analysed profiled sheeting geometries would not result in reduction of shear resistance. Profiled steel sheeting with narrow and high ribs (for example T $b_0 = 82$ $h_p = 58$, see Figure 3.2) would influence larger reduction of X-HVB shear resistance, even for 60 %. However, for wide range of profiled sheeting geometries (R $b_0 = 104$ $h_p = 40$, R $b_0 = 113$ $h_p = 51$, T $b_0 = 132$ $h_p = 46$, T $b_0 = 110$ $h_p = 51$, T $b_0 = 150$ $h_p = 60$ and T $b_0 = 143$ $h_p = 60$, see Figure 3.2) reduction of shear resistance is not obtained for X-HVB shear connectors higher than 125.0 mm.

Reduction factor for X-HVB shear connectors is calculated using Eq. 2.5 [7], as presented in Chapter 2.3.3. Approximately the same expression is used for headed studs, according to EN 1994-1-1:2004 [11] for transversal positioning of profiled sheeting ribs relative to the steel beam axis. The value of coefficient in Eq. 2.5 for reduction factor $k_{t,1}$ of X-HVB shear connectors is 0.66 [7] in comparison to the 0.70 which is used for headed studs according to EN 1994-1-1:2004 [11]. Moreover, X-HVB shear connectors can be positioned transverse to the steel beam axis [7], with similar behaviour considering reduction of shear resistance (see Eq. 2.6 and Eq. 2,7), which is in detail explained in Chapter 2.3.3. Reduction factor for X-HVB 110 shear connector, which is used for experimental investigation presented in this thesis, is from 0.87 - 1.00 for wide range of profiled steel sheeting geometries, except narrow and high profiled ribs (T $b_0 = 82$ $h_p =$

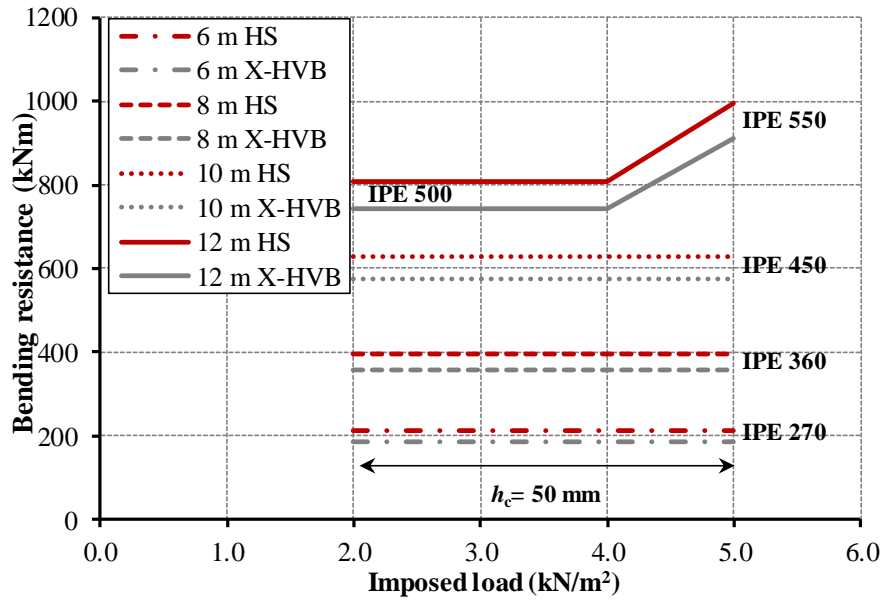
58, see Figure 3.2). Therefore, X-HVB shear connectors are competitive to the traditionally used welded headed studs, in solid and composite concrete slabs with profiled steel sheeting, considering their shear resistance, installation requirements and simple installation procedure.

3.3. Parametric analysis of X-HVB shear connectors in composite floor structures

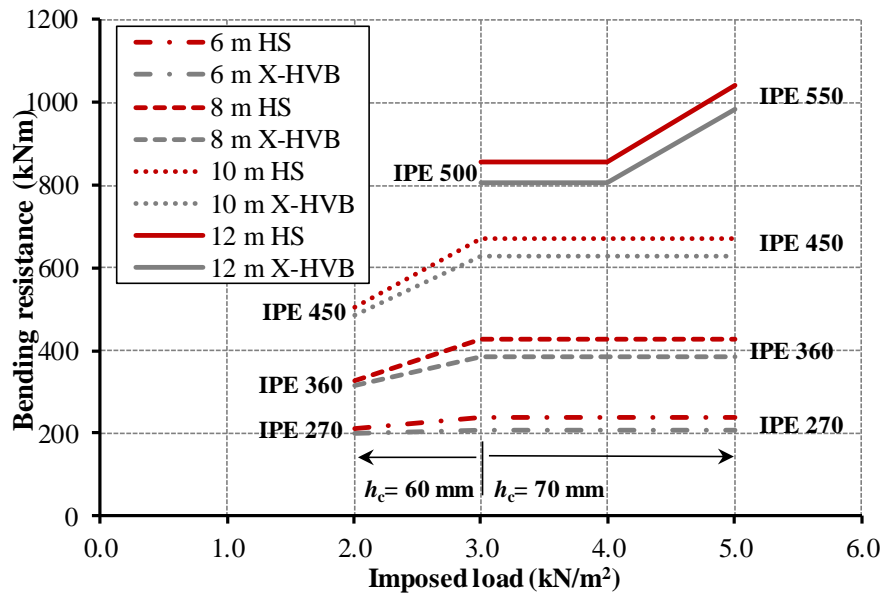
Comparative analysis of shear resistances of headed stud shear connector with 16.0 mm – 22.0 mm diameter with resistance of X-HVB 95 – X-HVB 125 shear connectors in composite concrete slabs with trapezoidal profiled sheeting ComFlor 60 (CF60 $b_0 = 149.0$ mm and $h_p = 60.0$ mm) and re-entrant profiled sheeting Comflor 51+ (CF51+ $b_0 = 110.0$ mm and $h_p = 51.0$ mm) is presented by Samardžić [46]. Analysis included composite beams with span from 6.0 m to 15.0 m with distances between beams (composite floor span) from 3.0 m to 5.0 m. Also, parametric analysis included various values of imposed loads, from 2.0 kN/m² to 5.0 kN/m². The aim of presented parametric analysis was to investigate decrease of bending resistance of composite beam when headed stud shear connector is replaced with X-HVB shear connector through partial shear connection, according to recommendations given in EN 1994-1-1:2004 [11] and ETA-15/0876 assessment [7].

Reduction of bending resistance of composite beam cross-section when one headed stud is replaced with two X-HVB shear connectors for various spans and imposed loads is presented in Figure 3.3. Presented results are obtained for beam distances (composite floor span) of 3.0 m. Relatively uniform reduction of composite beam bending resistance is obtained for all analysed beam spans and imposed loads when one headed stud shear connector with diameter of 16.0 mm is replaced with two X-HVB 110 or X-HVB 125 shear connectors, as presented in Figure 3.3. Height of the concrete h_c above the profiled sheeting was set as 50.0 mm for trapezoidal profiled sheeting CF60 for whole range of imposed loads and composite beam spans, while height of the concrete h_c of 60.0 mm and 70.0 mm was set for re-entrant profiled sheeting CF51+, as presented in Figure 3.3. Concrete height h_c of 60.0 mm was adopted for imposed load lower than 3.0 kN/m², while higher concrete above profiled sheeting is applied for imposed load of 3.0 kN/m² and larger. Change in bending resistance of composite cross-section for specific value of imposed load presented in Figure 3.3, is obtained due to change of steel cross-section in

order to satisfy design recommendations. Accomplished reduction of bending resistance, for wide range of imposed loads and beam spans, when one headed stud shear connector is replaced with two X-HVB shear connectors, is up to 13 %, due to obtained partial shear connection, as shown in Figure 3.3.



a) trapezoidal profiled sheeting CF60



b) re-entrant profiled sheeting CF51+

Figure 3.3. Reduction of composite beam bending resistance for 3.0 m distance of composite beams (composite floor span)

Lower limit of partial shear connection of composite beams in buildings with headed studs is 40 %, according to EN 1994-1-1:2004 [11]. This lower limit of partial

shear connection is accomplished for results presented in Figure 3.3, for both analysed shear connector types, i.e. headed studs and X-HVB shear connectors. Due to lower shear resistance of X-HVB shear connectors in comparison to the headed studs, aforementioned lower limit of partial shear connection often can not be satisfied when this type of shear connector is applied considering recommendations for minimal distances between connectors given in ETA-15/0876 assessment [7]. According to the parametric analysis presented in the work of Samardžić [46], when analysed trapezoidal profiled sheeting is applied (CF60), lower limit of partial shear connection can be satisfied for composite beam spacing up to 4.0 m (including beam spacing of 4.0 m) and beam spans up to 12.0 m but only for low values of imposed loads (approximately up to 2.0 kN/m²). For analysed re-entrant profiled sheeting (CF51+), lower limit of partial shear connection can be satisfied for beam distances up to 3.0 m and beam spans up to 15.0 m for whole range of imposed loads, from 2.0 kN/m² to 5.0 kN/m².

3.4. Summary

The aim of this investigation is to perform comparative analysis of headed stud and X-HVB shear connector resistance in solid and composite floor structures with profiled steel sheeting. Parametric analysis included various composite floor and beam spans in order gain better insight in application of X-HVB shear connectors in composite floor structures.

Lower limit of partial shear connection which is given in EN 1994-1-1:2004 [11] as 40 % is often compromised when X-HVB shear connectors are applied for composite floor structures with larger distances between composite beams than 3.0 m and meeting the requirements for minimal shear connector distances given in ETA-15/0876 assessment [7]. Positioning of shear connectors with distances smaller than minimal recommended can result in increase of shear connectors number over the beam span and therefore in accomplishment of the aforementioned requirements of partial shear connection given in EN 1994-1-1:2004 [11] for composite floor structures of buildings. Experimental and FE analysis of group arrangement of X-HVB shear connectors at distances which are smaller than minimal recommended is presented further in this thesis.

Chapter 4. Experimental work

Experimental work was separated into two distinct investigation programs: push-out tests of mechanically fastened X-HVB 110 shear connectors and shear and tension tests of X-ENP-21 HVB cartridge fired pins. Push-out tests were performed in order to investigate behaviour of mechanically fastened shear connectors in prefabricated concrete slabs. Behaviour of cartridge fired pins was analysed through pull-out resistance of variously loaded pins. The experimental results were used to calibrate numerical models and further, to perform parametric analysis with different steel and concrete material properties of push-out tests.

4.1. Experimental program of push-out tests

Geometrical properties of X-HVB 110 shear connector and X-ENP-21 HVB cartridge fired pins, which were used in push-out tests are presented in Figure 4.1. Push-out tests were divided into three phases, in which seventeen push-out specimens were prepared and examined, according to recommendations given in EN 1994-1-1:2004 [11].

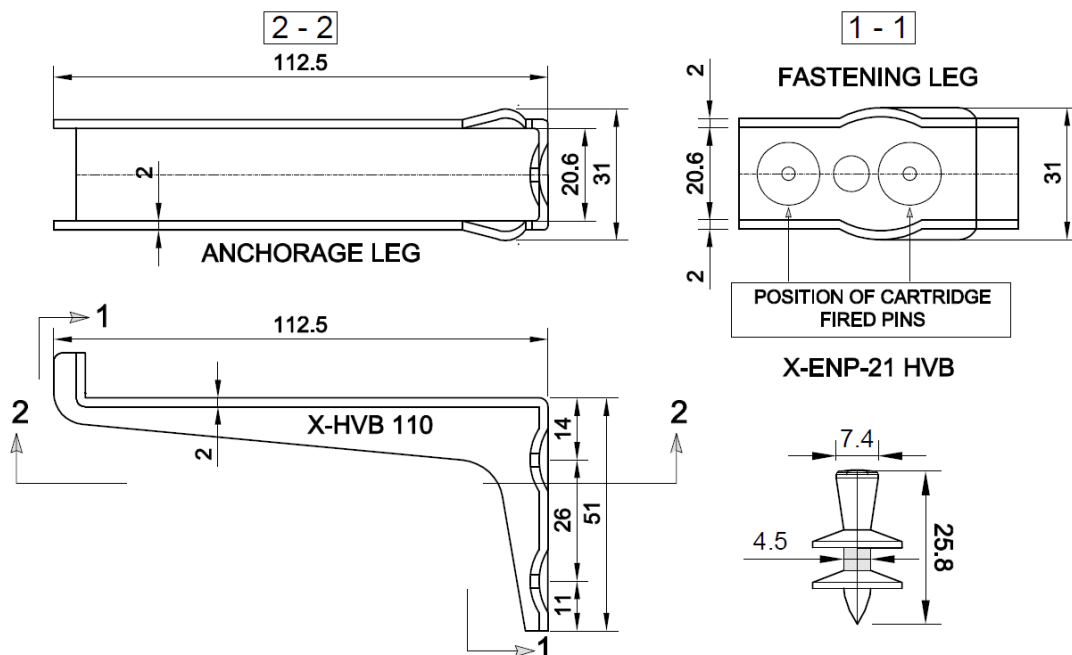


Figure 4.1. Geometrical properties of shear connector and cartridge fired pin

X-HVB 110 shear connectors were positioned into the envisaged openings of the prefabricated concrete slabs, four shear connectors on each HEB 260 (S275) steel beam

flange, eight shear connectors per specimen in total. Experimental phases of push-out tests were:

- Phase 1: X-HVB shear connectors were positioned at minimal longitudinal and transversal distances, which are recommended by ETA-15/0876 assessment [7]. In this experimental phase, behaviour of shear connectors was analysed through two orientations relative to the shear force direction, forward orientation (HSF series) and backward orientation (HSB series), as shown in Figure 4.2. Four specimens for each orientation were examined, eight specimens for first phase in total. Installation of cartridge fired pins was performed with nominal prescribed installation power level of 3.5.
- Phase 2: Forward orientation of shear connectors was further examined through second phase (HSFg series), with group arrangement of shear connectors, which were installed with reduced longitudinal and transversal distances, as shown in Figure 4.2. Installation power level which was used for installation of cartridge fired pins for HSFg test series was 2.0. Four test specimens within this push-out phase were examined.
- Phase 3: Group arrangement of forward oriented shear connectors with reduced distances and identical installation power level as for first phase was analysed through HSFg-2 push-out specimens of third phase. Five push-out specimens were examined.

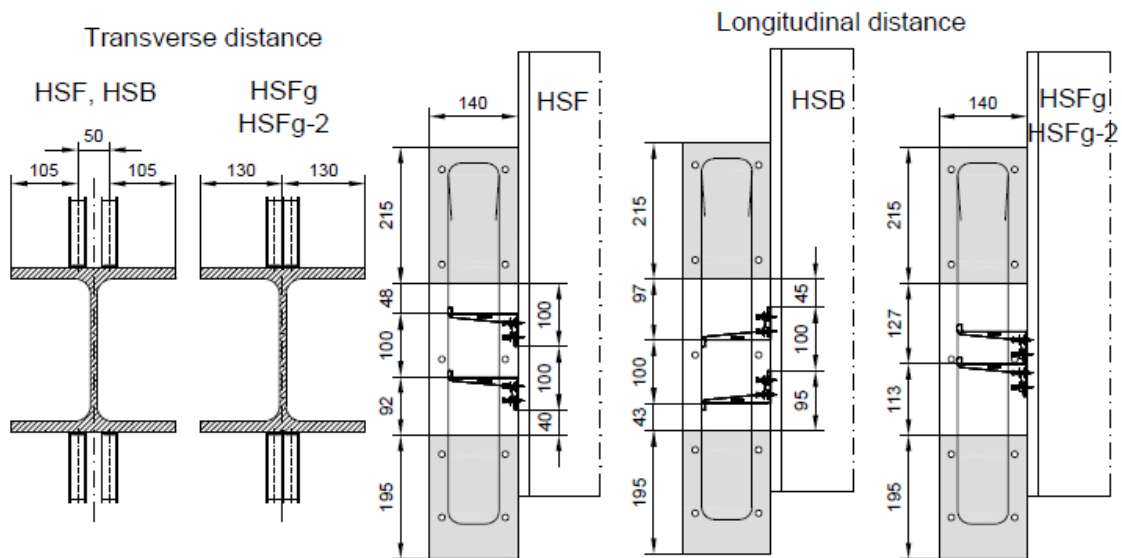
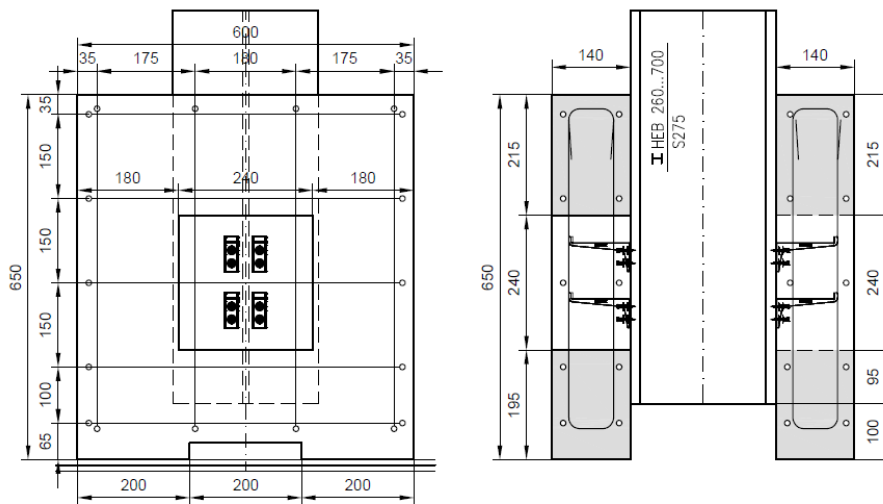
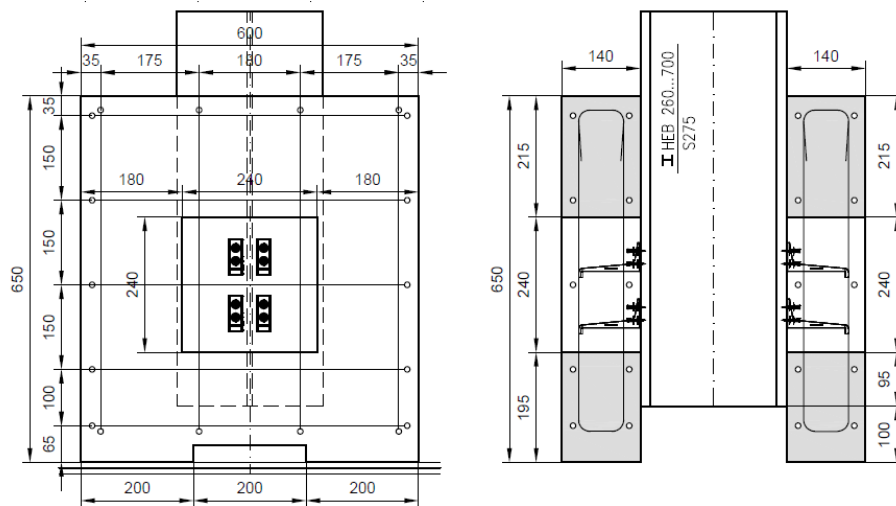


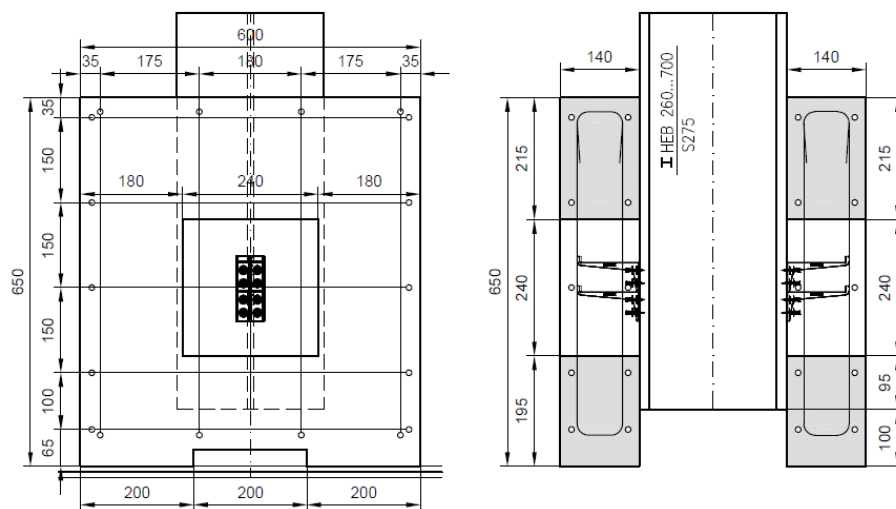
Figure 4.2. Position of shear connectors in envisaged openings



a) HSF specimens



b) HSB specimens



a) HSFg and HSFg-2 specimens with different installation power levels

Figure 4.3. Push-out test specimens layout

Table 4.1. Geometrical properties of push-out specimens

Series	Specimes number	Connectors number	Connectors spacing		Concrete slabs		Power level
	N_{spc}	N_{con}	longit. (mm)	transv. (mm)	depth (mm)	dimensions (mm)	
HSF	4	8	100	50	140	600x650	3.5
HSB	4	8	100	50	140	600x650	3.5
HSFg	4	8	0	0	140	600x650	2.0
HSFg-2	5	8	0	0	140	600x650	3.5

Push-out specimens were prepared and tested in the Laboratory of Materials at the University of Belgrade, Faculty of Civil Engineering. Examined test series, are designated in Figure 4.3 and presented in Table 4.1.

4.2. Specimens preparation

Concrete slabs with dimensions of 600x650x140 mm and openings in the middle of the slab were prefabricated by casting them in horizontal position in “ASA IBELIK” plant in Velika Plana, as shown in Figure 4.4.



Figure 4.4. Prefabrication of concrete slabs in “ASA IBELIK” concrete plant

The same dimensions of openings (240x240 mm), which were envisaged for later assembly of shear connectors, were adopted for all examined specimens. Concrete slabs were reinforced with standard reinforcement layout with 10.0 mm diameter ribbed bars and B500B grade, as shown in Figure 4.3. Two horizontal ribbed bars, in upper and

bottom reinforcement layer, were positioned between shear connectors of all examined specimens, as shown in Figure 4.3 and Figure 4.5.



Figure 4.5. *Push-out specimens assembling*

Installation of X-ENP-21 HVB cartridge fired pins for push-out test specimens was performed using DX 76 MX direct fastening tool (piston X-76-P-HVB) [15], with cartridges 6.8/18 M blue colour code (Figure 4.6). Minimum and maximum level for power regulation on the fastening tool for installation of pins is 1 and 4, respectively. Installation power levels, which were applied for connectors installation of HSF, HSB, HSFg and HSFg-2 specimens is shown in Table 4.1. Installation of cartridge fired pins for push-out tests was performed by technical staff of Hilti Company in Belgrade.



Figure 4.6. *Installation of X-ENP-21 HVB cartridge fired pins*

In order to avoid effects of bond between steel flanges and infill concrete used for envisaged openings, connecting surfaces of steel beams were greased. After the installation procedure of shear connectors was performed and steel flanges were greased, prefabricated concrete slabs were positioned on steel beam flanges. Afterwards, inner surfaces of envisaged openings were cleaned and treated with the layer of structural adhesive (Sikadur™ 30) as the continuing layer between infill and old concrete, as shown in Figure 4.5.



a) specimens after concreting

b) specimens prepared for testing

Figure 4.7. Specimens after assembling

Envisaged openings were filled in horizontal position with three-fraction concrete. After concreting of envisaged openings and in order to minimize initial cracks due to shrinkage, specimens were kept in the wet condition during first three days. After three days, half assembled specimens were turned in order to perform the same assembling procedure on the other specimen side. Half assembled specimens of experimental phase 1 and specimens prepared for push-out testing procedure are shown in Figure 4.7.

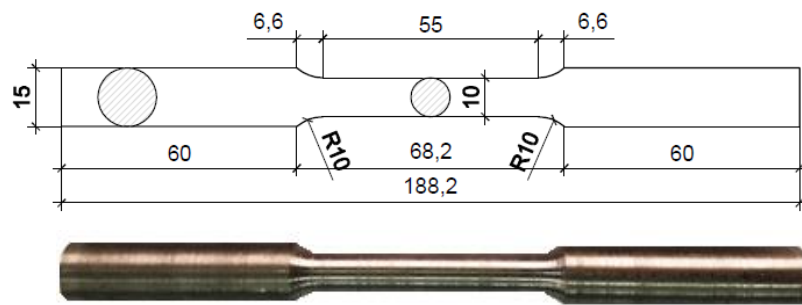
4.3. Material properties

Material properties of steel beams HEB 260, X-HVB 110 shear connectors, infill concrete and concrete of prefabricated slabs which were used in push-out tests were obtained by the standard experiments, which were performed in the Laboratory of Materials, Faculty of Civil Engineering. Material properties of X-ENP-21 HVB cartridge fired pins were provided by kindness of Hilti Company. As they are considered as proprietary, those are not explained here in detail. Statistical evaluations of examined material properties were performed, according to EN 1990:2010, Annex D [47]. Coefficient of variation V_x and characteristic value X_k of a specific material property were

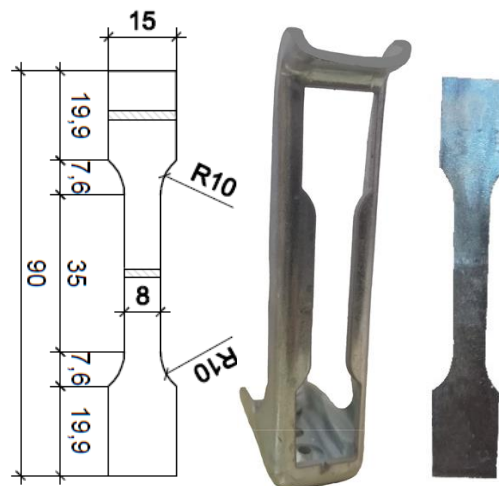
determined based on factor k_n for 5 % characteristic value, according to the number of examined specimens and considering the case that there is no prior knowledge of value of coefficient of variation V_x . Therefore, adopted value of factor k_n was 3.37 and 2.63 for three and four specimens, respectively.

4.3.1. Steel profile and X-HVB shear connector

Material properties of steel beam and shear connector were examined through coupon tensile tests. Tensile coupons were longitudinally cut from steel beam flange and shear connector anchorage leg, four coupons from each, as shown in Figure 4.8. Tensile coupons prior the testing along with their dimensions are shown in Figure 4.8. Round tensile coupons from steel beam flange with 10.0 mm diameter were built with 55.0 mm gauge length, L_0 . Flat tensile coupons were built with 36.0 mm gauge length L_0 and 1.9 mm to 2.0 mm thickness, which was determined with thickness of shear connector. Total length of flat coupons was 90.0 mm, which was the maximum tensile coupon length that can be built from X-HVB 110 shear connector.



a) round test coupons - beam flange



b) flat test coupons - shear connector

Figure 4.8. Tensile test coupons

Testing procedure was set according to recommendations given in EN 10002-1:2001 [48]. A uniform strain rate of 0.1 mm/min for the initial part of the tests, up to approximately 1 % strain increasing to 2.2 mm/min thereafter, was prescribed for each tensile test coupon. Figure 4.9 shows tensile coupons prior to fracture and after the testing procedure. Figure 4.9 shows tensile coupons prior to fracture and after the testing procedure.



a) tensile tests of round coupons

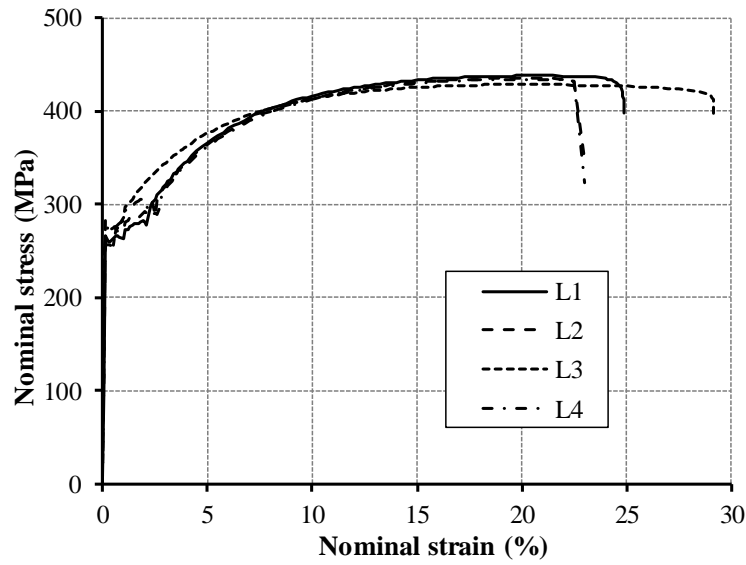


b) tensile tests of flat coupons

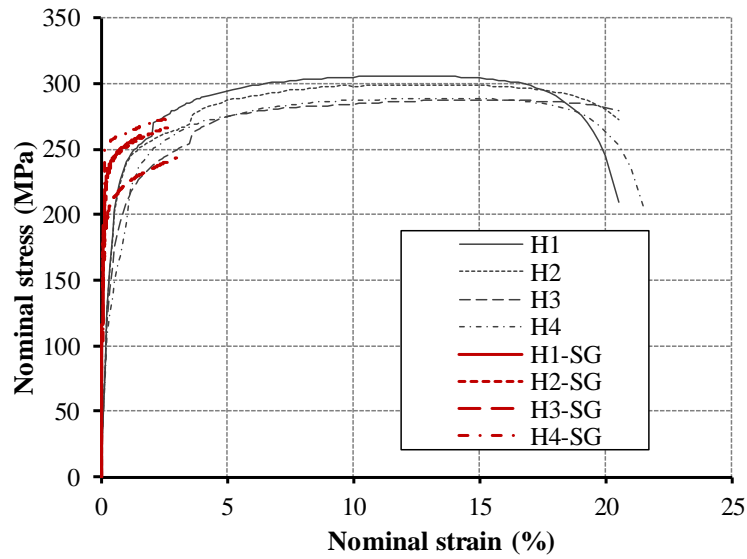
Figure 4.9. Tensile tests procedure and test coupons after fracture

All tests were performed in the servo-hydraulic testing machine Shimadzu, with a capacity of 300.0 kN. The elongations of the round coupons were monitored using a digital extensometer with a measuring range of 25 %, as shown in Figure 4.9a. Due to specific geometry of flat coupons, elongation measurements with digital extensometer was not applicable. Therefore, one electronic strain gauge with length of 10.0 mm was mounted on each side of flat tensile coupon (two strain gauges per one tensile coupon) in order to monitor the elongation, according to recommendations which Arrayago et al.

presented in his work [49], as shown in Figure 4.9b. All data were recorded using a data acquisition system.



a) beam flange



b) shear connector

Figure 4.10. Nominal stress-strain curves

Nominal stress-strain curves for both examined types of test coupons are shown in Figure 4.10. Material properties of all examined test coupons of steel beam and shear connectors are presented in Table 4.2 and Table 4.3, respectively, with statistical evaluation of obtained results. It can be seen from Figure 4.10a that yield strength is distinctly pronounced for steel beam material. According to the obtained results for beam flange tensile coupons, average value of yield strength and tensile strength was 266.4

MPa and 433.6 MPa, respectively for four examined tensile coupons. Therefore, material properties of steel beam of push-out tests correspond to the steel grade S235.

Table 4.2. *Steel beam material properties*

Specimen	Test coupon geometry		Material properties		
	diameter	cross-section area	yield strength	ultimate strength	modulus of elasticity
	d (mm)	A (mm ²)	f_y (N/mm ²)	f_u (N/mm ²)	E (GPa)
L1	9.81	75.58	259.7	437.6	197.6
L2	10.0	78.54	273.8	434.7	223.3
L3	10.0	78.54	255.5	428.1	-
L4	9.90	76.98	276.5	434.1	207.4
Mean			266.4	433.6	209.4
St. deviation			10.3	4.0	
Variation (%)			3.9	0.9	
Characteristic			239.2	423.1	

X-HVB shear connectors were built from material which obtained predominately nonlinear stress-strain relationship, as shown in Figure 4.10b. Initial part of the stress-strain curves, up to 3 % of strain, was obtained from measurements of strain gauges, which is given in Figure 4.10b with curves H1-SG to H4-SG. Nominal stress-strain curves denoted with H1 to H4 represent measurements from testing machine based on the displacement of the machine grips and gauge length of 36.0 mm.

Table 4.3. *Shear connector material properties*

Specimen	Test coupon geometry		Material properties		
	thickness	cross-section area	proof stress	ultimate strength	modulus of elasticity
	t (mm)	A (mm ²)	f_{02} (N/mm ²)	f_u (N/mm ²)	E (GPa)
H1	1.90	15.20	236.2	305.7	234.0
H2	1.90	15.20	233.0	299.1	218.0
H3	1.90	15.20	202.1	287.2	202.0
H4	1.98	15.84	255.9	288.7	208.7
Mean			231.8	295.2	215.6
St. deviation			22.2	8.8	
Variation (%)			9.6	3.0	
Characteristic			173.4	272.1	

Average value of 0.2 % proof stress f_{02} obtained from measurements of strain gauges for four tensile coupons is 231.8 MPa. Average tensile strength is 295.2 MPa.

Nominal material properties of base material DC04 (Material Number 1.0338), according to EN 10130:2006 [14], are: conventional yield strength $R_e = 140$ to 210 N/mm², tensile strength $R_m = 270$ to 350 N/mm² and $A_{80} \geq 38$ %. Lower yield strength should be used for design purposes, according to EN 10130:2006 [14]. Development and examination of tensile coupons from round parts of shear connectors were not possible due to specific geometry and relatively small dimensions of shear connector. Analysing experimentally obtained data, it can be concluded that manufacturing process of X-HVB shear connectors leads to material strength-enhancement, both in flat and round parts of shear connector which is introduced in material models of push-out tests specimens FE analysis.

4.3.2. Concrete

Prefabricated concrete slabs were casted using four batches of concrete within four days in “ASA IBELIK” plant. Infill concrete for envisaged openings of prefabricated slabs was produced for three separate phases of push-out tests and was made at the Laboratory of Materials with three fractions of aggregate. For infill concrete, Portland cement LAFARGE PC 20M(S-L) 42.5R was used. In order to reduce shrinkage of infill concrete, two types of concrete admixtures were applied: Sika[®] concrete admixture ControlTM 40 and Sika[®] superplasticizer admixture ViscoCreteTM 1020X. Infill concrete composition is given in Table 4.4. Concrete admixture was adopted according to comparable research programs in the field of composite steel-concrete structures performed by Spremić [3] and Pavlović [4] at the Faculty of Civil Engineering.

Table 4.4. Quantities of infill concrete admixtures

Water (kg/m ³)	Cement (kg/m ³)	Aggregate (kg/m ³)			Admixtures (kg/m ³)	
		0-4 mm	4-8 mm	8-16 mm	Control TM 40	ViscoCrete TM 1020X
162	320	822	478	611	6.4	1.92

In order to investigate concrete material properties of prefabricated concrete slabs and infill concrete used for three phases of experimental research, standard experiments for determination of concrete compressive strength ($f_{c,cube}$ and $f_{c,cyl}$), splitting tensile strength $f_{ct,sp}$ and elastic modulus E_{cm} were performed, as shown in Figure 4.11.

In order to determine axial tensile strength of infill concrete, splitting tensile strengths $f_{ct,sp}$ of concrete cylinders were converted to axial tensile strength f_{ctm} , according to Eq. 4.1, EN 1992-1-1:2004 [50].

$$f_{ctm} = 0.9 \cdot f_{ct,sp} \quad (4.1)$$

In previous expression:

f_{ct} is the axial tensile strength of concrete;

$f_{ct,sp}$ is the splitting tensile strength of concrete.

Push-out tests were performed in different periods: phase 1 in October 2014; phase 2 in June 2015 and phase 3 in February 2016. Therefore, examined material properties of prefabricated concrete slabs were normalized at the age of 28 days and at the age of push-out tests.



a) elastic modulus examination b) splitting tensile strength examination

Figure 4.11. Standard tests to determine the material properties of concrete

In order to compare experimental results of concrete material properties with concrete classes defined in EN 1992-1-1:2004 [50], normalized values of material properties at 28 days of prefabricated slabs and infill concrete were calculated according Eq. 4.2, Eq. 4.3 and Eq. 4.4. Normalized values of material properties at the age of 28 days are shown in Annex A. Normalized value of compressive strengths of 15.0 cm cubes and D15x30 cm cylinders at age t was obtained according to Eq. 4.2 using aging coefficient β_{cc} . Normalized value of axial tensile strength of concrete at 28 days and at age

t was obtained according to Eq. 4.3, while modulus of elasticity was determined using Eq. 4.4.

$$f_{cm}(t) = \beta_{cc}(t) \cdot f_{cm} \quad (4.2)$$

$$f_{ctm}(t) = [\beta_{cc}(t)]^\alpha \cdot f_{ctm} \quad (4.3)$$

$$E_{cm}(t) = [f_{cm}(t) / f_{cm}]^{0.3} \cdot E_{cm} \quad (4.4)$$

with:

$$\beta_{cc}(t) = \exp \left\{ s \cdot \left[1 - \left(\frac{28}{t} \right)^{1/2} \right] \right\} \quad (4.5)$$

In previous expression:

$f_{cm}(t)$ is the mean concrete compressive strength at an age of t days;

f_{cm} is the mean compressive strength at 28 days, according to EN 1992-1-1:2004 [50];

$f_{ctm}(t)$ is the axial tensile strength at an age of t days;

f_{ctm} is mean value of axial tensile strength of concrete, according to EN 1992-1-1:2004 [50];

$E_{cm}(t)$ is the modulus of elasticity at an age of t days;

E_{cm} is the secant modulus of elasticity of concrete, according to EN 1992-1-1:2004 [50];

$\beta_{cc}(t)$ is a coefficient which depends on the age of the concrete t ;

t is the age of the concrete in days;

α is the coefficient which value depends on the age of the concrete t , and should be adopted as 1.0 for $t < 28$ days and as 2/3 for $t \geq 28$ days;

s is a coefficient which depends on the type of cement and should adopted according to recommendations given in EN 1992-1-1:2004 [50].

The major importance of creating a FE models is to define concrete material properties at the age of push-out tests. Normalized values of concrete compressive and tensile strength and modulus of elasticity at the age of testing for three push-out phases are given in Table 4.5, Table 4.6 and Table 4.7.

Table 4.5. Concrete material properties at the age of push-out tests - phase 1

	Compressive strength (cube)	Compressive strength (cylinder)	Axial tensile strength	Modulus of elasticity
	$f_{cm,cube}(t)$ (MPa)	$f_{cm,cyl}(t)$ (MPa)	$f_{ctm}(t)$ (MPa)	$E_{cm}(t)$ (GPa)
Prefabricated slabs FV	33.21	28.51	-	27.64
Prefabricated slabs FP	32.54	27.70	-	28.55
Age at testing	97	97	-	97
β_{cc}	1.097	1.097	-	1.097
Normalized value	36.06	30.83	-	30.82
Infill concrete	39.42	29.81	2.54	27.75

* determination of normalized concrete strength given in Annex A

Table 4.6. Concrete material properties at the age of push-out tests - phase 2

	Compressive strength (cylinder)	Axial tensile strength	Modulus of elasticity
	$f_{cm,cyl}(t)$ (MPa)	$f_{ctm}(t)$ (MPa)	$E_{cm}(t)$ (GPa)
Prefabricated slabs FV	28.51	-	27.64
Prefabricated slabs FP	27.70	-	28.55
Age at testing	342	-	342
β_{cc}	1.153	-	1.153
Normalized value	32.42	-	32.41
Infill concrete	33.11	2.64	32.90

* determination of normalized concrete strength given in Annex A

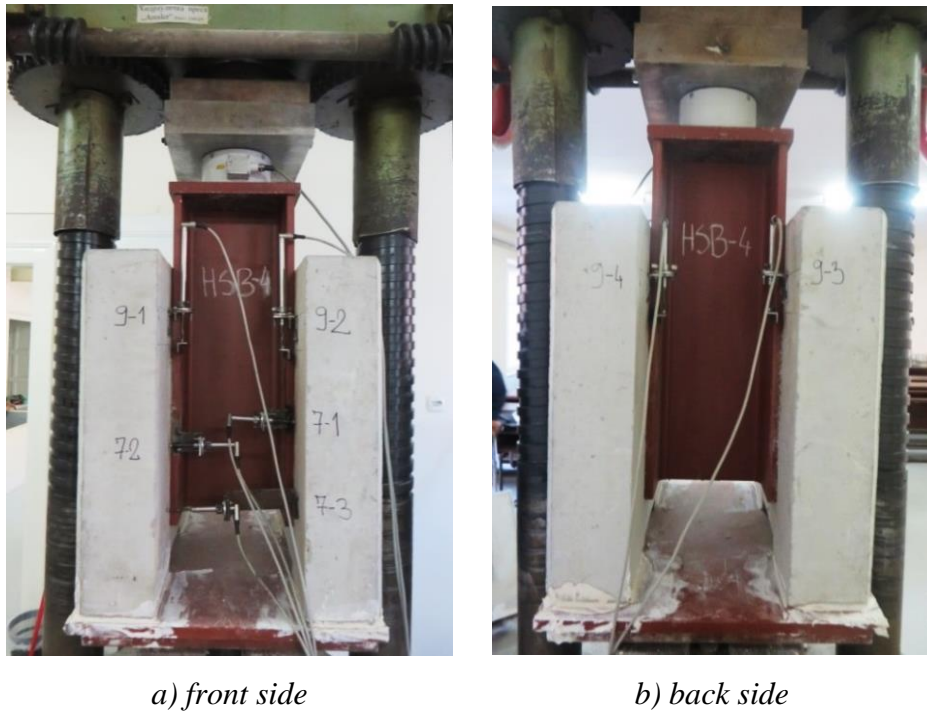
Table 4.7. Concrete material properties at the age of push-out tests - phase 3

	Compressive strength (cylinder)	Axial tensile strength	Modulus of elasticity
	$f_{cm,cyl}(t)$ (MPa)	$f_{ctm}(t)$ (MPa)	$E_{cm}(t)$ (GPa)
Prefabricated slabs FV	28.51	-	27.64
Prefabricated slabs FP	27.70	-	28.55
Age at testing	600	-	600
β_{cc}	1.170	-	1.170
Normalized value	32.88	-	32.86
Infill concrete	34.86	2.76	34.67

* determination of normalized concrete strength given in Annex A

4.4. Push-out test set-up

After the assembling procedure was completed, push-out tests were performed, according to the recommendations given in EN 1994-1-1:2004, Annex B [11]. Test set-up of all examined specimens is shown in Figure 4.12. In order to reduce load eccentricity and to provide good contact of the specimen and the supporting surface of the jack, the specimens concrete slabs were placed into the layer of fresh gypsum. Moreover, force was applied to the specimen steel beam through upper testing frame hinge over thick steel plate, in order to ensure that force application is performed centrally.



a) front side *b) back side*
Figure 4.12. Push-out specimen during examination

Each specimen was equipped with seven inductive displacement transducers to measure the slip and separation between the concrete slab and steel profile, as shown in Figure 4.13. Longitudinal slip between steel profile and both concrete slabs was measured with four sensors (V1-V4), two on each side of steel beam flange. Uplift between steel profile and concrete slabs was measured on the front side (H1 and H2), as close as possible to shear connectors. Separation between concrete slabs was measured on the front side, 15 cm above the slab support (S1). No strain measurements were made.

Force applied on specimen was measured by a load cell at the top, with 1000.0 kN capacity. Data acquisition and recording were performed in 1.0 Hz frequency with multichannel acquisition device. The loading regime was adopted as specified in EN

1994-1-1:2004, Annex B [11]. Force controlled cycling loading was applied in 25 cycles ranging from $P_{\min} = 15.0$ kN to $P_{\max} = 110.0$ kN, corresponding to approximately 5 % and 40 % of assumed shear resistance, as shown in Figure 4.14. Also, first step of cycling loading was divided in three phases (Figure 4.14). Assumed shear resistance of eight connectors in one specimen is 280.0 kN, based on characteristic shear resistance of one X-HVB 110 connector in solid concrete slabs, $P_{Rk} = 35.0$ kN, according to ETA-15/0876 assessment [7]. Failure loading was applied in one step, after the cyclic loading. Constant displacement rate was set during failure loading; such that failure does not appear in less than 15 minutes. Approximatively, 0.3 kN/s was applied during the failure loading.

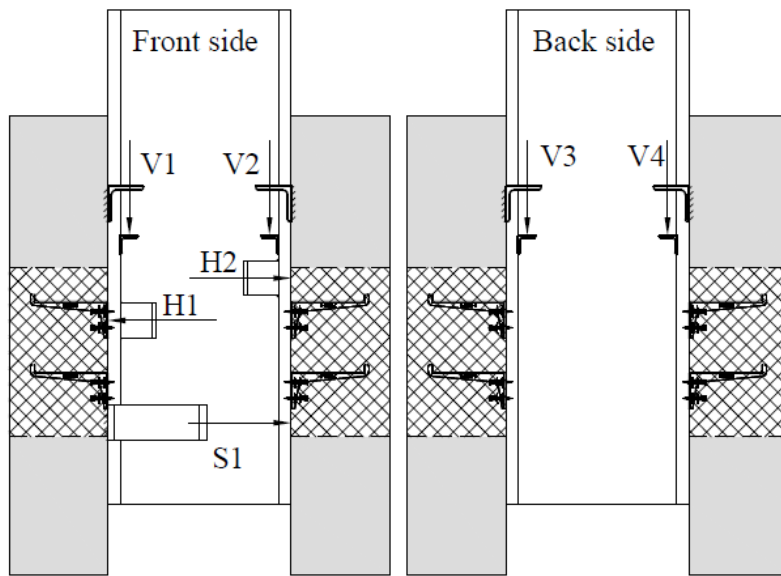


Figure 4.13. Layout of measurements for push-out specimens

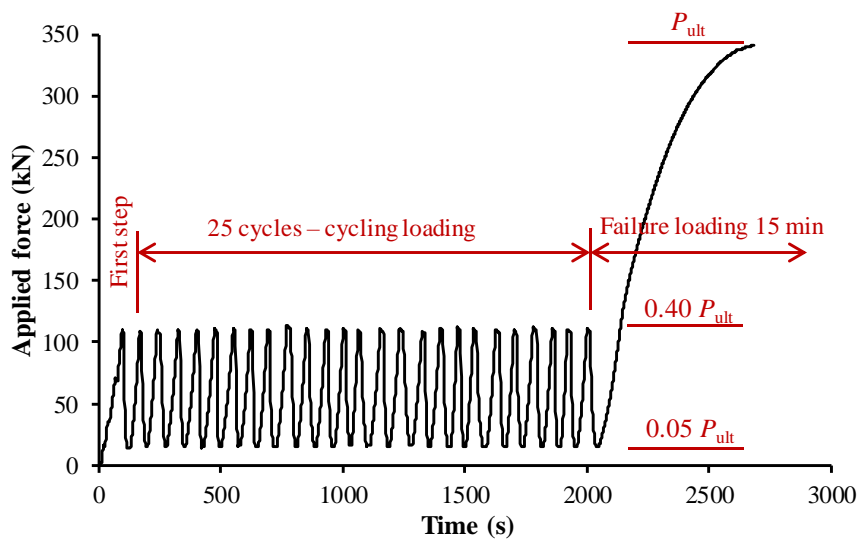


Figure 4.14. Loading regime for push-out tests

4.5. Experimental results of push-out tests

Typical force-slip curve which was obtained from push-out tests of X-HVB 110 shear connectors in prefabricated concrete slabs is presented in Figure 4.15. Shear force P_{ult} was defined as total ultimate force for all shear connectors of one specimen or shear resistance. Longitudinal slip $\delta_{u,tot}$ was divided into initial slip accumulated during cyclic loading δ_{init} and characteristic value of slip capacity δ_{uk} . Characteristic value of slip capacity δ_{uk} was obtained for 90 % of ultimate shear force on descending branch of load-slip curve and used as a main property of shear connectors, with respect to ductility, according to EN 1994-1-1:2004 [11]. Total slip obtained through testing procedure was designated as $\delta_{u,tot} = \delta_{init} + \delta_{uk}$, as presented in Figure 4.15. Introduced designation of main properties will be used for presentation of push-out test results.

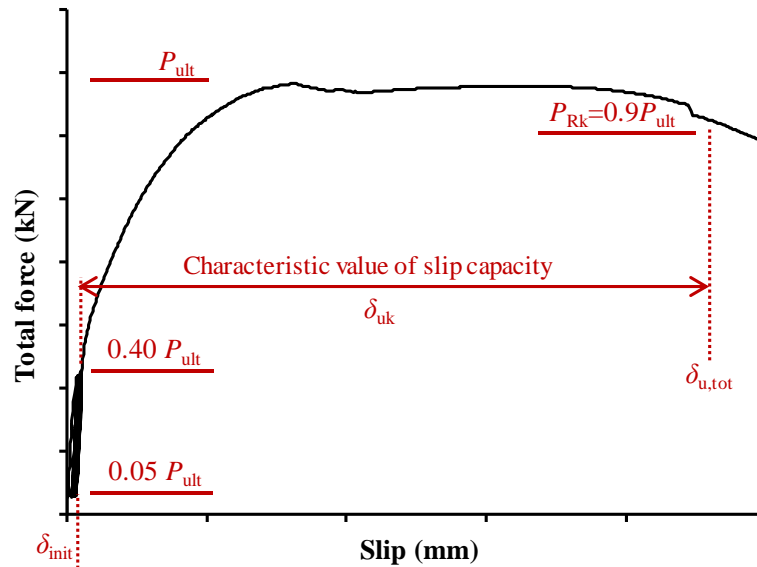


Figure 4.15. Designation of main parameters for push-out tests analysis

Statistical evaluation of experimentally gained results of push-out tests was performed according to recommendations given in EN 1990:2010, Annex D [47] with adopted value of factor k_n of 3.37 and 2.63 for three and four specimens in one test series, as previously explained in Chapter. 4.3. Also, characteristic value of ultimate shear force and slip capacity were determined according to recommendations given in EN 1994-1-1:2004, Annex B [11], where characteristic value should be taken as the minimum value of analysed property reduced by 10 %, if three tests on nominally identical specimens are carried out and the deviation of any individual test result from the mean value obtained from all tests does not exceed 10 %.

Two test specimens from HSFg-2 test series obtained unexpected failure mechanism due to mistakes of installation procedure, which is explained in detail in Annex B. Results of these test specimens, HSFg1-2 and HSFg5-2, were not used for statistical evaluation of HSFg-2 test series.

4.5.1. Cyclic loading

Force-slip curves obtained for all examined tests specimens during cycling loading are presented in Figure 4.16. Uniform behaviour off all test specimens within one tests series was obtained, with the exception of HSFg1-2 and HSFg5-2 test specimens of HSFg-2 test series, as shown in Figure 4.16d. Therefore, found installation mistakes for these test specimens resulted in significant influence on force-slip curves, even for cyclic loading, i.e. for loading levels lower than 40 % of shear resistance.

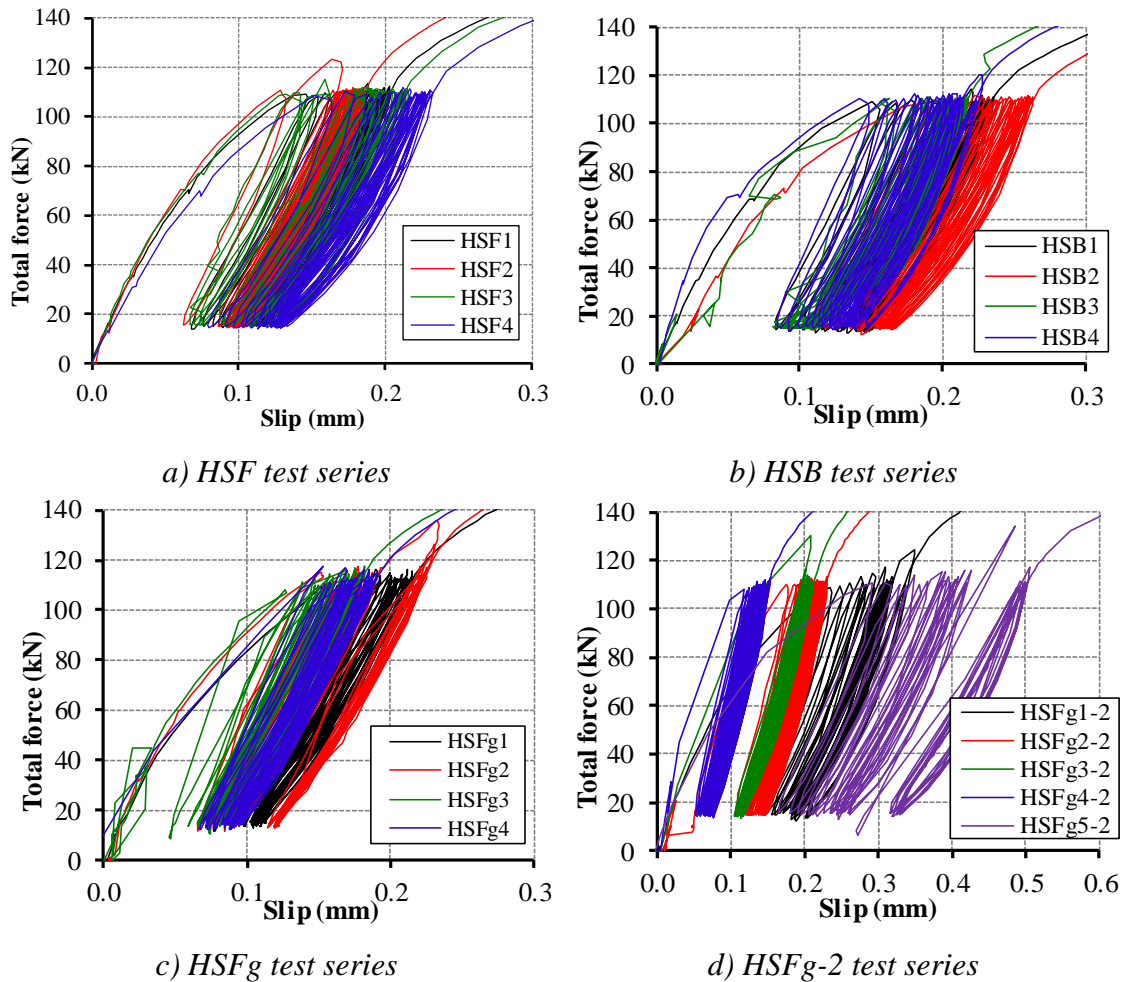


Figure 4.16. Force-slip curves for cyclic loading

4.5.2. Failure loading

Experimental results of failure loading for first phase of push-out tests are presented in Figure 4.17 and Figure 4.18. This experimental phase included two test series, HSF and HSB, with two orientations of shear connectors relative to the shear force direction and minimal recommended distances between connectors. Installation procedure was performed with 3.5 installation power level, for both test series.

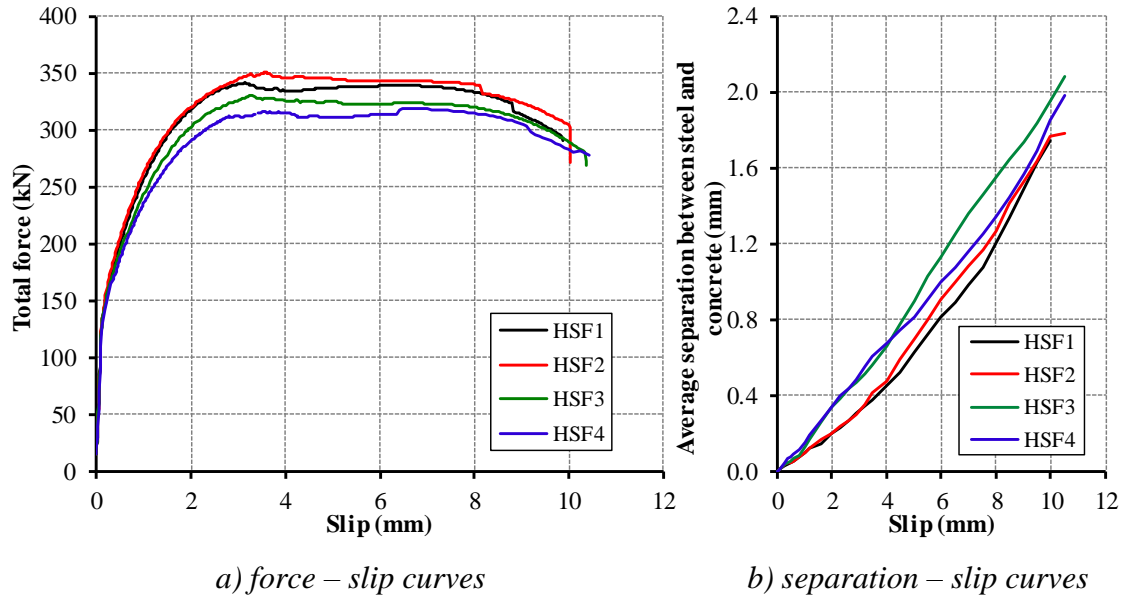


Figure 4.17. Experimental results for failure loading - HSF test series

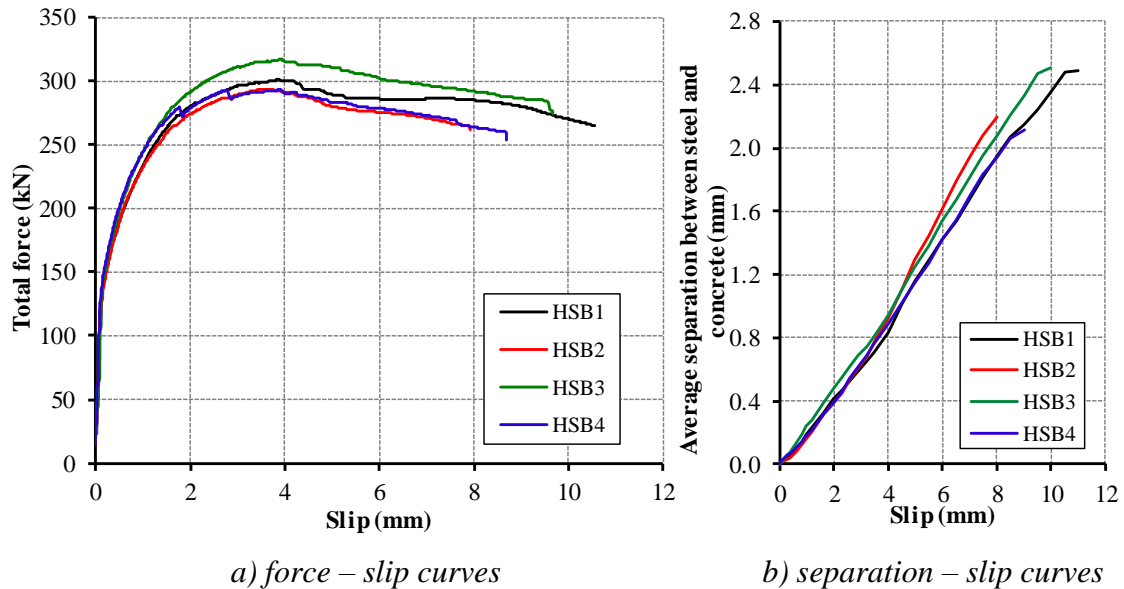


Figure 4.18. Experimental results for failure loading - HSB test series

Force-slip curves and average separation between steel beam and concrete slab are presented in Figure 4.17 and Figure 4.18. The longitudinal slip was obtained as average

measurement from four sensors (V1-V4), while separation between steel beam and concrete slab was obtained as average measurement from two sensors on specimen front side (H1 and H2 for left and right side of the test specimen). Experimentally gained results of these two test series are also presented in Table 4.8 and Table 4.9.

Table 4.8. Results of standard push-out tests - HSF series

Specimen	Ultimate force (kN)	Average slip (mm)			Average separation (mm)	
		initial	characteristic	total	between slabs	steel to concrete
	P_{ult}	δ_{init}	δ_{uk}	$\delta_{u,tot}$		
HSF1	341.7	0.12	9.69	9.81	2.32	1.69
HSF2	350.5	0.10	10.02	10.12	2.32	1.78
HSF3	330.6	0.13	9.59	9.72	2.13	1.86
HSF4	318.6	0.14	9.20	9.34	2.39	1.64
Mean	335.4	0.12	9.63	9.75	2.29	1.74
St. deviation	13.8		0.3			
Variation (%)	4.1		3.5			
Characteristic	299.0* (286.7**)		8.7* (8.3**)			

* according to EN 1990:2010 [47]; ** according to EN 1994-1-1:2004 [11]

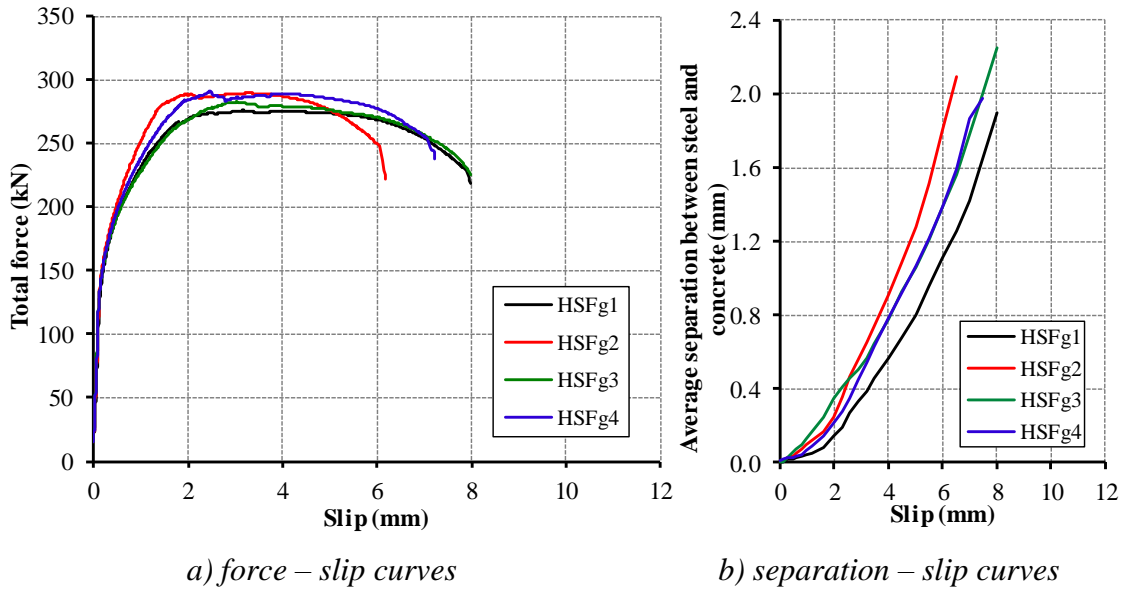
Table 4.9. Results of standard push-out tests - HSB series

Specimen	Ultimate force (kN)	Average slip (mm)			Average separation (mm)	
		initial	characteristic	total	between slabs	steel to concrete
	P_{ult}	δ_{init}	δ_{uk}	$\delta_{u,tot}$		
HSF1	301.3	0.15	10.19	10.34	2.82	2.40
HSF2	293.9	0.17	7.36	7.53	2.41	2.04
HSF3	317.0	0.11	9.67	9.78	2.74	2.51
HSF4	289.1	0.15	7.60	7.75	2.10	1.86
Mean	300.3	0.15	8.71	8.85	2.52	2.20
St. deviation	12.2		1.4			
Variation (%)	4.1		16.5			
Characteristic	268.2* (260.2**)		4.9* (6.6**)			

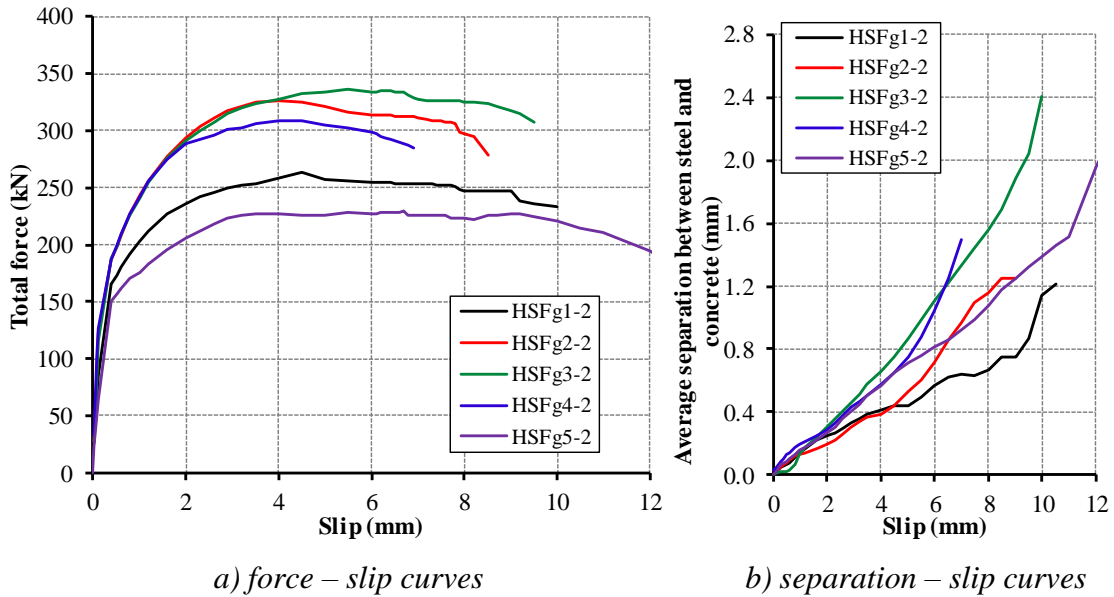
* according to EN 1990:2010 [47]; ** according to EN 1994-1-1:2004 [11]

Push-out specimens of second and third phase of experimental investigation were performed with reduced distances between shear connectors and different installation procedures. Four push-out specimens were examined within HSFg test series and five specimens within HSFg-2 test series. Lower installation power level, 2.0, was used for

test series HSFg, while for HSFg-2 tests series same installation procedure was used as for HSF and HSB test series. Experimental results of failure loading for these test series are presented in Figure 4.19 and Figure 4.20. Results of experiment of HSFg and HSFg-2 test series are also presented in Table 4.10 and Table 4.11.



a) force – slip curves *b) separation – slip curves*
Figure 4.19. Experimental results for failure loading - HSFg test series



a) force – slip curves *b) separation – slip curves*
Figure 4.20. Experimental results for failure loading - HSFg-2 test series

Table 4.10. Results of standard push-out tests - HSFg series

Specimen	Ultimate force (kN)	Average slip (mm)			Average separation (mm)	
		initial	characteristic	total	between slabs	steel to concrete
	P_{ult}	δ_{init}	δ_{uk}	$\delta_{u,tot}$		
HSFg1	275.7	0.11	6.22	6.33	1.79	1.17
HSFg2	289.4	0.12	5.44	5.56	1.81	1.49
HSFg3	282.6	0.09	6.38	6.47	1.80	1.53
HSFg4	290.7	0.10	6.53	6.63	1.83	1.63
Mean	284.6	0.11	6.14	6.25	1.81	1.46
St. deviation	6.9		0.5			
Variation (%)	2.4		7.9			
Characteristic	266.4* (248.1**)		4.9* (4.9**)			

* according to EN 1990:2010 [47]; ** according to EN 1994-1-1:2004 [11]

Table 4.11. Results of standard push-out tests - HSFg-2 series

Specimen	Ultimate force (kN)	Average slip (mm)			Average separation (mm)	
		initial	characteristic	total	between slabs	steel to concrete
	P_{ult}	δ_{init}	δ_{uk}	$\delta_{u,tot}$		
HSFg1-2	266.0	0.21	9.16	9.37	1.32	0.77
HSFg2-2	326.3	0.14	8.50	8.64	2.11	1.25
HSFg3-2	335.9	0.12	7.35	7.47	2.16	1.53
HSFg4-2	309.1	0.08	6.96	7.04	1.92	1.49
HSFg5-2	229.1	0.33	10.91	11.24	1.40	1.65
Mean	323.8	0.11	7.60	7.72	2.06	1.42
St. deviation	13.6		0.8			
Variation (%)	4.2		10.5			
Characteristic	278.0* (278.2**)		4.9* (6.3**)			

* according to EN 1990:2010 [47]; ** according to EN 1994-1-1:2004 [11]

4.5.3. Analysis of experimental results

Average force-slip curves of four analysed push-out tests series are presented in Figure 4.21. Comparison of characteristic shear resistance and characteristic value of slip capacity determined according to EN 1990:2010 [47] and EN 1994-1-1:2004 [11] with characteristic shear resistance of X-HVB 110 shear connector according to ETA-15/0876 assessment [7] for eight shear connectors $P_{Rk} = 8 \cdot 35.0 \text{ kN} = 280.0 \text{ kN}$ and characteristic

value of slip capacity $\delta_{uk} = 6.0$ mm in order to obtain shear connector as ductile is presented in Table 4.12.

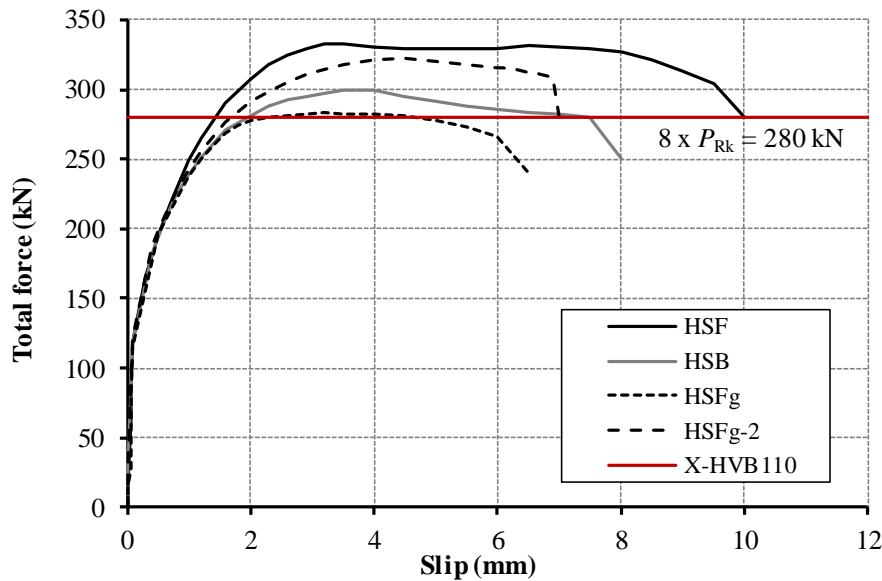


Figure 4.21. Average results of push-out tests series

By comparing the mean ultimate shear force P_{ult} and characteristic value of slip capacity δ_{uk} , forward orientation of shear connectors with minimal recommended distances between connectors, can be considered as more favourable. Approximately 12 % higher average ultimate shear force and 11 % higher characteristic value of slip capacity are obtained for HSF test series in comparison to the HSB series. These distinguishing features may be caused by (a) orientation of shear connector fastening leg; i.e. cartridge fired pins are positioned behind the anchorage leg, relative to the shear force direction and (b) possible confinement conditions in concrete developed behind the connector anchorage leg and beyond the fasteners. A detail investigation of X-HVB 110 shear connector behaviour is substantiated with detail FE analysis and presented in Chapter 8.

As a result of more favourable behaviour, forward orientation of shear connectors was further analysed through two test series with reduced distances between shear connectors. Two analysed parameters were: reduced longitudinal and transverse distance and different installation power levels. Approximately 14 % higher shear resistance is obtained for HSFg-2 series in comparison to the HSFg series. Considering the same specimens layout for both test series, lower shear resistance for HSFg test series is a consequence of lower depth of pin installation in steel base material due to lower

installation power level (approximately 2.0 instead 3.5 power level which was used for pins installation of HSF, HSB and HSFg-2 series). Also, lowering of installation power level reduced the characteristic value of slip capacity for approximately 19 %.

Table 4.12. Comparison of experimental results with recommendations given in ETA-15/0876 assessment [7] and EN 1994-1-1:2004 [11]

Series	Characteristic value			Experimental vs. recommendations	
	Shear force per specimen	Shear force per connector	Slip	Shear force	Slip
	P_{Rk} (kN)	P_{Rk} (kN)	(mm)	ETA-15/0876 [7]	EN 1994-1-1:2004 [11]
HSF	299.0*	37.38*	8.7*	1.07	1.45
	286.7**	35.84**	8.3**	1.02	1.38
HSB	268.2*	33.53*	4.9*	0.96	0.82
	260.2**	32.53**	6.6**	0.93	1.10
HSFg	266.4*	33.30*	4.9*	0.95	0.82
	248.1**	31.02**	4.9**	0.89	0.82
HSFg-2	278.0*	34.75*	4.9*	0.99	0.82
	278.2**	34.78**	6.3**	0.99	1.05

* according to EN 1990:2002 [47]; ** according to EN 1994-1-1:2004 [11]

The influence of group arrangement of shear connectors with reduced distances can be analysed based on the experimental results gained from HSF and HSFg-2 test series. Mean value of ultimate shear force for HSFg-2 test series is approximately 4 % lower in comparison to the HSF test series. Minimal and maximum shear resistance obtained from individual specimens of HSFg-2 test series are within the range of obtained results of HSF test series, as presented in Table 4.8 and Table 4.11. Group arrangement of shear connectors, when they are positioned one next to another, did not significantly influenced shear resistance, but obtained mean value of slip capacity is 20 % lower in comparison to the HSF specimens. Lowering of installation power level and group arrangement of shear connectors resulted in approximately same reduction of slip capacity (HSFg-2 vs. HSFg and HSF vs. HSFg-2 test series).

Also, only for HSF specimens with minimal recommended distances between shear connectors, characteristic shear resistance and characteristic value of slip capacity obtained through statistical evaluation of experimental results are higher than same values obtained through design recommendations, as given in Table 4.12. Comparative relation

of HSB, HSFg and HSFg-2 with HSF test series based on mean values of ultimate shear force and slip capacity is presented in Table 4.13.

Table 4.13. Comparison of experimental results of four push-out test series

Series	Mean value		Comparison within test series	
	Ultimate shear force	Slip	Ultimate shear force	Slip
	(kN)	(mm)	$P_{ult,i} / P_{ult,HSF}$	$\delta_{uk,i} / \delta_{uk,HSF}$
HSF	335.4	9.63	/	/
HSB	300.3	8.71	0.90	0.90
HSFg	284.6	6.14	0.85	0.64
HSFg-2	323.8	7.60	0.97	0.79

Table 4.14. Shear resistance per one cartridge fired pin

Series	Ultimate shear force		Shear force per one fastener	
	Characteristic	Mean	Characteristic	Mean
	[kN]	[kN]	[kN]	[kN]
HSF	299.0*	335.4	18.69	20.96
	286.7**		17.92	
HSB	268.2*	300.3	16.76	18.77
	260.2**		16.26	
HSFg	266.4*	284.6	16.63	17.79
	248.1**		15.51	
HSFg-2	278.0*	323.8	17.38	20.24
	278.2**		17.39	

* according to EN 1990:2002 [47]; ** according to EN 1994-1-1:2004 [11]

Accomplished characteristic and mean value of shear resistance per one cartridge fired pin for all analysed push-out test series are given in Table 4.14. Approximately 21.0 kN of pull-out resistance is achieved for HSF test series. Group arrangement of shear connectors in HSFg-2 test series did not influence significantly lower pull-out resistance per one cartridge fired pin.

For loads which are significantly below ultimate loads and correspond to day to day life of structure we refer to the structure behaviour at service loads or serviceability limit state, SLS. Analysis of shear connector stiffness and slip for SLS, corresponding to approximately $0.7P_{ult}$ is presented in Figure 4.22. Uniform behaviour of all analysed tests series is acquired for this loading level. Initial stiffness of one shear connector for all analysed test series is approximately the same and amounts 150 kN/mm, as shown in Figure 4.22. Initial stiffness of X-HVB 110 shear connector is lower than stiffness of 16

mm diameter headed studs and bolted shear connector, which amounts 300 kN/mm and 165 kN/mm, respectively, as presented by Pavlović et al. [51]. Stiffness corresponding to the SLS for one shear connector is the largest for HSFg test series, approximately 48 kN/mm, while the lowest value is obtained for HSF test series and amount approximately 35 kN/mm, in comparison to the 122 kN/mm for headed studs and 68 kN/mm of bolted shear connectors [51]. Obtained slip for SLS, given in Figure 4.23, is in the range from 0.52 mm for HSFg series to 0.83 mm for HSF series, respectively. Linear behaviour of shear connectors corresponding to service load levels is uniform, both for all analysed connectors layouts and different installation power levels, as presented in Figure 4.23.

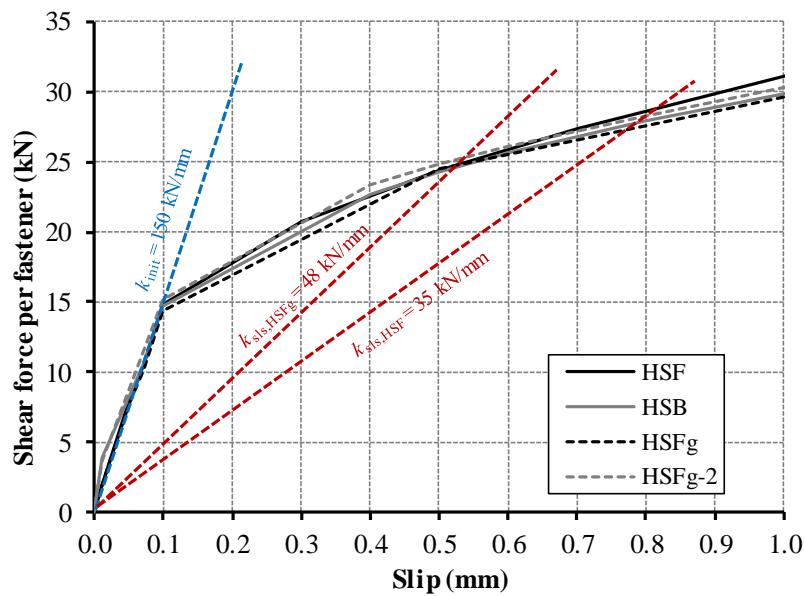


Figure 4.22. Stiffness of X-HVB shear connectors

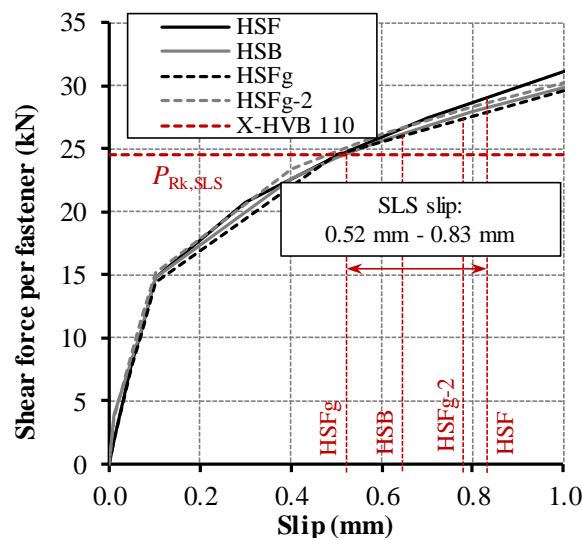


Figure 4.23. Experimentally obtained slip corresponding to the serviceability limit state

Also, for all experimentally investigated push-out test series, the mean value of characteristic slip δ_{ik} is higher than 6.0 mm which is the minimum required according to EN 1994-1-1:2004 [11] to consider this type of shear connector as ductile. X-HVB 110 shear connectors reached ultimate shear force at slip of approximately 4.0 mm, for all analysed test series. This is lower in comparison to the headed studs, according to experimental results presented by Spremić et al. [52] and approximately the same value as for bolted shear connectors, presented by Pavlović et al. [51].

4.5.4. Characteristic failure mechanisms

Characteristic failure mechanisms of headed studs in solid concrete slabs are well known and explained in various literature [53]. Load transfer is determined with deformation of shear connector and high bearing resistance of concrete influenced by confinement condition and triaxial restraint of surrounding concrete.

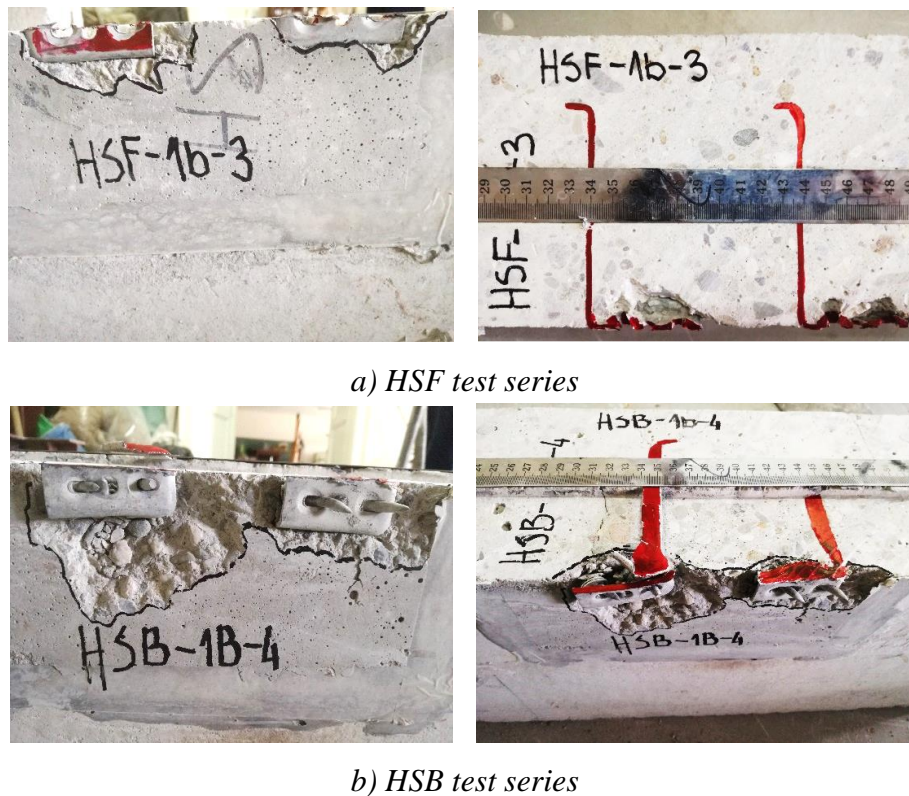
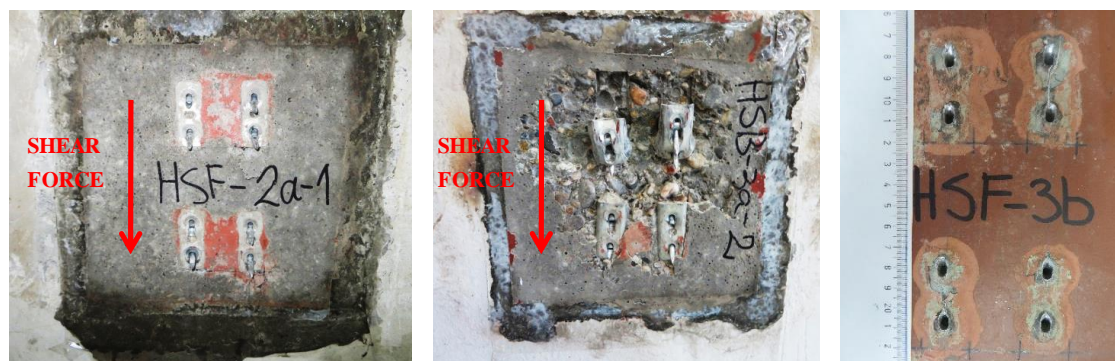


Figure 4.24. Specimens of phase 1 after testing procedure - cut through concrete slab

In comparison to the headed studs, failure mechanisms of mechanically fastened shear connectors are not still analytically explained. Their overall behaviour and failure mechanisms are related to deformation of shear connector and bearing resistance of concrete, but mostly governed with deformation and resistance of fasteners. Therefore,

embedded depth of cartridge fired pins into steel base material is of paramount importance for development of proper anchorage mechanisms. Global cracks in prefabricated concrete slabs or separation of contact layer between infill concrete and prefabricated slab are not obtained in examined specimens of all test series. All failure mechanisms are obtained in infill concrete of envisaged openings. Infill concrete zone of HSF and HSB specimens after the testing procedure are shown in Figure 4.24 and Figure 4.25. Figure 4.24 represents concrete slabs which were cut through shear connectors after testing procedure. Achieved failure mechanism of forward orientations of shear connectors (HSF series) is: pull-out failure of most pins and shear failure of some pins without significant damage in concrete and deformation of connectors. Deformation of concrete is only located at the surrounding zone of fasteners head, which is related to deformation of fasteners and their pull-out from base material. Backward orientation of shear connectors resulted in extensively different failure mechanism. Significant deformation of shear connectors is followed with notable damage of concrete and subsequent fasteners pull-out from base material, as presented in Figure 4.24 and Figure 4.25. Possible confinement condition and triaxial restraint of concrete behind forward oriented shear connectors are located in the surrounding zone of cartridge fired pins, resulting in low deformation of concrete and failure of fasteners anchorage mechanisms. By positioning of connectors anchorage leg and fasteners in front of concrete confined zone for backward oriented shear connectors, less favourable behaviour is achieved. Pull-out failure of cartridge fired pins is followed by a severe deformation of holes in a steel beam, for both orientation of shear connectors. Steel beam after testing procedure for forward orientation of shear connectors is shown in Figure 4.25c.



a) HSF test series

b) HSB test series

c) hole deformation

Figure 4.25. Infill concrete zone and steel beam after testing of phase 1

Similar failure mechanisms are obtained for specimens with reduced transversers and longitudinal distance between connectors, HSFg and HSFg-2 test series. Infill concrete zone after testing procedure for two specimens with the highest achieved shear resistance, HSFg2 and HSFg3-2 specimens is shown in Figure 4.26. Failure of these specimens is followed with lower concrete damage in comparison to the HSF specimens, which is again located beyond the pins head of the first shear connector row. Obtained failure mechanism of all HSFg specimens is pull-out of all fasteners. HSFg-2 test specimens, with approximately two times higher installation power level in comparison to the HSFg specimens failed due to shear failure of most fasteners (HSFg3-2 and HSFg2-2 specimens). Cracking of the infill concrete zone is obtained at the top of the fastener anchorage leg, for HSFg3-2 specimen. HSFg4-2 specimens with the lowest shear resistance within HSFg-2 test series failed due to pull-out failure of all fasteners.



a) HSFg test series

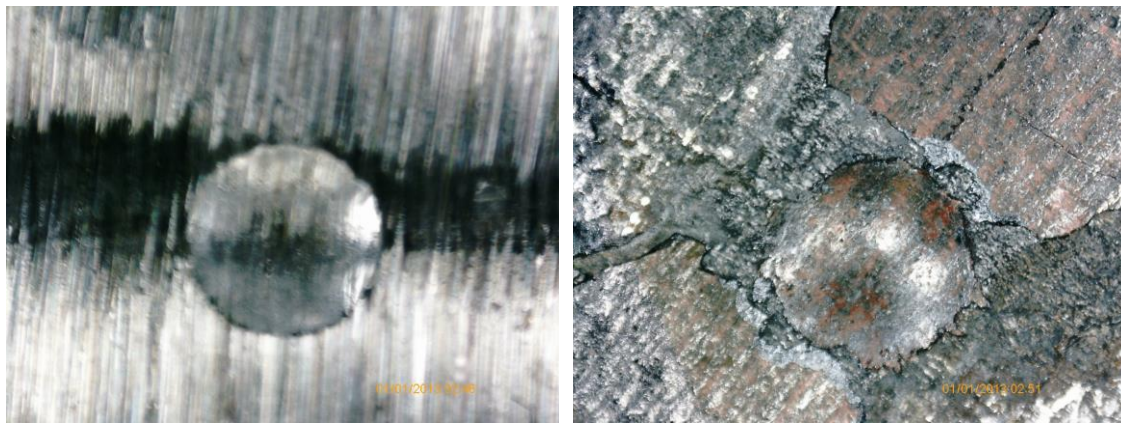


b) HSFg-2 test series

Figure 4.26. Specimens after testing procedure - reduced distance between shear connectors - phase 2 and 3

Considering obtained failure mechanisms presented in previous figures, ductile behaviour of shear connectors according to EN 1994-1-1:2004 [11] is mostly obtained from deformation capacity of cartridge fired pins and concerned anchorage mechanisms during the installation procedure. Deformation of cartridge fired pins can be obtained only through deformation of concrete and development of tensile forces in fasteners, until the complete failure of anchorage mechanisms and fasteners pull-out is achieved. Shear

(Chapter 4.3.1), as shown in Figure 4.27a. Steel beam, which was firstly used for HSF-2 test specimen and afterwards for HSFg3-2 specimen, was used for determination of material hardness at positions on steel beam flange (3E - 6E) and close to the cartridge fired pins hole (1 - 8), as shown in Figure 4.27a. Examination positions 1, 2, 3, 6, 7 and 8 were located as close as possible to the cartridge fired pins hole, and positions 4 and 5 at the centre of steel beam flange (midway between two shear connectors), as shown in Figure 4.27b. Diameters of both impresses, on check test piece and tested material, were photographed using high quality camera with magnification of 40 times.



a) check test piece

b) tested material

Figure 4.28. *Impresses obtained for measuring position 4*

Comparison of check test piece and tested material impresses for examination position 4 is shown in Figure 4.28. Magnified photographs were used for determination of impress diameter through measurement of two diagonal distances of impress for every examination position. Measured impresses diameters are given in Table 4.15. Hardness of tested material H_x was calculated according to Eq. 4.6.

$$H_x = H_e \cdot \frac{D - \sqrt{D^2 - d_e^2}}{D - \sqrt{D^2 - d_x^2}} \quad (4.6)$$

In previous expression:

H_e is the hardness of check test piece, adopted based on examination as 1320 MPa;

D is the diameter of the steel ball used for examination, adopted as 10.0 mm;

d_e is the diameter of the impress on the check test piece;

d_x is the diameter of the impress on the tested material.

Tensile strength of tested material was calculated for all measuring positions using two procedures. Firstly, tensile strength $f_{u,relation}$ was determined through relation presented in Eq. 4.7. Hardness coefficient k was adopted as 0.35, which is recommended value for metallic materials. Secondly, tensile strength $f_{u,tensile\ test}$ was determined according to results of tensile test coupons. Mean value of tensile strength of four tensile coupons (Figure 4.28b) is 433.6 MPa, as presented in Table 4.2. Therefore, value of hardness coefficient was determined according to Eq. 4.8.

$$f_{u,relation} = k \cdot H_x \quad (4.7)$$

$$k = f_{u,mean} / H_{x,1E} = 433.6\text{MPa} / 1363.0\text{MPa} = 0.32 \quad (4.8)$$

In previous expression:

k is the hardness coefficient;

$f_{u,mean}$ is the mean value of tensile strength of four tensile test coupons;

$H_{x,1E}$ is the hardness of tested material for measuring position 1E.

Table 4.15. Results of hardness measurement with Poldi hammer

Measuring position	Measuring position description	Diameter		Hardness	Tested material strength	
		Check test piece	Tested material	Tested material	Relation	Tensile tests
		d_e	d_x	H_x	$f_{u,relation}$	$f_{u,tensile\ test}$
		(mm)	(mm)	(MPa)	(MPa)	(MPa)
1	Surrounding zone of pin 1	2.80	2.76	1359.3	475.8	432.4
2		2.82	2.78	1359.1	475.7	432.4
3		2.84	2.72	1441.6	504.6	458.6
4	Between connectors	2.96	3.02	1266.9	443.4	403.0
5		2.84	2.92	1247.1	436.5	396.7
6	Surrounding zone of pin 2	3.06	2.90	1473.4	515.7	468.7
7		2.88	2.68	1528.9	535.1	486.4
8		2.90	2.70	1527.3	534.6	485.9
1E	Test coupons	2.56	2.52	1363.0	477.0	433.6
2E		2.68	3.06	1006.6	352.3	320.2
3E	Beam flange	2.70	2.56	1471.2	514.9	468.0
4E		2.60	2.50	1429.6	500.4	454.8
5E	Range of connector	2.42	2.70	1056.4	369.7	336.1
6E		2.28	2.60	1010.9	353.8	321.6

Based on the hardness test measurements, increase of base material strength is evident. Mean value of tensile strength of material in surrounding region of cartridge fired pins, presented in Table 4.15 is 460.7 MPa, determined with hardness coefficient 0.32 (Eq. 4.8). In comparison to the mean value of tensile strength of test coupons, tensile strength of base material is increased up to 50 MPa (surrounding zone of pin 2, see Table 4.15). Average increase of base material tensile strength in surrounding zone of cartridge fired pins amounts approximately 6 % in comparison to the results obtained through tensile test coupons which results are given in Table 4.2.

4.7. Shear and tension tests of cartridge fired pins

In order to obtain a better insight in behaviour of cartridge fired pins as part of X-HVB shear connectors, additional tests of X-ENP-21 HVB cartridge fired pins were performed. Scope of the examination were tests on cartridge fired pins in order to investigate the pull-out failure of pins loaded in shear and tension, according to recommendations given in ECCS publication [38]. The same, failure mechanism of cartridge fired pins is the most common in push-out tests of X-HVB 110 shear connectors in solid and prefabricated concrete slabs, as presented in Chapter 2 and 4.

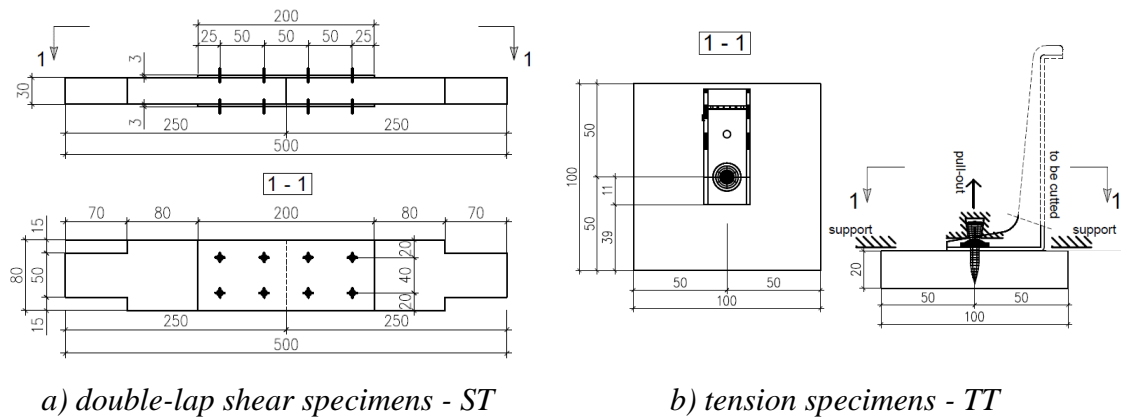


Figure 4.29. Shear and tension test specimens

Double-lap shear test specimens (ST) were built with baseplate thickness of 30.0 mm and steel sheets thickness of 3.0 mm, as shown in Figure 4.29a. Number of cartridge fired pins per one cover plate was eight, and total number per specimen was sixteen. Installation of cartridge fired pins was performed with installation power level 3.5, which is the same installation power level which was applied for phase 1 and 3 of push-out tests.

Four shear test specimens (ST) were examined. Geometrical properties of ST specimens were adopted in order to achieve pull-out failure of cartridge fired pins loaded in shear.

Table 4.16. *Tension test specimens properties*

Series	Installation power level	Number of specimens	Base plate thickness
		N_{spc}	(mm)
TT2-2	2	4	20
TT3-2	2	2	20
TT3-3.5	3.5	3	20

Tension tests with cartridge fired pins were performed on specimens which are shown in Figure 4.29b. Single cartridge fired pin was installed over X-HVB 110 shear connector in the midpoint of the base plate. Base plate with dimensions 100x100x20 mm was adopted for all examined specimens. Parameters that were analysed are steel grade of base plate and installation power level, as shown in Table 4.16 and Table 4.17. Nine tension specimens were examined within this experimental phase. The thickness of the base plates for shear and tension test specimens of 30.0 and 20.0 mm respectively, was adopted in order to fulfil the requirements of solid steel installation, as explained in Chapter 2.3.3 and therefore to mostly diminish its influence.

Table 4.17. *Average values of base plate material properties*

Specimen	Average material properties from coupon tensile tests		Achieved steel grade according to EN 10025-2 [8]
	yield strength	ultimate strength	
	f_y (N/mm ²)	f_u (N/mm ²)	
ST	413.9	562.1	S355
TT2-2	336.1	479.6	S275
TT3-2, TT3-3.5	468.2	534.6	S355

The material properties of base plates were examined through standard coupon tensile tests. Four round tensile coupons were examined for shear test base plates (ST) and tension test base plates (TT2 and TT3). Examined material properties with nominal stress-strain curves and statistical evaluation of obtained results are presented in detail in Annex C. Average material properties for ST, TT2 and TT3 base plate specimens are presented in Table 4.17 with determination of achieved steel grade according to EN 10025-2 [8]. Achieved steel grade for base plate of ST specimens is S355 and for TT specimens is S275 and S355, as presented in Table 4.17.

Specimens for shear and tension tests (ST and TT) after installation of cartridge fired pins are shown in Figure 4.30. The ends of the base plate of ST specimens were formed on both sides according to geometry presented on Figure 4.29a in order to accomplish geometry proper for testing machine grips and to maintain centric force flow. Shear and tension tests of cartridge fired pins were performed in the Laboratory of Materials at the University of Belgrade, Faculty of Civil Engineering, according to recommendations given in ECCS publication [38]. All tests were performed in the servo-hydraulic testing machine Shimadzu, with a capacity of 300.0 kN.



a) shear test specimens - ST

b) tension test specimens - TT

Figure 4.30. Specimens after installation of cartridge fired pins



Figure 4.31. Examination of shear test specimens - ST



Figure 4.32. Examination of tension test specimens - TT

Shear test specimens (ST) were equipped with four inductive displacement transducers in order to measure relative displacement between steel base material close to the machine grips and cover plate for each cartridge fired pins group, as shown in Figure 4.31. The sensors measurement base was 85.0 mm.

Tension test specimens (TT) were equipped with one sensor in order to measure relative displacement between steel base plate and acquired device to hold pins head, as shown in Figure 4.30b and Figure 4.32. The same testing procedure was prescribed, both for tension test (TT) and shear test (ST) specimens, according to recommendations given in ECCS publication [38]. The rate of loading was applied in order not to exceed 1.0 kN/min and rate of deformation controlled through movement of machine grips did not exceed 1.0 mm/min. Data acquisition and recording was performed with multichannel acquisition device.

Force-deformation curves, obtained through measurement of relative displacement of sensors placed on the same cover plate (U1 + U2, U3 + U4, Figure 4.31) are presented in Figure 4.33. Results of shear test specimens examination (ST) are presented in Figure 4.34 and Table 4.18. During the testing procedure of ST-3 specimen, it was observed that sensor U3 was not working, as presented through results given in Figure 4.33c and Table 4.18. Average value of fastener stand-off h_{NVS} measured as distance between fastener head and cover plate was approximately 12.0 mm. Comparison of obtained results of all

examined shear test specimens and characteristic failure mechanism are presented in Figure 4.34 and Table 4.18.

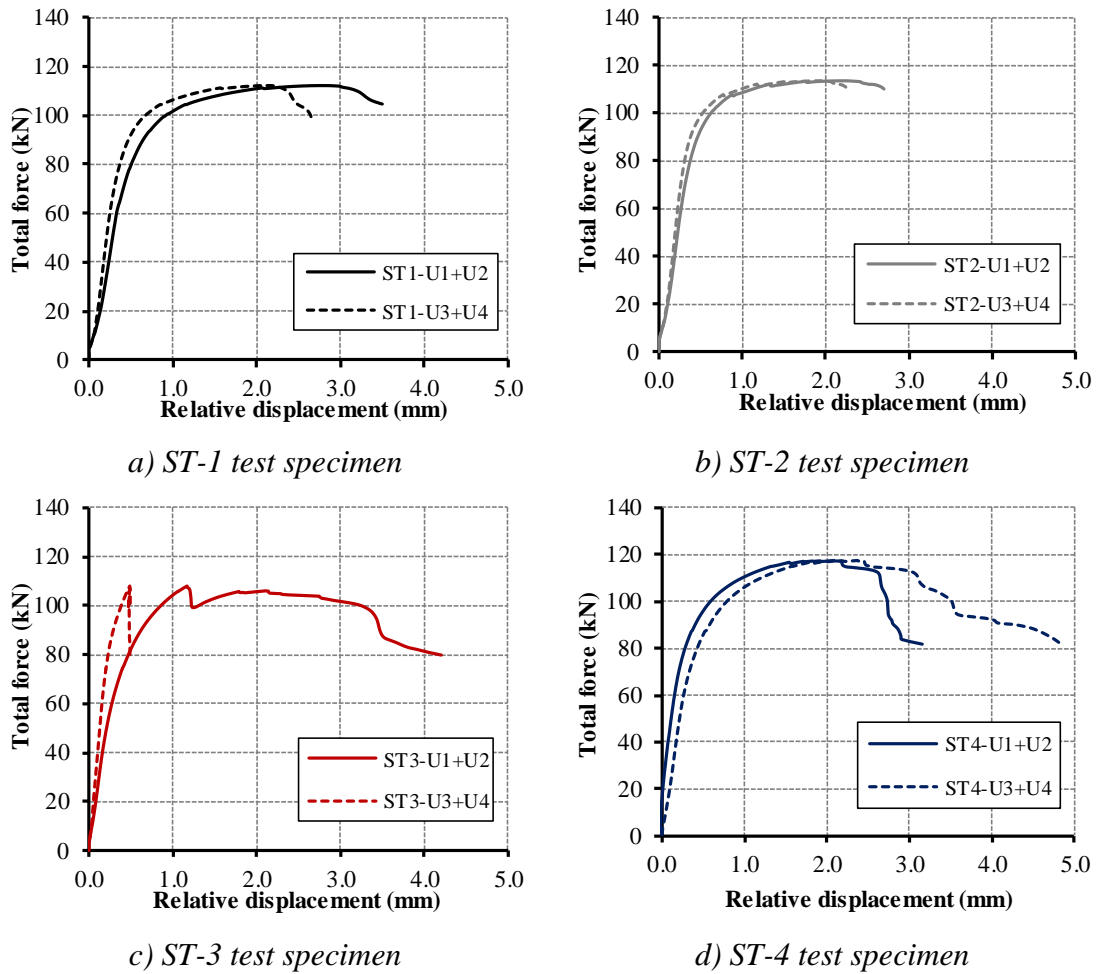
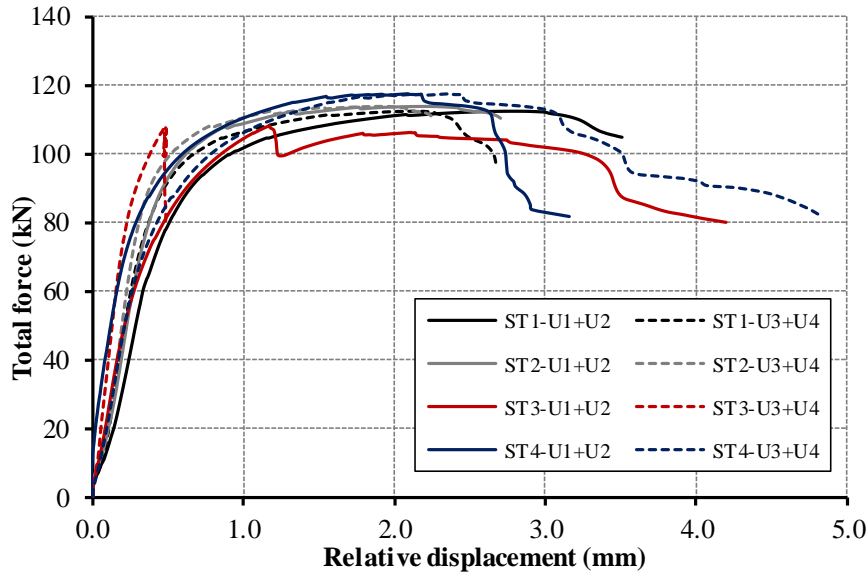


Figure 4.33. Force-relative deformation curves of shear test specimens - ST

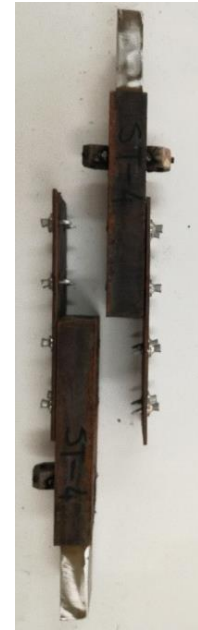
Ultimate shear force P_{ult} , force obtained for 3.0 mm of relative displacement P_{δ_3} and relative displacement of four sensors $\delta_{u1} - \delta_{u4}$ corresponding to shear resistance, δ_{ult} are presented in Table 4.18. In shear tests, failure loading should be determined as peak load in deformation of 3.0 mm, according to ECCS publication [38]. Statistical evaluation of experimentally gained results from shear test specimens (ST) was performed according to EN 1990:2010, Annex D [47] with adopted value of factor k_n of 2.63 for four specimens in one test series. Relatively uniform behaviour of four examined test specimens is obtained, with mean value of shear resistance of 112.8 kN and mean value of failure loading of 110.4 kN, as presented in Table 4.18.

Table 4.19 represents ultimate shear force and force obtained for relative deformation of 3.0 mm per one cartridge fired pin. Mean value of shear resistance per one

cartridge fired pin is 14.11 kN for four examined shear tests. Mean value of ultimate shear force per one cartridge fired pin of four series of push-out test specimens is from 17.79 kN to 20.96 kN, as presented in Table 4.14. The obtained difference of one cartridge fired pin resistance is from 20 % to 30 % for analysed shear tests and push-out test specimens, respectively.



a) comparison of force-deformation curves



b) failure mechanism

Figure 4.34. Results of shear test specimens (ST) examination

Table 4.18. Results of shear test specimens (ST) examination

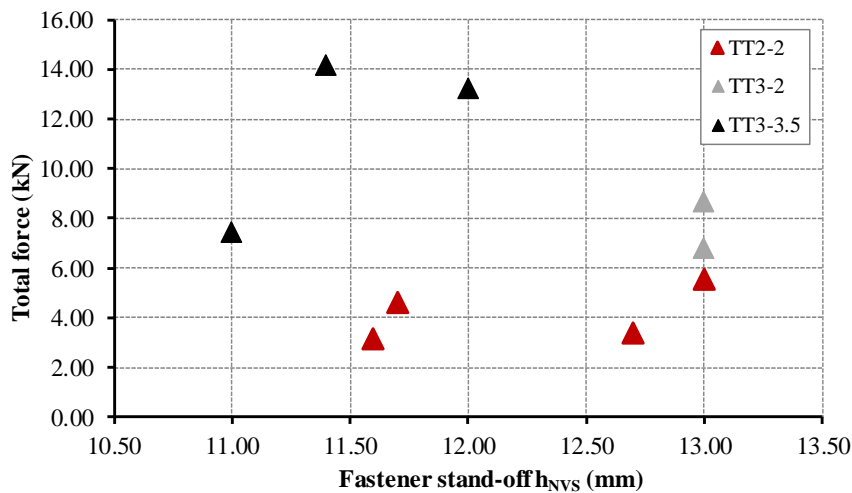
Specimen	Ultimate force (kN)	Force at 3 mm of total slip (kN)	Relative deformation (mm)				
			U1	U2	U3	U4	total
	P_{ult}	$P_{\delta 3}$	δ_{u1}	δ_{u2}	δ_{u3}	δ_{u4}	δ_{ult}
ST-1	112.2	109.3	0.890	1.986	1.250	0.931	5.056
ST-2	113.7	112.8	0.786	1.493	1.165	0.796	4.239
ST-3	108.1	104.3	0.673	0.498	0.000	0.486	1.657
ST-4	117.4	115.2	1.608	0.484	1.514	0.854	4.460
Mean	112.8	110.4					3.853
St. deviation	3.8	4.7					
Variation (%)	3.4	4.3					
Characteristic	102.8	94.4					

Lower shear resistance is related to the lower depth of penetration of cartridge fired pins for shear test specimens (ST) in comparison to the push-out specimens of HSF test series (fastener stand-off h_{NVS} is 12.0 mm for ST specimens in comparison to the 8.0 mm of HSF specimens). Also, higher shear resistance per one cartridge fired pin of HSF tests series is obtained due to concrete confinement conditions achieved in the region of cartridge fired pins head, which is further explained in Chapter 8.

Table 4.19. Pull-out resistance per cartridge fired pin of ST specimens

Specimen	Ultimate force per fastener (kN)	Force at 3 mm of total slip per fastener (kN)
	$P_{ult, pin}$	$P_{\delta 3, pin}$
ST-1	14.02	13.66
ST-2	14.21	14.10
ST-3	13.52	13.04
ST-4	14.67	14.40
Mean	14.11	13.80
Characteristic	12.85	12.24

Results of three tension test series (TT) are presented in Figure 4.35 and Table 4.20. Fastener stand-off h_{NVS} was measured as distance between fastener head and shear connector. Three tests series with different base material properties and installation power levels were analysed. Force-deformation curves of all examined tension test specimens are presented in Figure 4.36.



a) pull-out resistance



b) specimen failure

Figure 4.35. Tension test (TT) specimens results

Table 4.20. Results of tension test specimens - TT

Specimen	Ultimate force (kN)	Mean value of ultimate force (kN)	Fastener stand-off (mm)	Relative deformation (mm)
	$P_{ult,pin}$	$P_{ult,pin}$	h_{NVS}	δ_{ult}
TT2-2-1	3.19	4.19	11.60	0.04
TT2-2-2	4.61		11.70	0.16
TT2-2-3	5.55		13.00	0.21
TT2-2-4	3.41		12.70	0.09
TT3-2-1	6.82	7.77	13.00	0.77
TT3-2-2	8.72		13.00	0.21
TT3-3.5-1	7.46	11.65	11.00	0.21
TT3-3.5-2	14.22		11.40	0.69
TT3-3.5-3	13.28		12.00	0.32

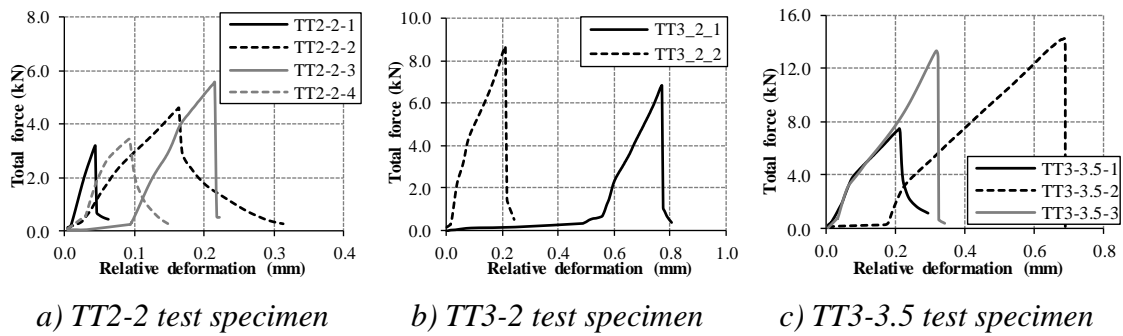


Figure 4.36. Force-deformation curves for tension test specimens (TT)

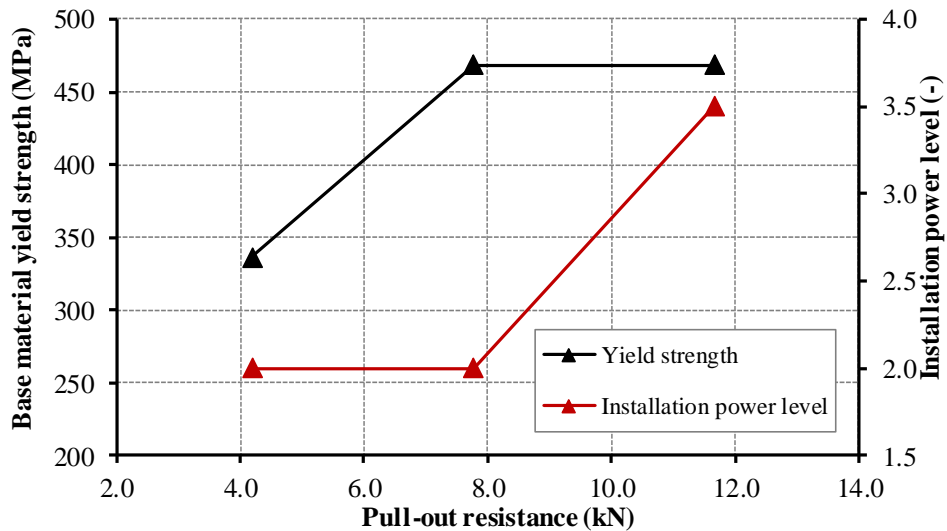


Figure 4.37. Pull-out resistance of cartridge fired pins

Obtained mean values of pull-out resistance of TT2, TT3 and TT3.5 test series are 4.19 kN, 7.77 kN and 11.65 kN, respectively. Pull-out resistance is mainly related to the base material properties and installation power level, than to the fastener stand-off, as presented in Figure 4.35 and Table 4.20. Specimens with the highest value of installation power levels and base material properties have obtained the highest pull-out resistance, or the largest fastener “hold” in the base material, as presented in Figure 4.37.

4.8. Summary

Presented experimental investigation emphasizes the possible application of X-HVB shear connectors in prefabricated composite construction, when shear connectors are discontinuously positioned in envisaged openings of concrete slabs. Experimental investigation included analysis of connectors orientation, variation of connectors distances and influence of pins installation power levels. Four test series were examined, seventeen push-out test specimens in total. Besides, experimental investigation included shear and tension tests of cartridge fired pins in order to obtain pull-out resistance of fasteners. Four shear test specimens and nine tension test specimens were examined. Standard tests were conducted to determine material properties of steel base plates and profiles, concrete slabs and shear connectors. Based on experimental investigation, the following conclusions can be drawn:

1) Positioning of X-HVB shear connector fastening leg relative to the shear force direction influences shear resistance, slip capacity and failure mechanisms. When shear connectors are positioned at minimal recommended transversal and longitudinal distances, it is shown that forward orientation of shear connectors is more favourable. Up to 12 % higher ultimate shear force and 11 % higher characteristic value of slip capacity is obtained for HSF test series in comparison to the HSB test series, based on the mean values of shear resistance obtained within one test series.

2) Pull-out and shear failure of cartridge fired pins is characteristic failure mechanism obtained for forward orientation of shear connectors for HSF, HSFg and HSFg-2 test series. Concrete damage is located in the surrounding zone of cartridge fired pins, mostly of first connectors row. Backward orientation is characterized with significant damage of concrete, deformation of connectors fastening leg and subsequent pull-out of fasteners.

3) Group arrangement of shear connectors without clear spacing between connectors at both directions, transversal and longitudinal, does not significantly influence shear resistance or obtained failure mechanisms. Only, 4 % lower shear resistance is obtained for HSFg-2 test series in comparison to the HSF test series with same installation power level.

4) Approximately 50 % lower installation power level for HSFg test series resulted in 14 % lower shear resistance and 19 % lower characteristic slip in comparison to the HSFg-2 test series with same specimens layout. Pull-out failure of all fasteners is obtained as characteristic failure mechanism of all specimens within HSFg test series. Low installation depth of fasteners into steel base material resulted in failure of anchorage mechanisms at lower loading levels.

5) Global cracks in prefabricated concrete slabs or separation of contact layer between infill concrete and prefabricated slab are not observed in examined specimens of all test series. Concrete damage of all specimens are obtained in infill concrete of envisaged openings.

6) Stiffness of single X-HVB 110 shear connector at serviceability loads is in the range from 35 kN/mm to 48 kN/mm. Stiffness is reduced up to 70 % when compared to headed studs and up to 30 % in comparison to the bolted shear connectors due to the failure of pins anchorage mechanisms and pull-out of fasteners.

7) X-HVB 110 shear connectors in prefabricated concrete slab obtained ductile behaviour for all analysed tests specimens, according to recommendations given in EN 1994-1-1:2004 [11].

8) High-speed installation procedure of cartridge fired pins significantly influences the base material properties. According to the hardness test of base material, average increase of base material tensile strength in surrounding zone of cartridge fired pins amounts approximately 6 % in comparison to the results obtained through tensile test coupons.

9) Pull-out resistance of cartridge fired pins obtained through shear tests with 3.0 mm thickness of double cover plates and installation power level of 3.5 is up to 30 % lower than resistance of push-out specimens of HSF and HSFg-2 test series with same

power installation level. Lower shear resistance is mostly related to the lower depth of penetration of cartridge fired pins for shear test specimens.

10) Pull-out resistance of single cartridge fired pin installed over X-HVB 110 shear connector, obtained through tension tests is influenced with base material properties and installation power level. Pull-out resistance of test series TT3-3.5 with installation power level of 3.5 is approximately 30 % higher in comparison with TT3-2 test series with lower installation power level and same base material properties. Lower base material properties of TT2-2 test series resulted in approximately 46 % lower pull-out resistance in comparison to the TT3-2 test series with same installation power level 2.0.

Chapter 5. Numerical analysis

5.1. Introduction

Extensive finite element analysis was conducted in this research in order to develop and calibrate FE models based on the results of presented experimental research. FE analysis included complete push-out models conforming to the standard push-out tests and models conforming to the shear and tension tests of cartridge fired pins, which experimental results are presented in Chapter 4. Previously calibrated FE models were further used for parametric FE analysis. FE analysis was conducted using Abaqus/Explicit code, version 6.12-3 [54].

FE models matching the push-out tests of four test series with X-HVB 110 shear connectors and shear and tension test specimens of cartridge fired pins were built and presented here with parameters which were varied through experimental analysis. The geometry, boundary conditions, load application, analysis methods, material models and applied mesh of FE models are also presented. The results gained through FE analysis were validated through comparison with experimental results.

5.2. FE modelling of push-out experiments

5.2.1. Geometry and boundary conditions

Complete FE models of push-out specimens (HSF, HSB, HSFg and HSFg-2 test series) were built consisting all specimen components used in push-out tests: prefabricated concrete slabs, reinforcement bars, steel beam, X-HVB 110 shear connectors and X-ENP-21 HVB cartridge fired pins. Quarters of real specimens were built with double vertical symmetry boundary conditions in order to accomplish shorter time required for calculation, as shown in Figure 5.1.

Double vertical symmetry boundary conditions are shown in Figure 5.2. Nodes at the top of the steel section were coupled to a reference point named “Jack”. Rough tangential behaviour between bottom surface of the concrete slab and shell element named “Support” was defined to account for possible uplift of the concrete slab at the bearing surface. Nodes of the shell element “Support” were coupled to a reference point named “Support” and assigned with a fully fixed boundary condition except for a lateral translation U3, which correspond to the global Z direction, as shown in Figure 5.3.

Displacement controlled loading was defined in the reference point “Jack”, while the vertical reaction of the reference point “Support” was used to obtain force-slip curves.

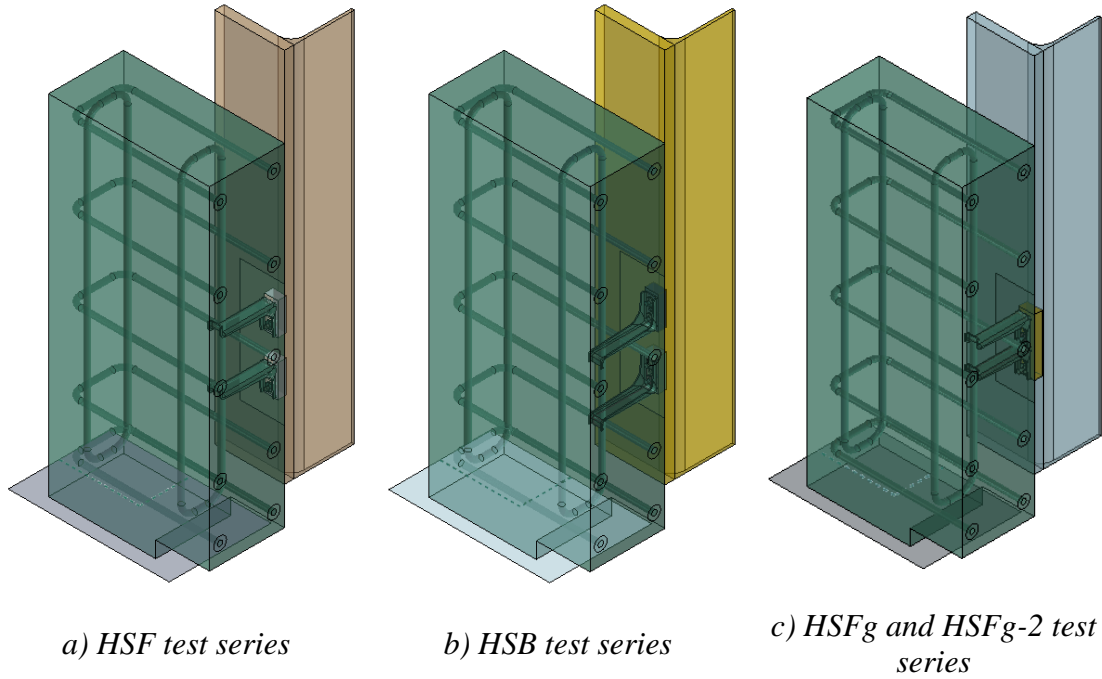


Figure 5.1. Geometry of FE models for push-out specimens

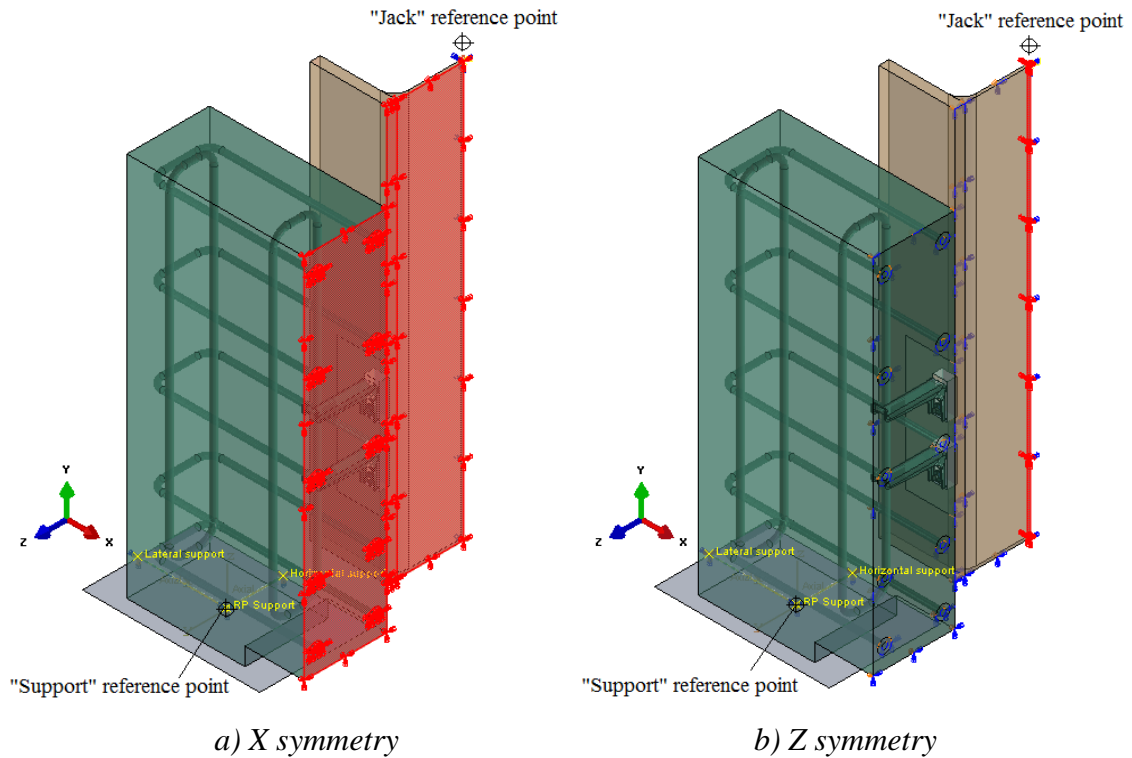


Figure 5.2. Double vertical symmetry boundary conditions of FE models

Lateral restraint of “Support” reference point was determined with the elastic stiffness k_{u3} in order to simulate an equivalent boundary condition of the concrete slab

lying on the layer of gypsum. The lateral restraint stiffness k_{u3} was calibrated to the value of $k_{u3} = 60 \text{ kN/mm}$ in order to match force-slip curves of both HSF and HSB push-out test series and also was used for development of FE models for HSFg and HSFg-2 test series. Influence of parameter lateral restraint stiffness k_{u3} on the results obtained from FE models is shown in Annex E.

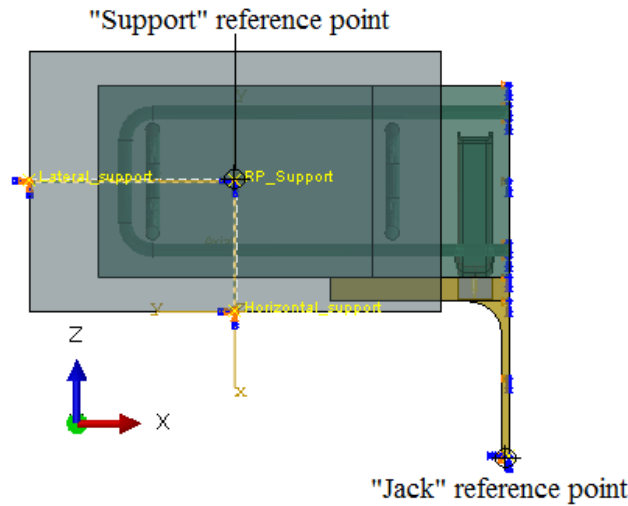


Figure 5.3. Support boundary conditions of FE models

Reinforcement bars were modelled as separate solid elements embedded in concrete slab, as shown in Figure 5.1. Contact surface of reinforcement bars and concrete was modelled as fully tied in order to preclude slip in this region. X-HVB 110 shear connector and X-ENP-21 HVB cartridge fired pins were modelled with exact geometry given in ETA-15/0876 assessment [7], as shown in Figure 5.4.

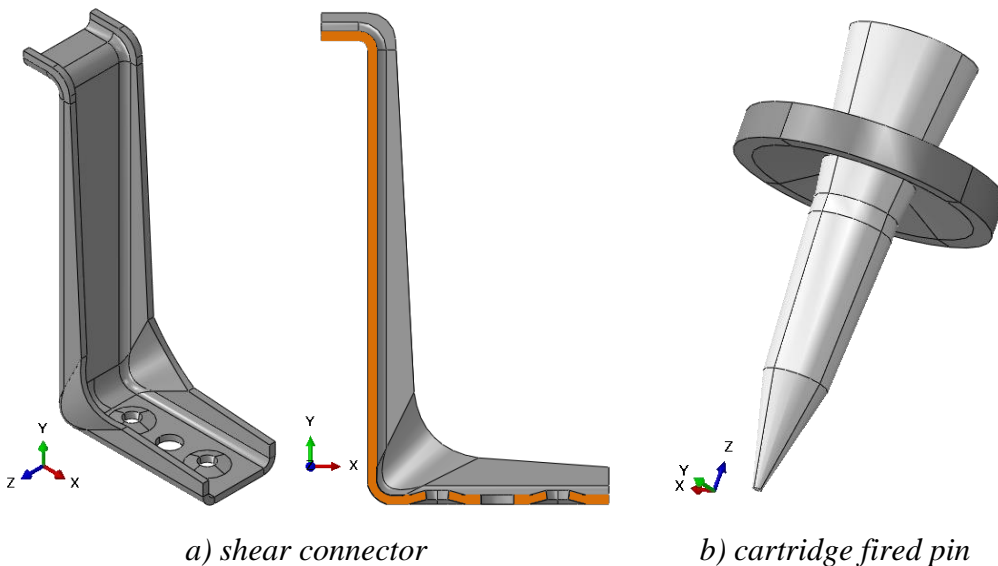


Figure 5.4. Geometry of shear connector and cartridge fired pin of FE models

In order to achieve good agreement between the FE analysis and experimental results, different geometry of the cartridge fired pins and the surrounding zone of the connector were investigated, as shown in Figure 5.5. First intention was to simplify FE model with flat geometry of the washer and connector in the zone of the pin, as shown in Figure 5.5a. Afterwards, curved geometry of washer and surrounding zone of the connector was set (see Figure 5.5b). For both analysed geometries, washer and pin were modelled as unique part of FE model. It was shown that the geometry of these parts gives a significant influence on stiffness, shear resistance and slip capacity of the push-out FE models. Finally, curved geometry of connector and washer was adopted and shown in Figure 5.4 and Figure 5.5c. Influence of the connector and cartridge fired pin geometry on results of FE analysis is presented in detail in Annex D. Fastener stand-off h_{NVS} from shear connector was adopted as 8.0 mm for HSF, HSB and HSFg-2 test series (installation power level 3.5) and 12.0 mm for HSFg test series (installation power level 2).

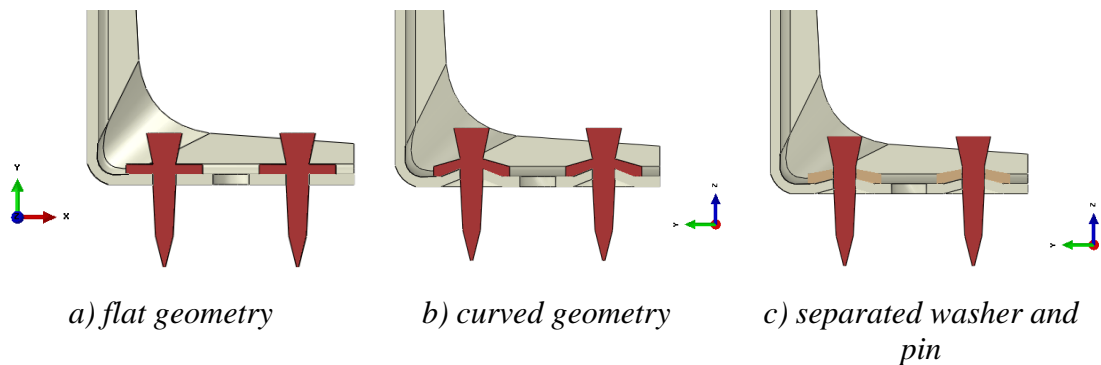


Figure 5.5. Various approaches for FE models of connector and cartridge fired pin

For all analysed FE models, Abaqus/Explicit solver was used with general contact interaction procedure. For normal and tangential behaviour “hard” and “penalty” friction formulation was used, respectively. Friction coefficient of 0.3 was set for contact surface between cartridge fired pin and steel base material, while for steel-concrete interface friction coefficient was 0.4, for all analysed push-out FE models. Influence of various values of friction coefficients on the results of FE analysis is presented for HSF and HSB test series in Annex E.

5.2.2. Loading phases

In order to achieve the stiffness and resistance obtained in experimental investigation two loading steps were applied for all push-out FE models: preloading and failure loading. The preloading step resembles installation procedure of the cartridge fired

pins. Certain slip resistance is present due to contact stresses between the connector and the steel base material. The origin of the contact stress between the shear connector and the base material lies in the installation procedure of cartridge fired pins. Shear connector and the steel base material are compressed against each other by the penetrating pin and washer, during high-speed installation. In FE models, this phenomenon is incorporated by introducing certain amount of preloading force in the pin.

The novelty in the modelling approach developed in this study is phenomenological simulation of consequence of firing the pins, thus resulting in preloading of the pins and interaction with the base material. For preloading of the cartridge fired pins various approaches were investigated as explained in more details in Annex D. Satisfying agreement of results of FE analysis with results of experimental investigation was achieved with preloading of the pins by imposing set of equivalent transverse and longitudinal strains to the body of the pins. Anisotropic expansion material properties were defined for the pin material and strains were engaged by using predefined temperature fields. The magnitude of the imposed strains was variable from 0 at the top of the pin to the maximum value at the bottom of the pin (part of the pin which is in contact with steel base material). Temperature change along the local Z direction of the pin is shown in Figure 5.6.

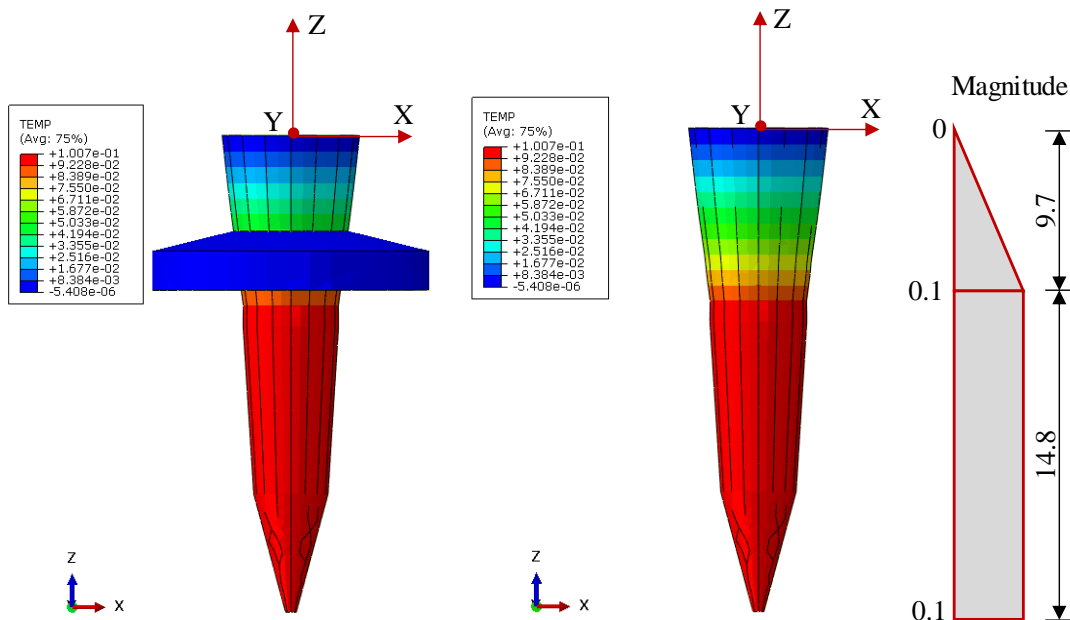


Figure 5.6. Predefined temperature fields of cartridge fired pins

As close as possible, the real pin deformation during installation was implemented by assigning the imposed transversal expansion and longitudinal shrinkage strains to the pin, therefore obtaining the clamping in the base material and preloading of the pins. The strains were assigned by anisotropic temperature expansion properties of the pin material. Deformed shape of pins (scale x5) after preloading step in FE analysis for HSF test series is presented in Figure 5.7. Transversal expansion and longitudinal shrinkage strains introduced into pins, obtaining the clamping in the base material and washer and preloading of the pins, are shown from FE analysis as Von Mises stresses at the end of the preloading step (see Figure 5.7).

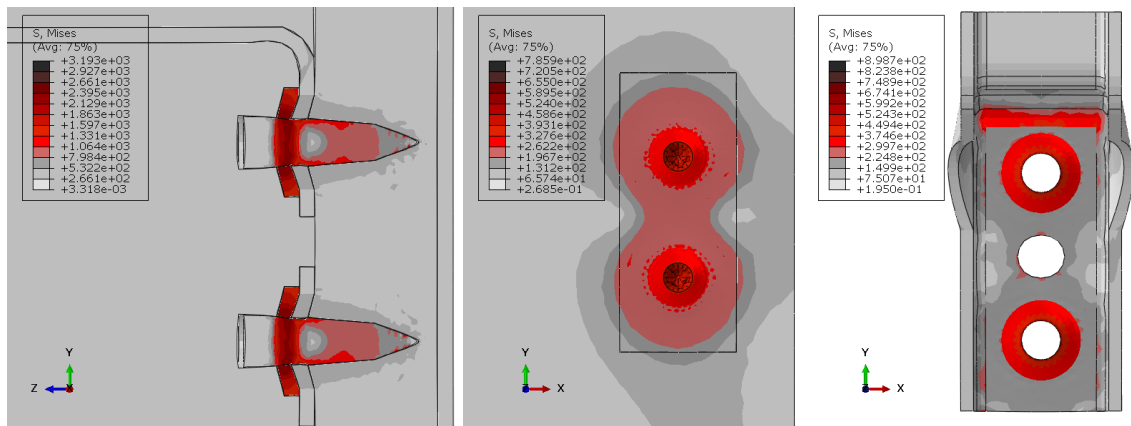


Figure 5.7. Von Mises stresses and deformed shape (scale x5) after the preloading step in FE analysis - HSF test series

The magnitude of imposed strains was iteratively calibrated to match the experimental results of push-out tests using same set of parameters for both test series, HSF and HSB. After calibration of parameters for HSF and HSB test series, the same parameters were used for development of FE model for HSFg-2 test series. The same installation power level was used for installation of HSF, HSB and HSFg-2 test series, as described in Chapter 4. Various parameters representing smaller installation power level used for installation of pins for HSFg test series were used developing FE models for specimens of this phase of experimental investigation. Various parameters are on interest for precise simulation of installation procedure of cartridge fired pins and definition of cartridge fired pin – shear connector – base material interaction. Those parameters were analysed through calibration procedure of pull-out resistance of pins loaded in tension and push-out FE models and in detail explained in Chapter 6.1 and Chapter 6.2.

Displacement controlled failure loading was applied in the second step. In this step, vertical displacement “U2” was applied to the “Jack” reference point to which the top steel section surface was constrained. Value of $U_2 = 10.0$ mm was used for FE models of HSF and HSFg-2 test series, while $U_2 = 15.0$ mm and $U_2 = 8.0$ mm was applied for HSB and HSFg test series, respectively. Preloading and failure loading were applied with time dependent amplitude functions in order to avoid large inertia forces in the quasi-static analysis. Time dependent amplitude functions for both loading steps of HSF push-out FE model are presented in Figure 5.8.

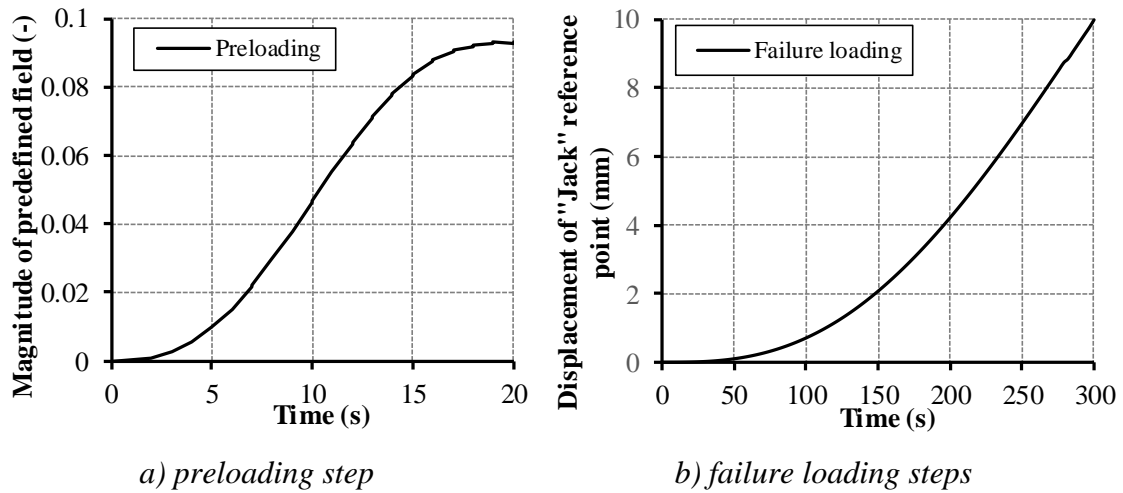


Figure 5.8. Smoothed amplitudes of FE analysis steps - HSF test series

FE analysis was performed as quasi-static using the dynamic explicit solver. Mass scaling with desired time increment of 0.001 s was used in both analysis steps (preloading and failure loading) for all analysed push-out series. Scaling factor was set as recomputed in every integration step and non-uniform (different for each finite element).

5.2.3. Finite element mesh

Different parts of the push-out FE models of all test series were meshed with various elements type and size. Complex geometry of connector and pins required smaller finite element size. Also smaller finite element size in the concrete and steel sections at the surrounding zone of connectors and pins was adopted, as shown in Figure 5.9 and Figure 5.10, while larger finite elements were used in distant areas.

Complex geometry of shear connectors and cartridge fired pins required tetrahedron finite element (C3D10M - 10-node modified quadratic tetrahedron). Connectors were meshed with approximate finite element size of 3.0 mm, cartridge fired

pins with approximate size of 1.0 mm and washer which was modelled as separate part, as previously explained, with approximate size of 2.0 mm. Also, connector holes which are envisaged for pins installation and washer contact region with cartridge fired pin were meshed with 1.0 mm element size. The same element size in concrete slab and steel profile in the contact zone with shear connector and cartridge fired pins was set, as shown in Figure 5.10. FE mesh of connectors and pins is shown in Figure 5.9.

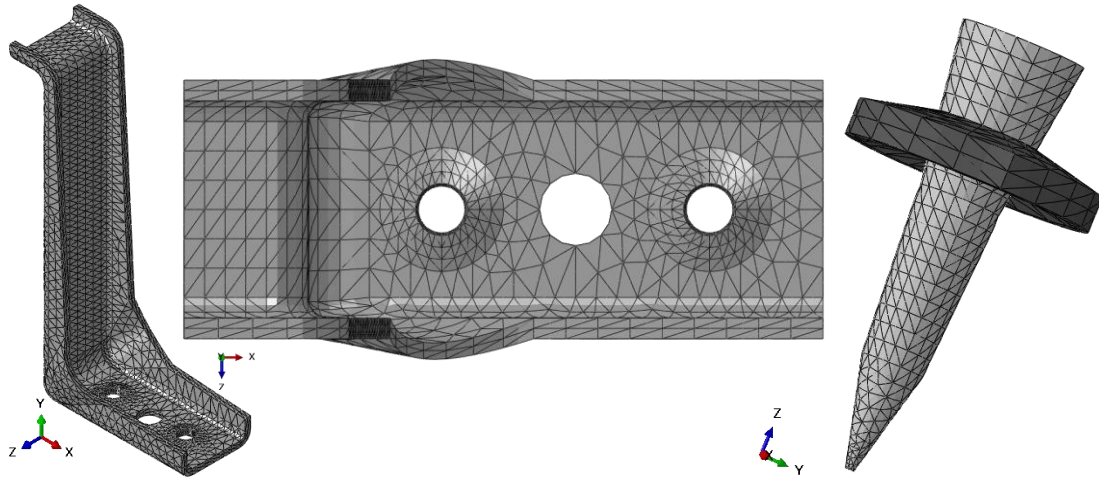


Figure 5.9. FE model mesh for shear connector and pin

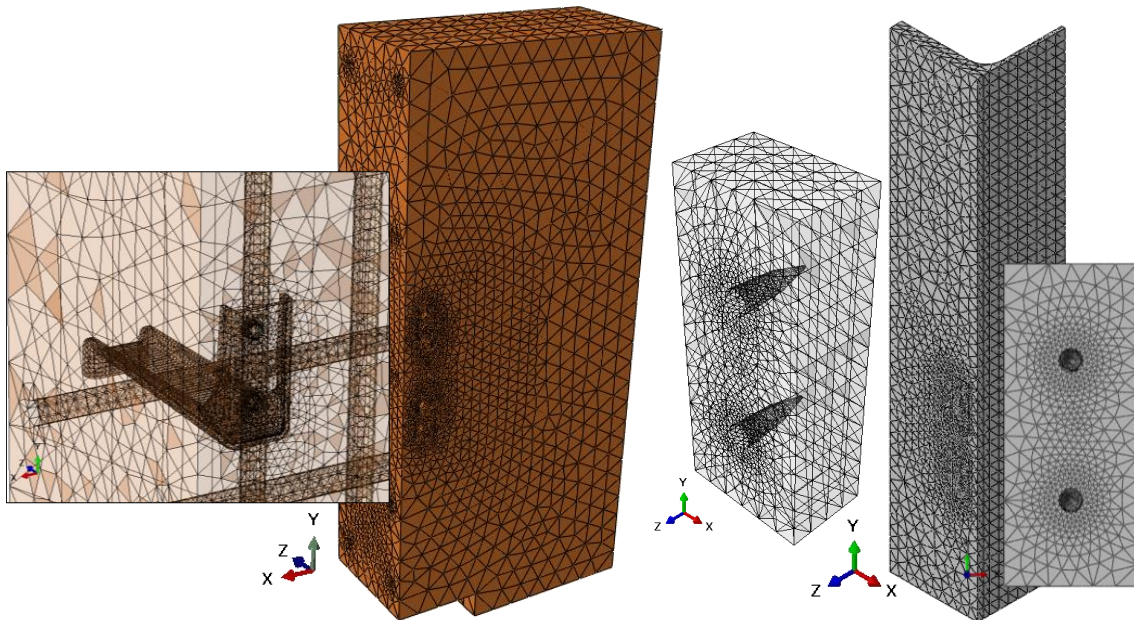


Figure 5.10. FE model mesh for concrete slab and steel profile

Concrete slab was meshed with approximate size of 25.0 mm of finite elements with C3D4 (4-node linear tetrahedron) finite elements. Steel profile was meshed with C3D10M tetrahedron finite element with approximate size of 15.0 mm. FE mesh of

concrete slab and steel profile is shown in Figure 5.10. Reinforcement bars were meshed with approximate size of 10.0 mm of finite elements with C3D4. After calibrating of FE mesh for HSF and HSB FE models in order to match the experimental results of phase 1, the same FE mesh was used for HSFg and HSFg-2 series (phase 2 and 3 of experimental investigation).

5.2.4. Material models

Examined material properties of shear connector, steel profile and concrete slab are presented in detail in Chapter 4 and used as input parameters for FE analysis of these components. Ductile damage material models for steel section, shear connectors, cartridge fired pins and reinforcement were not considered, as they are not of interest due to obtained failure mechanisms from experimental investigation.

5.2.4.1. Cartridge fired pins, shear connector and steel profile

Prescribed stress-strain relationship of X-ENP-21 HVB cartridge fired pins was simple elastic, linear hardening material model according to EN 1993-1-5:2009 [55], with tensile strength f_u of approximately 2800 MPa. Shear damage of cartridge fired pins was considered in FE models, since the shear failure of certain cartridge fired pins was obtained during experimental investigation of push-out specimens. Parameters of shear damage material model were defined based on the recommendation given by Pavlović [4] for damage material model of bolts. Shear stress ratio was defined for pure shear condition as $\theta_s = 1.732$. Shear damage model was defined in Abaqus [54] through damage initiation criterion and damage evolution law and calibrated to a constant value of equivalent plastic strain at the onset of damage. Equivalent plastic strain at the onset of damage was set as 0.08, equivalent plastic displacement at failure as 0.3 mm and exponential law parameter of 0.7.

Expansion material properties for cartridge fired pins were defined for the embedded part of the pin in steel base material and part of the pin beyond the steel base material in order to achieve desirable deformation fields that result in preloading of the pin and its binding to the base material. For the embedded part of the cartridge fired pin expansion coefficient was set as 0.8 in directions of pin local axis X and Y and 0 for local axis Z. Moreover, expansion coefficients were set as 0.8 in directions of material local axis X and Y and -1.0 for local axis Z for upper part of pin, as shown in Figure 5.11a. This allows clamping of the upper part of the pin in the washer and lower part in the base

material during the preloading step. Preloading accomplishes satisfying stiffness of complete push-out models in FE analysis for HSF, HSB and HSFg-2 test series, for which same installation power level was introduced during the installation procedure (approximately 3.5 as described in Chapter 4.1).

Expansion material properties for cartridge fired pins which were installed with lower installation power level were iteratively calibrated in order to accomplish satisfying agreement with experimental results of HSFg test series. For part of the pin which is beyond the steel base material, expansion coefficients were set as 0.8 in directions of material local axis X and Y and -1 for local axis Z, same as for the HSF, HSB and HSFg-2 series, as shown in Figure 5.11b. Lower installation power level was introduced through smaller expansion coefficients for embedded part of the cartridge fired pin, which were defined as 0.4 in directions of pin local axis X and Y and 0 for local axis Z, as shown in Figure 5.11b. Moreover, lower installation power level was introduced in FE analysis also through lower depth of penetration of cartridge fired pin in the steel base material, which leads to the higher pins stand-off from the base material upper surface. Prescribed cartridge fired pin stand-off was 8.0 mm for HSF, HSB and HSFg-2 FE models (installation power level 3.5) and 12.0 mm for HSFg FE models (installation power level 2).

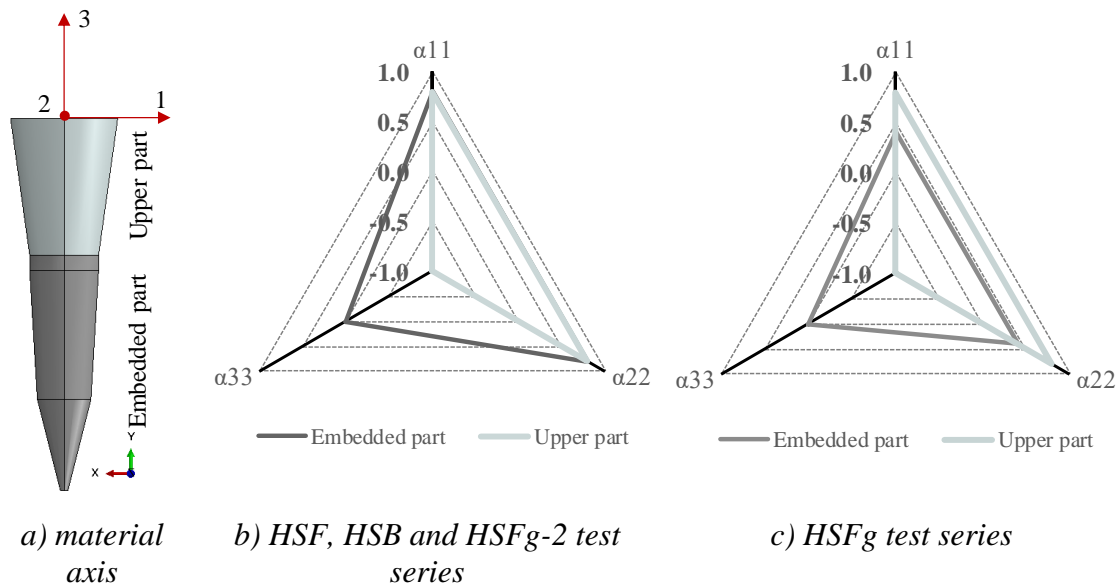
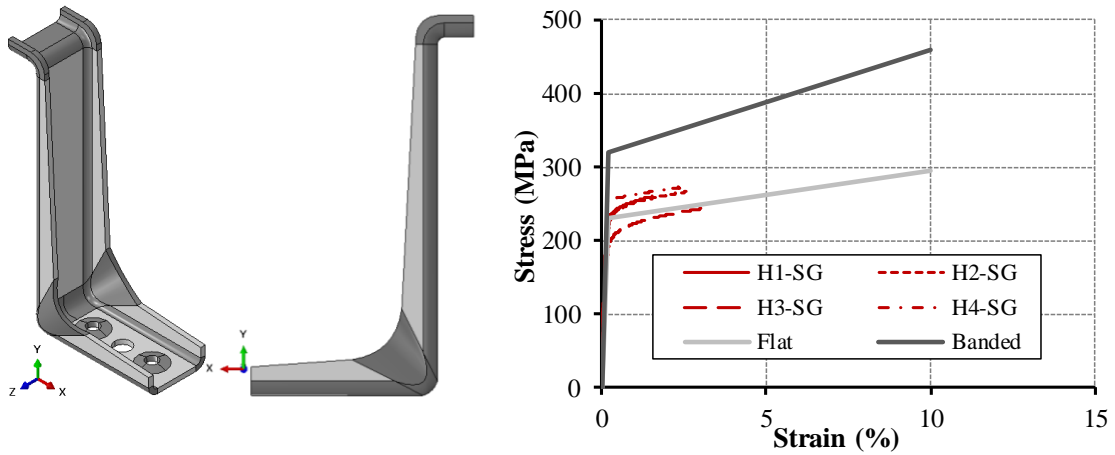


Figure 5.11. Orthotropic material properties of cartridge fired pins - preloading step in FE analysis

Material properties of shear connector for FE models were defined based on the experimental investigation results presented in Chapter 4.3.1. Elastic, linear hardening material model was used for FE analysis, according to EN 1993-1-5:2009 [55] as presented in Figure 5.12b. Material properties of flat parts of shear connector were defined based on tensile coupon test results, with proof stress f_{02} of 231.0 MPa and tensile strength f_u of 295.2 MPa with 0.1 strain rate, as the upper bound limit of nominal material properties. Examined tensile test coupons built from the flat part of connectors anchorage leg verified assumption of material hardening due to cold-forming process. Therefore, additional material hardening was introduced to the banded parts of shear connector, as shown in Figure 5.12a. Hardening was introduced using proof stress $f_{02} = 320$ MPa, and tensile strength $f_u = 460.0$ MPa, as shown in Figure 5.12b.



a) connector material arrangement

b) elastic, linear hardening model

Figure 5.12. Connector material properties - FE analysis

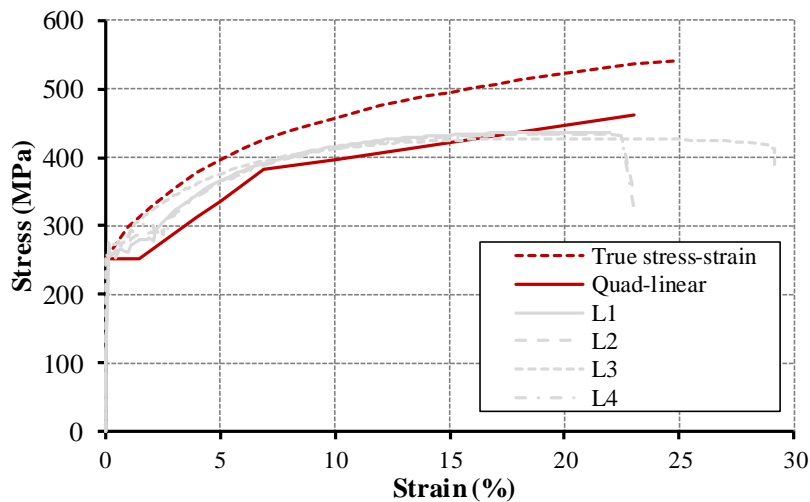


Figure 5.13. Quad-linear material model of steel profile - FE analysis

Steel base material properties in FE analysis were analysed through true stress-strain relation, according to EN 1993-1-5:2009 [55] and quad-linear material model which is proposed for hot-rolled steels by Yun and Gardner [56], as shown in Figure 5.13. True stress-strain relation is defined according to Eq. 5.1 from the tensile coupon test results presented in Chapter 4.3.1.

$$\sigma_{\text{true}} = \sigma \cdot (1 + \varepsilon) \quad (5.1)$$

$$\varepsilon_{\text{true}} = \ln \cdot (1 + \varepsilon) \quad (5.2)$$

The quad-linear material model includes an elastic response up to the yield point, yield plateau and strain hardening up to the ultimate tensile stress, as shown in Figure 5.13. The proposed material model is suitable for FE analysis of models with large plastic strains, such as design of connections [56]. The four stages of quad-linear stress-strain model are presented by Eq. 5.3. Increase of tensile strength of steel base material obtained from hardness test (Chapter 4.6) was introduced for definition of quad-linear material model. Average increase of 33.0 MPa, obtained from six measuring points close to the pins holes (1-3 and 6-8 measuring positions, see Table 4.15) was considered. Modulus of elasticity and yield stress were obtained from tensile coupon tests.

$$f(\varepsilon) = \begin{cases} E\varepsilon & \text{for } \varepsilon \leq \varepsilon_y \\ f_y & \text{for } \varepsilon_y < \varepsilon \leq \varepsilon_{\text{sh}} \\ f_y + E_{\text{sh}} \cdot (\varepsilon - \varepsilon_{\text{sh}}) & \text{for } \varepsilon_{\text{sh}} < \varepsilon \leq C_1 \cdot \varepsilon_u \\ f_{C1\varepsilon_u} + \frac{f_u - f_{C1\varepsilon_u}}{\varepsilon_u - C_1 \cdot \varepsilon_u} \cdot (\varepsilon - C_1 \cdot \varepsilon_u) & \text{for } C_1 \cdot \varepsilon_u < \varepsilon \leq \varepsilon_u \end{cases} \quad (5.3)$$

with:

$$\varepsilon_y = f_y / E \quad (5.4)$$

$$\varepsilon_{\text{sh}} = 0.1f_y / f_u - 0.055 \quad \text{but} \quad 0.015 \leq \varepsilon_{\text{sh}} \leq 0.03 \quad (5.5)$$

$$\varepsilon_u = 0.6 \cdot (1 - f_y / f_u) \quad \text{but} \quad 0.06 \leq \varepsilon_u \leq A \quad (5.6)$$

$$C_1 = \frac{\varepsilon_{\text{sh}} + 0.25 \cdot (\varepsilon_u - \varepsilon_{\text{sh}})}{\varepsilon_u} \quad (5.7)$$

$$E_{\text{sh}} = \frac{f_u - f_y}{C_2 \varepsilon_u - \varepsilon_{\text{sh}}} \quad (5.8)$$

$$C_2 = \frac{\varepsilon_{sh} + 0.4 \cdot (\varepsilon_u - \varepsilon_{sh})}{\varepsilon_u} \quad (5.9)$$

In previous expressions:

f_y is the yield stress;

f_u is the ultimate stress;

E is the modulus of elasticity;

E_{sh} is the strain hardening modulus;

ε_y is the yield strain;

ε_{sh} is the strain hardening strain;

ε_u is the ultimate strain;

A is the elongation after fracture defined in material specifications [8];

C_1 is the material coefficient that defines the transition point in the strain hardening region;

C_2 is the material coefficient;

$f_{Cl\epsilon_u}$ is the stress corresponding to transition point in the strain hardening region.

Implementation of quad-linear material model provided a better agreement with experimental results of four analysed push-out series, in comparison to the implementation of true stress-strain relation according to EN 1993-1-5:2009 [55]. This can be explained through complexity of base material modification due to installation procedure of cartridge fired pins. The influence of these two material models and various base material strengths on the results of push-put FE models of HSF and HSB test series is presented through parametric analysis given in Chapter 6.2.

5.2.4.2. Concrete

Concrete stress-strain relation for FE analysis was defined using experimentally obtained material properties of concrete cylinders, which is explained in Chapter 4.3.2 and based on recommendations given in EN 1992-1-1:2004 [50]. Normalized material properties of prefabricated concrete slabs at the age of push-out tests show close agreement with properties of infill concrete. Therefore, mean values of cylinder

compressive strength, axial tensile strength and modulus of elasticity were used to define stress-strain relation for FE analysis. Stress-strain relation was defined for each phase of push-out examination, for four push-out FE models. Concrete behaviour was described using concrete damage plasticity model in Abaqus [54]. Non-linear stress-strain relation presented in Eq. 5.10 and given in EN 1992-1-1:2004 [50] was used to describe concrete behaviour up to the 3.5 ‰ of strain:

$$\sigma_c = f_{cm} \cdot \frac{k\eta - \eta^2}{1 + (k-2) \cdot \eta} \quad \text{for } \eta \leq \varepsilon_{cu1} / \varepsilon_c \quad (5.10)$$

with:

$$\eta = \varepsilon_c / \varepsilon_{c1} \quad \text{and} \quad k = 1.05 \cdot \varepsilon_{c1} \cdot E_{cm} / f_{cm} \quad \text{defined according to EN 1992-1-1:2004 [50].}$$

In previous expression:

σ_c is the concrete uniaxial compressive stress;

ε_c is the uniaxial concrete compressive strain;

f_{cm} is the cylinder compressive strength;

E_{cm} is the modulus of elasticity;

ε_{c1} is the strain at peak stress, adopted as $2.05 \cdot 10^{-3}$ according to EN 1992-1-1:2004 [50];

ε_{cu1} is the nominal ultimate strain, adopted as $3.50 \cdot 10^{-3}$ according to EN 1992-1-1:2004 [50].

According to EN 1992-1-1:2004 [50], plasticity curve was defined only up to the nominal ultimate strain ε_{cu1} . High compressive and tensile strains are expected in the surrounding region of shear connectors in push-out FE models. Therefore, definition of stress-strain relation only up to the nominal ultimate strain ε_{cu1} would lead to unreal estimation of concrete strength. Also, definition of descending part of stress-strain relation for strains beyond the nominal ultimate strain ε_{cu1} depends of various factors and calibration according to experimental results should lead to the most precise definition.

Stress-strain relation for higher values of plastic strain is defined by several authors and standards. Chinese standard GB50010:2002 [57] defines stress-strain relation according to Eq. 5.11, with recommended values of factors $\alpha_a = 1.5$ and $\alpha_d = 2.8$.

$$\sigma_c = \begin{cases} f_{cm} \cdot \left[\alpha_a \cdot (\varepsilon_c / \varepsilon_{cu1}) + (3 - 2 \cdot \alpha_a) \cdot (\varepsilon_c / \varepsilon_{cu1})^2 + (\alpha_a - 2) \cdot (\varepsilon_c / \varepsilon_{cu1})^3 \right] & \text{for } \varepsilon_c / \varepsilon_{cu1} \leq 1 \\ f_{cm} \cdot (\varepsilon_c / \varepsilon_{cu1}) / \left[\alpha_d \cdot (\varepsilon_c / \varepsilon_{cu1} - 1)^2 + (\varepsilon_c / \varepsilon_{cu1}) \right] & \text{for } \varepsilon_c / \varepsilon_{cu1} > 1 \end{cases} \quad (5.11)$$

In previous expression:

α_a, α_d is the ascending and descending parameters for concrete compressive stress-strain curve according to [57].

Another definition of concrete stress-strain relation for descending part of stress-strain relation beyond the nominal ultimate strain ε_{cu1} is obtained by Carreira and Chu [58] and presented in Eq. 5.12.

$$\sigma_c = f_{cm} \cdot \frac{\gamma \cdot (\varepsilon_c / \varepsilon_{cu1})}{\gamma - 1 + (\varepsilon_c / \varepsilon_{cu1})^\gamma} \quad (5.12)$$

with:

$$\gamma = \left(\frac{f_{cm}}{32.4} \right)^3 + 1.55 \quad (5.13)$$

Sinusoidal extension of stress-strain relation beyond the nominal ultimate strain ε_{cu1} is proposed by Pavlović et al. [51] and presented in Eq.5.14.

$$\sigma_c = f_{cm} \cdot \left[\frac{1}{\beta} - \frac{\sin(\mu^{\alpha_{te}} \cdot \alpha_{te} \cdot \pi / 2)}{\beta \cdot \sin(\alpha_{te} \cdot \pi / 2)} + \frac{\mu}{\alpha} \right] \quad \text{for } \varepsilon_{cuD} < \varepsilon_c \leq \varepsilon_{cuE} \quad (5.14)$$

$$\left[f_{cuE} \cdot (\varepsilon_{cuF} - \varepsilon_c) + f_{cuF} \cdot (\varepsilon_c - \varepsilon_{cuE}) \right] / (\varepsilon_{cuF} - \varepsilon_{cuE}) \quad \text{for } \varepsilon_c > \varepsilon_{cuE}$$

with:

$$\mu = (\varepsilon_c - \varepsilon_{cuD}) / (\varepsilon_{cuE} - \varepsilon_{cuD}) \quad (5.15)$$

$$\beta = f_{cm} / f_{cu1} \quad (5.16)$$

In previous expressions μ is the relative coordinate of sinusoidal part of the stress-strain relation end points. Beginning of the sinusoidal extended part of stress-strain relation was defined as $\varepsilon_{cuD} = \varepsilon_{cu1}$ and $f_{cuD} = f_{cu1} = \sigma(\varepsilon_{cu1})$, according to Pavlović et al. [51]. Sinusoidal part of stress-strain relation has an end in the point with strain ε_{cuE} and with concrete strength reduced to f_{cuE} by factor $\alpha = f_{cm} / f_{cuE}$. Linear descending part of the stress-strain relation continue after sinusoidal part and ends at the point with strain ε_{cuF}

and final residual strength of concrete f_{cuF} . Pavlović et al. [51] proposed end strain $\varepsilon_{cuF} = 0.10$ large enough so as not to be achieved in the analyses.

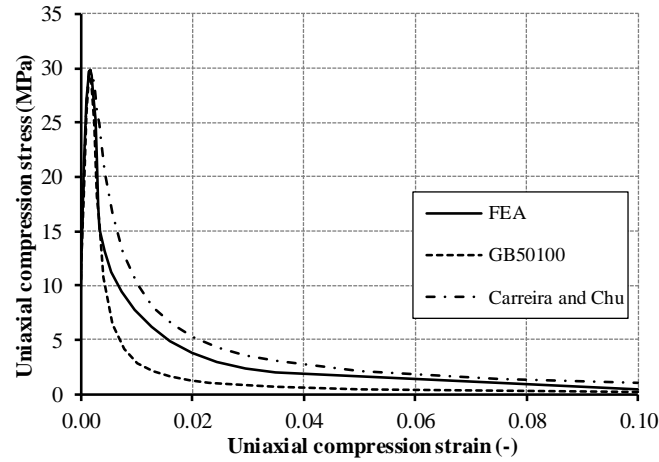


Figure 5.14. Stress-strain relation for concrete compression behaviour - HSF and HSB push-out FE models

After calibration of the parameters to match experimental results of three phases of push-out experimental analysis, further values of stress-strain relation parameters were adopted: final residual strength of concrete $f_{cuF} = 0.4$ MPa, reduction factor $\alpha = 15$ and end strain $\varepsilon_{cuE} = 0.0035$. Factors which governing tangent angels at the beginning and the end of sinusoidal part of the curve were set as $\alpha_{tD} = 0.5$ and $\alpha_{tE} = 0.9$. For presented FE analysis of push-out models, stress-strain relation proposed by Pavlović et al. [51] and given in Eq. 5.14 was defined and shown in Figure 5.14. Figure 5.14 represent a comparison of adopted stress-strain relation according to Pavlović et al. [51] with other relations given in Eq. 5.11 and Eq. 5.12, for push-out FE models of HSF and HSB test specimens of phase 1 of experimental investigation.

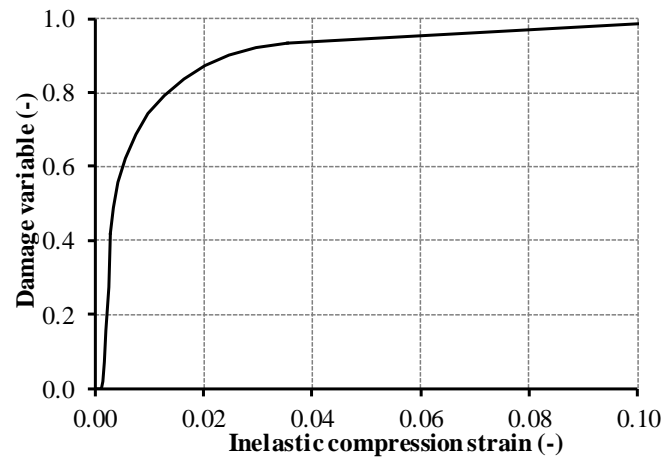


Figure 5.15. Compression damage - HSF and HSB push-out FE models

For definition of concrete compression behaviour in Abaqus, damage evolution law was defined as a function of inelastic strain and derived from the uniaxial stress-strain curve. Damage variable was determined by comparing undamaged and damaged concrete response beyond the ultimate compressive strength f_{cm} , as defined in Eq. 5.17. Concrete compression damage curve is shown in Figure 5.15.

$$D_c = 1 - f_{cm} / \sigma_c \quad (5.17)$$

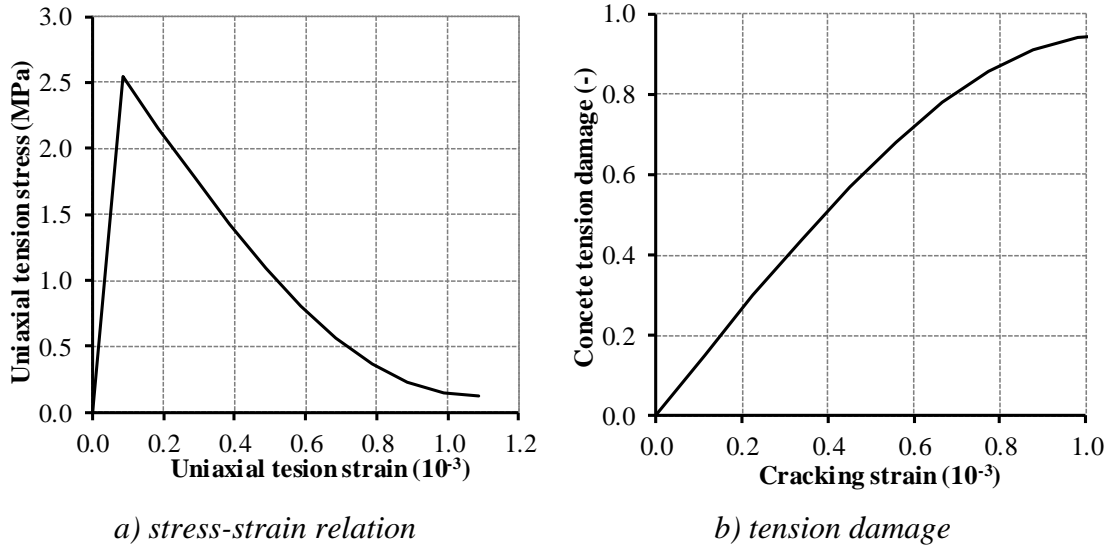


Figure 5.16. Concrete behaviour in tension - HSF and HSB push-out FE models

Plasticity parameters which were defined in concrete damage plasticity model in Abaqus were set according to recommendations given in Abaqus [54]. Flow potential eccentricity was set as $\varepsilon = 0.1$, biaxial/uniaxial compressive strength ratio $\sigma_{b0} / \sigma_{c0} = 1.2$ and dilatation angle $\psi = 36^\circ$. Parameter K which represent ratio of the second stress invariant on the tensile meridian to the compressive meridian was iteratively calibrated to match the results of push-out tests. It's default value according to Abaqus [54] is $2/3$ and $K = 0.57$ was defined for all FE models of push-out tests. Influence of parameter K on the results of push-out FE models of HSF and HSB test series is shown in Annex E.

Damage evolution law for concrete behaviour in tension was defined in Abaqus according to Eq. 5.18. Concrete behaviour in tension is shown in Figure 5.16.

$$D_t = 1 - f_{ctm} / \sigma_t \quad (5.18)$$

Stress-strain concrete relation in tension was described through linear increase of tensile stress along with modulus of elasticity E_{cm} (Figure 5.16a), up to the peak value f_{ctm} . After this point tension stress was degraded in sinusoidal manner until stress $f_{ctm} / 20$

assigned with a fully fixed boundary condition. Displacement controlled loading was defined in the reference point “Jack”, while the reaction of the reference point “Support” in the direction of the global X axis was used to obtain force-relative displacement curves. Same boundary conditions were applied for the tension test specimen (TT), as shown in Figure 5.17b. Definition of the “Jack” reference point was considered through two alternatives: coupling of the nodes of the pin head and coupling of the washer nodes. Preloading of pins, which was applied on upper part of cartridge fired pin (see Figure 5.11) resulted in less reliable results of pull-out resistance when coupling of pin head nodes to reference point “Jack” was applied. Therefore, coupling of the washer nodes, as shown in Figure 5.17b, was considered as close enough to the real conditions obtained during tension tests.

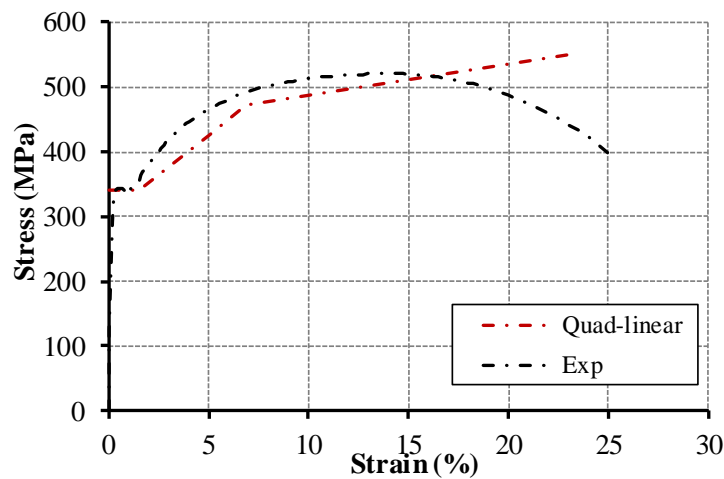
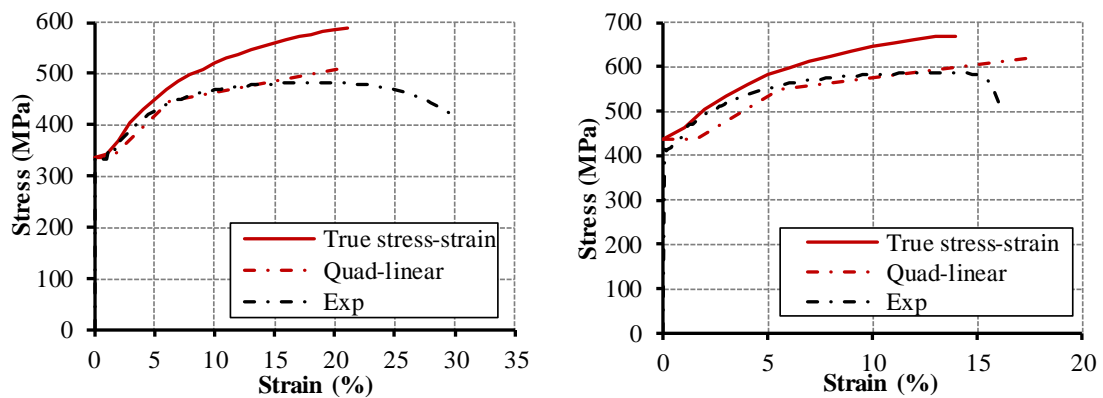


Figure 5.18. *Quad-linear material model of steel base material - FE models of ST specimen*

Abaqus/Explicit solver was used with general contact interaction procedure, for FE models of ST and TT specimens. For normal and tangential behaviour “hard” and “penalty” friction formulation was set, respectively. Friction coefficient of 0.3 and 0.25 was set for contact surface between cartridge fired pin and steel base material for FE model of ST and TT specimen. Lower value of interface friction coefficient of TT FE models was used for specimens with lower installation power level, which is in detail explained in Chapter 6. Friction coefficient of 0.4 was set to steel base plate – cover plate interface of ST specimen, and steel plate – shear connector interface for TT specimen. Cartridge fired pin stand-off from steel cover plate of ST specimen and shear connector

of TT specimens was set as 12.0 mm, which was obtained after measurement of test specimens (results are presented in Chapter 4.7.)

Two loading steps were applied, preloading and failure loading. Preloading step is applied in the same way as for push-out FE models, as previously described in Chapter 5.2.2. Displacement controlled failure loading was applied in the second step, through displacement “U1” and “U3” applied to the reference point “Jack” of ST and TT FE models, respectively. Value of U1 = 6.0 mm was used for FE model of ST test specimen, while U3 = 0.25 mm was applied for TT test specimens. Mass scaling with time increment of 0.001 s was used in both analysis steps (preloading and failure loading) for both FE models. Finite element mesh and material properties of cartridge fired pins and shear connector which were calibrated through FE analysis of push-out specimens (see Chapter 5.2.3 and 5.2.4) were used for ST and TT FE models.



a) TT2 specimen

b) TT3 specimen

Figure 5.19. Analysed material models of steel base material - FE models of TT specimen

Preloading of cartridge fired pins, which represents installation procedure, was defined for two installation power levels (2 and 3.5) through various material expansion properties as explained in detail in Chapter 5.2.4.1. Steel base material properties for shear tests specimens (ST) were defined as quad-linear material model, as shown in Figure 5.18. Tension test specimens of cartridge fired pins (TT) were analysed in FE analysis with true stress-strain relation of steel base material and with quad-linear material model, as shown in Figure 5.19. Influence of the analysed material models on pull-out resistance of cartridge fired pins through tension test FE models (TT) was presented in Chapter 6.

5.4. Comparison of FE analysis results with experimental investigation

5.4.1. Push-out FE models

Results of complete push-out FE models after calibration of all parameters are presented and compared with experimental results. The comparison of experimental and FE analysis results is performed for total force obtained for one test specimen, for all analysed test series. Comparison of the FE analysis and experimental results of the first phase of experimental investigation is given in Figure 5.20 and Figure 5.21. The same concrete material properties were used for both orientation of shear connectors (HSF and HSB test series) of the first push-out experimental phase.

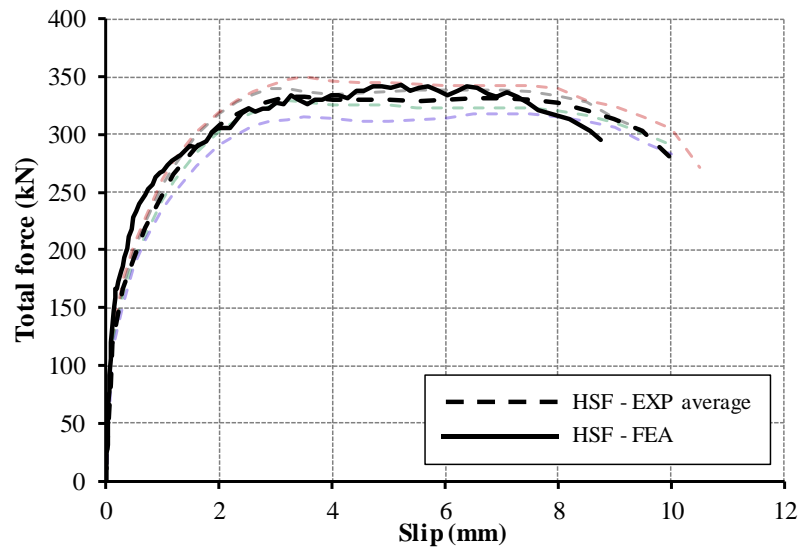


Figure 5.20. Experimental and FE analysis force-slip curves - HSF test series

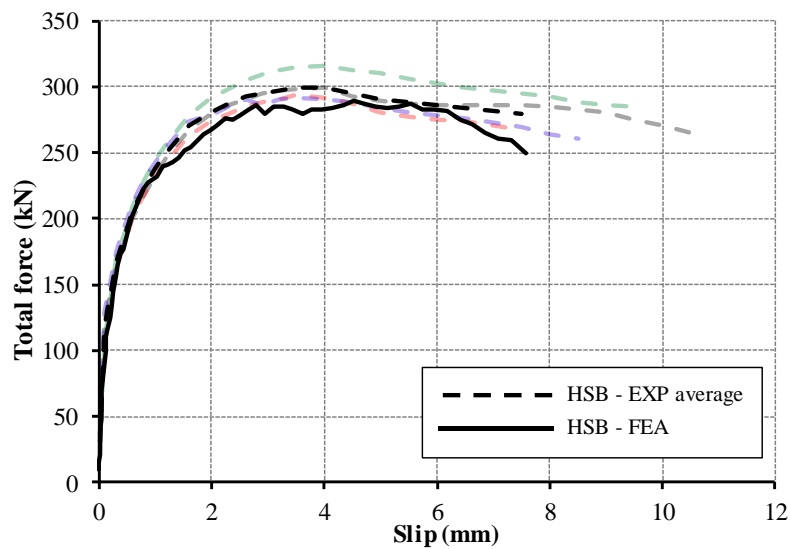


Figure 5.21. Experimental and FE analysis force-slip curves - HSB test series

Comparison of the second and third phase of push-out experimental results with results of FE analysis is given in Figure 5.22 and Figure 5.23, respectively. Concrete material properties were defined different from the HSF and HSB FE models, representing the experimentally obtained material properties of these push-out phases. Also, the same installation power level used for preparation of HSF, HSB and HSFg-2 test specimens was used for FE models. Material properties of steel base material, shear connector and cartridge fired pins were defined as the same values for all analysed FE test series. All parameters of significance, which represent interaction properties between different parts of complete FE models were defined as the same values for four analysed FE push-out models of three experimental phases.

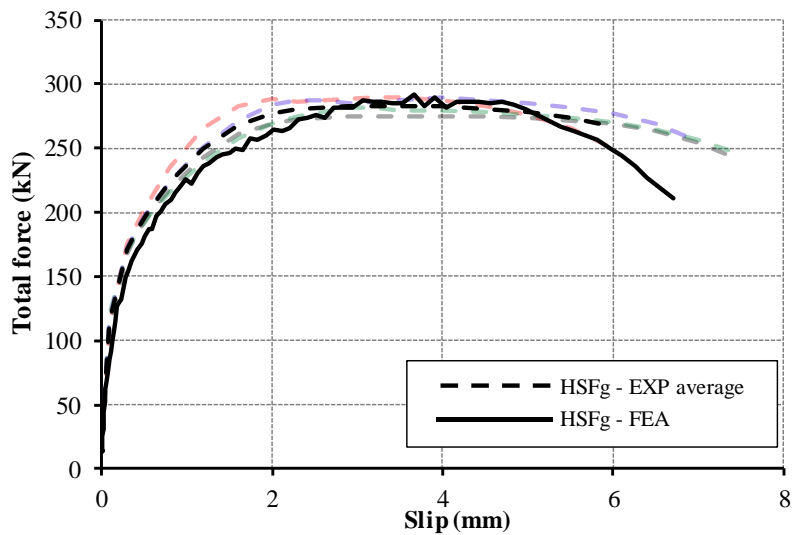


Figure 5.22. Experimental and FE analysis force-slip curves - HSFg test series

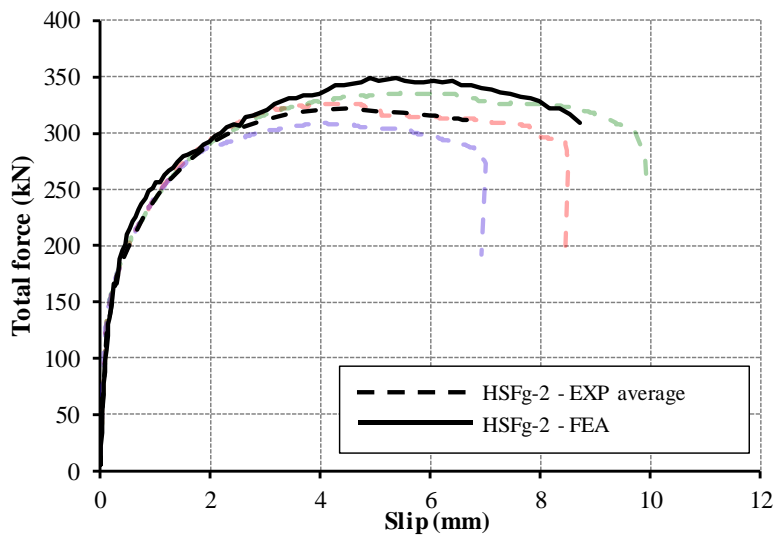


Figure 5.23. Experimental and FE analysis force-slip curves – HSFg-2 test series

Comparison of the obtained results is also presented in Table 5.1. Comparison is presented through ultimate shear force P_{ult} and characteristic value of slip capacity δ_{uk} , which are obtained as relative slip value corresponding to the 90% of ultimate shear force at descending part of force-slip curve. Good agreement of force-slip curves gained from FE analysis is obtained for all test specimens, considering ultimate shear force, initial stiffness and descending part of the force-slip curves, as shown in Figure 5.20, Figure 5.21, Figure 5.22, Figure 5.23.

Table 5.1. Experimental and FE analysis results of push-out specimens

Push-out specimen	Ultimate shear force (kN)			Characteristic value of slip (mm)		
	FEA	Experimental	Ratio	FEA	Experimental	Ratio
	$P_{ult,fea}$	$P_{ult,exp}$	$P_{ult,fea}/P_{ult,exp}$	$\delta_{uk,FEA}$	$\delta_{uk,test}$	$\delta_{uk,FEA}/\delta_{uk,test}$
HSF	342.7	335.4	1.02	8.38	9.63	0.87
HSB	288.9	300.3	0.96	7.09	8.71	0.81
HSFg	291.4	284.6	1.02	5.53	6.14	0.90
HSFg-2	348.4	323.8	1.08	8.53	7.60	1.12

FE analysis and experimental results of push-out specimens are compared through concrete compressive damage (DAMAGEC) for all analysed push-out test specimens, as shown in Figure 5.24. Interface layer between prefabricated concrete slab and steel beam is presented. Concrete compressive damage from FE analysis is presented at the end of calculation procedure, when pull-out of cartridge fired pins is observed. Good match between experimental and FE analysis results is achieved, considering presented concrete compressive damage variable which is analysed.

Higher compressive damage is achieved for HSF and HSB test specimens with shear connectors positioned at minimal recommended distances in comparison to their group arrangement, as shown in Figure 5.24. Moreover, the highest quantitative damage of concrete is achieved for HSB specimens, or backward orientation of shear connectors, which is also obtained through experimental results as less favourable orientation of shear connectors. Lower installation power level of HSFg test specimens, resulted in the lowest damage of concrete in the surrounding region of shear connectors. This also leads to the conclusion that lower installation power level results pull-out of cartridge fired pins from steel base material prior to reaching extensive crushing of concrete around the connectors.

Prefabricated concrete slabs were cut in longitudinal direction through shear connectors and cartridge fired pins. Sections are compared with corresponding results of

FE analysis, also through concrete compressive damage variable, as shown in Figure 5.25. Good agreement with results of experiments is achieved considering concrete compressive damage and deformation of shear connectors. Tensile strains in prefabricated concrete slab in the region of shear connector is given in Figure 5.26.

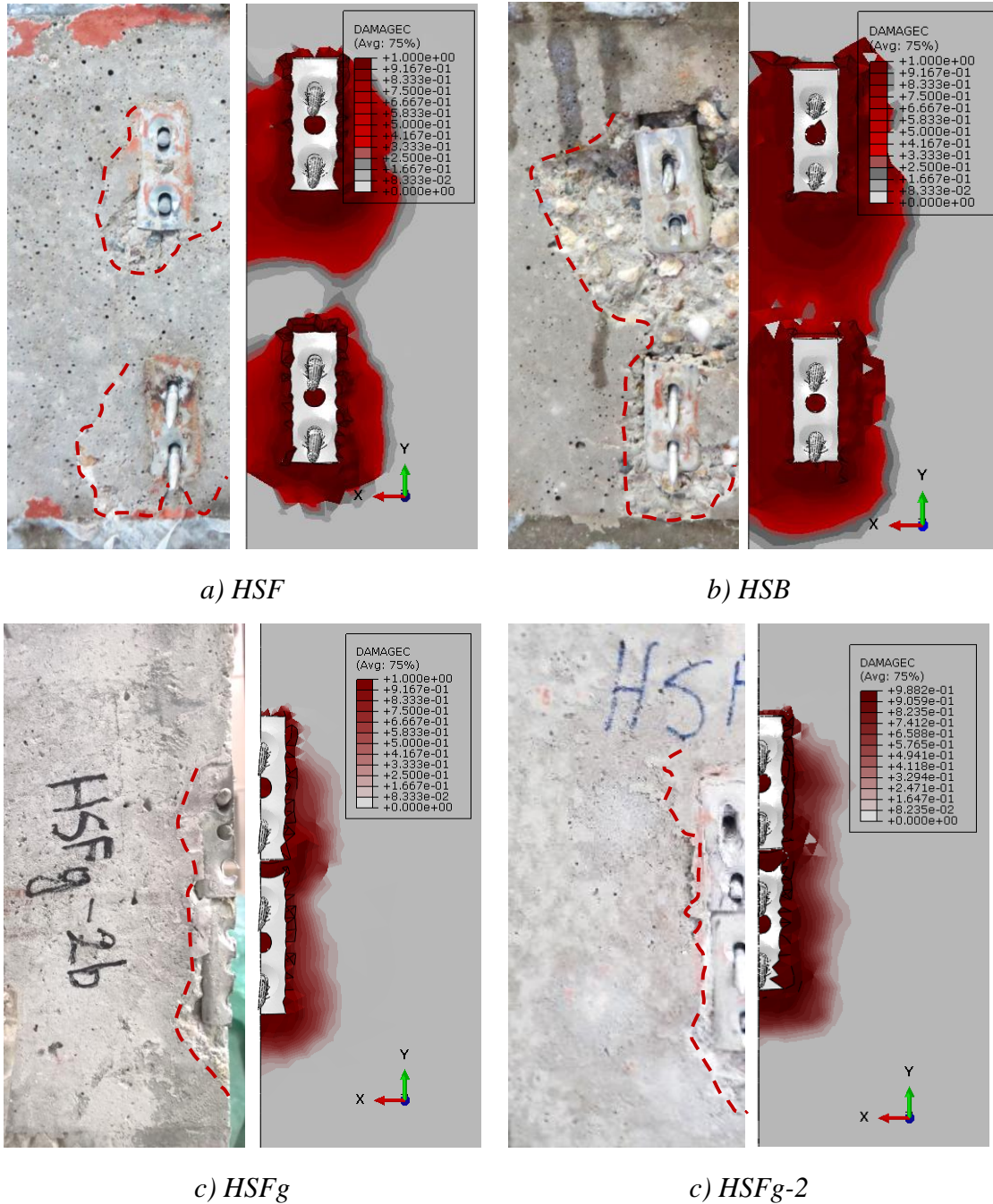
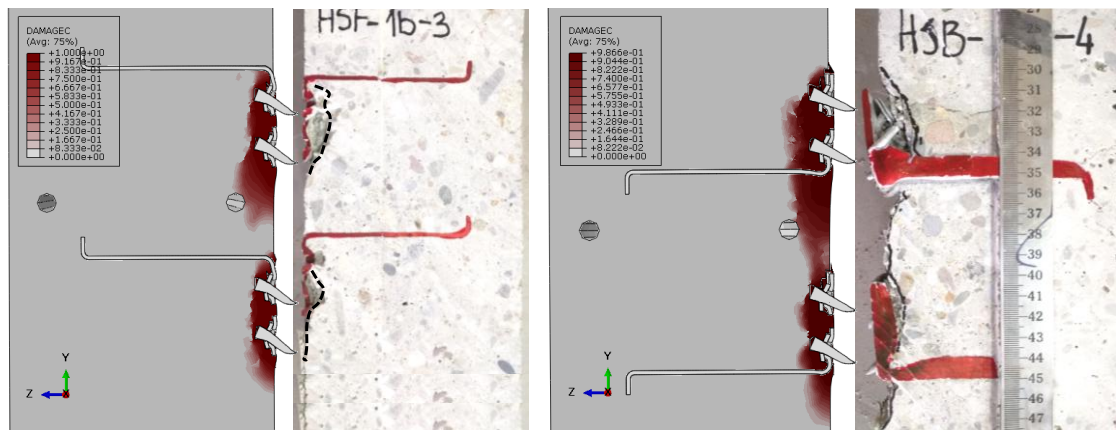
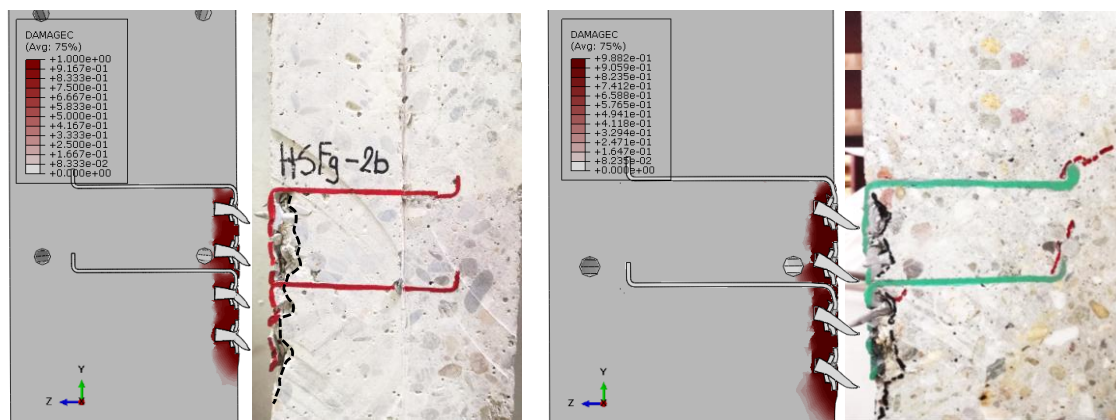


Figure 5.24. Experimental and FE analysis results – concrete compressive damage



a) HSF

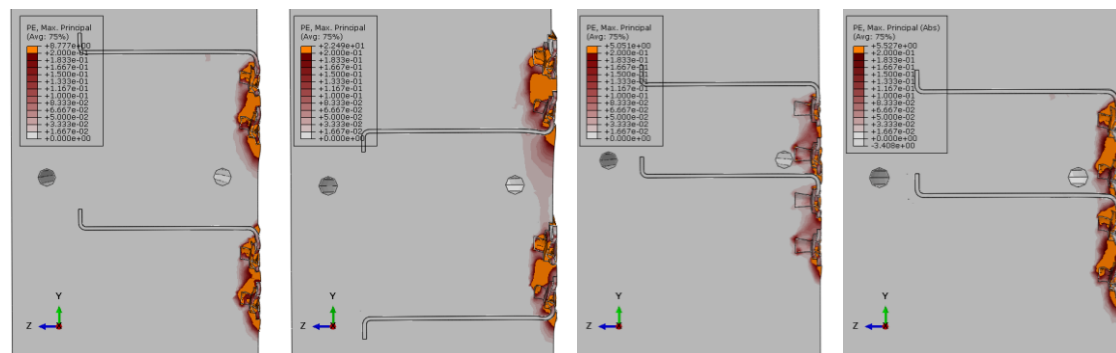
b) HSB



c) HSFg

c) HSFg-2

Figure 5.25. Experimental and FE analysis results – concrete compressive damage - cut through prefabricated concrete slabs



a) HSF

b) HSB

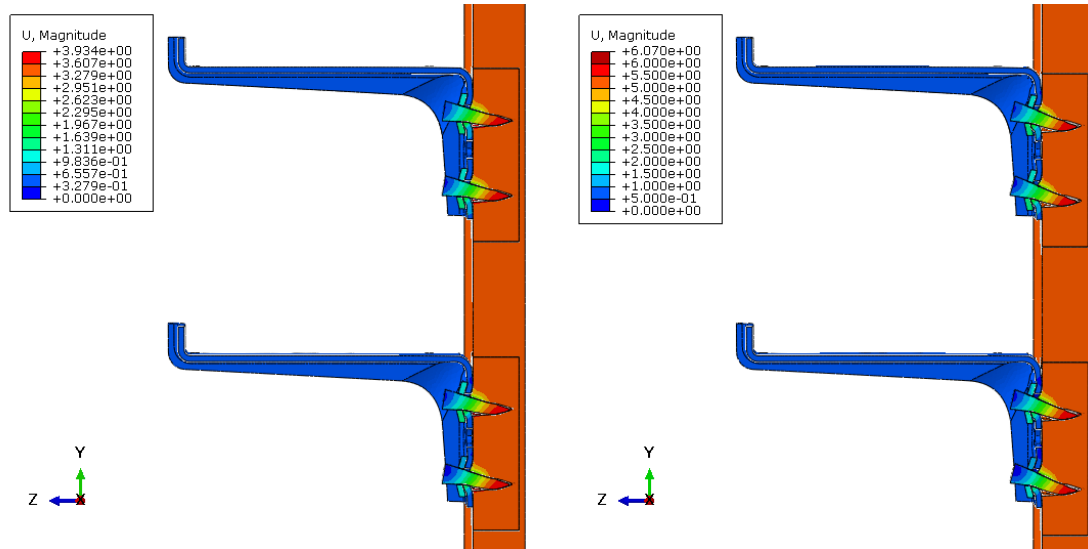
c) HSFg

c) HSFg-2

Figure 5.26. Tensile strains in prefabricated concrete slabs – FE analysis

Ductile connectors are those with sufficient deformation capacity to justify the assumption of ideal plastic behaviour of the shear connection in the structure. A connector may be taken as ductile if the characteristic slip capacity δ_{uk} is at least 6.0 mm, according to EN 1994-1-1:2004 [11]. Connectors deformation capacity can be obtained through

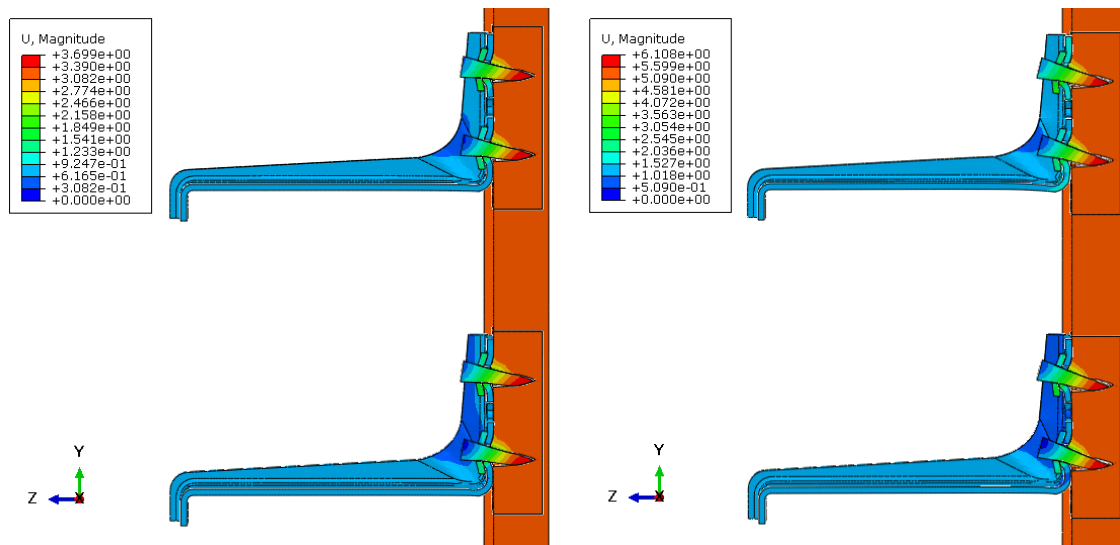
difference between shear connector displacement at the connector root (displacement at contact with steel profile) and top of the shear connector embedded in concrete, in the direction of the shear force. Deformation of X-HVB 110 shear connectors for two characteristic orientation of shear connector relative to the shear force direction, obtained from FE analysis is presented in Figure 5.27 and Figure 5.28.



a) 96 % of ultimate shear force

b) total slip of 6.0 mm

Figure 5.27. Deformation of shear connector – HSF FE model



a) 96 % of ultimate shear force

b) total slip of 6.0 mm

Figure 5.28. Deformation of shear connector – HSB FE model

Displacement of X-HVB 110 shear connector is uniform over it's height, which is obtained through experimental and FE analysis. This is also related to low degree of concrete failure, as previously explained. Deformation capacity of X-HVB 110 shear

connector for various loading levels and connector orientations is directly related to ductility of cartridge fired pins, as shown in Figure 5.27 and Figure 5.28. The deformation of anchorage leg of the connector in concrete contributes by 8 % and up to 15 % to total displacement of the connector, in case of HSF and HSB configuration respectively, as shown in Figure 5.27 and Figure 5.28. The remaining, main, part of the total deformation is contributed to deformation of cartridge fired pins in the holes. According to the ETA-15/0876 assessment [7] X-HVB shear connectors should be considered as ductile. Results obtained from experimental and numerical analysis of X-HVB 110 shear connectors presented herein, confirm this statement. Comparison of deformation capacity of X-HVB 110 shear connectors vs. other types of shear connectors, such as headed studs, perforated shear connectors and bolted shear connectors with mechanical couplers is presented also by Gluhović et al. [59].

5.4.2. FE models of shear and tension tests of cartridge fired pins

Comparison of experimental and FE analysis results of shear tests of cartridge fired pins (ST) is presented in Figure 5.29. Good agreement was obtained with experimental results, considering shear resistance and relative displacement. This indicate that assumptions developed during FE analysis of push-out specimens can be used also for FE analysis of shear connections with cartridge fired pins with pull-out failure.

Failure of shear test specimen (ST) due to pull-out of cartridge fired pins is presented in Figure 5.30 and Figure 5.31. Displacement of the shear test specimen in the direction of the applied force (global X direction) is presented in Figure 5.31. As presented in Figure 5.31, four groups of cartridge fired pins obtained similar displacement and pull-out of these groups was obtained in the same time. This was not obtained in the experimental test specimens (see Figure 4.34b) due to imperfections of installation procedure of cartridge fired pins. Therefore, relative displacement gained from FE analysis and presented in Figure 5.31 is given as displacement of each group of cartridge fired pins.

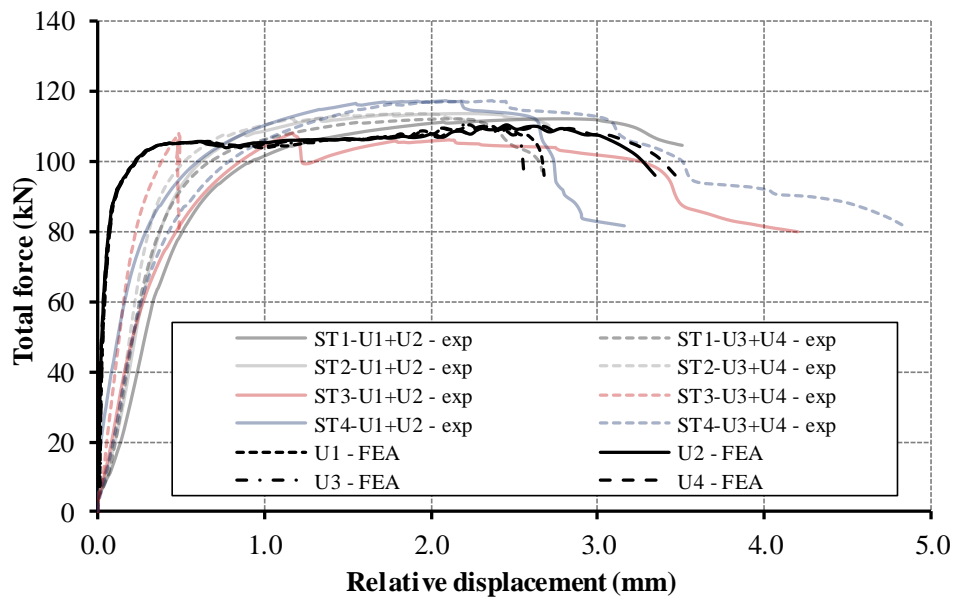


Figure 5.29. Experimental and FE analysis results - force-relative displacement curves for shear test specimens (ST)

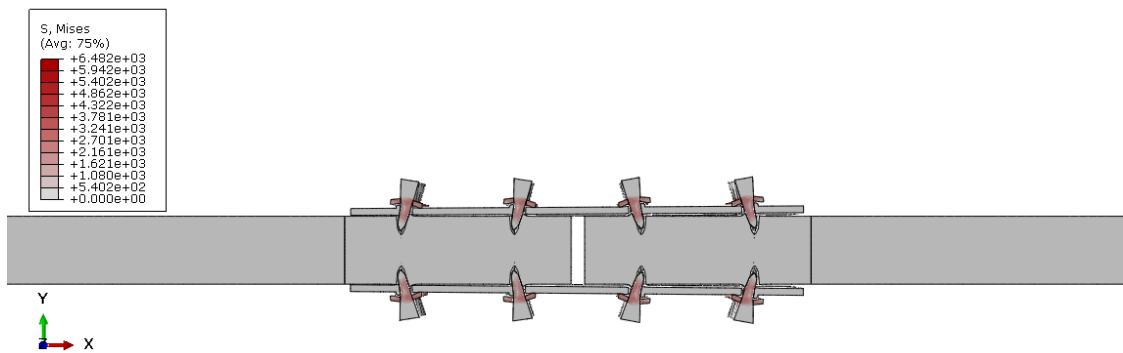


Figure 5.30. Failure of shear test specimen (ST) of cartridge fired pins - FE analysis

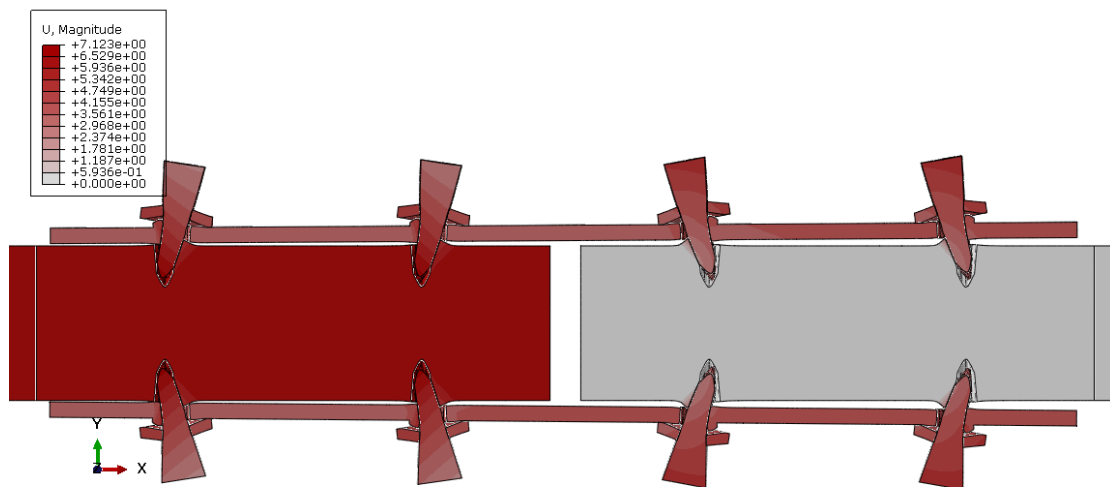


Figure 5.31. Deformation of shear test specimen (ST) - FE analysis

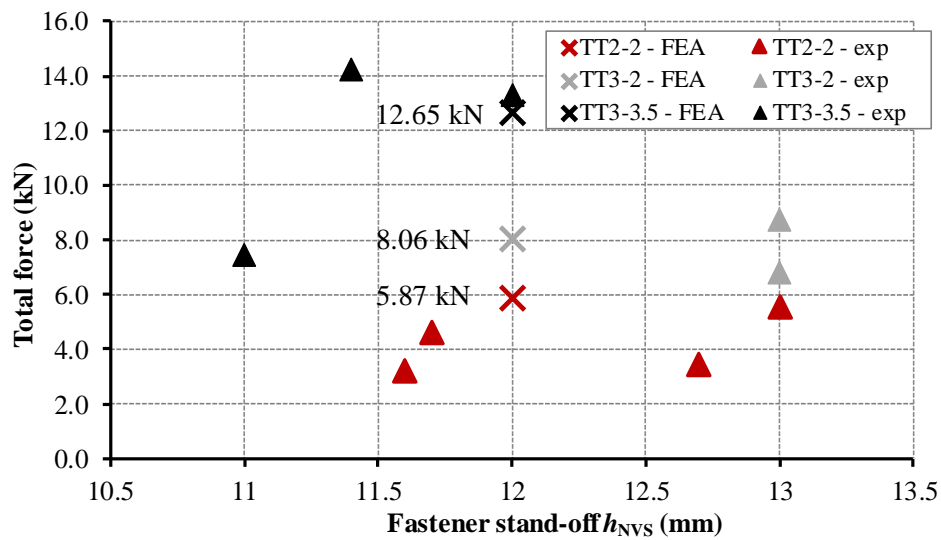


Figure 5.32. Experimental and FE analysis results - pull out resistance of tension test specimens (TT)

Comparison of experimental and FE analysis of pull-out resistance of tension test specimens (TT) is presented in Figure 5.32. Good match between obtained results is achieved indicating that parameters calibrated through FE analysis of push-out models and shear tests specimens are applicable also for tension test specimens. Both FE analysis results, for shear and tension test specimens are presented for quad-linear material model for steel base material (Figure 5.29 and Figure 5.32).

5.5. Summary

Complete FE models for comparison with push-out tests and shear and tension tests of cartridge fired pins were developed. Abaqus/Explicit solver was used for development and analysis of FE models. Exact geometry of all parts of experimental test specimens was analysed. Advanced analysis methods were employed in order to simulate installation procedure of cartridge fired pins. Further conclusions from FE analysis can be drawn:

1) Good agreement between experimental and FE analysis results is achieved for all analysed test specimens: push-out specimens, shear and tension test specimens of cartridge fired pins. Good prediction of behaviour of X-HVB 110 shear connector in prefabricated concrete slabs is achieved considering initial stiffness, shear resistance and characteristic value of slip capacity of push-out test specimens. FE analysis models of push-out test series matched the experimental results with up to 8% accuracy for shear resistance.

2) Developed FE models of push-out test series matched the failure mechanisms obtained through experimental investigation. Failure mechanisms of X-HVB shear connectors are mostly related to the deformation capacity and pull-out failure of cartridge fired pins. The deformation of anchorage leg of the connector in concrete contributes by 8 % and up to 15 % to total displacement of the connector, in case of HSF and HSB configuration respectively, according to the developed FE models.

3) Pull-out of cartridge fired pins in FE models is defined by equivalent compressive contact stresses and friction at the interface between the base material and pins modelled as separate parts. This resembles the physical mechanism of the load transfer of cartridge fired pins and is a recommended modelling procedure as it gives good agreement with experimental results. It was possible to properly calibrate FE models for experiments with different installation power levels (e.g. HSFg vs. HSFg-2) by keeping the friction coefficient in the model to value 0.3 for push-out FE models and varying the level of imposed contact stresses.

4) Parameters calibrated through FE analysis of push-out models is further employed for FE analysis of shear and tension tests of cartridge fired pins, with satisfying match considering obtained experimental and FE analysis results.

4) Quad-linear material model of steel base material and concrete damage plasticity model which are adopted for FE analysis resulted in good agreement between experimental and numerical results.

5) Simulation of two installation power levels which are used through experimental investigation is successfully achieved in FE analysis. This is confirmed through FE analysis of push-out models and shear and tension test models of cartridge fired pins.

Chapter 6. Calibration of numerical models and parametric analysis of X-HVB shear connector

6.1. Calibration of pull-out FE models for cartridge fired pins

Developed FE analysis procedure for simulation of cartridge fired pin installation is explained in detail in Chapter 5.2.2. Installation procedure was defined through preloading of pins by application of strains. This FE analysis approach was firstly developed for push-out specimens and afterwards applied to the shear and tension tests of cartridge fired pins. Good agreement with all experimental results was achieved, which is explained in previous chapter.

Table 6.1. *Analysed parameters of pin installation procedure for tension tests with base material S275 – true stress-strain material model*

Material tensile strength (MPa)	Installation power level (-)	Friction coefficient (-)	Analytical field (mm)	Predefined field magnitude (-)	Number of specimens (-)	Pull-out resistance (kN)
f_u	-	-	-	-	N_{spc}	P_{ult}
479.6	2.0	0.30	9.7	0.10	3	8.11
		0.25				6.31
479.6	3.5	0.20	9.7	0.10	3	4.14
		0.30				10.93
479.6	3.5	0.25	9.7	0.10	3	8.19
		0.20				5.71
479.6	3.5	0.30	9.7	0.08	2	10.21
				0.06		9.85
479.6	2.0	0.30	9.7	0.08	2	7.83
				0.06		7.49
479.6	3.5	0.30	12.7	0.10	2	11.33
			14.0			11.32
479.6	2.0	0.30	12.7	0.10	2	8.47
			14.0			8.82

For cartridge fired pins installation procedure, several parameters were introduced. Anisotropic thermal expansion material properties for upper and embedded part of cartridge fired pins (see Figure 5.11) were introduced for definition of two installation power levels - 2.0 and 3.5. Further, strains were engaged by using predefined temperature

fields (see Figure 5.6). Predefined temperature fields were engaged through analytical field, as variable over cartridge fired pin height. Linear change of temperature predefined field was applied for 9.7 mm from the pin upper part. Constant value of temperature field was further applied for embedded part of the cartridge fired pin (see Figure 5.6).

Calibration of pull-out FE models of cartridge fired pins is presented herein. Influence of previously explained parameters on pull-out resistance is analysed in order to define which parameter has the most important influence on obtained hold in the base material and therefore on pull-out resistance. Also, influence of friction coefficient in the contact surface between base material and embedded part of the pin and two steel grades (S275 and S355) is analysed in this parametric study. These parameters are analysed for two materials (S275 and S355) defined through true stress-strain and quad-linear material model. Obtained pull-out resistances are presented in Table 6.1, Table 6.2 and Table 6.3.

Table 6.2. *Analysed parameters of pin installation procedure for tension tests with base material S355 – true stress-strain material model*

Material tensile strength (MPa)	Installation power level (-)	Friction coefficient (-)	Analytical field (mm)	Predefined field (-)	Number of specimens (-)	Pull-out resistance (kN)
f_u	-	-	-	-	N_{spc}	P_{ult}
534.6	2.0	0.30	9.7	0.10	3	11.44
		0.20				6.11
534.6	3.5	0.30	9.7	0.10	3	14.53
		0.25				11.44
534.6	3.5	0.30	9.7	0.08	2	13.72
				0.06		12.95
534.6	2.0	0.30	9.7	0.08	2	11.04
				0.06		10.11
534.6	3.5	0.30	12.7	0.10	2	14.63
			14.0			14.75
534.6	2.0	0.30	12.7	0.10	2	11.66
			14.0			11.84

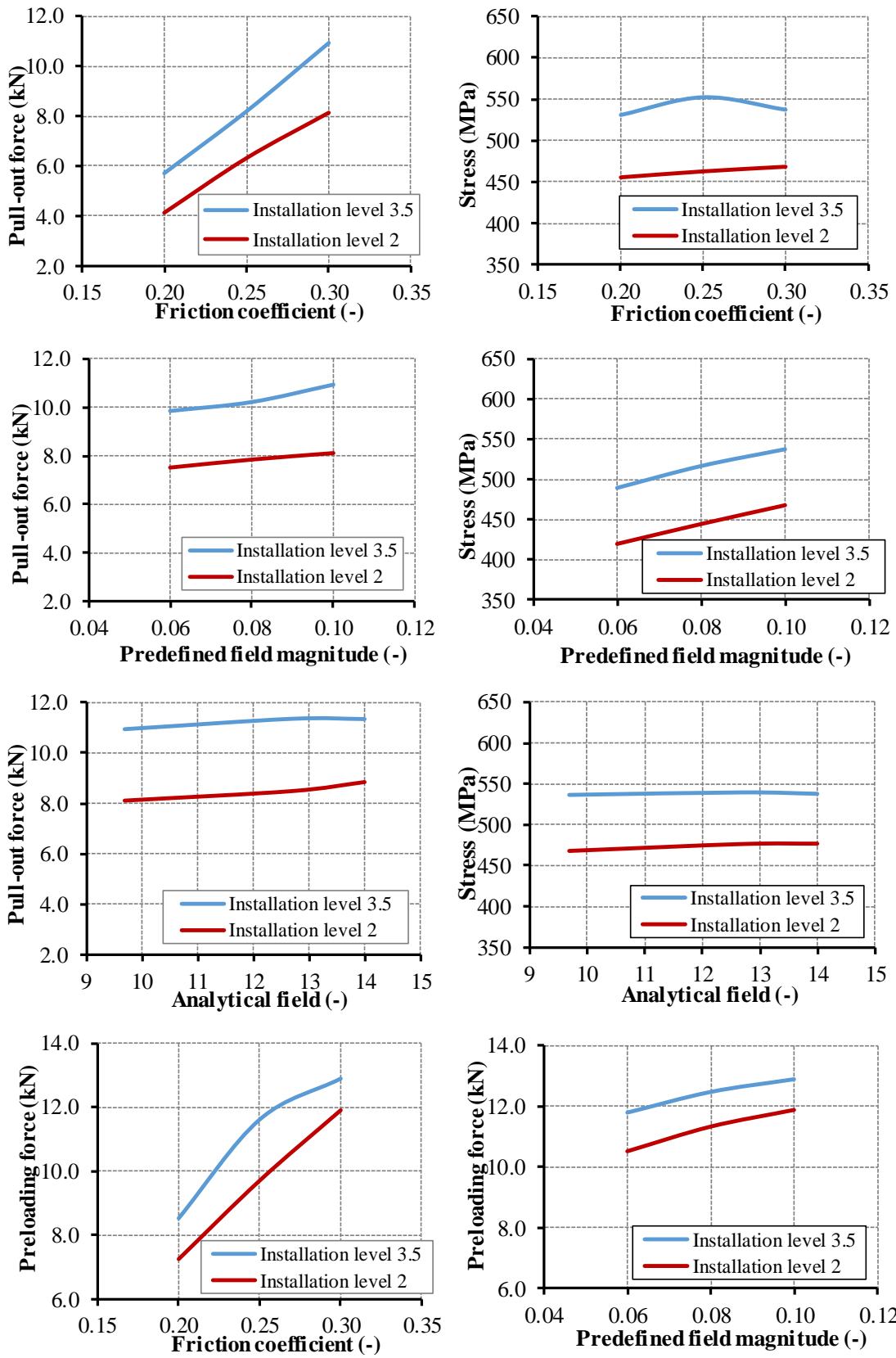


Figure 6.1. Parametric analysis results for pin installation procedure of tension tests – base material S275

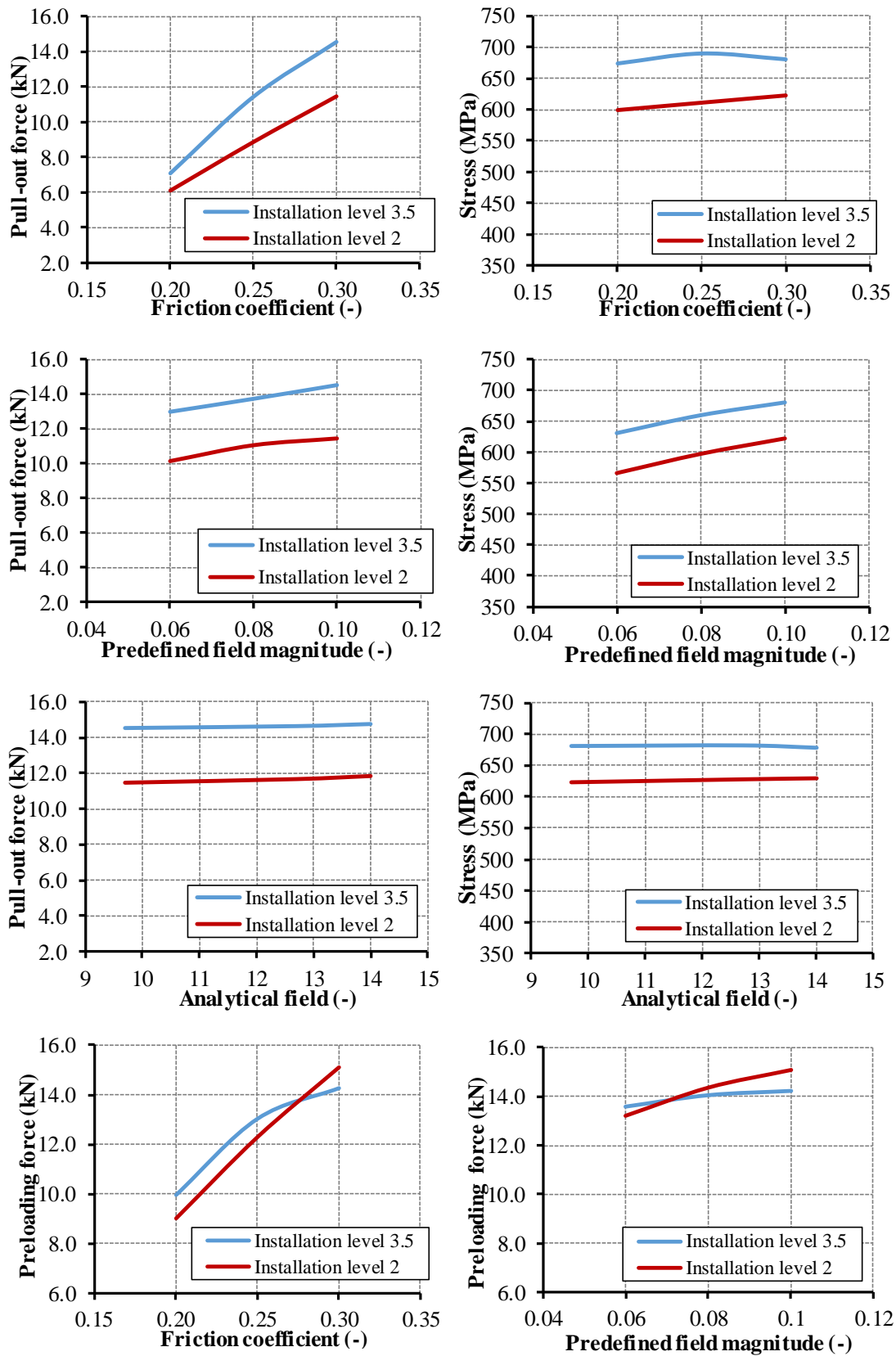


Figure 6.2. Parametric analysis results for pin installation procedure of tension tests—base material S355

Results of calibration procedure are also presented in Figure 6.1 and Figure 6.2. These results are obtained for true-stress strain base material model in FE analysis and two base material steel grades S275 and S355. Influence of parameters of interest is given through obtained pull-out resistance, stress developed after installation procedure in the steel base material and preloading force in the cartridge fired pin. Von Mises stress is obtained at the upper surface of steel base material at the edge of the base material hole. As given in Figure 6.1 and Figure 6.2, the major influence on pull-out resistance of cartridge fired pins and preloading force after installation procedure is obtained for various values of friction coefficient, for both analysed steel grades (S275 and S355). Analysed differences in definition of predefined field magnitude and analytical field resulted in small change of pull-out resistance of cartridge fired pin for both analysed parameters, as shown in Figure 6.1 and Figure 6.2. The major influence on accumulated stress in base material close to the cartridge fired pin is obtained for applied predefined field magnitude. Influence of other analysed parameters resulted in difference which is smaller than 10 %. Moreover, preloading force in cartridge fired pin during installation procedure is highly influenced by definition of friction coefficient in the contact surface with base material. Influence of predefined field magnitude on preloading force is more notable for installation power level 2.0, which is the result of the various orthotropic material properties for upper and embedded part of cartridge fired pin (see Figure 5.11).

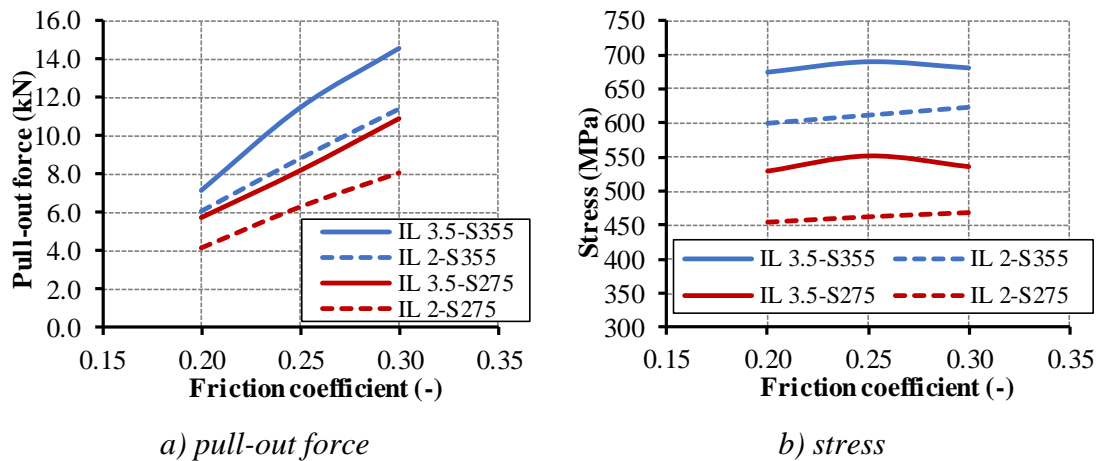


Figure 6.3. Comparison of parametric analysis results for pin installation procedure of tension tests – true stress-strain material model

Comparison of pull-out resistances and accumulated stress in steel base material after installation procedure for various values of friction coefficients and steel grades with

true stress-strain relation in FE analysis is given in Figure 6.3. Accumulated stress in steel base material after installation procedure is in direct relation with steel base material properties. Also, higher installation power level results in higher accumulated stress and pull-out resistance. Based on the presented calibration procedure, further parameters with the most significant influence on cartridge fired pins pull-out resistance can be accentuated: friction coefficient obtained between cartridge fired pin and base material, steel base material properties and introduced installation power level.

Table 6.3. *Analysed parameters for base material S275 and S355 – quad-linear material model*

Material tensile strength (MPa)	Installation power level (-)	Friction coefficient (-)	Analytical field (mm)	Predefined field magnitude (-)	Number of specimens (-)	Pull-out resistance (kN)
f_u	-	-	-	-	N_{spc}	P_{ult}
479.6	2.0	0.30	9.7	0.10	3	7.53
		0.25				5.87
		0.20				3.34
479.6	3.5	0.30	9.7	0.10	3	9.46
		0.25				7.31
		0.20				5.15
534.6	2.0	0.30	9.7	0.10	3	10.54
		0.25				8.06
		0.20				5.48
534.6	3.5	0.30	9.7	0.10	3	12.65
		0.25				9.90
		0.20				6.71

Moreover, quad-linear material model was applied in FE analysis for steel base material, for both materials (S275 and S355). Analysis was performed for both installation power levels and various values of friction coefficient, as presented in Table 6.3. Comparison of pull-out resistances for two material models, true stress-strain and quad-linear material model, and two values of installation power levels is given in Figure 6.4. Obtained difference between pull-out resistance is smaller for lower installation power levels and amounts approximately 10 % for installation power level 2.0 and up to 20 % for installation power level 3.5. The same behaviour is obtained for stress accumulated in steel base material after installation procedure. The best agreement with

average experimental results is obtained for defined friction coefficient of 0.3 for installation power level 3.5 and 0.25 for installation power level 2.0, which is in detail explained in Chapter 8.

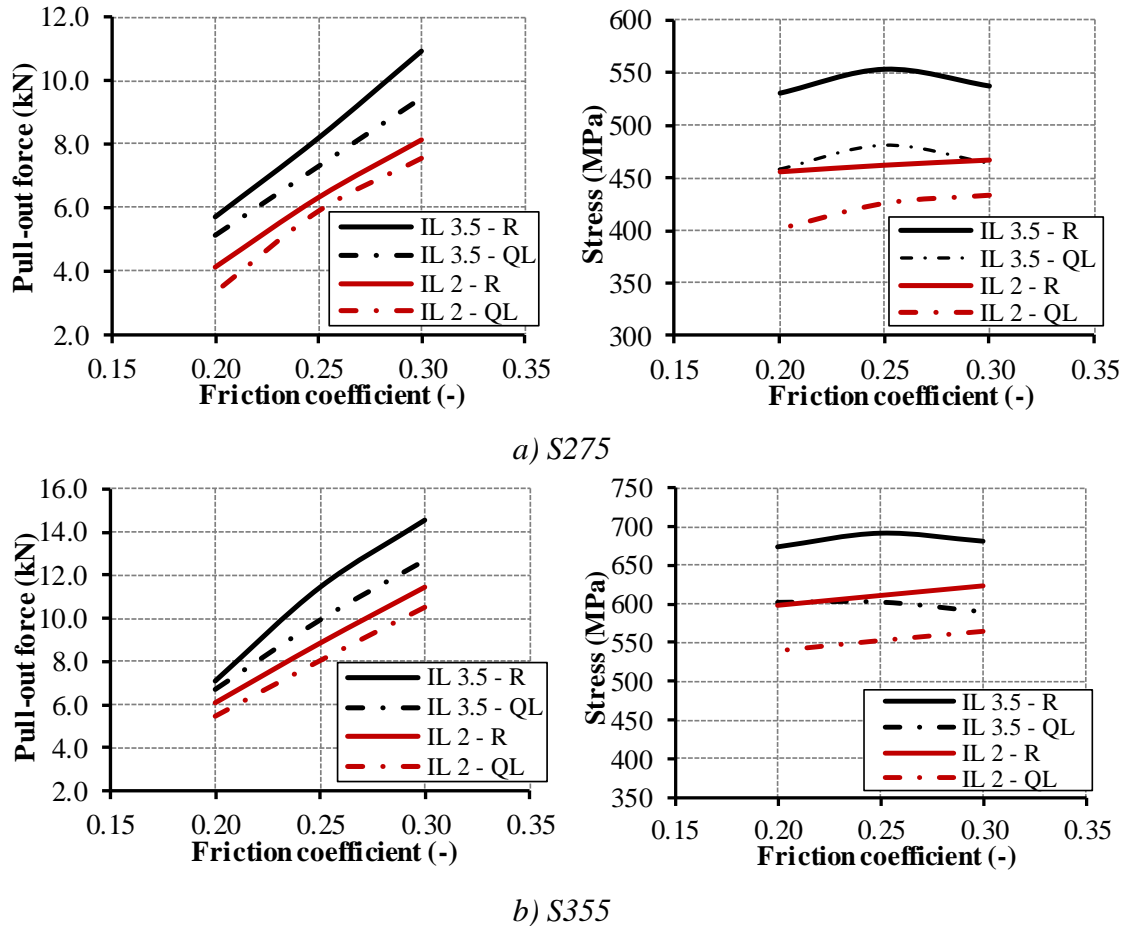


Figure 6.4. Comparison of parametric analysis results of tension tests – analysis of two material models influence

6.2. Sensitivity study of push-out FE models for various installation procedure parameters of cartridge fired pins

Described installation procedure of cartridge fired pins is further analysed through sensitivity study of push-out FE models with the most significant parameters and their influence on obtained shear resistance of X-HVB 110 shear connectors. Analysed parameters are presented in Table 6.4. Analysis is performed for HSF and HSB push-out test series. These two tests series with various shear connectors orientation are used for sensitivity study which is described in this chapter, considering several distinguishing features which are obtained from experimental analysis.

Table 6.4. Various installation procedure of cartridge fired pins – sensitivity study of push-out FE models

FE model	Analysed parameter	P1	P2	P3
P0	adopted values	0.10	0.8 / 0.8 / 0	0.8 / 0.8 / -1.0
P1	predefined field magnitude	0.06	0.8 / 0.8 / 0	0.8 / 0.8 / -1.0
P2	pin expansion material properties	0.10	0.5 / 0.5 / 0	0.5 / 0.5 / -0.8
P3	pin expansion material properties	0.10	1.0 / 1.0 / 0	1.0 / 1.0 / -1.2

Influence of FE modelling approach of installation procedure of cartridge fired pins on behaviour of X-HVB 110 shear connectors in prefabricated concrete slabs is given in Figure 6.5 and Figure 6.6, for two analysed test series. Analysed parameters resulted in small differences considering initial stiffness, shear resistance and characteristic value of slip capacity. Adopted parameters resulted in the best agreement with experimental results of four analysed test series. Also, adopted values of analysed parameters are in agreement with parameters defined for tension and shear tests of cartridge fired pins for same installation power levels.

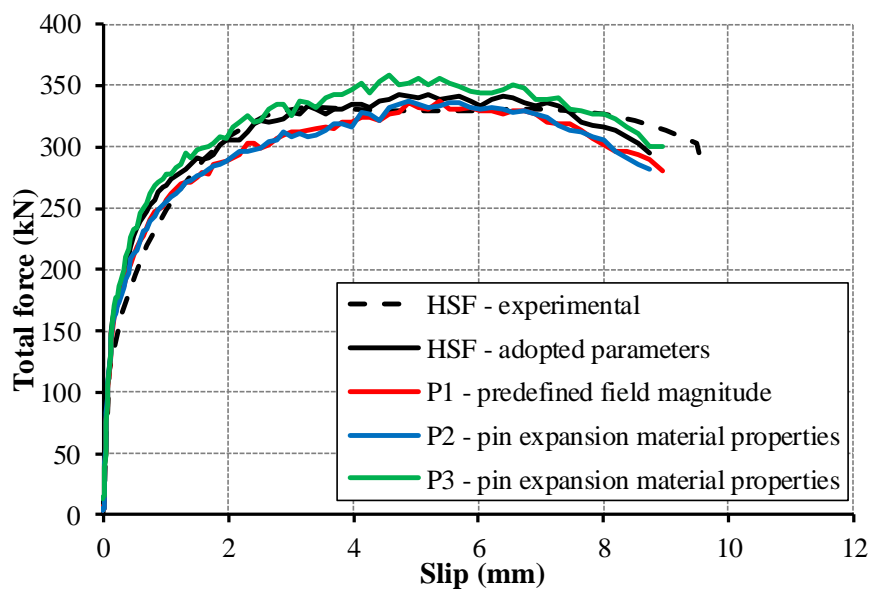


Figure 6.5. Sensitivity study results for various installation procedure of cartridge fired pins – HSF test series

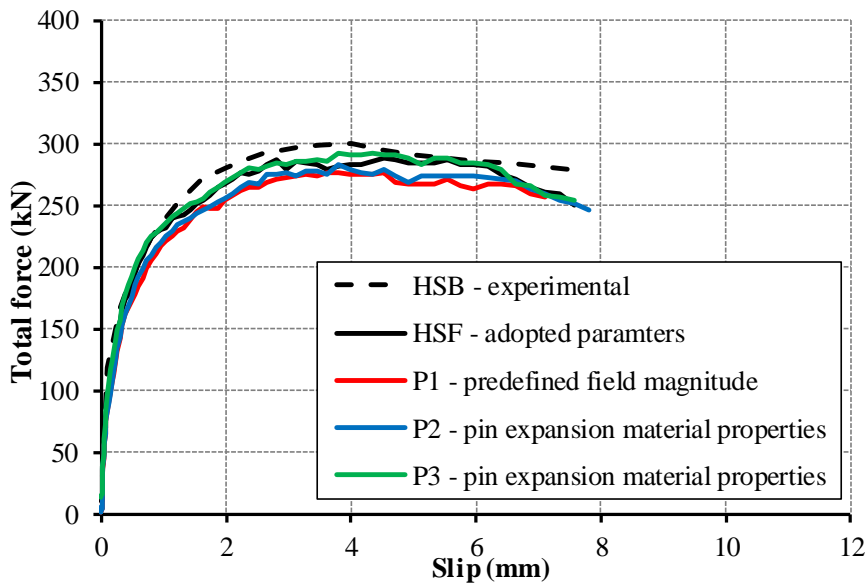


Figure 6.6. Sensitivity study results for various installation procedure of cartridge fired pins – HSB test series

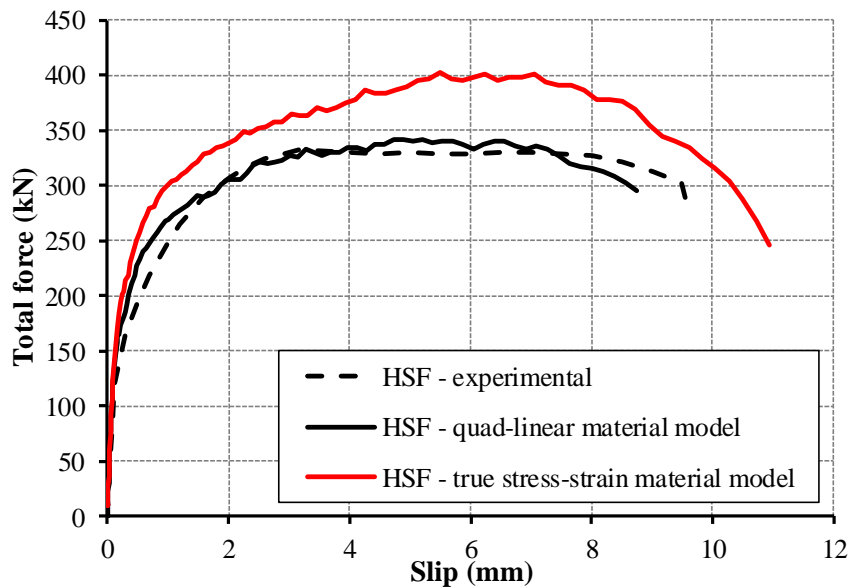


Figure 6.7. Influence of material model of steel base material on FE analysis results – HSF test series

Results presented for quad-linear material model in Figure 6.7 and Figure 6.8 are obtained from push-out FE model where this material model is applied only in the region close to the cartridge fired pins (15 mm distance from pins as presented with rectangle in Figure 5.7) and true stress-strain is applied for remaining part of steel profile. Push-out FE model with true stress-strain material model is developed when this material model is applied on whole steel profile and therefore in the region close to the cartridge fired pins.

Presented results strongly highlights the influence of high speed installation procedure on base material properties (see Chapter 4.6) and therefore on pull-out resistance of cartridge fired pins as part of X-HVB shear connectors. Quad-linear material model prescribed for FE models presented in this thesis resulted in good agreement with experimental results of X-HVB 110 shear connector push-out tests and shear and tension tests of cartridge fired pins.

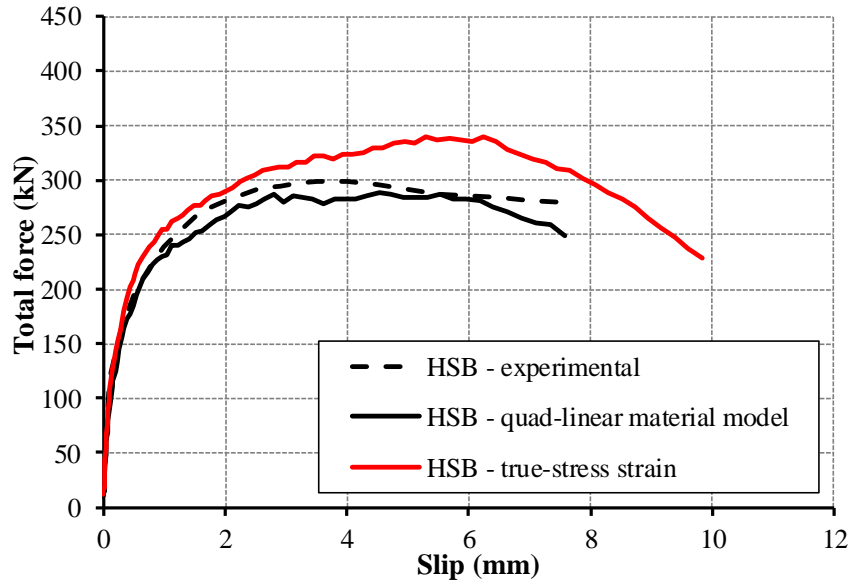


Figure 6.8. Influence of material model of steel base material on FE analysis results – HSB test series

6.3. Parametric analysis of X-HVB shear connector push-out FE models

Behaviour of X-HVB 110 shear connectors in prefabricated concrete slabs is further analysed through parametric analysis with various concrete classes, according to EN 1992-1-1:2004 [50] and various steel grades. Base material properties are obtained through tension tests presented in this thesis for various steel grades, S235, S275 and S355.

Influence of concrete class on X-HVB 110 shear connector resistance in prefabricated concrete slab is presented in Figure 6.9 and Figure 6.10. For both analysed shear connector orientations, various concrete classes did not result in significant difference in obtained shear resistance. Comparison with average experimental results and FE analysis results with examined concrete material properties of push-out phase 1 is also given in Figure 6.9 and Figure 6.10.

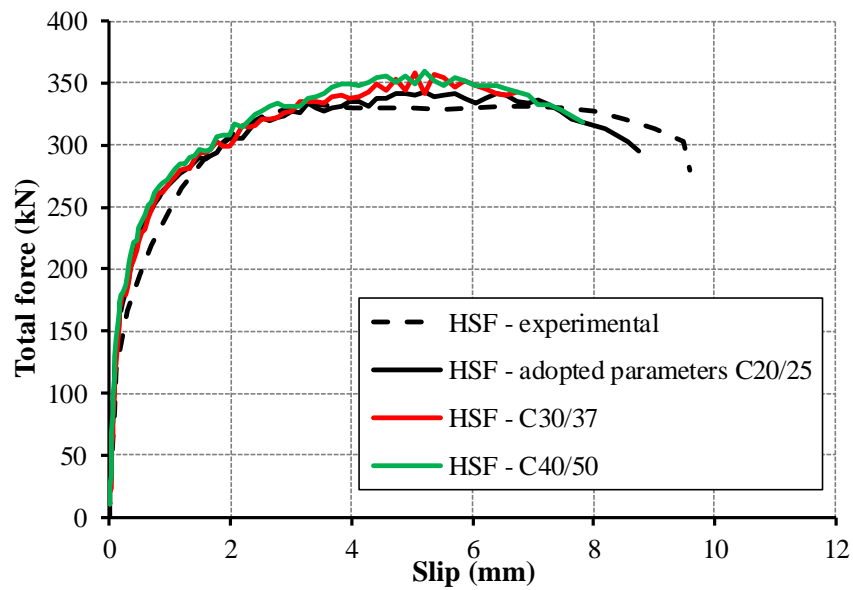


Figure 6.9. Influence of concrete class on shear resistance – HSF test series

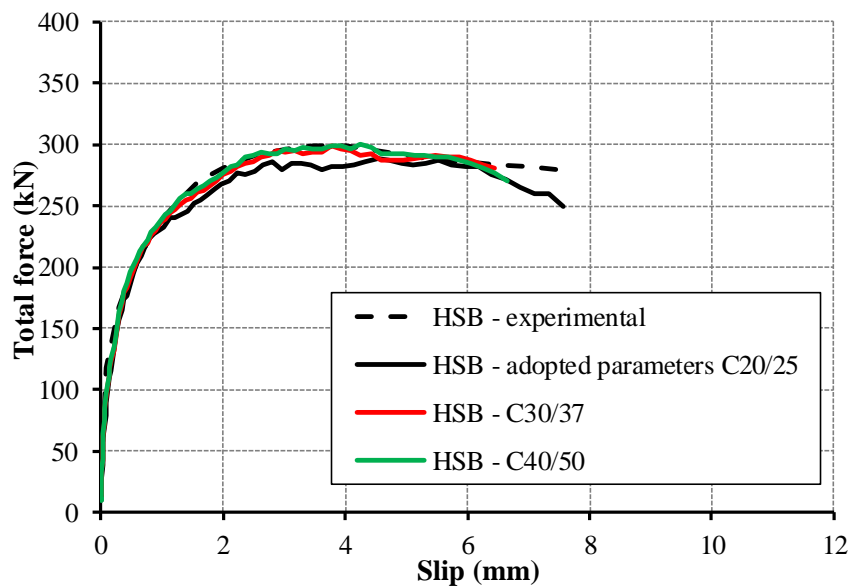


Figure 6.10. Influence of concrete class on shear resistance – HSB test series

Quad-linear material model for steel grade S275 and S355 is further applied in push-out FE models. Material model for steel grade S235 is developed based on tension test of coupons built from steel profile, as presented in Chapter 4.3. Material models for steel grade S275 and S355 are developed based on examined material properties of base plates used in shear and tension tests of cartridge fired pins (see Chapter 4.7 and Annex C). Approximate increase of base material strength of 33.0 MPa obtained from base material hardness tests (see Chapter 4.6) is applied for all analysed quad-linear material models. Introduced material models are given in Figure 5.13, Figure 5.18 and Figure 5.19.

Influence of base material steel grade on behaviour of X-HVB 110 shear connector in prefabricated concrete slabs is given in Figure 6.11 and Figure 6.12. Increase of shear resistance up to 20 % is achieved with higher steel grades. Also, higher steel grades resulted in higher characteristic values of slip capacity for both orientations of shear connectors.

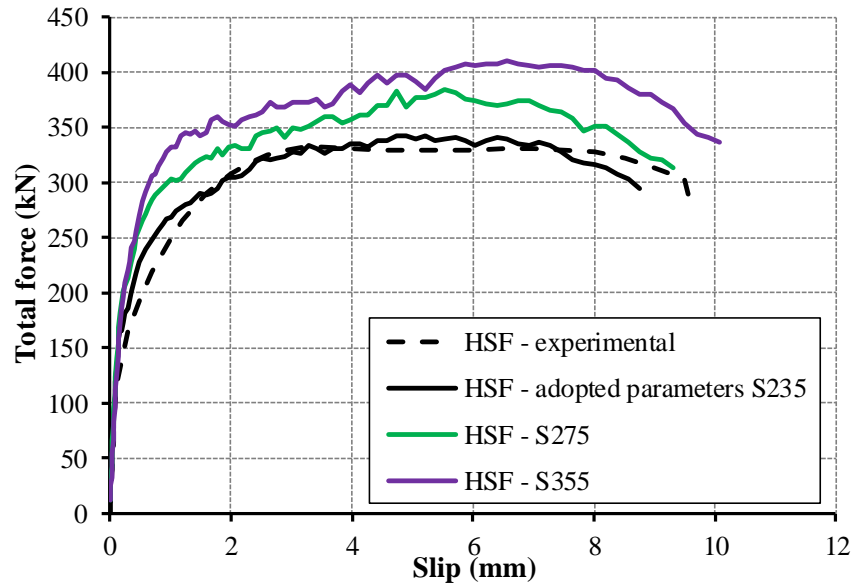


Figure 6.11. Influence of steel base material strength on FE analysis results – HSF test series

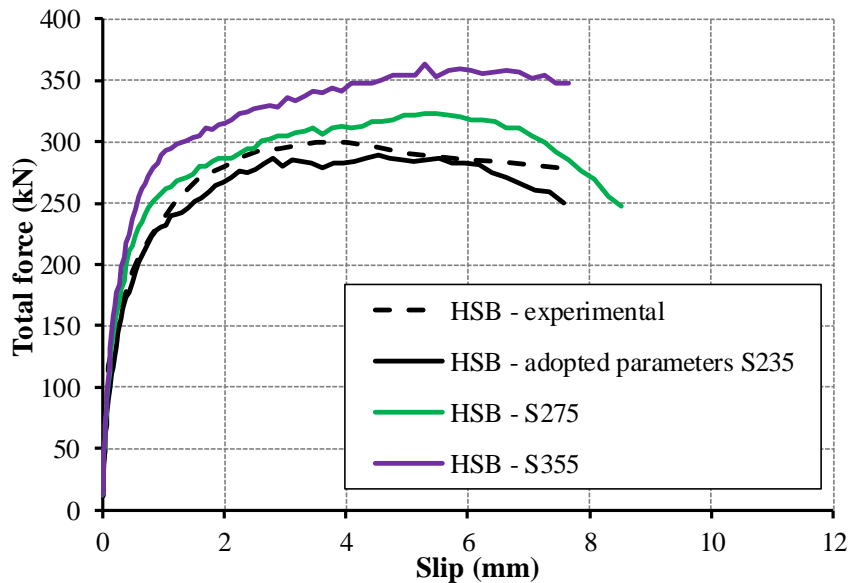


Figure 6.12. Influence of steel base material strength on FE analysis results – HSB test series

6.4. Summary

Presented sensitivity study and parametric analysis was performed for X-HVB 110 shear connectors in standard push-out tests and tension tests of X-ENP 21 HVB cartridge fired pins. Sensitivity study included all parameters which were used to describe installation procedure of cartridge fired pins in FE models. Also, through presented parametric analysis influence of concrete class of prefabricated slab and steel grade of base material on shear resistance of X-HVB 110 shear connector was obtained. Further statements can be drawn from presented results:

1) Variation of all parameters which are used for definition of installation procedure of cartridge fired pins in FE analysis resulted in approximately 10 % difference in obtained shear resistance of X-HVB 110 shear connectors and pull-out resistance of cartridge fired pins loaded in tension.

2) Pull-out resistance of cartridge fired pins loaded in tension is mostly influenced with friction coefficient between embedded part of cartridge fired pin and base material, steel base material strength and obtained installation power level.

3) Variation of concrete class does not have significant influence on behaviour of X-HVB 110 shear connector in prefabricated concrete slabs, considering shear resistance and characteristic value of slip capacity.

4) Implementation of various steel base material models in FE analysis resulted in variation of obtained shear resistance of X-HVB 110 shear connectors up to 20 %. High speed installation procedure of cartridge fired pin reflects in change of base material properties near to the cartridge fired pins. Application of quad-linear material model in this close region gives better prediction of experimental results considering shear resistance of X-HVB shear connectors and pull-out resistance of cartridge fired pins.

5) Increase of steel grade of base material for approximately 100 MPa (from steel grade S235 to S355) resulted in approximately 20 % higher shear resistance of X-HVB 110 shear connector. Also, higher characteristic value of slip capacity is obtained for both shear connector orientations which is related to the obtained “hold” of cartridge fired pin into steel base material.

6) Behaviour of X-HVB shear connectors in prefabricated concrete slabs is determined with obtained “hold” of cartridge fired pin into steel base material which is

described also as anchorage mechanisms. In presented parametric analysis, anchorage mechanisms are analysed through friction coefficient developed between pin embedded part and steel base material and accumulated stress in steel base material. This modelling approach highlights the clamping as the most characteristic anchorage mechanism.

7) Friction coefficient and accumulated stress into steel base material, which are recognized as the most important features of installation procedure through presented parametric analysis are also recognized as the most important features of pull-out resistance based on the previous experimental investigation (see Chapter 2.3.4). Therefore, developed FE simulation of installation procedure is considered as reliable in high percentage.

Chapter 7. Pull-out resistance of cartridge fired pins loaded in tension

7.1. Behaviour of cartridge fired pins through tension loading

Experimentally and numerically gained data for pull-out resistance of cartridge fired pins was compared with results obtained from literature for various types of fasteners and presented herein. Two most important parameters for behaviour of cartridge fired pins loaded in tension were accentuated in Chapter 6: friction coefficient between embedded part of cartridge fired pin and steel base material and stress accumulated into base material after installation procedure. Those parameters determine the hold of cartridge fired pin into base material. The aim of the analysis presented in this chapter is to validate FE models not only through own experimental investigation of X-HVB shear connectors and cartridge fired pins, but also through comparison with results of various types of fasteners. Finally, prediction models for determination of pull-out resistance of cartridge fired pins are given. Defined prediction models are developed through experimental investigation and FE analysis presented in this thesis.

Figure 7.1 gives comparison of own experimental results with pull-out resistance of various types of powder actuated fasteners. Mujagic et al. [37] presented in their work results of 127 individual tests of different powder actuated fasteners with smooth shank. Information about base material strength for presented experimental results is not given in this work [37]. As explained in Chapter 2.3.4, certain experimental results are determined as underestimation of results due to installation process mistakes, which is presented also in Figure 7.1. Experimental results of TT3-2 test series with lower installation power level 2.0 are in the range of presented results, while specimens of TT2-2 test series with lower base material strength and installation power level 2.0 can be considered as underestimated results. Also, one experimental result of TT3-3.5 test series with installation power level 3.5 will be considered as underestimated result, as presented in Figure 7.1 and would be disregarded for further analysis of behaviour of cartridge fired pins subjected to tension loading. As presented in Figure 7.1, significant dissipation of experimental results is obtained for embedded depth lower than 10.5 mm. This embedded depth is analysed through FE analysis of tension tests specimens which results is presented in previous chapters. For galvanized powder actuated fasteners with knurled shank and diameter of 4.5 mm, which characteristic pull-out resistances are presented in

Figure 7.2, approximate embedded depth which leads to satisfying pull-out resistance of fasteners is from 12.0 to 18.0 mm [12].

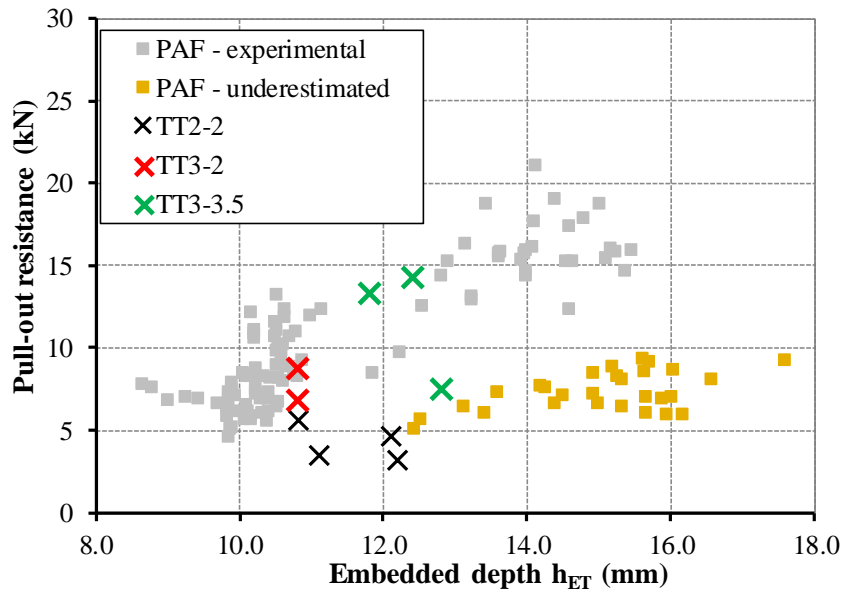
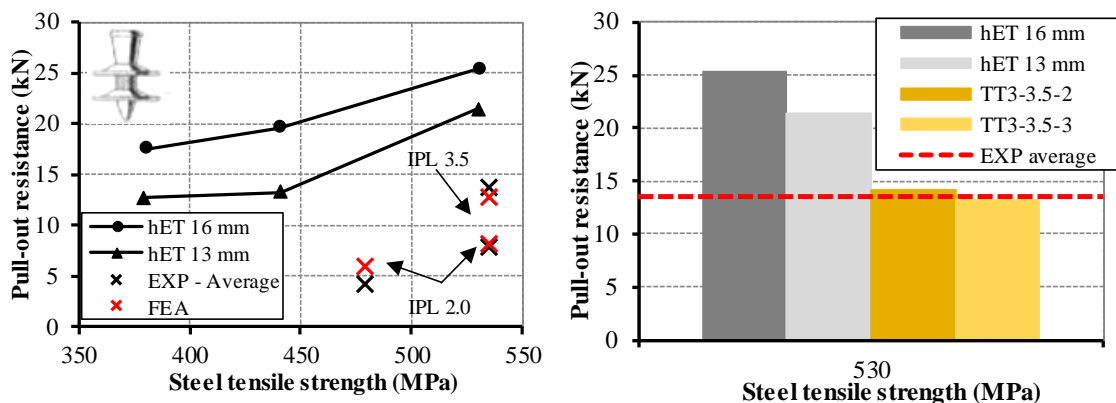


Figure 7.1. Comparison of experimental and FE analysis results with pull-out resistances for smooth shank powder actuated fasteners, adapted from [37]



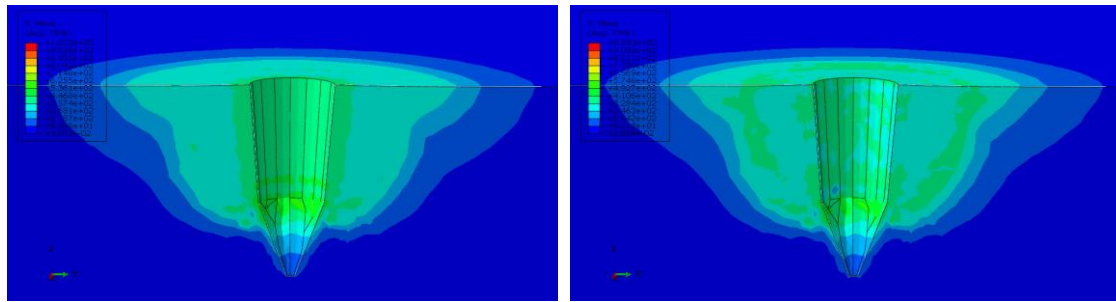
a) comparison of tension test series, adapted from [12]

b) TT3-3.5 test series

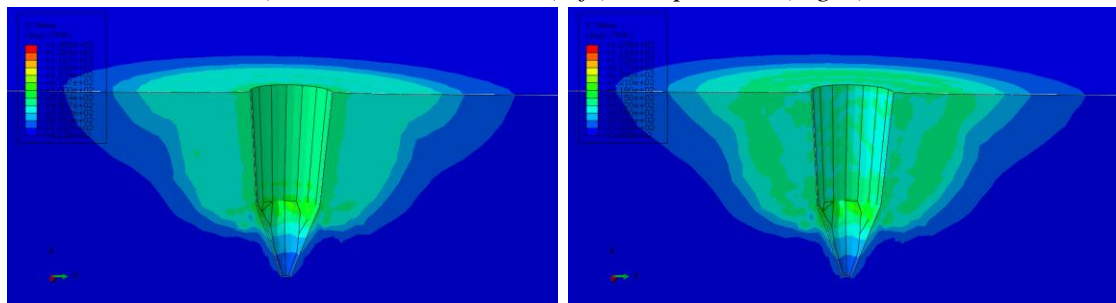
Figure 7.2. Comparison with characteristic resistance of ENP2-21 L15MXR fastener

Comparison of experimental and FE analysis results of X-ENP-21 HVB cartridge fired pin with characteristic resistance of similar ENP2-21 L15MXR fastener which is used for profiled sheeting connection is presented in Figure 7.2. Presented characteristic pull-out resistance is gained based on 90 individual tension tests for each base material strength and embedded depth. Significantly lower shear resistance is obtained for same base material tensile strength due to lower embedded depth. FE analysis results presented

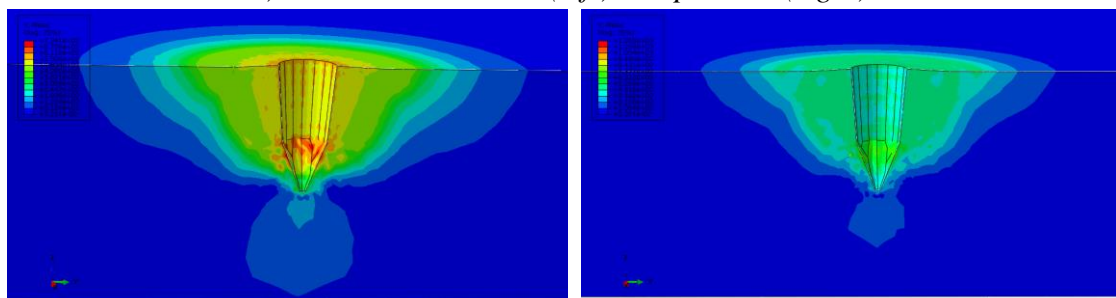
in Figure 7.2 are obtained for 10.5 mm of embedded depth (approximate 12.0 mm of pin stand-off over X-HVB shear connector). Also, lowering of installation power level resulted in further reduction of pull-out resistance for same base material strength (approximately 530 MPa). Relatively proportional lowering of pull-out resistance in relation to the embedded depth is obtained for test specimens with installation power level 3.5 and base material strength of approximately 530 MPa, as shown in Figure 7.2b.



a) TT2-2 – installation (left) and pull-out (right)



b) TT3-2 – installation (left) and pull-out (right)



c) TT3-3.5 – installation (left) and pull-out (right)

Figure 7.3. *Stress accumulated in steel base material after installation procedure and corresponding to pull-out of cartridge fired pin*

Stress accumulated in steel base material after installation procedure and corresponding to pull-out of cartridge fired pin obtained from FE models developed for three test series is given in Figure 7.3. Accumulated stress is spread over wide region around cartridge fired pin. This region decreases approximately from 4 diameters at the top surface of base material to the 2 diameters of pin embedded part at the end of the pin.

Also, influence of the tip of the pin at the obtained hold in base material is highly pronounced only for the installation power level 3.5, as shown in Figure 7.3. Preloading force in cartridge fired pin after installation procedure is given in Figure 7.4. The highest preloading force is obtained for the highest installation power level, as shown in Figure 7.4c. Lowering of installation power level from 3.5 to 2.0 with same base material strength resulted in lower preloading force for approximately 15 %. For same installation power level 2.0, preloading force in cartridge fired pin decreased from 11.45 kN to 9.24 kN, due to lower base material strength for approximately 55.0 MPa, as shown in Figure 7.4a and Figure 7.4b.

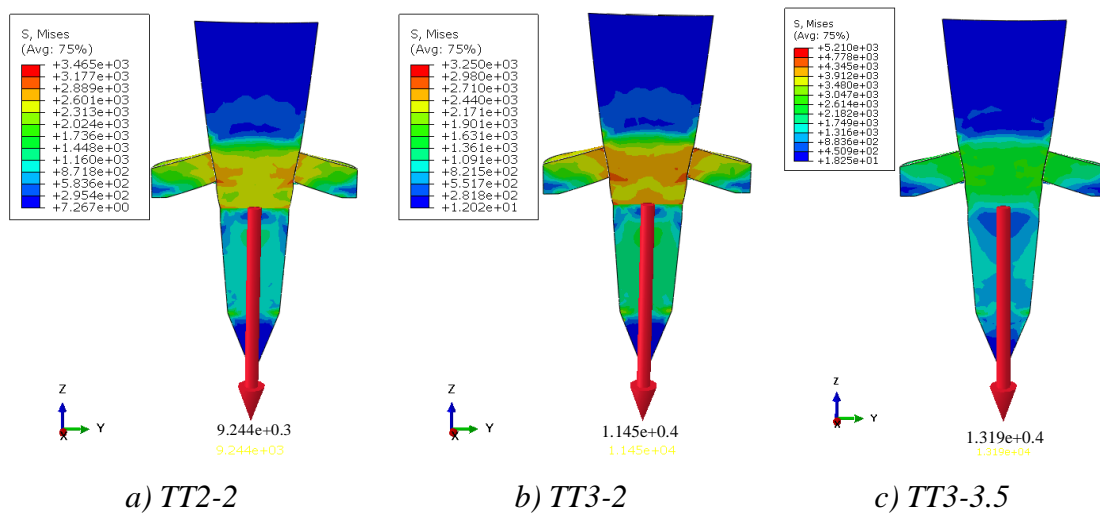


Figure 7.4. Stress and preloading force in cartridge fired pin after installation procedure

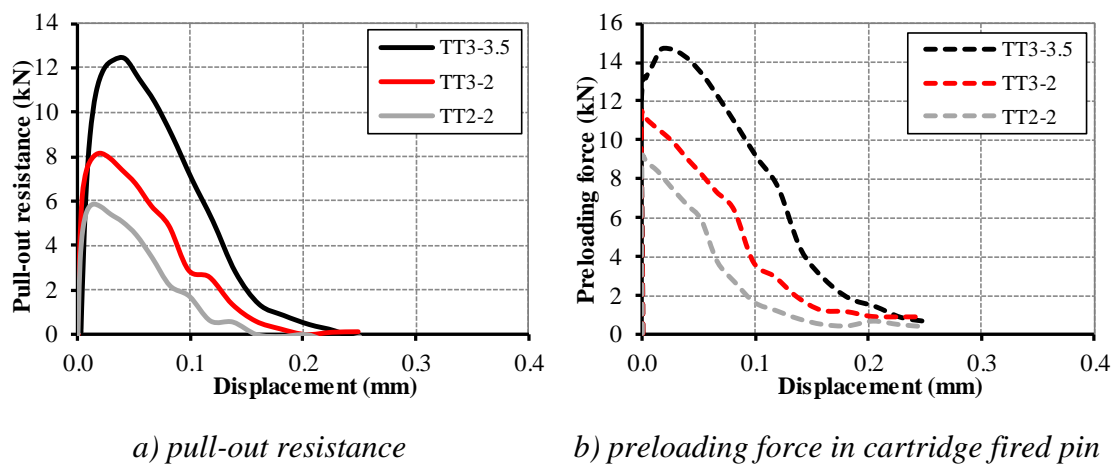


Figure 7.5. FE analysis results for tension test specimens

Pull-out resistance in function of relative displacement of cartridge fried pin from steel base material, obtained for three analysed FE models, is presented in Figure 7.5a.

Also, Figure 7.5b presents decrease of preloading force in cartridge fired pin through testing procedure. Decrease of preloading force when the testing procedure starts is constant for lower installation power level 2.0, as shown in Figure 7.5b. For higher installation power level 3.5, slight increase of preloading force is noticed till the achievement of pull-out resistance, as shown in Figure 7.5b. This increase is less than 10 % and is obtained due to higher friction coefficient, 0.3 for installation power level 3.5 in comparison to the 0.25 for installation power level 2.0.

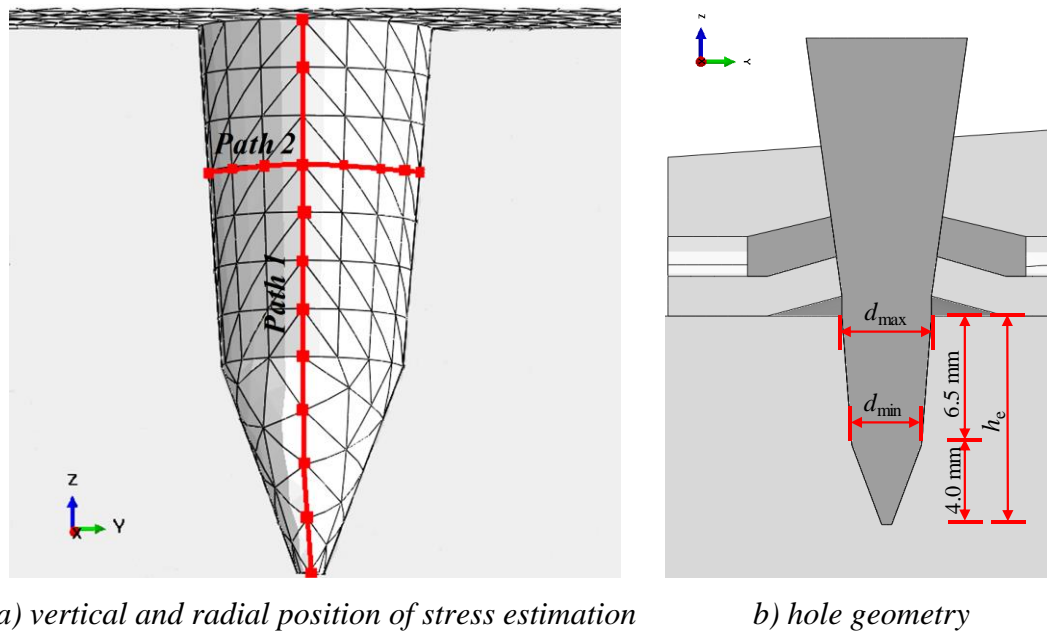
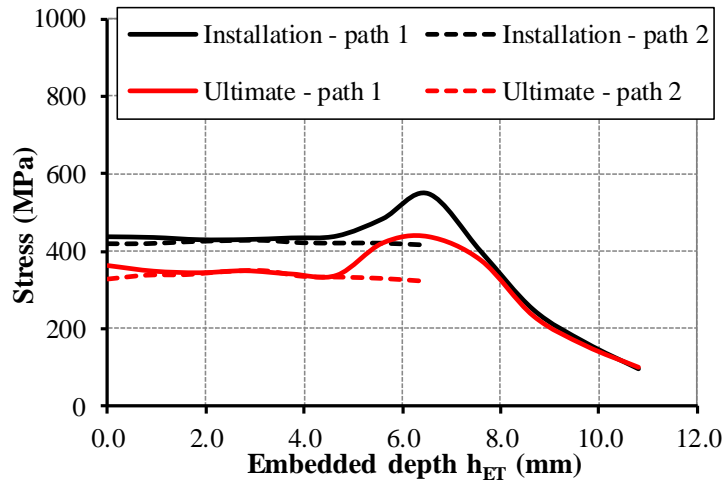
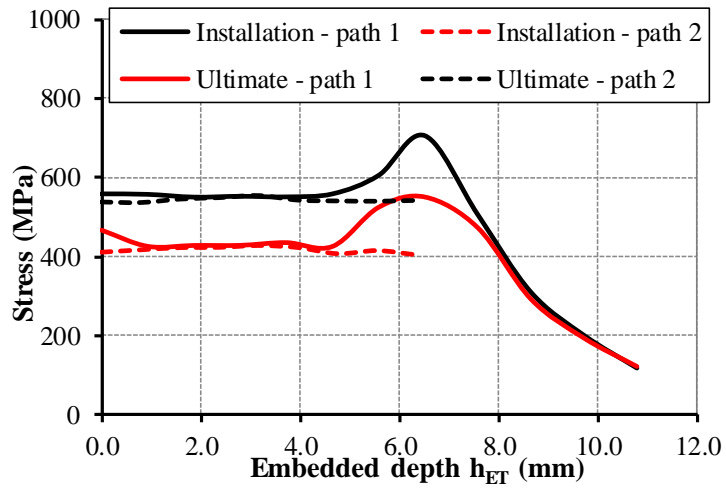


Figure 7.6. Geometry of steel base plate hole

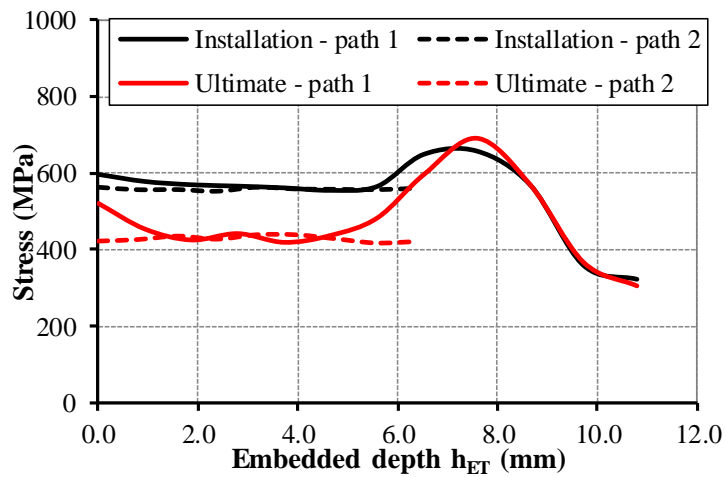
For further analysis of cartridge fired pins behaviour when they are subjected to the tension force, stress in the steel base material at the contact surface with embedded part of cartridge fired pin is analysed. Accumulated stress is obtained for two paths, as given in Figure 7.6a. Path 1 is used for stress analysis over the embedded depth, while path 2 is used to obtain stress over perimeter of cartridge fired pin hole, approximately 3.0 mm from the top surface of steel base material, as shown in Figure 7.6b. The stress is analysed at the end of installation procedure of cartridge fired pin and at the loading step with maximum pull-out force, or the step when hold obtained in base material is overcome. The analysed results for three different FE models are given in Figure 7.7.



a) TT2-2

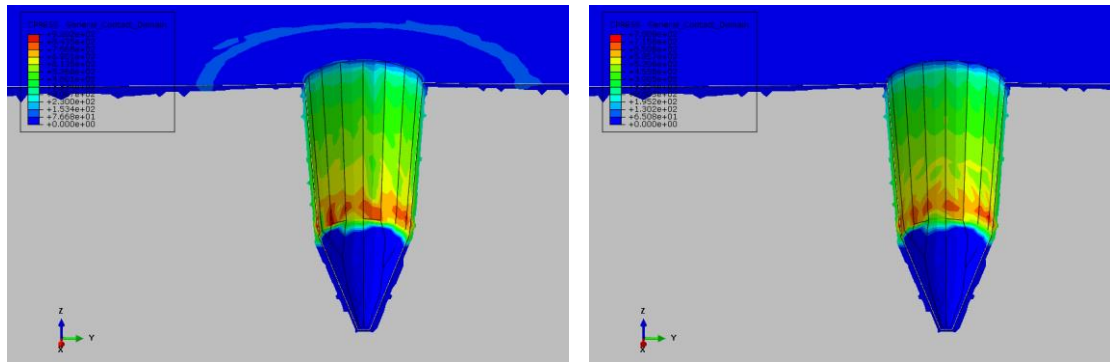


b) TT3-2

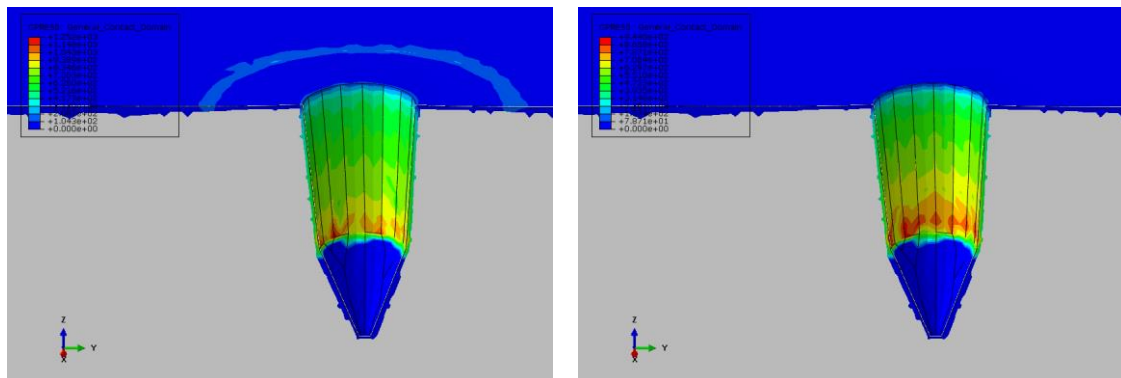


c) TT3-3.5

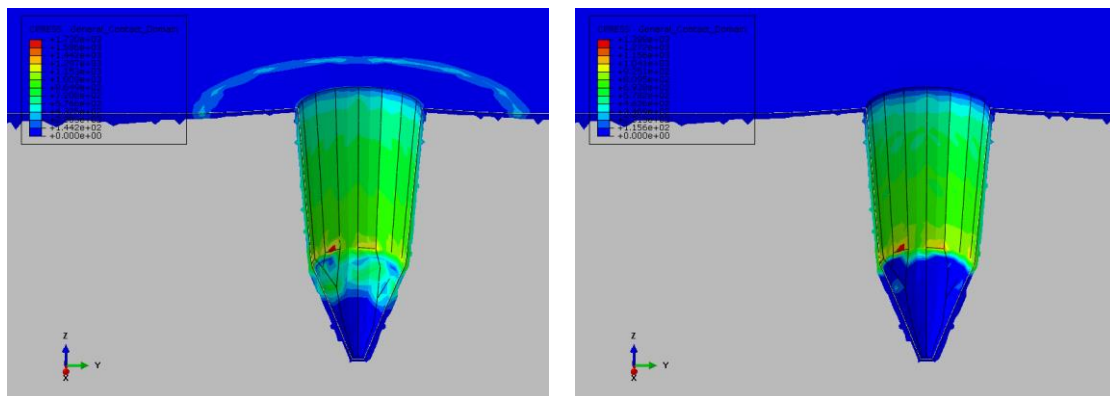
Figure 7.7. Stress obtained over cartridge fired pin hole height (path 1) and perimeter (path 2)



a) TT2-2 – installation (left) and pull-out (right)



b) TT3-2 – installation (left) and pull-out (right)



c) TT3-3.5 – installation (left) and pull-out (right)

Figure 7.8. Contact pressure on steel base material after installation procedure and corresponding to pull-out of cartridge fired pin

Accumulated stress over height of cartridge fired pin hole has the same value as stress obtained over perimeter of hole at approximately 3.0 mm distance from the base plate top surface. Therefore, accumulated stress can be obtained as constant value over the conical part of pin hole from base material top surface till part with d_{\min} diameter, as shown in Figure 7.6 and Figure 7.7. Certain increase of stress is obtained for the part of hole with minimal diameter d_{\min} , which is considered as localized increase due to sharp

change of hole geometry, as shown in Figure 7.7. Approximately, 2.5 mm from the part of hole with minimal diameter d_{\min} , accumulated stress is decreased for more than 50 %, as shown in Figure 7.3 and Figure 7.7. When the pull-out force is reached, accumulated stress in steel base material is decreased for approximately 150 MPa and is in the range of yield stress of base material, as shown in Figure 7.7.

Contact pressure developed during installation procedure of cartridge fired pin and corresponding to pull-out resistance is presented in Figure 7.8. Lower installation power level results in lower activation of embedded surface which will transfer the tension loading. Higher installation power level results in larger embedded surface, which is also related to accumulated stress in steel base material, which is presented in Figure 7.3 and Figure 7.7. The highest influence on embedded surface which is activated for tension force transfer has embedded depth and also base material strength.

7.2. Prediction model for pull-out resistance of cartridge fired pins

Results which are obtained from FE analysis of cartridge fired pins loaded in tension and presented pull-out resistance of cartridge fired pin is further used for development of prediction model to obtain pull-out resistance of X-ENP-21 HVB cartridge fired pin. Proposed prediction model is given in Eq. 7.1. Main parameters for pull-out resistance is accentuated and given in following equations: friction coefficient of pin embedded part μ_e and pressure force F_{press} developed during installation procedure between cartridge fired pin and steel base material. This pressure force is influenced with power level introduced during installation procedure, embedded depth of pin in steel base material and therefore embedded surface of pin in steel base material A_e and base material tension stress f_u as presented in Eq. 7.2. Pull-out resistance of cartridge fired pin with lower installation power level 2.0, can be calculated using Eq. 7.3. For cartridge fired pins with knurled tip, pull-out resistance should be calculated according Eq. 7.4.

$$P_{\text{pull}} = \mu_e \cdot F_{\text{press}} \quad (7.1)$$

$$F_{\text{press}} = A_e \cdot f_u \quad (7.2)$$

$$P_{\text{pull}} = 0.65 \cdot \mu_e \cdot F_{\text{press}} \quad (7.3)$$

$$P_{\text{pull}} = 1.75 \cdot \mu_e \cdot F_{\text{press}} \quad (7.4)$$

when $h_e \leq 11.0$ mm embedded surface should be calculated according Eq. 7.5 for whole range of base material strengths; when $f_u > 440$ MPa and $h_e > 11.0$ mm embedded surface should be increased and calculated according to Eq. 7.6 and for lower values of base material strength according Eq. 7.5:

$$A_e = \frac{(d_{\max} + d_{\min})}{2} \cdot (h_e - 4) \cdot \pi \quad (7.5)$$

$$A_e = \frac{(d_{\max} + d_{\min})}{2} \cdot (h_e - 4) \cdot \pi + 10\text{mm}^2 \quad (7.6)$$

In previous expressions:

μ_e is the friction coefficient of embedded part of pin which should be adopted as 0.25 for installation power level 2.0 and 0.3 for installation power level 3.5;

A_e is the embedded surface cartridge fired pin, determined according Eq. 7.5 and Eq. 7.6;

d_{\max} is the maximum hole (pin) diameter, adopted as 4.5 mm;

d_{\min} is the minimum hole (pin) diameter, adopted as 3.5 mm;

h_e is the embedded depth of cartridge fired pin;

f_u is the base material tensile strength.

Table 7.1. Comparison of experimental and FE analysis results with prediction model of pull-out resistance of X-ENP-21 HVB cartridge fired pin

Base material strength	Friction coefficient	Embedded geometry		Pull – out resistance (kN)			Ratio	
		depth	surface	EXP	FEA	Eq. 7.1 Eq. 7.2	anl/exp	anl/fea
f_u (MPa)	μ_e (-)	h_e (mm)	A_e (mm ²)	$P_{\text{pull,exp}}$	$P_{\text{pull,fea}}$	$P_{\text{pull,anl}}$	(-)	(-)
534.6	0.30	10.5	81.64	13.75	12.65	13.09	0.95	1.03
534.6	0.25	10.5	81.64	7.77	8.06	7.09	0.91	0.88
479.6	0.25	10.5	81.64	4.19	5.87	6.35	1.52	1.08

Comparison of experimental and FE analysis results of X-ENP-21 HVB cartridge fired pin subjected to tension loading with prediction model given in Eq. 7.1 and Eq. 7.3 is presented in Table 7.1 and Figure 7.9. Good agreement with obtained experimental and FE analysis results is achieved. Only disagreement which is not on the safe side of prediction is obtained for experimental results of TT2-2 test series. This test series

obtained very low pull-out resistance when lower installation power level is applied for base material with low tensile strength. This situation could be considered as installation mistake and is in the range of high experimental results dissipation.

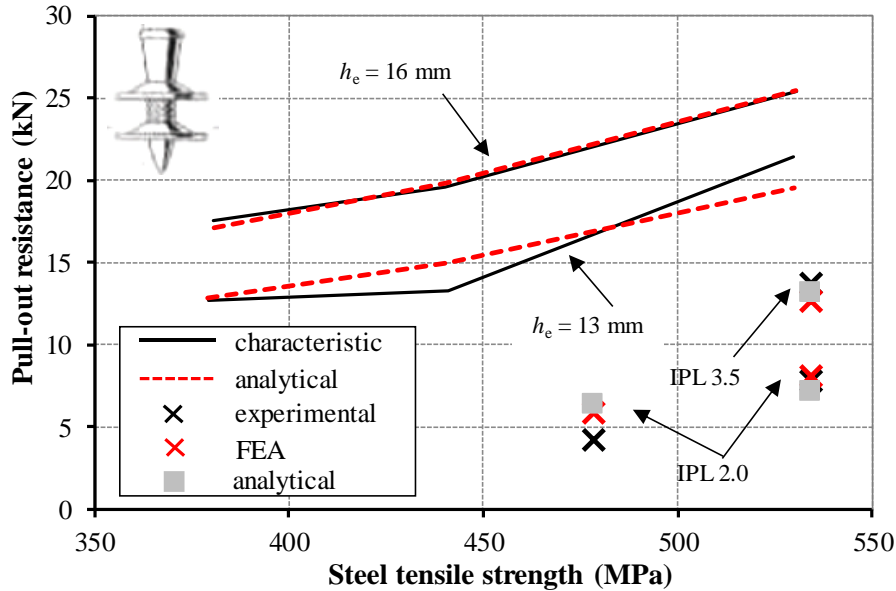


Figure 7.9. Analytical vs. experimental results of ENP2-21 L15MXR and X-ENP-21 HVB cartridge fired pin

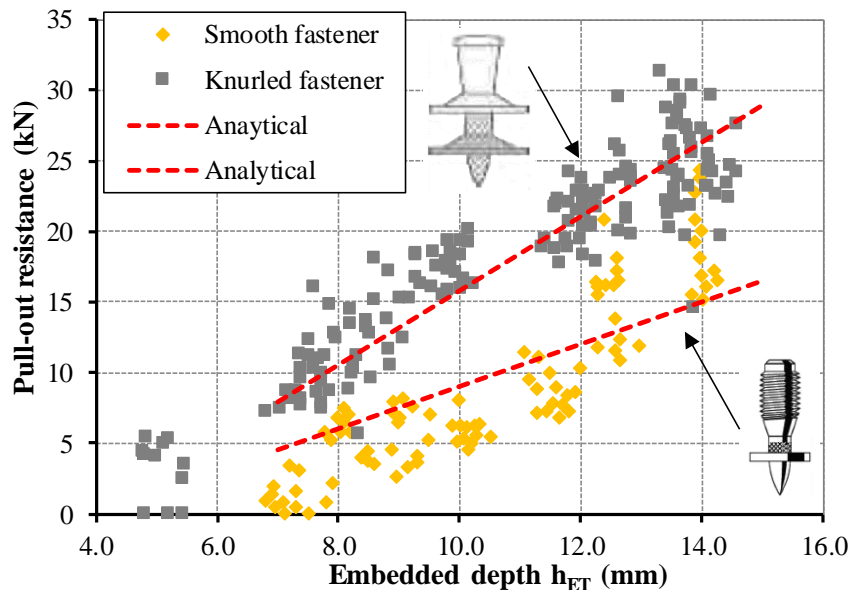


Figure 7.10. Comparison of proposed prediction model with experimental results of various types of fasteners, $f_u=400$ MPa

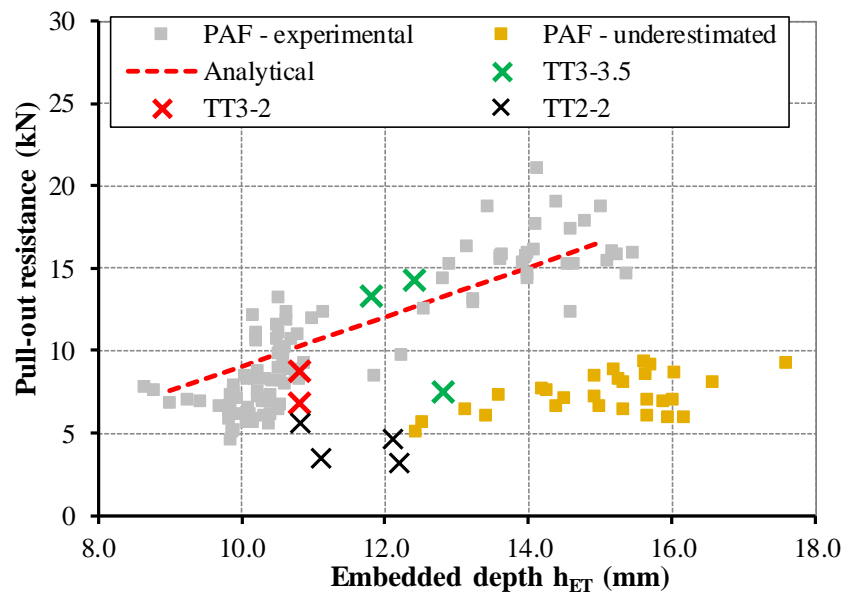


Figure 7.11. Comparison of proposed prediction model with experimental results of various types of fasteners with smooth shank, $f_u=400$ MPa

Developed prediction model is applied and compared with characteristic pull-out resistance of ENP2-21 L15MXR fastener and presented in Figure 7.9. Good agreement with characteristic pull-out resistance of presented fastener is achieved. Developed prediction model are applied for various types of powder actuated fasteners and compared with available experimental results, as presented in Figure 7.10 and Figure 7.11. Analytically obtained pull-out resistances presented in Figure 7.10 and Figure 7.11 for smooth tip fasteners are obtained using Eq. 7.1, while for knurled tip fastener enlargement coefficient of 1.75 is used, as presented in Eq. 7.4.

7.3. Summary

Presented analysis of pull-out behaviour of cartridge fired pins can lead to following conclusions:

1) Developed FE procedures for simulation of installation procedure of cartridge fired pins can be considered as reliable for various embedded depths, installation power levels and different types of fasteners.

2) Accumulated stress in steel base material after installation procedure is in the range of base material tensile strength and is relatively uniform over cylindrical part of pin and perimeter. This stress is decreased to approximately level of yield stress tension force corresponding to pull-out resistance.

3) Main parameters which reflect the behaviour of cartridge fired pins subjected to tension loading is friction coefficient, embedded depth and base material strength. Friction coefficient which is developed between embedded part of cartridge fired pin and base material strength is 0.3 for higher installation power levels.

4) Proposed prediction models for pull-out resistances of cartridge fired pins obtained satisfying agreement with experimental and FE analysis results of own investigation presented in this thesis and can be applied for other types of fasteners with smooth and knurled tip.

Chapter 8. Behaviour of X-HVB shear connectors in prefabricated concrete slabs

Comparative analysis of experimental and FE analysis results of X-HVB 110 shear connectors in prefabricated concrete slabs is presented in Chapter 5 and parametric analysis results are presented in Chapter 6. This chapter in detail describes behaviour of X-HVB 110 shear connectors in prefabricated concrete slabs for all examined test series.

Two distinctive failure mechanisms are obtained for forward and backward orientation of shear connectors. Comparison of obtained results from experimental and FE analysis is given in Figure 8.1. Considerable higher deformation of connector's fastening leg is obtained for backward orientation of shear connectors (HSB test series) as given in Figure 8.1 and Figure 8.2. Deformation of shear connector and cartridge fired pins for HSF and HSB test series corresponding to shear resistance is presented in Figure 8.2.

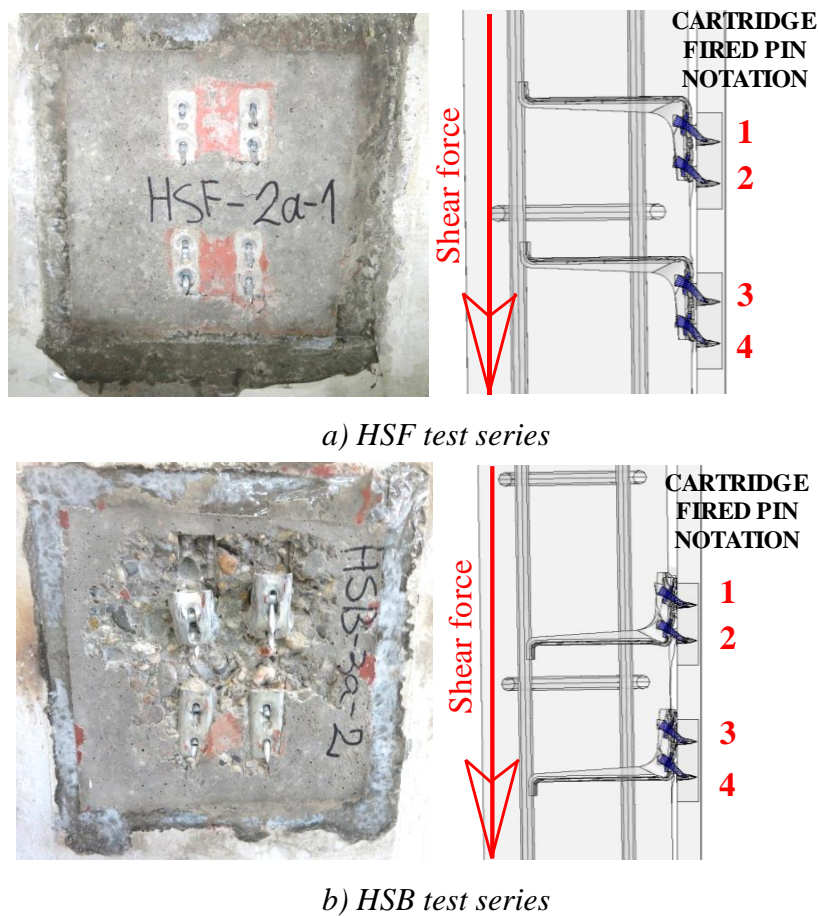


Figure 8.1. Failure mechanisms of X-HVB shear connectors – experimental vs. FE analysis

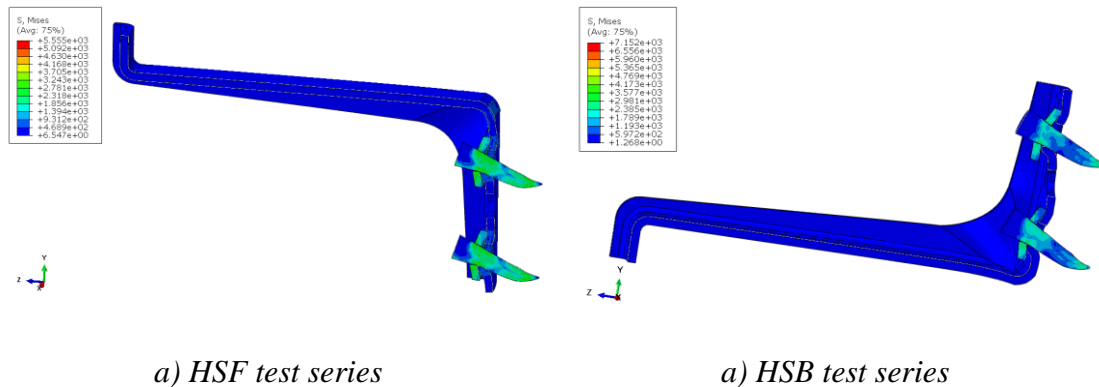
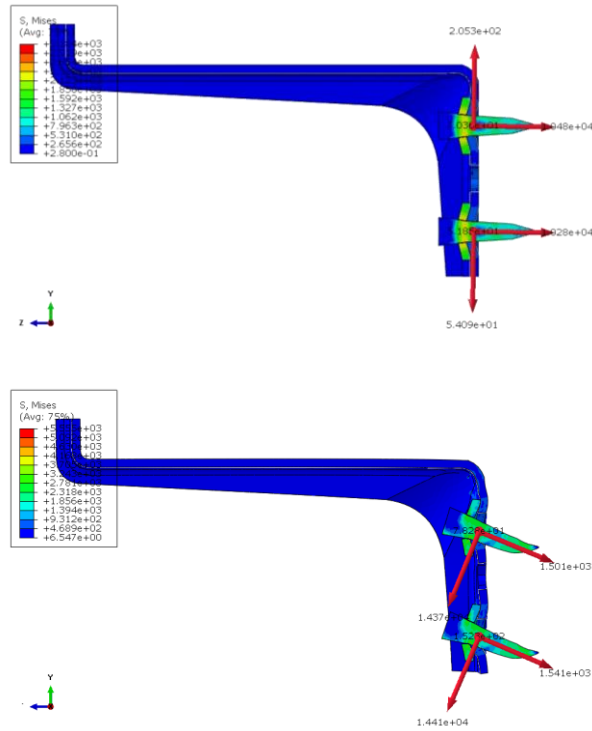


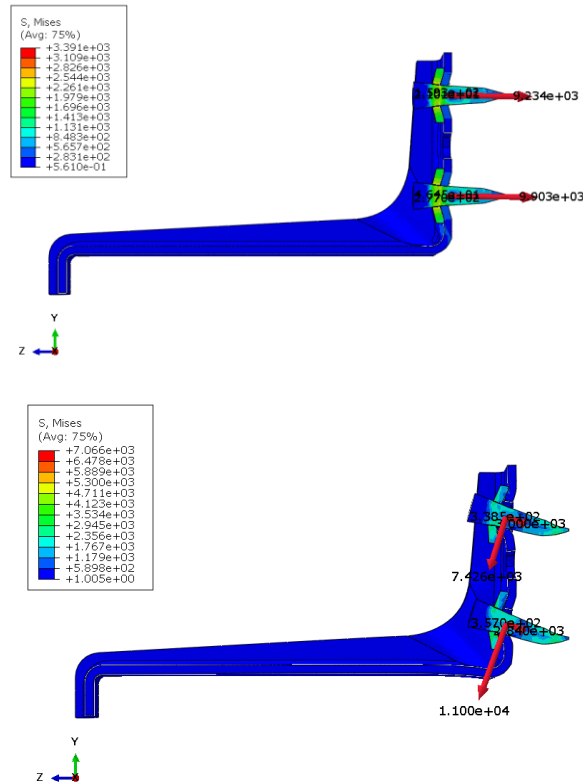
Figure 8.2. Deformation of connector and cartridge fired pins – FE analysis

Considering obtained failure mechanisms, two most significant parameters for behaviour of X-HVB shear connectors is concrete failure in close region to the cartridge fired pins head and cartridge fired pin – steel base material interaction. Behaviour of X-HVB shear connectors can be analysed through growth of cartridge fired pins forces during testing procedure. First shear connector row for two test series, HSF and HSB, with accompanying cartridge fired pins is presented in Figure 8.3. Upper figures present developed forces in cartridge fired pins during installation procedure and bottom figure deformation and accompanying forces corresponding to shear resistance of X-HVB 110 shear connector.

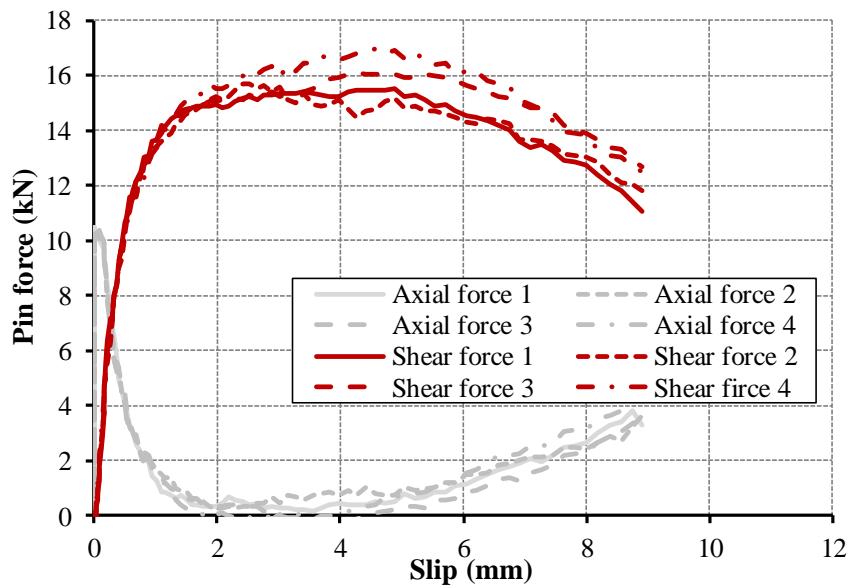
Growth of axial and shear force of cartridge fired pins during testing procedure in function of relative slip is presented in Figure 8.4 and Figure 8.5. Notation of pins forces from 1 to 4 represent a pins row relative to the shear force direction, as presented in Figure 8.1. Preloading force generated by simulation of the installation procedure is approximately 10.5 kN for 3.5 installation power level and 9.0 kN for 2.0 installation power level. In case of HSF test specimen (forward orientation of shear connectors), all cartridge fired pins are equally engaged in load transfer (see Figure 8.4a). This holds as well for the group arrangement of shear connectors (HSFg and HSFg-2 test series), as presented in Figure 8.5. Push-out test specimen with lower installation power level (HSFg test series) resulted in rapid loss of preloading force in comparison to the test specimens with higher installation power level (HSF, HSB and HSFg-2 test series).



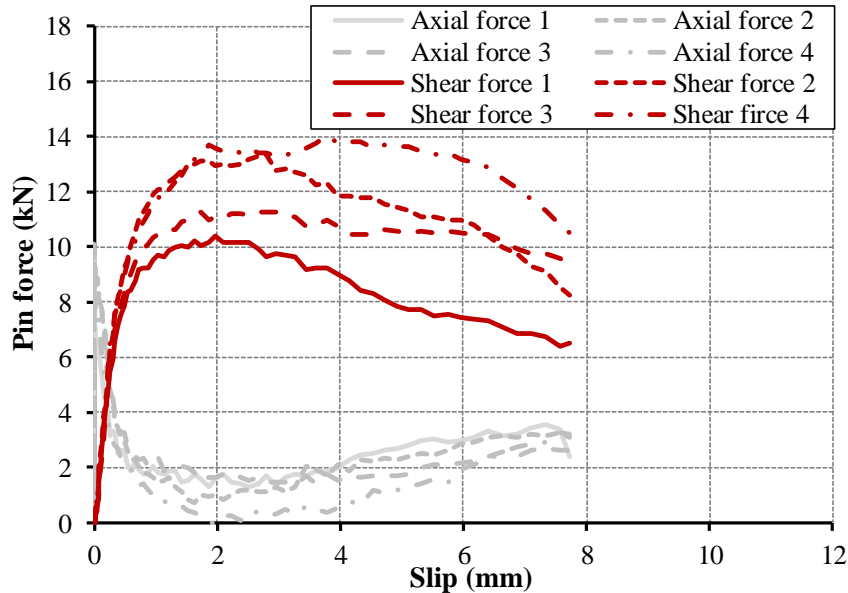
a) HSF test series - installation (upper figure) and shear resistance (bottom figure)



a) HSB test series - installation (upper figure) and shear resistance (bottom figure)
Figure 8.3. Cartridge fired pins forces – first row of shear connectors relative to the shear force direction



a) HSF test series

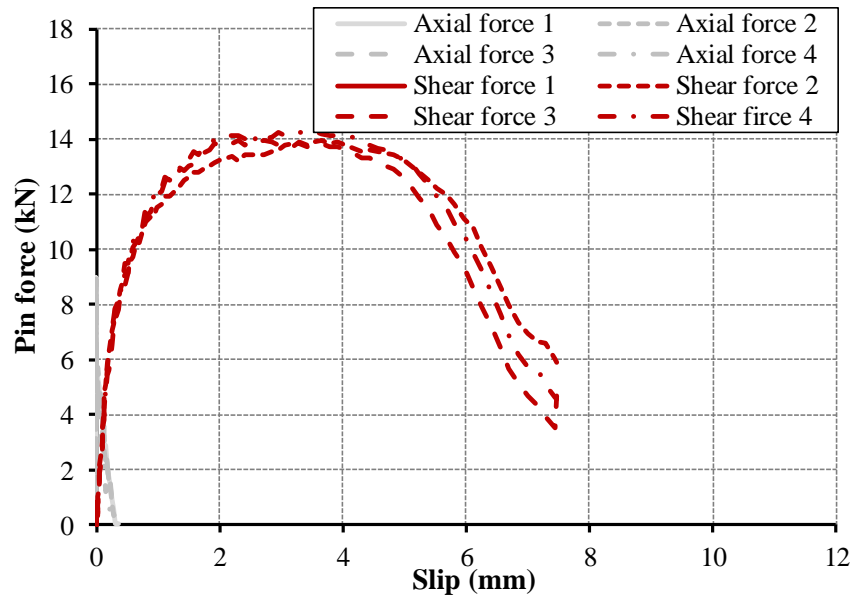


b) HSB test series

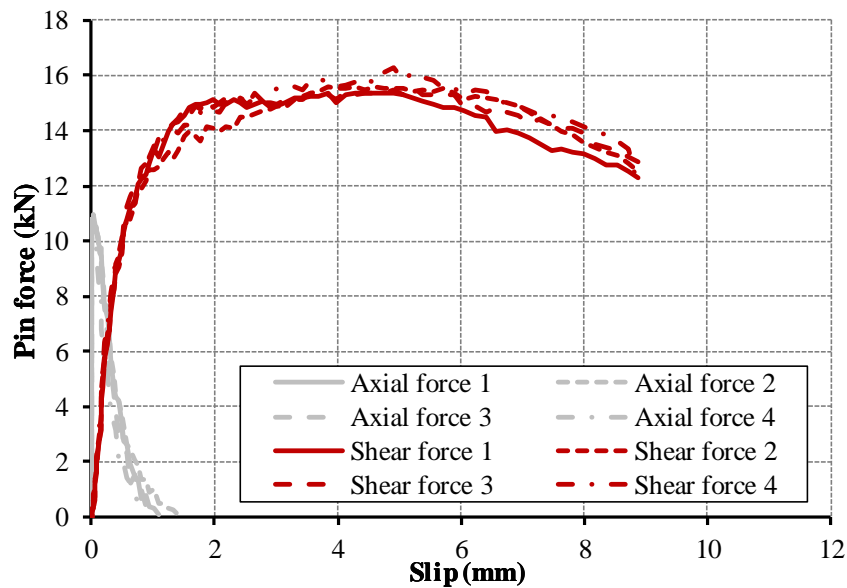
Figure 8.4. Axial and shear force in cartridge fired pins – minimal distance between shear connectors

For the backward orientation of shear connectors (HSB test series), cartridge fired pins variously participate in shear load transfer, as shown in Figure 8.4b. The lowest shear force is developed for cartridge fired pin 1 and 3 (first pin row for both shear connectors, see Figure 8.1b). This is related to the higher concrete damage obtained for the first row of cartridge fired pins, which is primary failure mechanism. Second cartridge fired pin of both shear connectors failed due to pull-out from base material, but smaller shear force is

still obtained in comparison to the forward orientation of shear connector with same installation power level (HSF and HSFg-2 test series).



a) HSFg test series

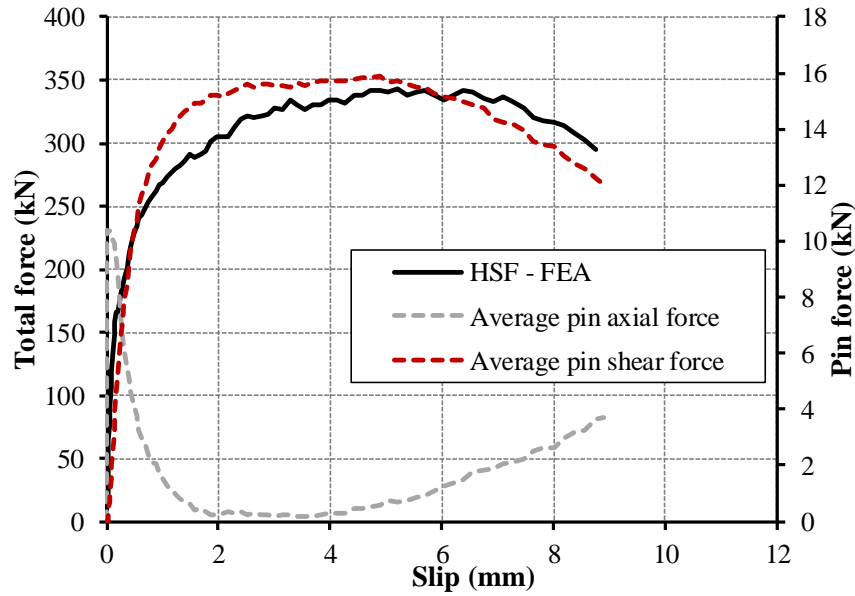


b) HSFg-2 test series

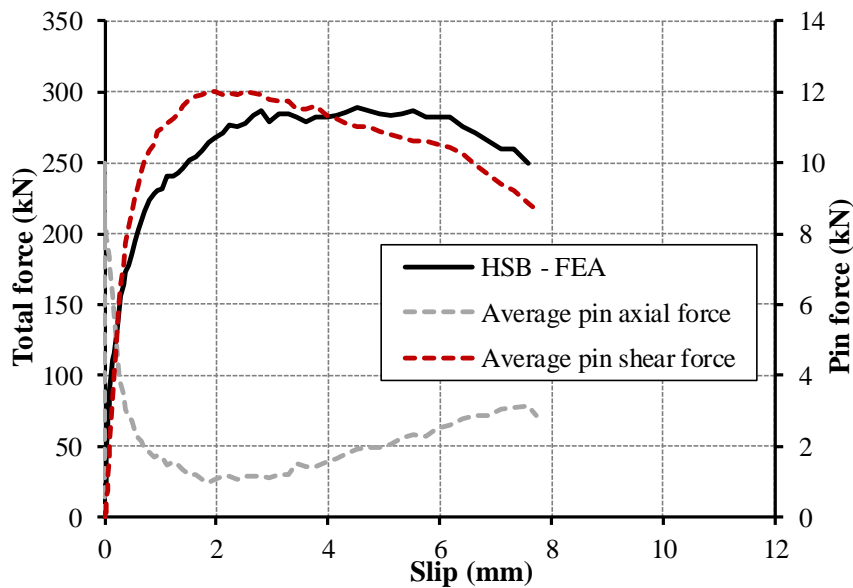
Figure 8.5. Axial and shear force in cartridge fired pins – group arrangement of shear connectors

Comparative analysis of average pins forces with shear force-relative slip curves of push-out tests is presented in Figure 8.6 and Figure 8.7. Complete reduction of preloading force accumulated during installation procedure is obtained for loading which is in the range from 0.7 to 0.9 of ultimate shear force P_{ult} , for installation power level 3.5.

For lower installation power level 2.0 of HSFg test series, preloading force is completely reduced for loading which is considerably below loads which correspond to serviceability limit state, approximately 0.5 of shear resistance P_{ult} . Subsequent increase of preloading force is obtained due to deformation and pull-out of cartridge fired pins, as given in Figure 8.6.

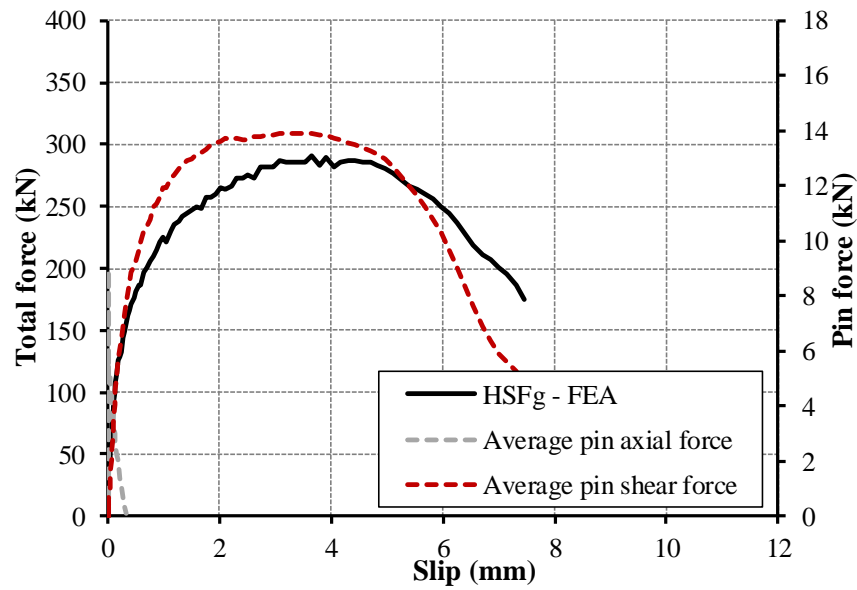


a) HSF test series

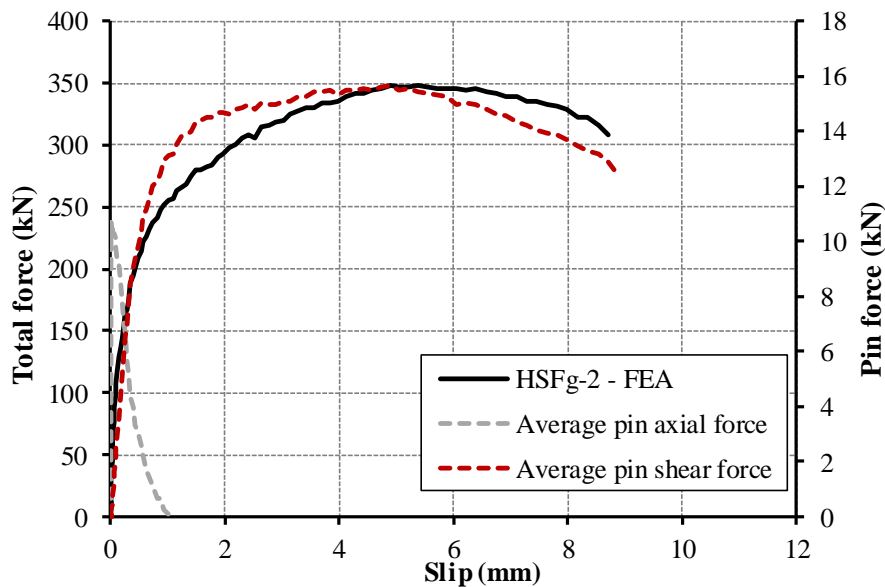


b) HSB test series

Figure 8.6. Average pins forces relative to shear resistance and slip capacity - minimal distance between shear connectors



a) HSFg test series



b) HSFg-2 test series

Figure 8.7. Average pins forces relative to shear resistance and slip capacity - group arrangement of shear connectors

Reduction of preloading force in cartridge fired pins is followed with increase of shear force. For forward orientation of shear connectors and same installation power level 3.5, average value of shear force per one cartridge fired pin is 16.0 kN (HSF and HSFg-2 test series). Group arrangement of shear connectors does not influence obtained failure mechanisms and obtained pins forces. Relatively higher ultimate shear force obtained from FE analysis of HSFg-2 test series is a result of concrete confinement conditions

behind shear connectors which are more pronounced for reduction of shear connector distances, as given in Figure 8.8. Maximal value of developed shear force for lower installation power level 2.0 of HSFg test series is 13.9 kN, which is approximately 13 % lower in comparison to the HSF and HSFg-2 test series with higher installation power level 3.5. Backward orientation of shear connectors obtained approximately 12.0 kN of shear force per cartridge fired pin. This clearly indicates that another failure mechanism is obtained for this orientation of shear connectors, which is mostly related to concrete damage and deformation of shear connectors prior to pull-out of cartridge fired pins, as presented in Figure 8.1 and Figure 8.6b.

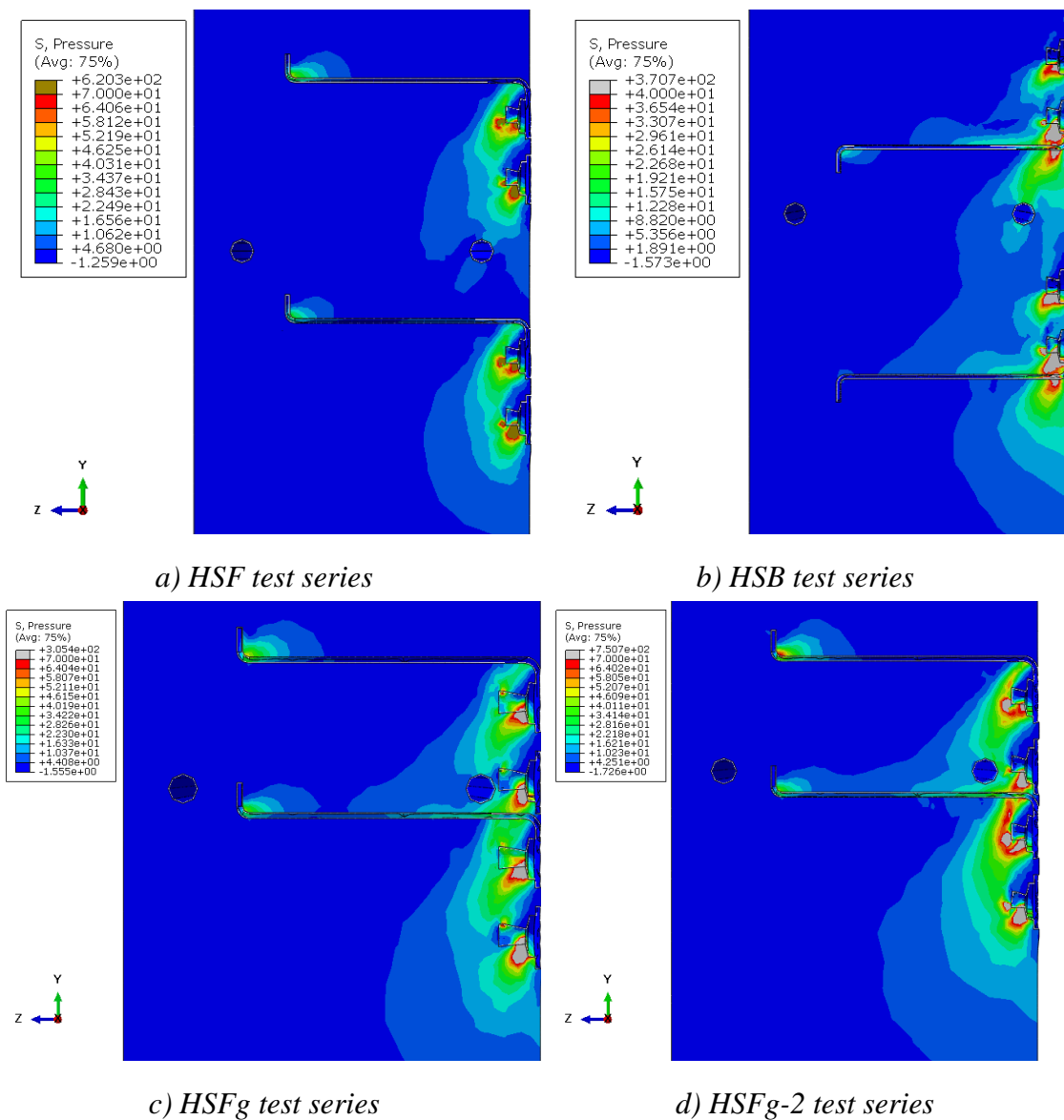
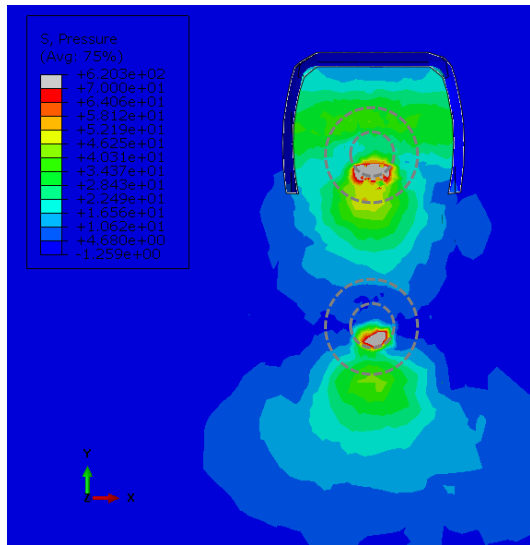
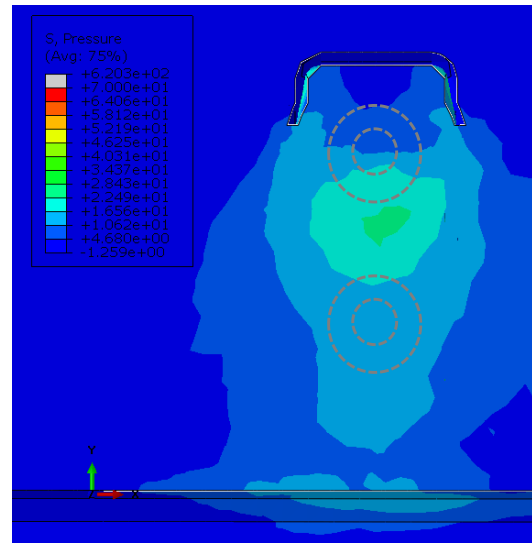


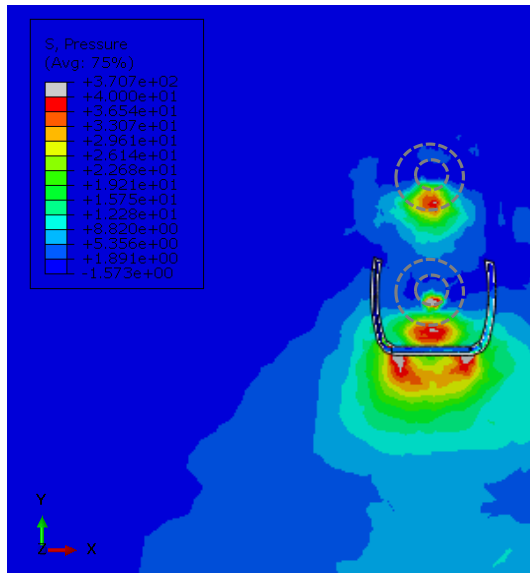
Figure 8.8. Concrete pressure corresponding to 90 % of shear resistance



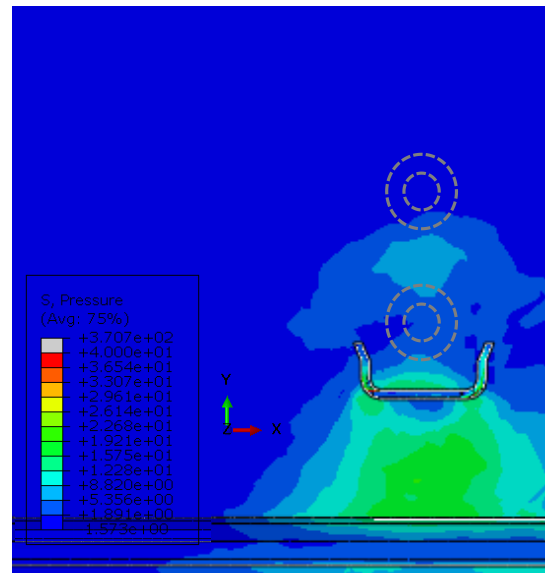
a) HSF series – 11 mm from steel plate



b) HSF series - 20 mm from steel plate



c) HSB series – 11 mm from steel plate

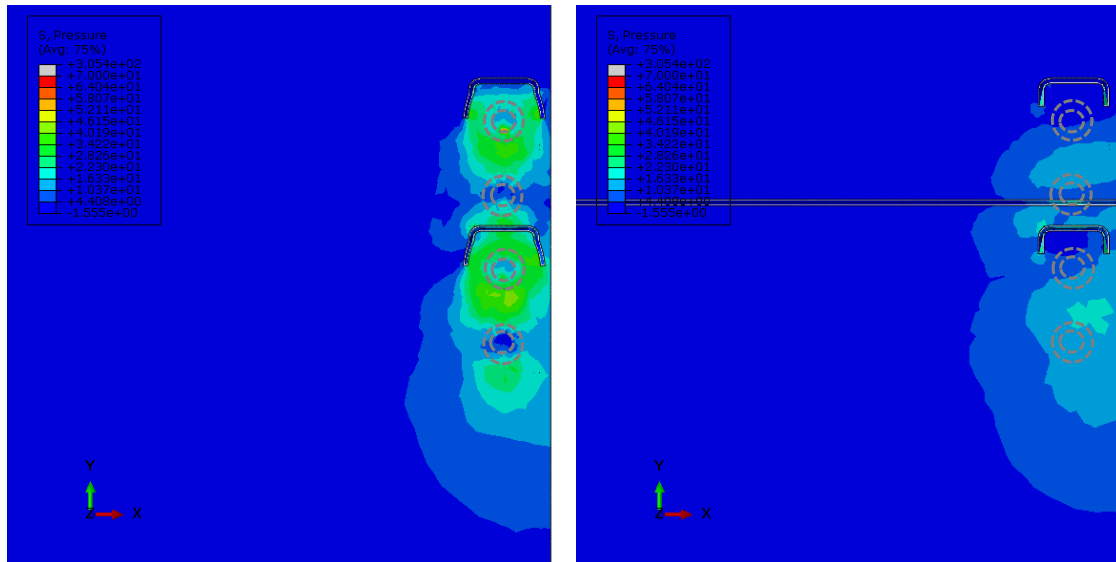


d) HSB series - 20 mm from steel plate

Figure 8.9. Concrete pressure corresponding to 90 % of shear resistance – minimal distance of shear connectors

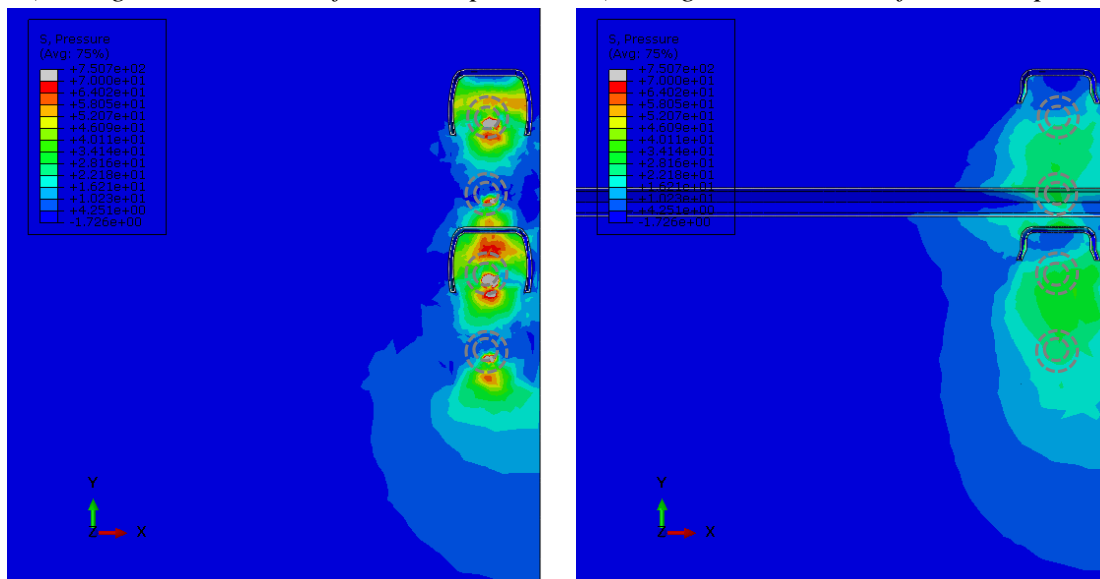
Pressure which is developed in concrete for various test series is given in Figure 8.8, Figure 8.9 and Figure 8.10. Loading level corresponding to presented concrete pressure is approximately 90 % of shear resistance obtained from FE analysis. Figure 8.8 gives presentation of concrete pressure over height of concrete prefabricated slab in the middle of shear connector. Spread of concrete pressure over the width of prefabricated concrete slab for various heights above the steel base material (bottom of concrete slab) is given in Figure 8.9 and Figure 8.10. Left side of Figure 8.9 and Figure 8.10 represents concrete pressure immediately above the cartridge fired pins, while left side represents

concrete pressure developed 20.0 – 25.0 mm from the bottom of concrete slab. Also, position of cartridge fired pins is indicated. Figure 8.9 gives presentation of concrete pressure in the region of first shear connector. Pressure in concrete is spread in the range which is approximately equal to the width of shear connector for both orientation of shear connectors. Moreover, for backward orientation of shear connector concrete pressure is localized behind shear connector anchorage leg.



a) HSFg series – 15 mm from steel plate

b) HSFg series - 25 mm from steel plate



a) HSFg-2 series – 11 mm from steel plate

b) HSFg-2 series - 20 mm from steel plate

Figure 8.10. Concrete pressure corresponding to 90 % of shear resistance – reduced distance between shear connectors

For both orientations and minimal distances between shear connectors, pressure in concrete is significantly reduced 20.0 mm above steel base material and is in the range of concrete compressive strength, without localized increase which is characteristic for lower concrete layers, as shown in Figure 8.9. Group arrangement of shear connectors obtained similar behaviour for same installation power level 3.5. Comparing same concrete layers for HSF and HSFg-2 test series, concrete pressure is spread over larger height for group arrangement of shear connectors. This is also a reason for slightly higher shear resistance of HSFg-2 test series obtained from FE analysis in comparison to the HSF test series. Also, lower installation power level of HSFg test series results in lower transfer of pressure from shear connector to concrete. Concrete pressure for this test series is significantly reduced in the layer which is 25.0 mm above steel base material, as shown in Figure 8.10b.

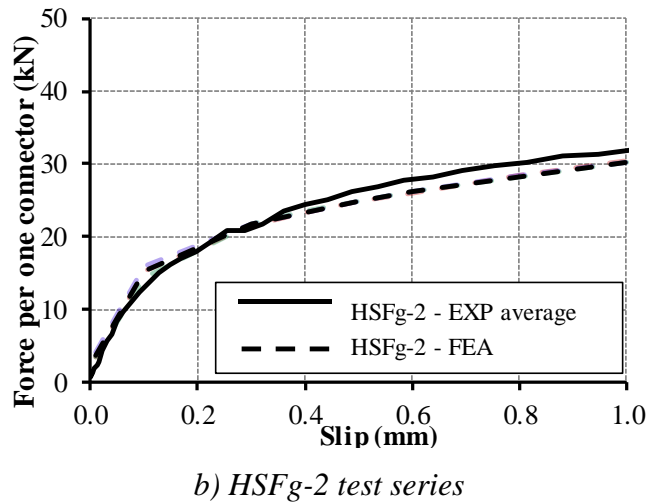
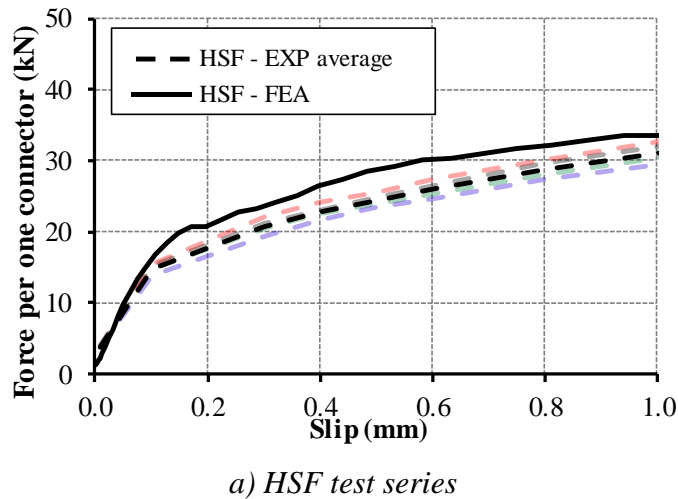


Figure 8.11. Shear resistance for one shear connector – installation power level 3.5 and forward orientation of shear connectors

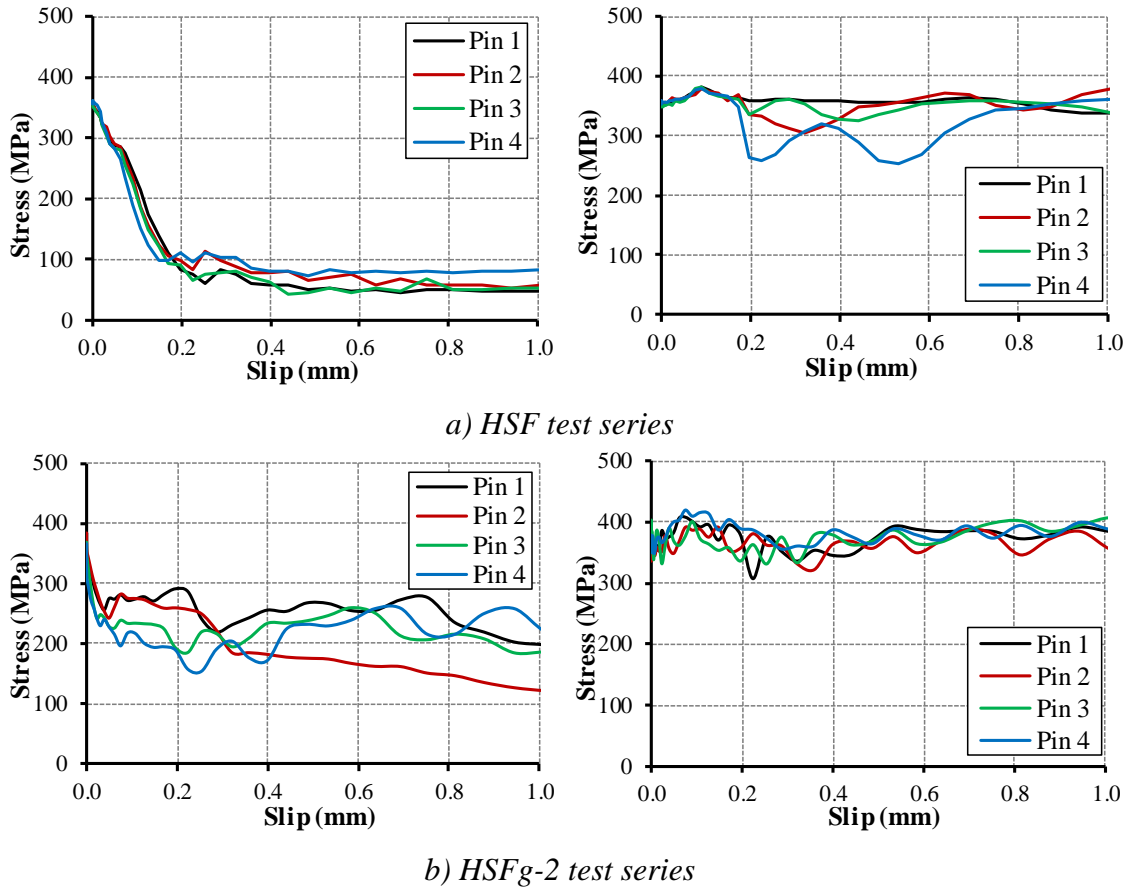
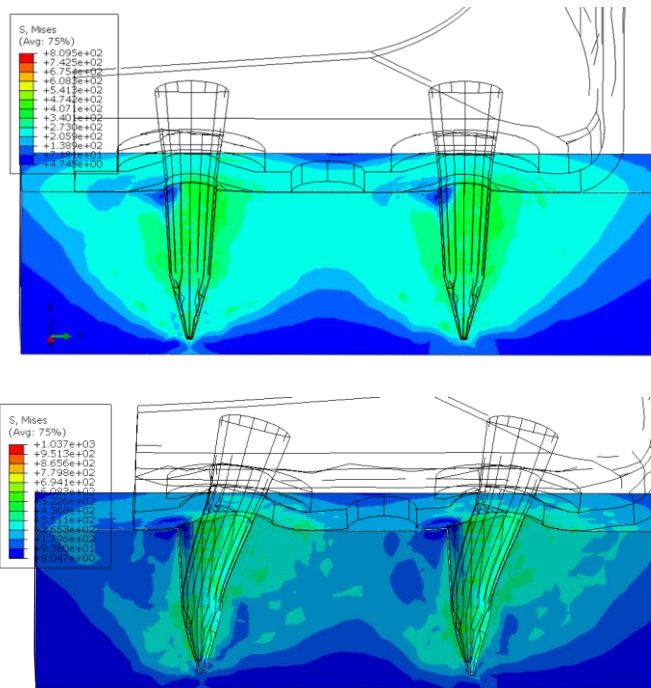


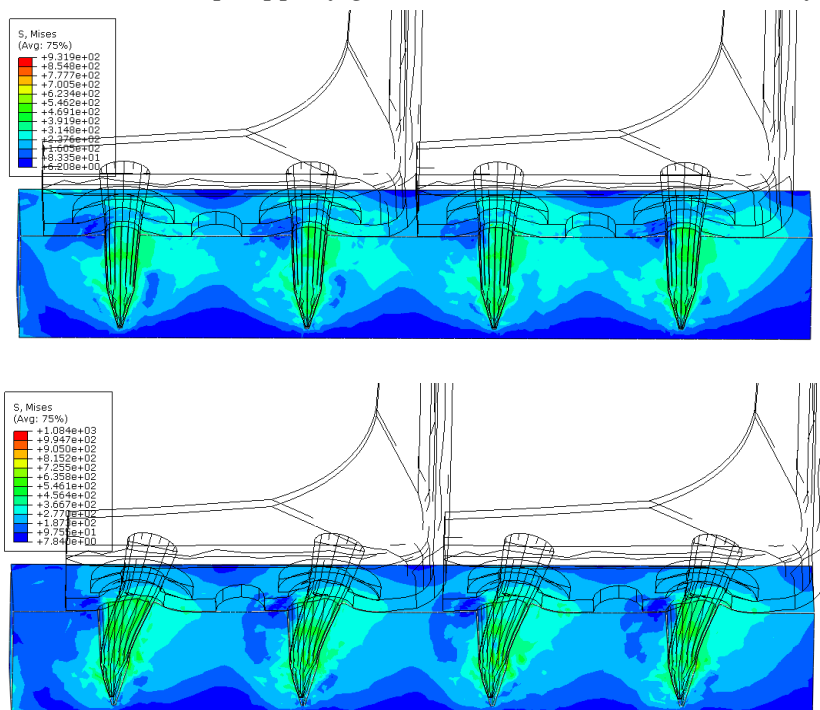
Figure 8.12. Steel base material stress – behind pin (left) and in front of pin (right) relative to the shear force direction

Behaviour of X-HVB shear connectors should be analysed through behaviour of concrete and cartridge fired pins. Figure 8.11 represents shear resistance per one fastener of forward orientation and higher installation power level 3.5, up to the 1.0 mm of relative slip. Significant reduction of initial stiffness is obtained for approximate resistance of one fastener of 20.0 kN and relative slip of 0.2 mm according to FE analysis, which is indicated in Figure 8.11. This stiffness reduction is obtained for all analysed test series through experimental investigation (see Figure 4.22). Reduction of longitudinal and transversal distances between connectors resulted in slightly lower reduction of stiffness at the force level of approximately 20.0 kN, as presented in Figure 8.11b. Shear resistance of 20.0 kN is obtained also as the loading level for which pull-out of fasteners is obtained. This is determined also as force level for which stress in steel base material behind cartridge fired pins (relative to the shear force direction) is starting to reduce, as presented in Figure 8.12 and Figure 8.13 (upper figures). Reduction of stress in steel base material

behind pins relative to shear force direction is propagated till shear resistance is achieved, as shown in Figure 8.13 (bottom figure).



a) HSF series – 0.2 mm slip (upper figure) and shear resistance (bottom figure)



b) HSFg-2 series - 0.2 mm slip (upper figure) and shear resistance (bottom figure)
Figure 8.13. Stress in steel base material for forward orientation of shear connectors and installation power level 3.5

Change of stress at the upper surface of steel base material through loading phases behind and in front of cartridge fired pin relative to shear force direction is presented in Figure 8.12. Stress in steel base material behind cartridge fired pin is reduced for more than 50 % for relative slip of 0.2 mm for HSF test series. This reduction is also obtained for group arrangement of shear connectors (HSFg-2 test series), but reduction of stress is lower, corresponding to slip of 0.2 mm. This is in direct relation with group positioning of shear connectors and developed confinement conditions of steel base material after the installation procedure.

Based on the presented analysis it can be concluded that resistance of X-HVB shear connector is divided on the resistance obtained by concrete pressure behind shear connector relative to the shear force direction and additional resistance by pull-out of cartridge fired pins. Prediction model defined in Chapter 7 for pull-out resistance of cartridge fired pins loaded in tension is slightly modified and applied also for definition of prediction model for shear resistance of X-HVB shear connector. Prediction model which describes shear resistance of X-HVB shear connector which is defined based on the experimental and FE analysis presented in this thesis is given in Eq. 8.1. First part of the prediction model given in Eq. 8.1 is related to the resistance of concrete and influences the behaviour of X-HVB shear connector through initial stiffness and subsequent pull-out of cartridge fired pins. Embedded depth h_e which was introduced for FE analysis of push-out tests with installation power level 3.5 is 14.5 mm. Comparison of shear resistance of push-out test specimens with forward orientation of shear connectors and minimal recommended distances between shear connectors (see Chapter 6) obtained through FE analysis and prediction model (see Eq. 8.1) is given in Figure 8.14 and Table 8.1. Presented comparison is performed for various steel grades which were used for parametric analysis of X-HVB 110 shear connector and concrete compressive strength $f_{cm}=29.87$ MPa obtained from experimental investigation of material properties of HSF test series and is given in Chapter 6.

$$P_{ult} = k \cdot h_{sc} \cdot b_{sc} \cdot \left(\frac{f_{cm}}{28} \right)^{0.2} + 2 \cdot \mu_e \cdot \frac{F_{press}}{1.6} \quad (8.1)$$

with:

$$F_{press} = A_e \cdot f_u \quad (8.2)$$

$$A_e = \frac{(d_{\max} + d_{\min})}{2} \cdot (h_e - 4) \cdot \pi \quad (8.3)$$

$$A_e = \frac{(d_{\max} + d_{\min})}{2} \cdot (h_e - 4) \cdot \pi + 10\text{mm}^2 \quad (8.4)$$

In previous expression:

h_{sc} is the height of shear connector [mm], according to ETA-15/0876 assessment [7];

b_{sc} is the width of shear connector [mm], according to ETA-15/0876 assessment [7];

f_{cm} is the concrete cylinder compressive cylinder strength [MPa];

k is the coefficient which depends of shear connector orientation relative to the shear force direction and should be adopted as 8.5 for forward orientation of shear connectors and 6.8 when shear connector orientation is not prescribed;

μ_e is the friction coefficient of embedded part of pin is prescribed as 0.3;

F_{press} is the pressure force developed during installation procedure between cartridge fired pin and pins hole in steel base material;

A_e embedded surface of pin's hole, determined according Eq. 8.3 and Eq. 8.4 which should be determined according to recommendations given in Chapter 7;

d_{\max} is the maximum hole (pin) diameter (see Chapter 7);

d_{\min} is the minimum hole (pin) diameter (see Chapter 7);

h_e is the embedded depth of cartridge fired pin (see Chapter 7);

f_u is the base material tensile strength.

Table 8.1. Shear resistance for forward orientation of shear connectors – comparison with prediction model for various base material strengths

Base material strength	Friction coeff.	Embedded geometry		Shear resistance (kN)			Ratio	
		depth	surface	EXP	FEA	ANL Eq. 8.1.	anl/exp	anl/fea
f_u (MPa)	μ_e (-)	h_e (mm)	A_e (mm ²)	$P_{ult,exp}$	$P_{ult,fea}$	$P_{ult,anl}$	(-)	(-)
433.6	0.30	14.5	131.9	335.4	342.7	331.2	0.99	0.97
479.6	0.30	14.5	141.9	-	384.0	363.8	-	0.95
534.6	0.30	14.5	141.9	-	411.1	387.2	-	0.94

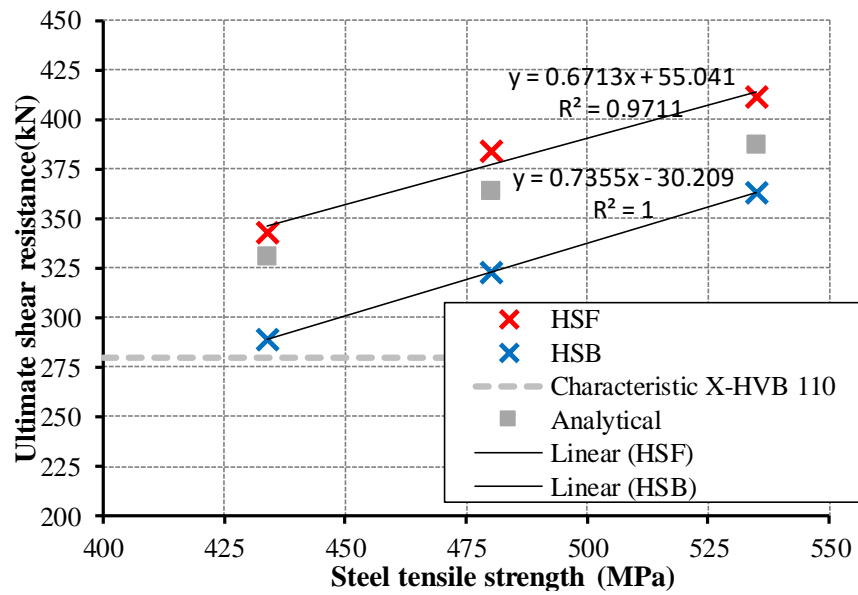


Figure 8.14. Comparison of shear resistance for FE analysis results and according to prediction model

Table 8.2. Shear resistance for forward orientation of shear connectors – comparison with prediction model for various concrete classes

Concrete class	Friction coeff.	Embedded geometry		Shear resistance (kN)			Ratio	
		depth	surface	EXP	FEA	ANL Eq. 8.1.	anl/exp	anl/fea
f_{cm} (MPa)	μ_e (-)	h_e (mm)	A_e (mm ²)	$P_{ult,exp}$	$P_{ult,fea}$	$P_{ult,anl}$	(-)	(-)
29.87	0.30	14.5	131.9	335.4	342.7	331.2	0.99	0.97
38.0	0.30	14.5	131.9	-	358.2	339.1	-	0.95
48.0	0.30	14.5	131.9	-	359.3	347.1	-	0.97

Comparison of shear resistances of X-HVB 110 shear connector for various concrete classes of prefabricated concrete slabs obtained through FE analysis (see Figure 6.9) and through prediction model given in Eq. 8.1 is presented in Table 8.2. Defined prediction model obtains good agreement with results of FE analysis.

According to ETA-15/0876 assessment [7], characteristic shear resistance of various heights of X-HVB shear connectors is obtained for normal-weight concrete classes C20/25 - C50/60 and for structural steel base material S235, S275 and S355 (see Table 2.1). As presented in Figure 8.11, experimental shear resistance is slightly lower on comparison to the FE analysis results. Considering that ETA-15/0876 assessment [7] gives characteristic resistance of X-HVB shear connectors for various concrete and steel base material strengths, lowest values from the specified ranges are adopted, according

to EN 1992-1-1:2004 [50] and EN 10025-2 [8]. Comparison of characteristic shear resistance obtained according to ETA-15/0876 assessment [7] and Eq. 8.1. is presented in Table 8.3. Adopted compressive cylinder strength f_{cm} is 28.0 MPa, base material strength f_u is 360 MPa, friction coefficient μ_e is 0.3 and embedded depth h_e is 14.5 mm. Embedded surface A_e is calculated according to Eq. 8.3, considering recommendations given in Chapter 7. Coefficient k defined in Eq. 8.1 is determined based on the FE analysis results of HSF test series in order to determine the height of active concrete pressure behind shear connector which represent the first part of shear resistance determined according to this prediction model. Characteristic shear resistance of X-HVB 110 shear connectors given in ETA-15/0876 assessment [7] are lower in comparison to the results presented in this thesis. Therefore, value of coefficient k in Eq. 8.1 is determined in order to achieve better agreement of proposed prediction model with characteristic shear resistances obtained by manufacturer. Also, ETA-15/0876 assessment [7] does not explicitly determines the relation between proposed characteristic shear resistance and orientation of X-HVB shear connectors relative to the shear force direction. It is proposed that value of coefficient k of 8.5 should be used for forward orientation of shear connectors, while value of 6.8 should be used when orientation of shear connectors relative to the shear force direction is not prescribed.

Table 8.3. Characteristic shear resistance of X-HVB shear connectors - ETA-15/0876 assessment [7] and prediction model

X-HVB shear connector	Connector geometry [7]		Shear resistance (kN)		Ratio
	height	width	ANL Eq. 8.1.	Characteristic [7]	anl/chr
(-)	h_{sc} (mm)	b_{sc} (mm)	$P_{ult,anl}$	P_{Rk}	(-)
40	43	24.3	24.91	29.0	0.86
50	52	24.3	26.40	29.0	0.91
80	80	24.3	31.02	32.5	0.95
95	95	24.3	33.50	35.0	0.96
110	112.5	20.6	33.56	35.0	0.96
125	127.5	20.6	35.66	37.5	0.95
140	142.5	20.6	37.77	37.5	1.01

Table 8.4. Shear resistance of X-HVB shear connector

X-HVB shear connector	Shear resistance (kN)			Ratio	
	Concrete	Pins	ANL Eq. 8.1.	con / anl	pin / anl
(-)	$P_{ult,con}$	$P_{ult,pin}$	$P_{ult,anl}$	$P_{ult,con} / P_{ult,anl}$	$P_{ult,pin} / P_{ult,anl}$
40	7.11	17.80	24.91	0.25	0.61
50	8.60	17.80	26.40	0.30	0.61
80	13.22	17.80	31.02	0.41	0.55
95	15.70	17.80	33.50	0.45	0.51
110	15.76	17.80	33.56	0.45	0.51
125	17.86	17.80	35.66	0.48	0.47
140	19.96	17.80	37.77	0.53	0.47

Prediction model given in Eq. 8.1 represents shear resistance of X-HVB shear connectors through concrete compressive strength and pull-out resistance of cartridge fired pins. Particular influence of these two resistances in shear resistance is presented in Table 8.4. Concrete compressive strength represent less than 50 % of shear resistance of X-HVB shear connector and increases with increase of connector height.

8.1. Summary

Presented analysis of X-HVB shear connector behaviour can lead to following conclusions:

1) Developed FE models with simulation of installation procedure of cartridge fired pins can be considered as reliable for analysis of X-HVB shear connectors.

2) According to developed FE models for forward orientation of shear connectors, pressure in concrete developed through shear loading is transferred through width of shear connector to the approximately one third of connector height.

3) Main parameters which reflect behaviour of X-HVB shear connectors is concrete compressive strength, steel base material strength, embedded depth of cartridge fired pins and friction coefficient. Friction coefficient which is developed between embedded part of cartridge fired pin and base material strength is prescribed as 0.3.

4) Prediction model which describes shear resistance of X-HVB shear connector which is defined based on the experimental and FE analysis presented in this thesis. First part of the prediction model is related to the resistance of concrete and influences the

behaviour of X-HVB shear connector through initial stiffness and subsequent pull-out of cartridge fired pins.

5) Proposed prediction model for shear resistance of X-HVB shear connectors obtained satisfying agreement with FE analysis results calibrated based of own experimental investigation. This prediction model gives safe side prediction for characteristic shear resistance given in ETA-15/0876 assessment [7].

5) Participation of concrete compressive resistance in total resistance of X-HVB shear connectors is from 25 % to 55 % and increases with connector height.

Chapter 9. Conclusions and future work

X-HVB 110 shear connector, connected to the steel base material with X-ENP-21 HVB cartridge fired pins, is analysed through 4 tests series, 17 push-out specimens in total with prefabricated concrete slabs. Different orientations and distances of connectors, as well as tensile and shear behaviour on the cartridge fired pins alone are tested in experiments and validated by FE analysis. Following conclusions are drawn:

1) Shear resistance and slip capacity of X-HVB 110 shear connectors in prefabricated concrete slabs with envisaged openings are not reduced in comparison to those values in solid concrete slabs cast in situ.

2) Average slip capacity of the tested series ranges from 6.1 mm to 9.6 mm. Being larger than 6.0 mm, the behaviour of X-HVB 110 connectors in prefabricated solid concrete slabs is considered as ductile according to recommendations given in EN 1994-1-1:2004 [11]. Average shear resistance of all analysed test series in push-out experiments ranges from 35.6 kN to 41.9 kN per connector, which is higher than characteristic shear resistance of 35.0 kN obtained by ETA-15/0876 assessment [7] for this type of shear connector.

3) When shear connectors are positioned at minimal recommended transversal and longitudinal distances, up to 12 % higher shear resistance and 11 % higher slip capacity is obtained in the case of forward orientation (HSF series) in comparison to the backward orientation (HSB series). The forward orientation of the shear connectors, i.e. anchorage leg of the connector facing ahead and the pins and the fastening leg following the flow of the shear force in concrete is more favourable, considering obtained shear resistance and failure mechanisms.

4) The pull-out of the cartridge fired pins from the steel flange is the characteristic failure mechanism for the forward orientation of the shear connectors with very little damage in concrete, i.e. only limited crushing around the first row of pins. The backward orientation is characterized by significant crushing damage of concrete, deformation of the fastening leg of connector and subsequent pull-out of pins. However, concrete damage is confined only to zone around connectors. No global cracks in the prefabricated concrete slabs nor the separation of contact layer between the infill concrete and the prefabricated slab were found.

5) It was found that the orientation of shear connector relative to the shear force direction strongly influences shear resistance, slip capacity and failure mechanisms. However, making the group arrangement of shear connectors positioned at distances smaller than recommended did not result in significant reduction of shear resistance.

6) Grouped connectors of HSFg-2 test series, where 4 connectors are tightly clustered in 2x2 arrangement, obtained only 4 % lower shear resistance compared to the HSF test series. Obtained results could be considered as significant feature of X-HVB shear connectors, considering their grouped arrangement in composite concrete slabs with profiled steel sheeting and agreement with requirements for minimal partial shear connection degree.

7) Pull-out of cartridge fired pins in the push-out and pin experiments is modelled in FE analysis by equivalent compressive contact stresses and friction at the interface between the base material and pins modelled as separate parts. This resembles the physical mechanism of the load transfer of fired pins and is a recommended modelling procedure as it gives good agreement with experimental results. It was possible to properly calibrate FE models for experiments with different installation power levels (e.g. HSFg vs. HSFg-2) by keeping the friction coefficient in the model to value 0.3 of push-out FE models and varying the level of imposed contact stresses.

8) Behaviour of X-HVB shear connectors in prefabricated concrete slabs is determined with obtained “hold” of cartridge fired pin into steel base material which is described also as anchorage mechanisms. Variation of concrete class does not have significant influence on shear resistance of X-HVB shear connectors. Increase of steel grade of base material for approximately 100 MPa (from steel grade S235 to S355) resulted in approximately 20 % higher ultimate shear resistance of X-HVB shear connector. Also, higher characteristic value of slip capacity is obtained for both shear connector orientations which is related to the obtained “hold” of cartridge fired pin into steel base material.

9) Pull-out resistance of cartridge fired pins loaded in tension is mostly influenced with friction coefficient between embedded part of cartridge fired pin and base material, embedded depth and steel base material grade. FE modelling approach defined for installation procedure highlights the clamping of fastener into base material as the most

important anchorage mechanism. Proposed prediction model for determination of pull-out resistance of cartridge fired pins is applicable for various range of cartridge fired pins. Tension loading is transferred mostly over cylindrical part of cartridge fired pin.

10) Proposed prediction model of shear resistance of X-HVB shear connectors obtained satisfying agreement with FE analysis results of own experimental investigation and characteristic shear resistance obtained by ETA-15/0876 assessment [7]. Participation of concrete compressive strength in total resistance of X-HVB shear connectors is from 25 % to 55 % and influences the behaviour of shear connector through initial stiffness and subsequent initiation of pull-out of cartridge fired pins. Pull-out of cartridge fired pins is obtained for relative slip of approximately of 0.2 mm.

Based on conclusions which are drawn above, following recommendations for future work can be given:

1) Additional experimental investigation of cartridge fired pins for shear and tension test with various types of pins, installation power levels and base material properties should be performed in order to validate proposed prediction models.

2) Detail investigation of base material properties in close region to the cartridge fired pins after installation procedure should be performed in order determine steel material model which can be used for FE analysis procedures of this type of connections.

3) Developed FE models should be used for development of FE models with composite concrete slabs with profiled steel sheeting. Further, beam tests with composite concrete slabs should be performed in order to investigate lower limit of partial shear connection which should be applied for this type of shear connector.

4) Beam tests with prefabricated concrete slabs and X-HVB shear connectors positioned in envisaged openings should be performed in order to investigate influence of this type of composite construction on bending resistance and obtained slip.

5) Application of cartridge fired pins and X-HVB shear connectors with high strength steels should be further investigated for various contemporary structures, such as composite beams with cold-formed sections and composite columns.

REFERENCES

- [1] "XMA-17A/95 Summary of Push Tests X-HVB Shear Connector System", Hilti Aktiengesellschaft, Schaan, Fürstentum Liechtenstein, 1996.
- [2] A. G. J. Way, T. C. Cosgrove, and M. E. Brettle, *SCI Publication P351 Precast concrete floors in steel framed buildings*, Berkshire, UK, SCI The Steel Construction Institute, 2007.
- [3] M. Spremić, *Analiza ponašanja grupe elastičnih moždanika kod spregnutih nosača od čelika i betona*, doktorska disertacija, Univerzitet u Beogradu, Građevinski fakultet, Beograd, 2013.
- [4] M. Pavlović, *Resistance of bolted shear connectors in prefabricated steel-concrete composite decks*, doctoral dissertation, University of Belgrade, Faculty of Civil Engineering, Belgrade, 2013.
- [5] "HILTI X-HVB system Solutions for composite beams", Hilti Aktiengesellschaft, Schaan, Fürstentum Liechtenstein, 2017.
- [6] *European Assessment Document EAD 200033-00-0602 Nailed shear connector*, Brussels, Belgium, European Organisation for Technical Assessment, 2016.
- [7] *European Technical Assessment ETA-15/0876*, Berlin, Germany, Deutsches Institut für Bautechnik, 2016.
- [8] *EN 10025-2 Hot rolled products of structural steels – Part 2: Technical delivery conditions for non-alloy structural steels*, Brussels, Belgium, CEN European Committee for Standardization, 2004.
- [9] J.C. Badoux, "TECHNICAL ASSESSMENT The behaviour and strength of steel-to-concrete connection using Hilti HVB shear connectors", Schaan, Fürstentum Liechtenstein: Hilti AG Befestigungstechnik, 1988.
- [10] J.C. Badoux, "TECHNICAL ASSESSMENT The behaviour and strength of steel-to-concrete connection using HVB shear connectors", Schaan, Fürstentum Liechtenstein: Hilti AG Befestigungstechnik, 1989.
- [11] *EN 1994-1-1 Eurocode 4: Design of composite steel and concrete structures - Part 1-1: General rules and rules for buildings*, Brussel, Belgium, CEN European Committee for Standardization, 2004.
- [12] H. Beck, M. Siemers, and M. Reuter, *Steel Construction Calendar 2011 - Powder-actuated fasteners and fastening screws in steel construction*, Ernst & Sohn, 2011.
- [13] *Deutsches Institut für Bautechnik ANSTALT DES OFFENTLICHEN RECHTS*, no. Z-26.4-46, Berlin, Germany, Deutsches Institut für Bautechnik, 2008.
- [14] *EN 10130:2006 Cold rolled low carbon steel flat products for cold forming – Technical delivery conditions*, Brussels, Belgium, CEN European Committee for Standardization, 2006.
- [15] "HILTI DX 76", Hilti Corporation, Schaan, Fürstentum Liechtenstein, 2013.
- [16] M. Crisinel, "Partial-interaction analysis of composite beams with profiled sheeting and non-welded shear connectors", *J. Constr. Steel Res.*, vol. 15, pp. 65–98, 1990.
- [17] *ANSI/AISC 360-05 An American National Standard - Specification for structural steel buildings*, Chicago, Illinois, American Institute of Steel Construction, 2005.
- [18] *Standard specifications for steel and composite structures*, JSCE Japan Society of

- Civil Engineers, Tokyo, 2009.
- [19] B. J. Daniels, D. O. Leary, and M. Crisinel, "The analysis of composite slabs with profiled sheeting using a computer based semi-empirical partial interaction approach", in *10th International Specialty Conference on Cold-Formed Steel Structures*, 1990.
 - [20] M. Fontana and R. Bärtschi, "New types of shear connectors with powder-actuated fasteners", Institute of Structural Engineering Swiss Federal Institute of Technology Zurich, Zurich, December, 2002.
 - [21] M. Fontana and H. Beck, "Novel Shear Rib connectors with powder actuated fasteners".
 - [22] R. Bärtschi, "*Schubtragfähigkeit von gelochten Blechleisten mit Hilti – Setzbolzen*", Zürich, Switzerland, ETH Eidgenössische Technische Hochschule Zürich, 1999.
 - [23] F. W. Klaiber, T. J. Wipf, J. R. Reid, and M. J. Peterson, "Investigation of Two Bridge Alternatives for Low Volume Roads", vol. 2, Iowa Department of Transportation College of Engineering Iowa State University, 1997.
 - [24] R. Bärtschi, "Load-bearing behaviour of composite beams in low degrees of partial shear connection", Swiss Federal Institute of Technology, Zurich, 2005.
 - [25] *European Technical Assessment ETA-18/0447*, Nordhavn, Denmark, ETA-Denmark A/S, 2018.
 - [26] M. Tahir, P. N. Shek, and C. S. Tan, "Push-off tests on pin-connected shear studs with composite steel – concrete beams", *Constr. Build. Mater.*, vol. 23, no. 9, pp. 3024–3033, 2009.
 - [27] *European Technical Assessment ETA-18/0355*, Nordhavn, Denmark, ETA-Denmark A/S, 2019.
 - [28] *EN 1993-1-3 Eurocode 3: Design of steel structures - Part 1-3: general rules - Supplementary rules for cold-formed members and sheeting*, Brussels, Belgium, CEN European Committee for Standardization, 2009.
 - [29] N. J. Glaser and M. D. Engelhardt, "*An overview of power driven fastening for steel connections in the US construction industry*", Ferguson Structural Engineering Laboratory, The University of Texas at Austin, 1994.
 - [30] *ISO 11148-13 Hand-held non-electric power tools - Safety requirements - Part 13: Fastener driving tools*, Geneva, ISO International Standard Organization, 2017.
 - [31] *EN 15895:2018 - Cartridge operated hand-held tools - Safety requirements - Fixing and hard marking tools*, Brussels, Belgium, BSI British Standards Institution, 2018.
 - [32] "HILTI Direct Fastening Technology Manual 2013", Hilti Aktiengesellschaft, Schaan, Fürstentum Liechtenstein, 2013.
 - [33] H. Beck, M. Engelhardt, and N. Glaser, "Static pullout strength of power actuated fasteners in steel: state-of-the-art review", *Eng. J.*, vol. Second Qua, pp. 99–110, 2003.
 - [34] *European Technical Approval ETA-08-0040*, Berlin, Germany, Deutsches Institut für Bautechnik, 2018.
 - [35] *European Technical Approval ETA-04/0101*, Berlin, Germany, Deutsches Institut

- fur Bautechnik, 2018.
- [36] F. Goldspiegel, K. Mocellin, and P. Michel, "Numerical modelling of high-speed nailing process to join dissimilar materials: Metal sheet formulation to simulate nail insertion stage", *J. Mater. Process. Technol.*, vol. 267, no. October 2018, pp. 414–433, 2019.
- [37] U. J. R. Mujagic, P. S. Green, and W. G. Gould, "Strength prediction model for power acutated fasteners connecting steel members in tension and shear-North American Applications", in *20th International Specialty Conference on Cold-Formed Steel Structures*, 2010.
- [38] *The testing of connections with mechanical fasteners in steel sheeting and sections*, ECCS - European Convention for Constructional Steelwork, Portugal, 2009.
- [39] *EN 1993-1-8 Eurocode 3: Design of Steel Structures - Part 1-8: Design of joints*, Brussels, Belgium, CEN European Committee for Standardization, 2005.
- [40] *Preliminary European recommendations for the testing and design of fastenings for sandwich panels*, Portugal, ECCS - European Convention for Constructional Steelwork / CIB International Council for Research and Innovation in Building and Construction Joint Committee, 2009.
- [41] *AISI S905-08 w/SI-11 AISI Standard - AISI S905- Test methods for mechanically fastened cold-formed steel connections*, Washington, D.C, American Iron and Steel Institute, 2012.
- [42] *AISI S100-16 - North American specification for the design of cold-formed steel structural members*, AISI American Iron and Steel Institute, 2016.
- [43] *E 1190-95 Standard test methods for strength of power-actuated fasteners installed in structural members*, Reapproved 2000, West Conshohocken, ASTM International, 2004.
- [44] H. Beck and M. D. Engelhardt, "Net section efficiency of steel coupons with power actuated fasteners", *J. Struct. Eng.*, pp. 12–21, 2002.
- [45] N. Gluhović, Z. Marković, M. Spremić, and M. Pavlović, "Experimental investigation and specific behaviour of X-HVB shear connectors in prefabricated composite decks", in *Ce/Papers EUROSTEEL 2017*, 2017, vol. 1, no. 2–3, pp. 2080–2089.
- [46] S. Samardžić, Uperedna analiza nosivosti različitih sredstava za sprezanje sa primerom primene na spregnutoj međuspratnoj konstrukciji stambeno-poslovnog objekta, Master rad, u pripremi, Univerzitet u Beogradu, Građevinski fakultet, 2019.
- [47] *EN 1990:2002+A1:2005 Eurocode — Basis of structural design*, CEN European Committee for Standardization, Brussels, Belgium, 2010.
- [48] *EN 10002-1 Metallic materials - Tensile testing - Part 1: Method of test at ambient temperature*, CEN European Committee for Standardization, Brussels, Belgium, 2001.
- [49] I. Arrayago, E. Real, and L. Gardner, "Description of stress–strain curves for stainless steel alloys", *Mater. Des.*, vol. 87, pp. 540–552, 2015.
- [50] *EN 1992-1-1 Eurocode 2: Design of Concrete Structures - Part 1-1: general rules and rules for buildings*, Brussels, Belgium, CEN European Committee for Standardization, 2004.

- [51] M. Pavlović, Z. Marković, M. Veljković, and D. Buđevac, "Bolted shear connectors vs. headed studs behaviour in push-out tests", *J. Constr. Steel Res.*, vol. 88, pp. 134–149, 2013.
- [52] M. Spremic, Z. Markovic, M. Veljkovic, and D. Budjevac, "Push-out experiments of headed shear studs in group arrangements", *Advanced Steel Construction*, vol. 9, no. 2. pp. 139–160, 2013.
- [53] D. J. Oehlers and M. A. Bradford, "Elementary behaviour of composite steel and concrete structural members". Oxford, Butterworth Heinemann, 1999.
- [54] ABAQUS User Manual, DS SIMULIA Corp, Providence, RI, USA, 2009.
- [55] *EN 1993-1-5 Eurocode 3: Design of steel structures - Part 1-5: Plated structural elements*, CEN European Committee for Standardization, 2009.
- [56] X. Yun and L. Gardner, "Stress-strain curves for hot-rolled steels", *J. Constr. Steel Res.*, vol. 133, pp. 36–46, 2017.
- [57] *GB50010-2002 - Code for Design of Concrete Structures*, Ministry of housing and urban–rural development of China, 2002.
- [58] D. Carreira and K.-H. Chu, "Stress-Strain Relationship for Plain Concrete in Compression", *ACI J.*, November-December, pp. 797–804, 1985.
- [59] N. Gluhović, M. Spremić, B. Milosavljević, Z. Marković, and J. Dobrić, "Ductility of different types of shear connectors - Experimental and Numerical Analysis", in *The International Colloquium on Stability and Ductility of Steel Structures*, 2019.

Annex A – Concrete material properties

From every batch of concrete, sets of four 15.0 cm cubes (16 cubes in total) and three cylinders D15x30 cm (12 cylinders in total) were made. Also, from every batch of concrete two cubes were cured in the same conditions as the slabs (FP) and two cubes in the water (FV). Also, eight cylinders were cured in water (CV) and four cylinders in the same conditions as the slabs (CP). Results of standard experiments of concrete used for prefabricated slabs (cube and cylinder compressive strength and elastic modulus) are shown in Table A.1.

Table A.1. Concrete material properties for prefabricated concrete slabs

Cubes series	Compressive strength (cube)	Cylinder series	Compressive strength (cylinder)	Modulus of elasticity
	$f_{c,cube}(t)$ [MPa]		$f_{c,cyl}(t)$ [MPa]	$E_{cm}(t)$ [GPa]
FV 1a	38.22	CV-2a	30.56	-
FV 1b	34.67	CV-2b	33.95	28.29
FV 2a	36.44	CV-2c	31.86	-
FV 2b	28.44	CV-3a	30.11	-
FV 3a	28.89	CV-3b	29.03	27.29
FV 3b	31.11	CV-4a	31.52	32.07
FV 4a	36.00	CV-4b	31.18	28.93
FV 4b	31.11	CV-4c	31.92	25.48
Mean	33.11	Mean	31.27	28.41
FP 1a	33.78	CP-3c	29.03	-
FP 1b	32.44	CP-1a	31.97	30.30
FP 2a	33.33	CP-1b	29.99	30.30
FP 2b	32.89	CP-1c	30.67	27.49
FP 3a	28.44			
FP 3b	30.22			
FP 4a	34.22			
FP 4b	34.22			
Mean	32.44	Mean	30.42	29.36

Two batches of concrete were made for concreting of the openings of one side, for the phase 1 push-out tests (eight push-out specimens of phase 1). From every mixture of infill concrete, sets of one 15.0 cm cube for compressive strength testing, one cylinder D15x15 cm for splitting tensile strength testing and one cylinder D15x30 cm for elastic modulus examination were made (three specimens of each mixture).

One batch of concrete was made for concreting of the openings of one side, for the phase 2 and phase 3 of push-out tests. From every mixture of infill concrete, sets of two

cylinders D15x15 cm and two cylinders D15x30 cm were made (four specimens of each mixture). Results of the standard test specimens for infill concrete are presented in Table A.2, Table A. 3 and Table A.4.

Table A.2. *Infill concrete material properties of phase 1 push-out tests*

Series	Compressive strength (cube)	Compressive strength (cylinder)	Splitting tensile strength	Axial tensile strength	Modulus of elasticity
	$f_{c,cube}(t)$ [MPa]	$f_{c,cyl}(t)$ [MPa]	$f_{ct,sp}(t)$ [MPa]	$f_{ct}(t)$ [MPa]	$E_{cm}(t)$ [GPa]
B1-1a	44.67	27.84	2.72	2.44	27.38
B1-1b	33.64	28.75	3.08	2.78	-
B1-2a	37.56	30.27	2.52	2.27	27.16
B1-2b	39.60	27.16	2.80	2.52	28.29
Mean	38.87	28.51	2.78	2.50	27.61

Table A. 3. *Infill concrete material properties of phase 2 push-out tests.*

Series	Compressive strength (cylinder)	Splitting tensile strength	Axial tensile strength	Modulus of elasticity
	$f_{c,cyl}(t)$ [MPa]	$f_{ct,sp}(t)$ [MPa]	$f_{ct}(t)$ [MPa]	$E_{cm}(t)$ [GPa]
B2-1a	37.52	2.55	2.29	30.30
B2-1b	32.82	3.40	3.06	-
B2-2a	32.26	2.83	2.55	35.96
B2-2b	32.14	3.11	2.80	32.89
Mean	33.68	2.97	2.67	33.05

Table A.4. *Infill concrete material properties of phase 3 push-out tests*

Series	Compressive strength (cylinder)	Splitting tensile strength	Axial tensile strength	Modulus of elasticity
	$f_{c,cyl}(t)$ [MPa]	$f_{ct,sp}(t)$ [MPa]	$f_{ct}(t)$ [MPa]	$E_{cm}(t)$ [GPa]
B3-1a	32.31	2.90	2.61	36.30
B3-1b	35.48	3.20	2.88	32.07
B3-2a	38.42	3.30	2.97	37.36
B3-2b	42.38	3.40	3.06	35.63
Mean	37.15	3.20	2.88	35.34

Material properties of prefabricated concrete slabs and infill concrete of three push-out test phases at 28 days, calculated according Eq. 4.2 - Eq. 4.5 given in Chapter 4.3.2 are given in Table A.5, Table A.6, Table A.7, Table A.8 and Table A.9, respectively.

Table A.5. Prefabricated concrete slabs strength at 28 days

Cubes series	Age at testing	Aging coeff.	Compressive strength (cube)	Cylinder series	Age at testing	Aging coeff.	Compressive strength (cylinder)
	t (days)	β_{cc}	$f_{cm,cube}$ [MPa]		t (days)	β_{cc}	f_{cm} [MPa]
FV 1a	29	1.0035	38.09	CV-2a	98		27.84
FV 1b			CV-2b	98	1.098	30.93	
FV 2a	28	1.0000	36.44	CV-2c	98		29.03
FV 2b			CV-3a	97	1.097	27.44	
FV 3a	27	0.9963	29.00	CV-3b	97		26.46
FV 3b			CV-4a	95		28.77	
FV 4a	25	0.9884	36.42	CV-4b	95	1.096	28.46
FV 4b			CV-4c	95		29.13	
Mean			33.21	Mean			28.51
FV 1a	29	1.0035	33.66	CP-3c	97	1.097	26.46
FV 1b			CP-1a	99		29.11	
FV 2b	28	1.0000	33.33	CP-1b	99	1.098	27.31
FV 3a			CP-1c	99		27.93	
FV 3b	27	0.9963	28.55				
FV 4a				30.33			
FV 4b	25	0.9884	34.62				
FV 1a				34.62			
Mean			32.54	Mean			27.70

Table A.6. Infill concrete strength of phase 1 at 28 days

Series	Age at testing	Aging coeff.	Compressive strength (cube)	Compressive strength (cylinder)	Axial tensile strength	Modulus of elasticity
	t (days)	β_{cc}	$f_{cm,cube}$ [MPa]	f_{cm} [MPa]	f_{ctm} [MPa]	E_{cm} [GPa]
B1-1a	26	0.9925	45.01	28.05	2.46	27.44
B1-1b	26		33.90	28.96	2.80	-
B1-2a	23	0.9795	38.34	30.91	2.31	27.33
B1-2b	23		40.43	27.73	2.57	28.47
Mean			39.42	28.91	2.54	27.75

Table A.7. Infill concrete strength of phase 2 at 28 days

Series	Age at testing	Aging coeff.	Compressive strength (cylinder)	Axial tensile strength	Modulus of elasticity
	t (days)	β_{cc}	f_{cm} [MPa]	f_{ctm} [MPa]	E_{cm} [GPa]
B2-1a	35	1.0213	36.73	2.26	30.11
B2-1b	35		32.14	3.01	-
B2-2a	32	1.0310	31.84	2.52	35.82
B2-2b	32		31.73	2.77	32.76
Mean			33.11	2.64	32.90

Table A.8. *Infill concrete strength of phase 3 at 28 days*

Series	Age at testing	Aging coeff.	Compressive strength (cylinder)	Axial tensile strength	Modulus of elasticity
	t (days)	β_{cc}	f_{cm} [MPa]	f_{ctm} [MPa]	E_{cm} [GPa]
B3-1a	62	1.0678	30.26	2.50	35.59
B3-1b	62		33.23	2.76	31.44
B3-2a	59	1.0642	36.11	2.85	36.67
B3-2b	59		39.83	2.94	34.97
Mean			34.86	2.76	34.67

Table A.9. *Modulus of elasticity of prefabricated concrete slabs at 28 days*

Cylinder series	Age at testing	Aging coeff.	Modulus of elasticity
	t (days)	β_{cc}	E_{cm} [GPa]
CV-2a	98		-
CV-2b	98	1.098	27.51
CV-2c	98		-
CV-3a	97	1.097	-
CV-3b	97		26.54
CV-4a	95		31.20
CV-4b	95	1.096	28.15
CV-4c	95		24.79
Mean			27.64
CP-3c	97	1.097	29.46
CP-1a	99		29.46
CP-1b	99	1.098	27.49
CP-1c	99		-
Mean			28.55

Annex B – Installation requirements

Comparison of failure loading of HSFg1-2 and HSFg5-2 specimens with average force-slip curve of HSFg-2 test series is presented in Figure B.1. Inappropriate installation of X-ENP-21 HVB cartridge fired pins and installation mistakes obtained during concreting of envisaged openings of concrete slabs, resulted in 18 % to 29 % lower ultimate shear resistance of HSFg1-2 and HSFg5-2 specimens, respectively. Moreover, different behaviour of shear connectors is noticed through comparison of initial and stiffness corresponding to SLS, as shown in Figure B.1b. Experimental results of these two specimens were not included in statistical evaluation of results of HSFg-2 series, as previously explained.

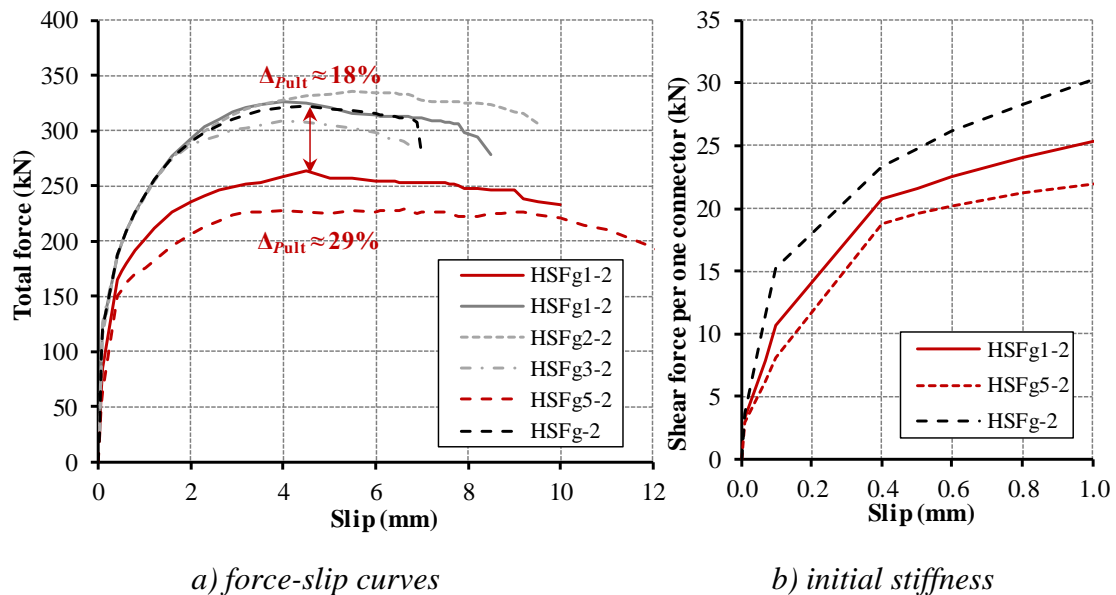
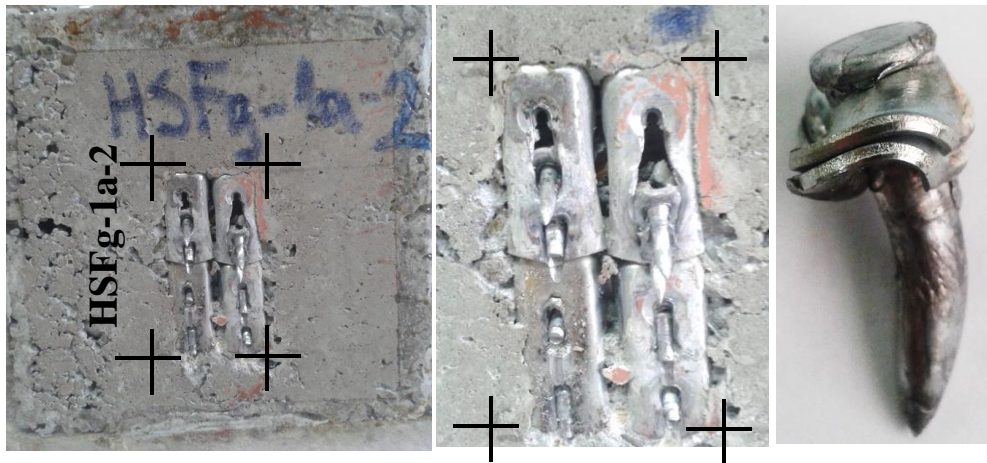


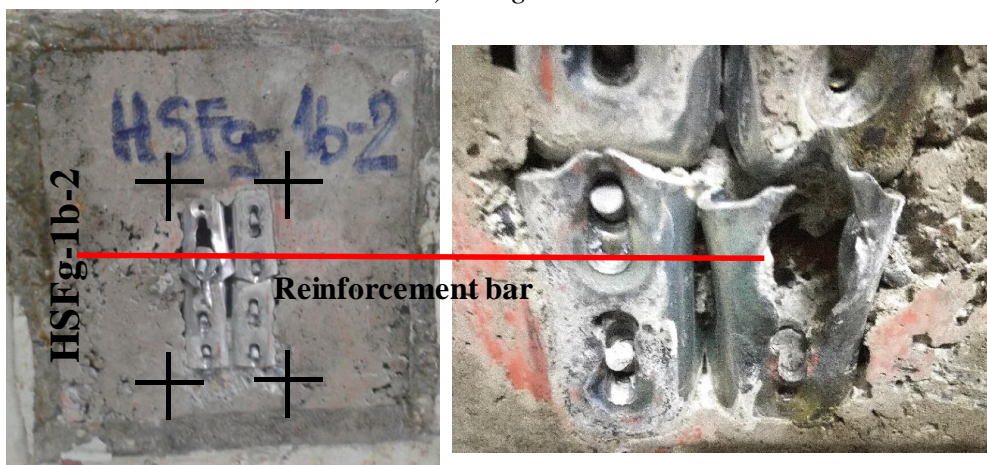
Figure B.1. Shear resistance reduction due to inappropriate installation

Through the installation of second cartridge fired pin at the first row connector of the HSFg1-2 specimen *a* side (sensors V1, V3 and H1, see Figure 4.13) installation mistake occurred. During the positioning of the fastening tool, fastener guide was not turned into the position for installation of the second pin, according to operating instructions [15]. Installation of the second pin was attempted above already installed first pin, which resulted in significant deformation and inappropriate installation of first pin, as shown in Figure B.2a. Moreover, throughout installation of the cartridge fired pins at *b* side of the specimen (sensors V2, V4 and H2, Figure 5) two pins at two different connectors and one pin at *a* side of specimen, were not installed in holes that are provided for that at connector fastening leg, which is shown in Figure B.2. Moreover, porous

structure of infill concrete close to the horizontal reinforcement bar was noticed in Figure B.2b. Position of reinforcement bar is highlighted with red line in Figure B.2b and outwardly visible after testing procedure. Beside the aforementioned installation mistakes of pins, poor quality of infill concrete at the surrounding zone of the reinforcement bar resulted in insufficient bearing resistance of the concrete and bearing failure of connector anchorage leg prior to pull-out failure of fasteners.



a) HSFg1a-2



b) HSFg1b-2

Figure B.2. Installation mistakes - HSFg1-2 specimen

Inappropriate quality of the infill concrete was also noticed for HSFg5-2 test specimen, as presented in Figure B.3. Although, cartridge fired pins were installed properly, reduced bearing resistance of infill concrete beyond the fastener head resulted in different failure mechanism. Shear transfer from steel beam to concrete slab is obtained through local bearing of connector anchorage leg. Hole elongation was noticed for shear

connectors on both specimen slabs. Therefore, failure of pin anchorage mechanism was not obtained prior the bearing failure of connector and deformation of pins.



Figure B.3. Installation mistakes - HSFg5-2 specimen

Experimentally gained ultimate shear resistance for HSFg1-2 and HSFg5-2 specimens is compared with analytical expressions for bearing resistance of cover material due to cartridge fired pins loaded in shear. Design resistance of cartridge fired pins is defined in various standards, as explained in Chapter 2.3.6. Bearing resistance of cartridge fired pins loaded in shear is defined in EN 1993-1-3:2009 [28] (Eq. B.1), AISI S100-16 [42] and SIA 161/1990 [22] (Eq. B.2). Analytical expressions for characteristic bearing resistance defined in AISI S100-16 [42] and EN 1993-1-3:2009 [28] are identical, as explained in more details in Chapter 2.3.6.

For analysis of bearing resistance, further geometric properties are adopted: thickness of shear connector $t = 2.0$ mm; diameter of cartridge fired pin $d = 4.5$ mm; end distance from the centre of the fastener to the adjacent end of the connector $e_1 = 12.0$ mm and $e_1 / d = 2.67$. Material properties of shear connector, as material which is in contact with pin washer, are adopted as mean value of experimentally obtained data for yield and ultimate strength, $f_{02} = 232$ MPa and $f_u = 295$ MPa (see Table 4.3). Also, EN 1993-1-3:2009 [28] defines range of validity of analytical expressions for cartridge fired pin resistance, considering ratio of fastener end distance and diameter, $e_1 / d \geq 4.5$, which is not accomplished for analysed push-out specimens. Also, bearing resistance is presented by several authors; Dubas (Eq. B.3), modified Dubas expression (Eq. B.4) and Beck (B.5) [22]. The range of application of presented equations (Eq. B.2 – Eq. B.5), relative to edge distance of cartridge fired pins and pin's diameter, e_1 / d , is: $1.4 \leq e_1 / d \leq 3.0$ (Eq. B.2);

$e_1 / d \leq 3.0$ (Eq. B.3); $e_1 / d \geq 2.45$ (Eq. B.4) and are accomplished for X-HVB 110 shear connector.

$$F_{b,Rk} = 3.2 \cdot f_u \cdot d \cdot t \quad (\text{B.1})$$

$$L_R = 0.8 \cdot \frac{e_1}{d} \cdot f_u \cdot d \cdot t \quad (\text{B.2})$$

$$L_R = 1.12 \cdot \frac{e_1}{d} \cdot f_u \cdot d \cdot t \quad (\text{B.3})$$

$$L_R = 2.743 \cdot f_u \cdot d \cdot t \cdot k \quad (\text{B.4})$$

$$V_{ENP,Press} = n \cdot d \cdot t \cdot (6 \div 8) \cdot f_y \quad (\text{B.5})$$

In previous expressions:

f_u is the ultimate strength of shear connector material;

f_y is the yield strength of shear connector material, adopted as experimentally obtained proof stress f_{02} ;

d is the nominal diameter of cartridge fired pin shank;

t is the thickness of shear connector;

e_1 is the end distance from the centre of the fastener to the adjacent end of the connected part, in the direction of load transfer;

k is the factor depending on fastener stand-off after installation ($k = 2.23$ for range of appropriate installation [22]);

n is the number of cartridge fired pins.

Based on the observations of HSFg1-2 and HSFg5-2 specimens after the testing procedure, shown in Figure B.2 and Figure B.3, further statement is adopted: for HSFg1-2 specimen shear failure of nine pins and bearing failure of seven pins is observed; for HSFg5-2 specimen shear failure of ten pins and bearing failure of six pins is observed. Bearing resistance is determined according to Eq. B.1 - Eq. B.5 and characteristic shear failure of one cartridge fired pin with 4.5 mm diameter is adopted as 20.2 kN [22], [32].

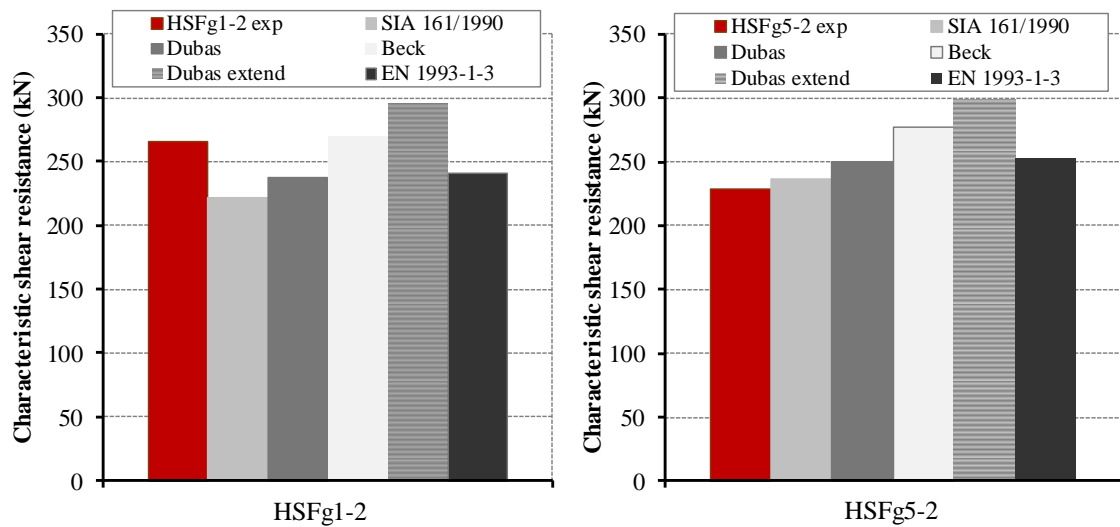


Figure B.4. Bearing resistance of cartridge fired pins

Experimentally obtained ultimate shear resistance for two analysed specimens is compared with analytically determined resistance of cartridge fired pins loaded in shear and presented in Figure B.4. For both analysed test specimens, recommendations given in EN 1993-1-3:2009 [28], SIA 161/1990 [22] and proposed by Dubas [22] represent a good prediction of ultimate shear resistance for analysed specimens.

The presented analysis emphasizes the need for visual inspection after installation of cartridge fired pins. Also, appropriate quality of the infill concrete should be provided for group arrangement of shear connectors positioned at distances smaller than minimal recommended. Poor quality of infill concrete for envisaged openings of prefabricated concrete slabs could result in bearing failure of shear connector fastening leg, prior to pull-out failure of cartridge fired pins.

Annex C – Base plate material properties of cartridge fired pins shear and tension tests

For determination of base plate material properties of shear and tension tests, sets of four round tensile coupons were examined for ST, TT2 and TT3 specimens, respectively. Tensile test coupons during the examination and prior the testing are presented in Figure C.1.



a) base plate tensile test coupons

b) tensile test

Figure C.1. Tensile test for determination of base material properties of ST, TT2 and TT3 specimens

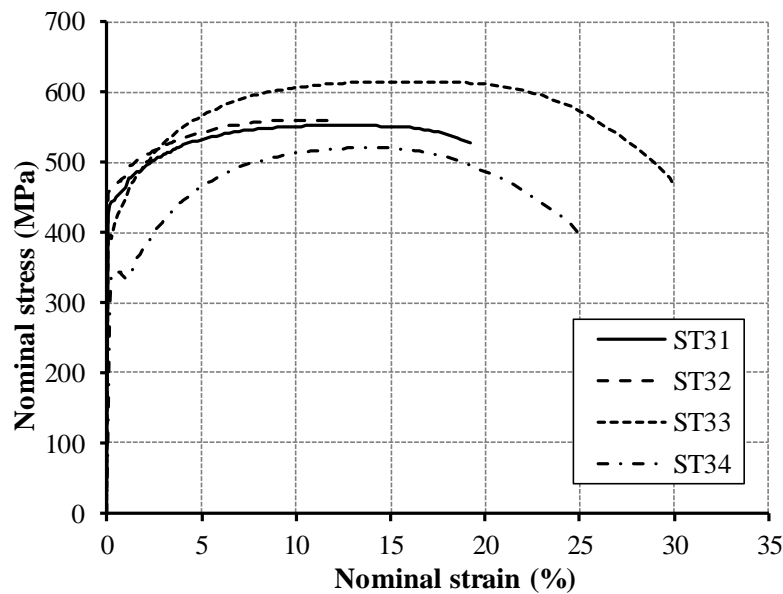


Figure C.2. Nominal stress-strain curves - ST specimens

Round tensile from base plates were built with 5.0 mm diameter and with 33.0 mm of gauge length, L_0 . Tensile tests were performed in the servo-hydraulic testing machine Shimadzu, with a capacity of 300.0 kN. The elongations were monitored using a digital

extensometer with a measuring range of 25%, as shown in Figure C.1b. Testing procedure was adopted according to recommendations given in EN 10002-1:2001 [48], and as previously explained in Chapter 4.3.1. Nominal stress-strain curves of base plate materials for shear tests of cartridge fired pins (ST specimens) and tension test with two distinct installation power levels (TT2-2, TT3-2 and TT3-3.5) are presented in Figure C.2, Figure C.3 and Figure C.4. Results of tension tests are also presented in Table C.1, Table C.2 and Table C.3, with statistical evaluation of obtained results.

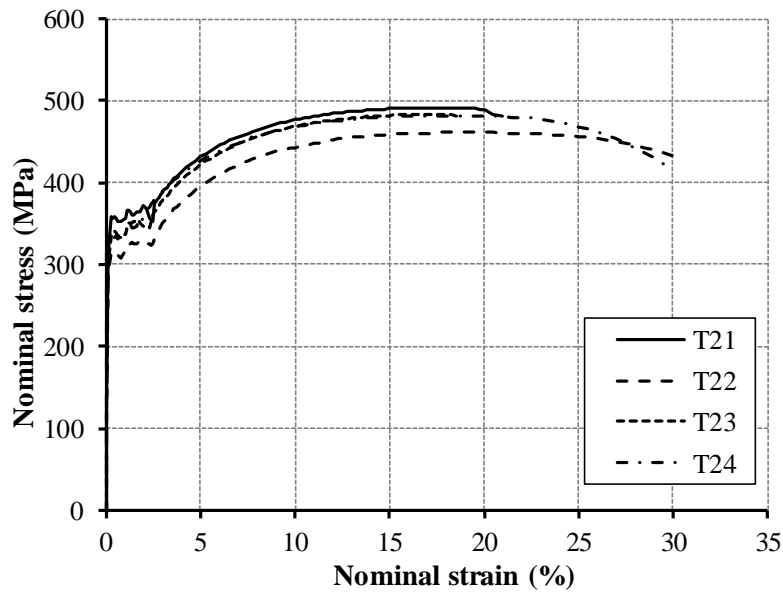


Figure C.3. Nominal stress-strain curves - TT2-2 specimens

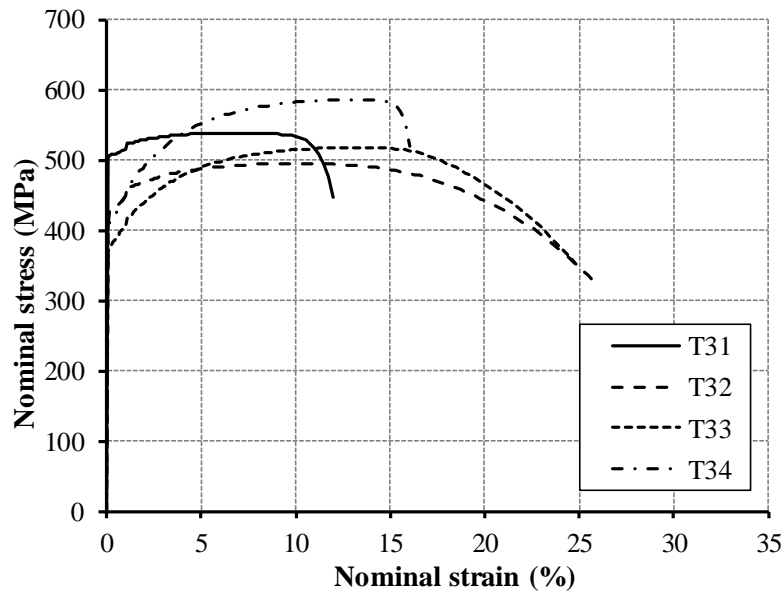


Figure C.4. Nominal stress-strain curves - TT3-2 and TT3-3.5 specimens

Table C.1. Base plate material properties - ST specimens

Specimen	Test coupon geometry		Material properties	
	diameter	cross-section area	yield strength	ultimate strength
	d (mm)	A (mm ²)	f_y (N/mm ²)	f_u (N/mm ²)
ST31	4.81	18.17	444.2	552.5
ST32	4.80	18.10	462.4	560.5
ST33	4.60	16.62	407.6	615.0
ST34	4.90	18.86	341.6	520.5
Mean			413.9	562.1
St. deviation			53.4	39.3
Variation (%)			12.8	7.0
Characteristic			273.6	458.8

Table C.2. Base plate material properties - TT2-2 specimens

Specimen	Test coupon geometry		Material properties	
	diameter	cross-section area	yield strength	ultimate strength
	d (mm)	A (mm ²)	f_y (N/mm ²)	f_u (N/mm ²)
T21	5.00	19.63	358.0	491.8
T22	5.00	19.63	316.5	461.1
T23	4.90	18.86	337.6	483.4
T24	4.90	18.86	332.5	482.0
Mean			336.1	479.6
St. deviation			17.4	13.0
Variation (%)			5.1	2.7
Characteristic			291.0	445.3

Table C.3. Base plate material properties - TT3-2 and TT3-3.5 specimens

Specimen	Test coupon geometry		Material properties	
	diameter	cross-section area	yield strength	ultimate strength
	d (mm)	A (mm ²)	f_y (N/mm ²)	f_u (N/mm ²)
T31	4.90	18.86	508.7	539.2
T32	5.00	19.63	431.0	495.1
T33	5.00	19.63	517.8	517.8
T34	4.60	16.62	415.5	586.3
Mean			468.2	534.6
St. deviation			52.5	38.9
Variation (%)			11.2	7.2
Characteristic			330.2	432.3

Based on average results of tensile tests, further statements can be adopted: material properties of base plate of ST specimens correspond to the steel grade S355, base plate of TT2 specimens correspond to the steel grade S275 and base plate of TT3 specimens correspond to the steel grade S355. All experimentally obtained average material properties have higher values than corresponding nominal values of yield strength and ultimate tensile strength of adopted steel grade, according to EN 10025-2 [8].

Annex D – Development of FE models

Influence of some of the most important parameters on the results of FE analysis, which are presented in Chapter 5, obtained during development of the complete push-out FE models, are shown in this Annex. Through development of FE models, different parameters were calibrated in order to validate results of experimental analysis. Considering described plan of experimental investigation, first FE models were developed for HSF and HSB test series.

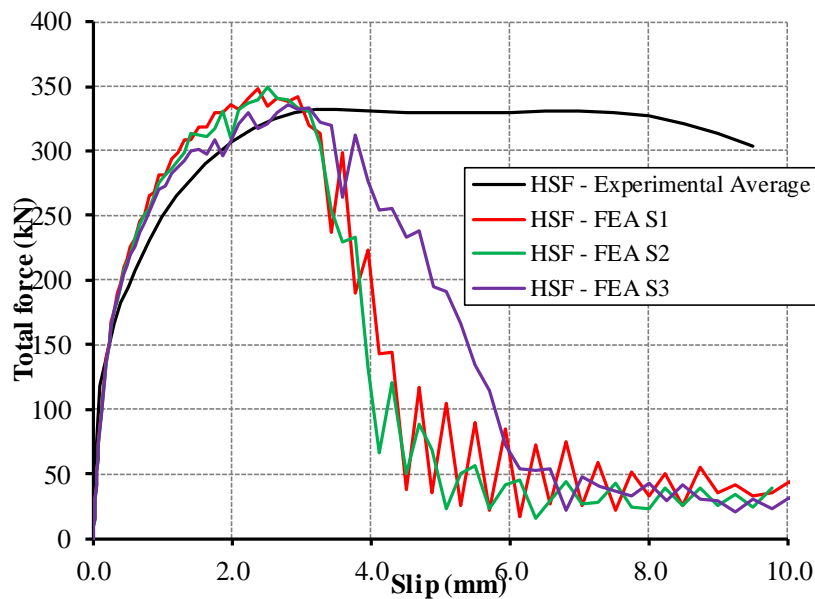


Figure D.1. FE analysis for flat geometry of connector and washer without preloading of the pins - HSF test series

Results of the FE analysis for some of the first models developed for forward orientation of shear connectors (HSF test series) are shown in Figure D.1. Shear failure of all cartridge fired pins were achieved in these FE models, which did not represent the real failure mechanism achieved during experimental investigation. Parameters that were calibrated during development of these models are shown in Table D.1. Preloading of the pins was not still introduced in these models. Flat geometry of washer and connectors in the zone of pins (see Figure 5.5a) was used in FE models which results are presented in Figure D.1. Also, material hardening in the curved regions of the shear connectors was investigated in the presented FE analysis results. Force-slip curves presented in Figure D.1 gained from FE analysis obtained significant difference in achieved slip capacity in comparison to the average curve of experimental results of HSF test series.

Table D.1. Calibration of parameters without preloading of pins in FE analysis – HSF test series

FE model	Geometry of connector and washer	Preloading of pins	Hardening of the connector material properties in the curved zones	Hardened yield strength
				f_y [MPa]
HSF – FEA S1	flat	no	yes	320
HSF – FEA S2	flat	no	yes	250
HSF – FEA S3	flat	no	no	-

Influence of different connector geometry in the zone of pin and washer on results of FE analysis is presented in Figure D.2 and Table D.2. Firstly, flat and curved geometry of connector in pin surrounding zone and washer was investigated, while cartridge fired pins and washer were modelled as unique part (see Figure 5.5). The results obtained from these FE models (HSF - FEA F and HSF - FEA C, see Figure D.2) did not accomplished good agreement with experimental results. Afterwards, cartridge fired pin and washer were modelled as separate parts in FE models (HSF - FEA S, see Figure D.2). This modelling approach resulted in satisfactory slip capacity and failure mechanism of cartridge fired pins. Pull-out failure of pins was achieved with this modelling approach. Initial stiffness and ultimate shear resistance still significantly differ from experimental results, as shown in Figure D.2.

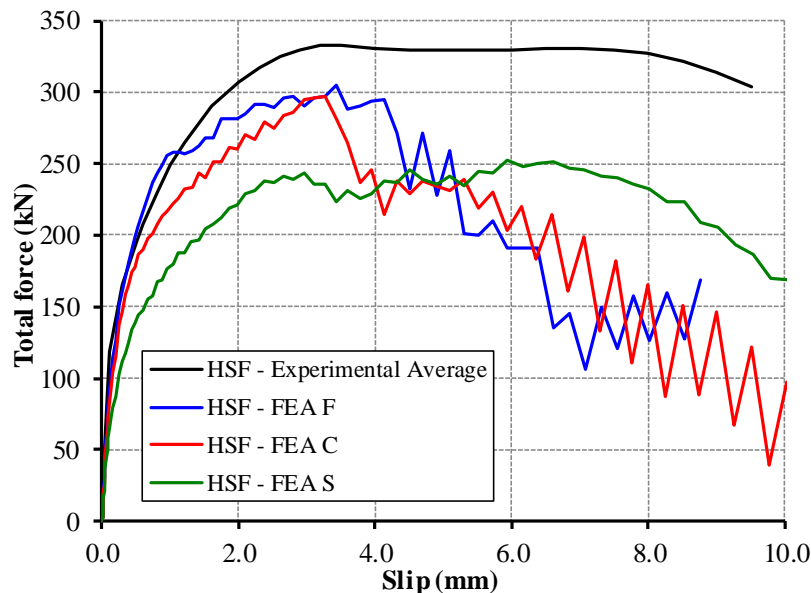


Figure D.2. FE analysis with different connector's geometry - HSF test series

Observing the results of different FE models developed during FE analysis, it was concluded that certain slip resistance is present due to contact stresses between the

connector and the steel profile. Possible improvement of load-slip behaviour, which is presented in Figure D.3, resulted in satisfactory agreement with experimental results of HSF test series. Additional slip resistance, which should be introduced in FE models, amounted approximately 80.0 kN per whole test specimen, or 5.0 kN per one cartridge fired pin. Therefore, introduction of the preloading force in the cartridge fired pins was the next step in FE analysis, which indicatively could improve the initial stiffness and ultimate shear resistance, as shown in Figure D.3.

Table D.2. Calibration of different connector and washer geometry in FE analysis - HSF test series

FE model	Geometry of connector and washer	Preloading of pins	Hardening of the connector material properties in the curved zones
HSF – FEA F	flat	no	no
HSF – FEA C	curved	no	yes
HSF – FEA S	separated	no	yes

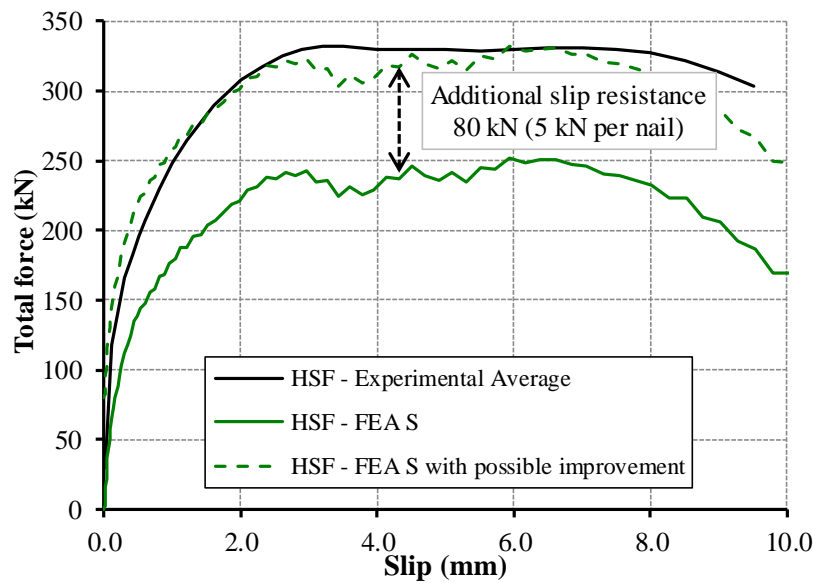


Figure D.3. Possible improvement of the load-slip behaviour by introducing initial slip resistance

First modelling approach which is developed in order to introduce preloading force in cartridge fired pins and necessary slip resistance for the complete push-out models considered extension of the pins during the preloading step. Extension of the pins was achieved using two additional parts of the FE model, holder and mover (fixed and

movable plate), as shown in Figure D.4. Preloading force was applied to the cartridge fired pins through their extension.

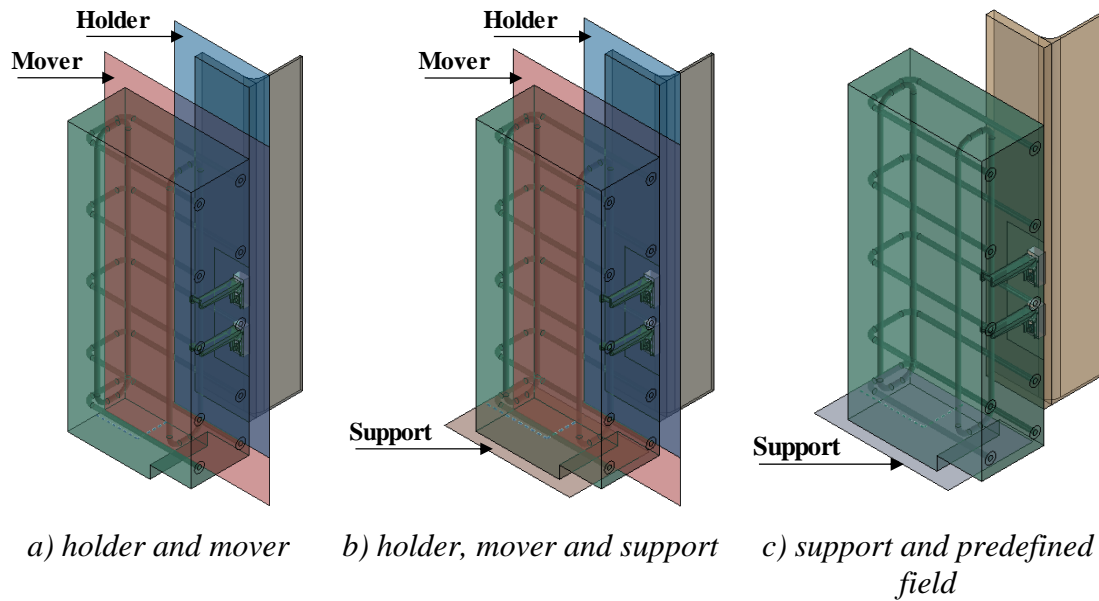


Figure D.4. Different modelling approaches of pins preloading in FE analysis – HSF test series

Concrete slab and steel profile were modelled with certain initial overlapping which represented the value which movable part of the FE model crossed during the preloading step, as shown in Figure D.5a. Extension of the pins during the preloading step and thus introduced stresses are shown in Figure D.5b.

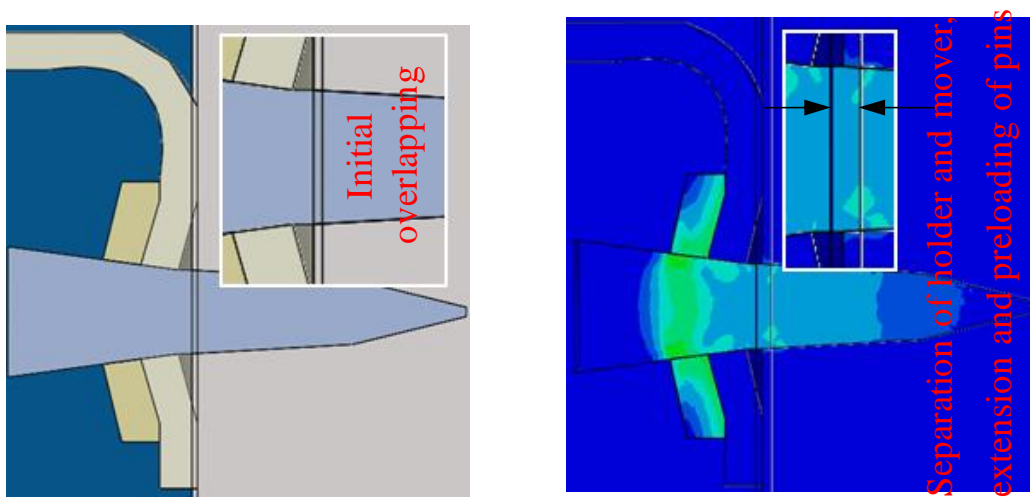


Figure D.5. Preloading of cartridge fired pins through their extension

Additional parts of the complete push-out FE model, introduced in order to implement preloading force in the pins (holder and mover), were excluded from the FE model during failure loading. This preloading method for pins resulted in very complex FE model with complicated interaction properties between different parts. Complexity of the model is enlarged using the parts which need to be excluded during further analysis (failure loading).

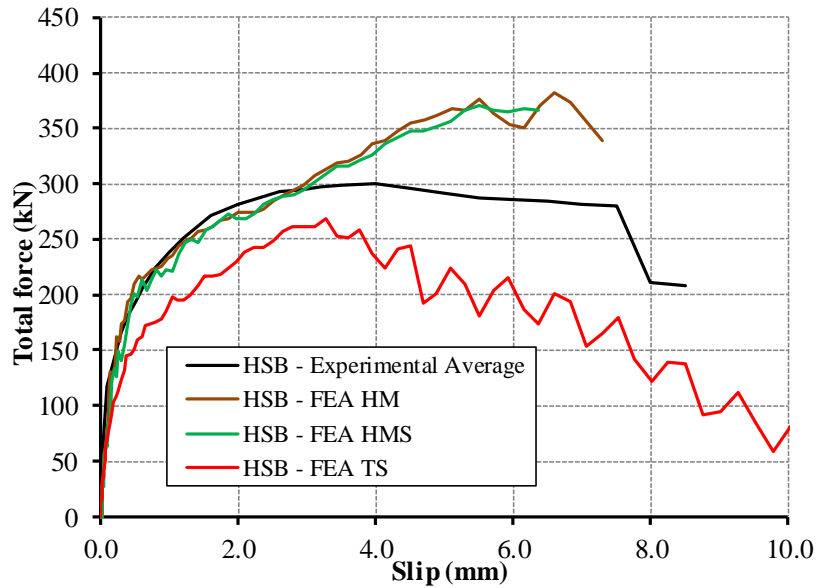


Figure D.6. Force-slip curves with different methods for introduction of pin preloading force - HSB test series

Force-slip curves which are the result of FE models of HSB test series, obtained from different approaches of pins preloading are given in Figure D.6. Analysed parameters are presented in Table D.3. Preloading of pins through their extension did not obtain satisfactory agreement with experimental results of HSF and HSB test series.

Table D.3. FE models for different approaches of pins' preloading - HSB test series

FE model	Support	Holder and Mover	Preloading of the pins
HSB – FEA HM	no	yes	extension
HSB – FEA HMS	yes	yes	extension
HSB – FEA TS	yes	no	temperature – predefined field

Second approach for pins preloading was similar to the adopted one presented in Chapter 5. Preloading of cartridge fired pins was conducted by application of strains to the part of the pin which is above the base material (HSB - FEA TS, see Figure D.6). Anisotropic expansion material properties were defined for the pin material ($\alpha_{11} = 0$, α_{22}

= 0, $\alpha_{33} = 1$) and strains are engaged by using predefined temperature fields. The magnitude of the temperature was adopted as constant value through part of the pin which was used for implementation of strains.

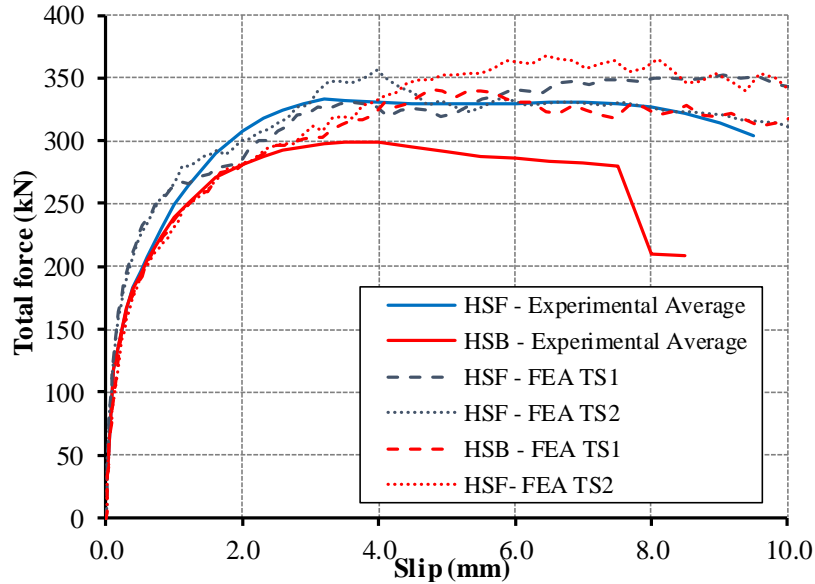


Figure D.7. FE analysis - preloading of pins through implementation of strains in upper part of the pin - HSF and HSB test series

Results of FE analysis for previously explained modelling approach for pins preloading forces implementation for HSF and HSB test series are shown in Figure D.7. Same parameters were adopted for both analysed test series. Parameters that were analysed are presented in Table D.4.

Table D.4. Calibration of parameters for preloading of upper part of the pin - HSF and HSB series

FE model	Predefined field magnitude	Global friction coefficient	Interaction properties for contact between pins and base material	
			Friction coefficient	Damage
HSF – FEA TS1	-0.06	0.4	0.5	235/150/150
HSB – FEA TS1	-0.06	0.4	0.5	235/150/150
HSF – FEA TS2	-0.06	0.4	0.3	235/90/90
HSB – FEA TS2	-0.06	0.4	0.3	235/90/90

Although, preloading of pins through application of strains resulted in behaviour which is close to those experimentally obtained, it included calibration of six different parameters, as shown in Table D.4. Calibration of those parameters through extensive FE

analysis did not result in distinct behaviour of push-out FE models for two different orientation of shear connectors, as shown in Figure D.7.

Finally adopted modelling approach for preloading of cartridge fired pins which gave satisfactory results in FE analysis for both orientation of shear connectors is explained in Chapter 5 and also used for FE analysis of complete push-out models for reduced distances of shear connectors (HSFg and HSFg-2 test series).

Annex E – Influence of different parameters on FE analysis results of push-out tests

Behaviour of push-out FE models is determined with several parameters which can be classified in three groups. First group represent geometric and material parameters which were determined through tests, such as material properties of steel profile, concrete slab, shear connector and cartridge fired pin and were used for development of FE models, as presented in Chapter 5.

Beside, several parameters which were not obtained from experimental investigation were adopted though calibration of FE analysis results with results of experimental investigation. Therefore, stiffness of lateral restraint of concrete slab k_{u3} , parameter K which represent ratio of the second stress invariant on the tensile meridian to the compressive meridian of concrete material model, definition of descending part of concrete compressive stress-strain curve and friction coefficient (global and friction on the contact of embedded part of cartridge fired pin and steel base material) are classified as second group of parameters. The influence of these parameters are presented herein. Concrete compressive stress-strain curve was analysed through sinusoidal definition proposed by Pavlović et al. [51] and though descending part of concrete compressive curve given in GB50010:2002 [57]. Analysed values of these parameters and adopted one are presented in Table E.1.

Third group of influence parameters are those which are used to describe installation procedure of cartridge fired pins in FE analysis. Those parameters are of particular importance considering that development of installation procedure had the most important influence on behaviour of push-out FE models, as presented in Annex D.

Table E.1. Influence of different parameters on push-out FE analysis results

FE model	Analysed parameter	K	k_{u3}	μ	μ_e	compressive curve
		(-)	(N/mm)	(-)	(-)	(-)
M0	adopted values	0.57	60000	0.40	0.30	sinusoidal
M1	parameter K	0.60	60000	0.40	0.30	sinusoidal
M2	lateral restraint k_{u3}	0.57	20000	0.40	0.30	sinusoidal
M3	global friction coefficient μ	0.57	60000	0.20	0.30	sinusoidal
M4	embedded friction coefficient μ_e	0.57	60000	0.40	0.20	sinusoidal
M5	concrete compressive curve	0.57	60000	0.40	0.30	GB50100

All parameters were calibrated in order to match experimental results of four groups of experimental push-out tests. The influence of parameters from the second group are presented herein, for two orientations of shear connectors relative to the shear force direction (HSF and HSB test series). Considering different failure mechanisms which were obtained for these two test series, calibration of same parameters in order to achieve results of experiment were of major importance.

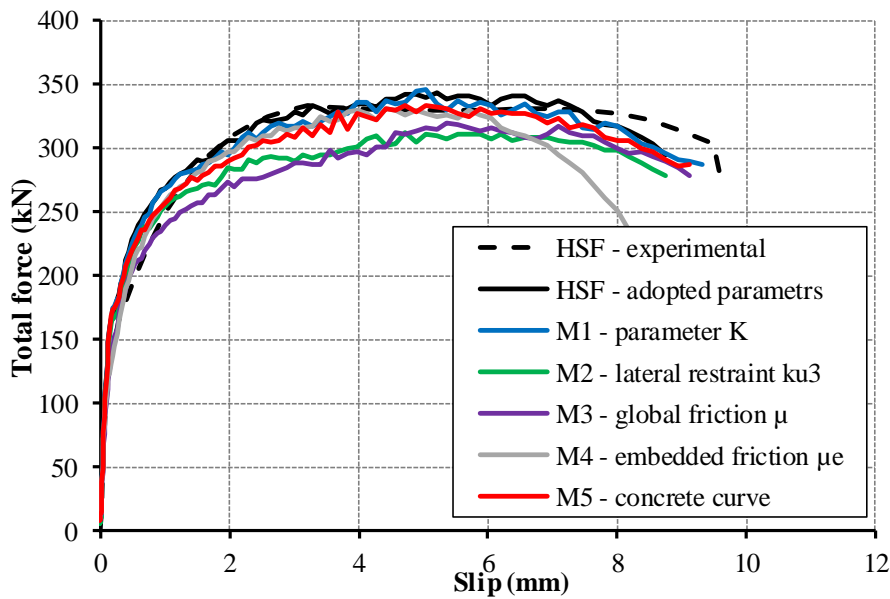


Figure E.1. Analysed parameters for HSF test series

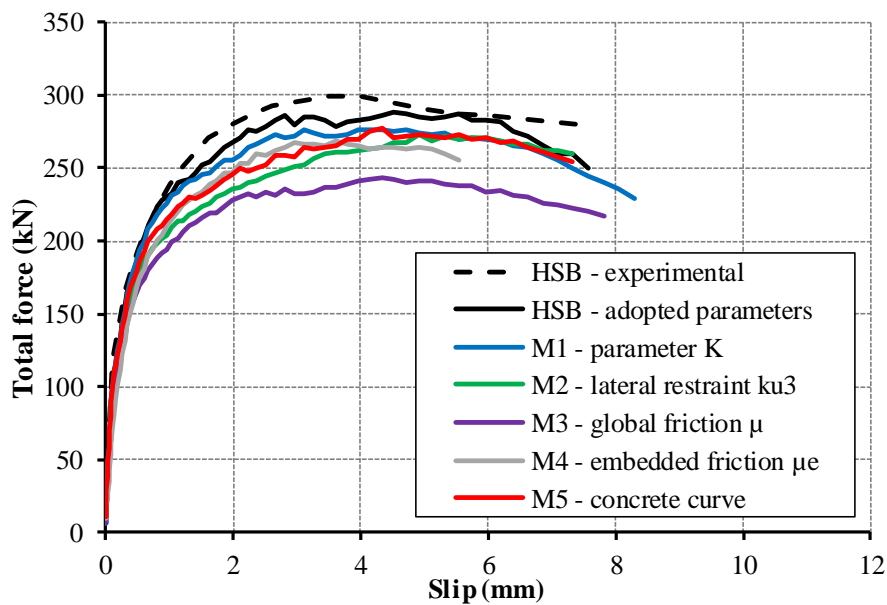


Figure E.2. Analysed parameters for HSB test series

Results of presented parametric analysis for two push-out test series are given in Figure E.1 and Figure E.2. For forward orientation of shear connectors (HSF test series) influence of the most parameters is negligible, as shown in Figure E.1. The largest influence on ultimate shear resistance is obtained for lower value of stiffness of lateral restraint k_{u3} and global friction coefficient μ . Also, lowering of friction coefficient μ_e for contact surface of cartridge fired pin embedded part and steel base material had a significant influence only for lowering of characteristic value of slip capacity, as shown in Figure E.1.

Beside, for backward orientation of shear connectors (HSB test series), significant influence on ultimate shear resistance is obtained for the most of the analysed parameters, as shown in Figure E.2. The smallest influence is obtained for variation of concrete parameter K . Considering obtained failure mechanism of HSB test series from experimental push-out tests, this test series is more sensitive for variation of analysed parameters. Therefore, calibration of adopted parameters of FE analysis was mostly governed by experimental results of HSB test series. Lowering of lateral restraint stiffness k_{u3} and friction coefficient μ_e for contact surface of cartridge fired pin resulted in significant lowering of initial stiffness. Lower value of global friction coefficient and definition of descending part of concrete compressive curve according to GB50100 resulted in significantly different global behaviour of push-out FE models, as shown in Figure E.2. Push-out force-slip curves for adopted values of analysed parameters which - closely describe behaviour of test specimens of two experimental test series and average experimental curves are also given in Figure E.1 and Figure E.2.

Curriculum vitae



Nina Gluhović was born on 20 September in 1989 in Rogatica, Bosnia and Hercegovina where she completed her preliminary and high school. She enrolled Faculty of Civil Engineering, University of Belgrade in 2008. After completing the undergraduate studies in 2012, she enrolled master studies. She graduated on the Faculty of Civil Engineering, University of Belgrade in 2013 in the field of steel structures. Since 2013 she is working as teaching assistant on the Faculty of Civil Engineering, University of Belgrade where she participates in preparation and the implementation of classes on undergraduate and master studies in the field of steel structures. She is supervising of graduate and master thesis.

Her master thesis was awarded in 2013 by the Foundation of prof. Branko Zarić for the best master thesis in the field of steel structures. In May 2015 she participated in the 1st Training School - Advances in Wind Energy Technology, organized by Department of Construction & Property Management University of Malta, through COST Action TU1304 – WINERCOST, Wind Energy Reconsideration to Enhance the concept of Smart Cities. She is participating in the project TR-36048, founded by the Serbian Ministry of Education, Science and Technological Development. She has authored and co-authored over twenty scientific papers published in the international and national journals and conferences at home and abroad.

She owns a Designer state license for structural engineering and she had performed design of different kind of steel structures according to the Eurocode, most of which are industry and commercial facilities.

Nina Gluhović is fluent in written and spoken English and has a basic level of Russian.

Биографија аутора



Нина Глуховић је рођена 20.09.1989. године у Рогатици, Босна и Херцеговина, где је завршила основну школу и гимназију. Грађевински факултет Универзитета у Београду, студијски програм грађевинарство, уписала је 2008. године. По завршетку основних студија, 2012. године, је уписала мастер студије на Одсеку за конструкције. Мастер студије завршила је 2013. године, када уписује докторске студије на Грађевинском факултету Универзитета у Београду. Од школске 2013/2014 године запослена је као асистент – студент докторских студија на Грађевинском факултету Унвиерзитета у Београду где је учествовала у припреми и извођењу наставе на предметима на основним и мастер студијама из области металних конструкција. Активно је учествовала у изради дипломских и мастер радова студената завршних година.

Добитник је награде из Фонда проф. Бранка Зарића за најбољи мастер рад из области Металних конструкција у школској 2012/2013. години. У мају 2015. године учествовала је у радионици 1st Training School - Advances in Wind Energy Technology, Department of Construction & Property Management University of Malta, May, 26th to 31th, 2015, COST Action TU1304 – WINERCOST, Wind Energy Reconsideration to Enhance the concept of Smart Cities, у организацији COST Action TU1304 и Универзитета на Малти. Као истраживач учествује у научном пројекту Министарства науке, просвете и технолошког развоја Републике Србије, евиденциони број пројекта TR-36048. Аутор је и коаутор преко двадесет научних радова који су објављени у међународним и националним часописима и зборницима са научно-стручних скупова у земљи и иностранству.

Поседује лиценцу за пројектовање објеката високоградње и у досадашњој каријери учествовала је изради пројеката за индустријске и трговинско-пословне објекте. Нина Глуховић течно говори и пише енглески језик и поседује основни ниво знања руског језика.

Изјава о ауторству

Име и презиме аутора: Нина Глуховић

Број индекса: 906/13

Изјављујем

да је докторска дисертација под насловом

BEHAVIOUR OF SHEAR CONNECTIONS REALISED BY CONNECTORS
FASTENED WITH CARTRIDGE FIRED PINS

Наслов на српском језику:

ПОНАШАЊЕ СМИЧУЋИХ СПОЈЕВА ИЗВЕДЕНИХ МОЖДАНИЦИМА СА
ЕКСЕРИМА СА ЕКСПЛОЗИВНИМ УПУЦАВАЊЕМ

- резултат сопственог истраживачког рада;
- да дисертација у целини ни у деловима није била предложена за стицање друге дипломе према студијским програмима других високошколских установа;
- да су резултати коректно наведени и
- да нисам кршио/ла ауторска права и користио/ла интелектуалну својину других лица.

Потпис аутора



У Београду, октобар, 2013

Изјава о истоветности штампане и електронске верзије докторског рада

Име и презиме аутора: Нина Глуховић

Број индекса: 906/13

Студијски програм: Грађевинарство

Наслов рада: BEHAVIOUR OF SHEAR CONNECTIONS REALISED BY
CONNECTORS FASTENED WITH CARTRIDGE FIRED PINS

Наслов на српском језику: ПОНАШАЊЕ СМИЧУЋИХ СПОЈЕВА ИЗВЕДЕНИХ
МОЖДАНИЦИМА СА ЕКСЕРИМА СА ЕКСПЛОЗИВНИМ УПУЦАВАЊЕМ

Ментор: Проф. др Златко Марковић

Изјављујем да је штампана верзија мог докторског рада истоветна електронској верзији коју сам предао/ла ради похрањена у **Дигиталном репозиторијуму Универзитета у Београду**.

Дозвољавам да се објаве моји лични подаци везани за добијање академског назива доктора наука, као што су име и презиме, година и место рођења и датум одбране рада.

Ови лични подаци могу се објавити на мрежним страницама дигиталне библиотеке, у електронском каталогу и у публикацијама Универзитета у Београду.

Потпис аутора



У Београду, октобар, 2013

Изјава о коришћењу

Овлашћујем Универзитетску библиотеку „Светозар Марковић“ да у Дигитални репозиторијум Универзитета у Београду унесе моју докторску дисертацију под насловом:

BEHAVIOUR OF SHEAR CONNECTIONS REALISED BY CONNECTORS
FASTENED WITH CARTRIDGE FIRED PINS

Наслов на српском језику:

ПОНАШАЊЕ СМИЧУЋИХ СПОЈЕВА ИЗВЕДЕНИХ МОЖДАНИЦИМА СА
ЕКСЕРИМА СА ЕКСПЛОЗИВНИМ УПУЦАВАЊЕМ

која је моје ауторско дело.

Дисертацију са свим прилозима предао/ла сам у електронском формату погодном за трајно архивирање.

Моју докторску дисертацију похрањену у Дигиталном репозиторијуму Универзитета у Београду и доступну у отвореном приступу могу да користе сви који поштују одредбе садржане у одабраном типу лиценце Креативне заједнице (Creative Commons) за коју сам се одлучио/ла.

1. Ауторство (CC BY)

2. Ауторство – некомерцијално (CC BY-NC)

3. Ауторство – некомерцијално – без прерада (CC BY-NC-ND)

4. Ауторство – некомерцијално – делити под истим условима (CC BY-NC-SA)

5. Ауторство – без прерада (CC BY-ND)

6. Ауторство – делити под истим условима (CC BY-SA)

(Молимо да заокружите само једну од шест понуђених лиценци.
Кратак опис лиценци је саставни део ове изјаве).

Потпис аутора

У Београду, октобар, 2013



1. **Ауторство.** Дозвољаваате умножавање, дистрибуцију и јавно саопштавање дела, и прераде, ако се наведе име аутора на начин одређен од стране аутора или даваоца лиценце, чак и у комерцијалне сврхе. Ово је најслободнија од свих лиценци.

2. **Ауторство – некомерцијално.** Дозвољаваате умножавање, дистрибуцију и јавно саопштавање дела, и прераде, ако се наведе име аутора на начин одређен од стране аутора или даваоца лиценце. Ова лиценца не дозвољава комерцијалну употребу дела.

3. **Ауторство – некомерцијално – без прерада.** Дозвољаваате умножавање, дистрибуцију и јавно саопштавање дела, без промена, преобликовања или употребе дела у свом делу, ако се наведе име аутора на начин одређен од стране аутора или даваоца лиценце. Ова лиценца не дозвољава комерцијалну употребу дела. У односу на све остале лиценце, овом лиценцом се ограничава највећи обим права коришћења дела.

4. **Ауторство – некомерцијално – делити под истим условима.** Дозвољаваате умножавање, дистрибуцију и јавно саопштавање дела, и прераде, ако се наведе име аутора на начин одређен од стране аутора или даваоца лиценце и ако се прерада дистрибуира под истом или сличном лиценцом. Ова лиценца не дозвољава комерцијалну употребу дела и прерада.

5. **Ауторство – без прерада.** Дозвољаваате умножавање, дистрибуцију и јавно саопштавање дела, без промена, преобликовања или употребе дела у свом делу, ако се наведе име аутора на начин одређен од стране аутора или даваоца лиценце. Ова лиценца дозвољава комерцијалну употребу дела.

6. **Ауторство – делити под истим условима.** Дозвољаваате умножавање, дистрибуцију и јавно саопштавање дела, и прераде, ако се наведе име аутора на начин одређен од стране аутора или даваоца лиценце и ако се прерада дистрибуира под истом или сличном лиценцом. Ова лиценца дозвољава комерцијалну употребу дела и прерада. Слична је софтверским лиценцама, односно лиценцама отвореног кода.